Integrated geospatial-geochemical catchment analysis of Newfoundland stream waters draining endmember silicate bedrock types (ultramafic-mafic rocks vs. granite)

By Gabrielle Maria Ledesma

A thesis submitted to the School of Graduate Studies in partial fulfillment of the requirements for the degree of

Master of Science

Department of Earth Sciences

Memorial University of Newfoundland

August 2024

Abstract

The dissolved inorganic element chemistry of stream waters is a reflection of local bedrock composition, but also other catchments properties such as hydrology, surficial geology, vegetation/soil type, and elevation. Studies from small hydrological catchments with a singular or restricted range of bedrock type(s) are ideal for isolating geologic controls on water chemistry from other physicochemical and environmental controls. This study assesses dissolved major, trace, and rare earth element data from streams at two study sites within the same (boreal) climate zone of Newfoundland that each drain a silicate-endmember bedrock composition: (1) Bay of Islands in western Newfoundland draining an ophiolite sequence of mafic/ultramafic bedrock, and (2) Burin Peninsula draining a large Devonian carboniferous granite pluton (St. Lawrence granite) that hosts fluorite mineralization. Through integrating geochemical data with geospatially quantified catchment property data, this study has isolated the elements most strongly controlled by: bedrock geology (Mg, Cr, Ni in ultramafic rock streams; Cs, Rb in granite streams; contrasting REE abundances and Eu anomalies); weathering/soil/vegetation effects and associated flux of dissolved organic matter to streams (K, Co, Ce anomalies); and short temporal events or local geological features such as the fluorite mineralization (elevated element flux, high Y/Ho). Several of these more local water chemical features were traceable into larger catchment areas of Newfoundland major rivers. The low-abundance trace element data are the first to be reported for any Newfoundland surface water and have exposed this research approach as useful to trace boreal catchment dynamics through the lens of trace element geochemistry.

General Summary

The type of rock waters interact with can control the composition of elements dissolved in stream waters in tandem with other surface features such as plants and soils. This study measured the chemistry of small streams in Newfoundland that drain two highly contrasting rock types and the physical properties of their catchments such as topography and vegetation in order to separate out the different controls on the stream chemical composition. This research approach allowed the attribution of specific stream water chemical features to different controls ranging from the composition of rocks in catchments, processes operating at wider catchment scale such as soil development, and unusual water chemistry related to localized geological features. Understanding these relationships is important for identifying areas where geology can lead to potential toxic element inputs to waters and for understanding the transport of dissolved elements from major rivers into oceans.

Acknowledgments

I would like to start by thanking my supervisor, Dr. Michael Babechuk for his support throughout the project. His dedication to his field and guidance throughout the research process has made me a better scientist. I would also like to thank my co-supervisor Dr. Penny Morrill, whose enthusiasm and recommendations throughout the project was much appreciated. This project would not have been accomplished without the help from Dr. Inês Nobre Silva, who provided guidance for all the clean lab work. I would also like to thank our field assistant Ajatshatru Balaji who traversed many rivers collecting valuable data during field work. Thank you to our collaborators, Dr. Huy Dang and Dr. Wei Wang, from Trent University for all their work in sample analysis.

A special acknowledgment is given to all the amazing friends I've met throughout the program. Graduate degrees come with many challenges but allow for the most beautiful friendships to which I will always treasure.

I would like to thank my family for their constant support. To Mom, Papa, Joey, Austin, Janice, Pat, Sean, Ella, Kelly, Amanda, Emily, and Brynn, who celebrate with me in my joys and are a comfort through challenges. Words fall short to describe how lucky I am to have all of you.

Finally, I would like to acknowledge my husband, James. Thank you for coming with me to an island in the North Atlantic. You are my anchor through everything, and life is better with you.

Funding for the research was provided by the NSERC Discovery Grant, awarded to Michael Babechuk.

Table of Contents

Abstract ……..….. ii
General Summary ……..... iii
Acknowledgements ……...….. iv
Table of Contents…….…… v
List of Tables and Appendices ……..... vii
List of Figures ……..... viii
Organization of Thesis ……..…….. xi
Chapter 1: Introduction and Background……..……..... 1
1.1. Motivation of Study……..… 1
1.2. Project Overview and Key Objectives ……..... 2
1.3. Advantage of multi-element aqueous geochemistry enabled by inductively coupled plasma mass spectrometry (ICP-MS) ..…….……...……... 4
1.4. Lithologic controls and dissolved trace element signatures in freshwater ……..… 7
1.5. Factors controlling the abundance and behavior of selected major and trace elements in freshwater ……..…… 10
1.5.1. Major cations ……...……... 11
1.5.2. Alkali trace elements ……...……..... 13
1.5.3. Thorium-Uranium ……...……...… 15
1.5.4. Nickel-Chromium-Cobalt ……..……...17
1.5.5. Rare Earth Elements…….. 20
1.6. Advantage of using geospatial data to study small-scale catchments …… 22
1.7. References ……..…….. 26
Co-Authorship Statement…….. 52
Chapter 2: Integrated geospatial-geochemical catchment analysis of Newfoundland streams waters draining endmember silicate bedrock types (ultramafic-mafic rocks vs. granitic) ……... 53
2.1. Abstract ……..... 53
2.2. Introduction ……... 54
2.3. Sample sites ……... 57
2.3.1. Western Newfoundland site …… 57
2.3.2. Burin Peninsula site …… 58
2.3.3. Major rivers …….……... 59
2.3.4. Roadside spring water sites …….……... 60
2.4. Material and methods ……..…….… 60
2.4.1. Field sampling …….…… 60
2.4.2. Sample analysis & quality assurance/quality control …….…….… 61
2.4.3. Spatial analysis …….……... 63
2.4.4. Data analysis …….……..… 64
2.5. Results ……..…….… 66
2.5.1. Lithology and sample watershed classification ……... 66
2.5.2. Watershed characteristics – size, surficial coverage, topography, and vegetation ……..… 67
2.5.3. Physicochemical properties and DIC/DOC of streams ……..…….… 69
2.5.4. Lithologic compositions ……..… 70
2.5.5. Stream geochemistry ……...… 71

2.6. Discussion ……..... 78
2.6.1. Geologic controls on stream water chemistry revealed by monolithologic and sub-monolithologic streams and applications to larger catchments ……..….. 78
2.6.2. Assessing interrelated controls on stream chemistry in small, ultramafic -mafic catchments of western Newfoundland ……..…….. 83
2.6.3. Assessing interrelated controls on stream chemistry in small, granite catchments of Burin Peninsula ……..… 88
2.6.4. REE+Y as tracers of both source rock input and catchment processes ….... 92
2.6.5. Anomalous samples and their geological and temporal influences at a localized scale ……... 97
2.6.6. Evaluation of trace elements in groundwater tapped for present day or historical drinking water ……... 99
2.7. Conclusions ……..… 100
2.8. References ……...… 104
2.9. Tables …….…….. 116
2.10. Figures ……..…….…… 121
Chapter 3: Conclusions …….…….. 145
3.1. References ……...…… 149
Appendix 1: Full watershed attributes and physicochemical properties of all streams/rivers….. 150
Appendix 2: Field observations for all streams/rivers ……..… 152
Appendix 3: Summary of measured AQUA-1 and SLRS-6 reference material values compared to certified and literature values. …… …… ...… 154
Appendix 4: Compiled major and trace element compositions for bedrock within study sites...157
Appendix 5: Full geochemical data for all streams/rivers ……...……..... 159

List of Tables and Appendixes

Table 1 Elemental abundance in different rock types/Earth reservoirs

Table 2 Detailed catchment bedrock geology used to derive the lithologic groupings of streams for this study.

Table 3 Summary of watershed attributes and physicochemical properties of streams divided into their lithologic groupings.

Table 4 Summary of selected geochemical data of streams divided into their lithologic groupings.

Appendix 1 Full watershed attributes and physicochemical properties of all streams/rivers.

Appendix 2 Field observations for all streams/rivers.

Appendix 3 Summary of measured AQUA-1 and SLRS-6 reference material values compared to certified and literature values.

Appendix 4 Compiled major and trace element compositions for bedrock within the study sites.

Appendix 5 Full geochemical data for all streams/rivers.

List of Figures

Figure 1 Simplified bedrock geology of western Newfoundland study site showing water sample locations and delineated catchments up until the point of sampling. Bedrock was visualized using the 1:1 Million Bedrock Geology file from the Geoscience Atlas and catchment delineation was done in ArcGIS Pro. Details of process and references can be found in Sections 2.4.3 and 2.5.1.

Figure 2 Simplified bedrock geology of Burin Peninsula study site showing water sample locations and delineated catchments up until the point of sampling. Bedrock was visualized using the 1:1 Million Bedrock Geology file from the Geoscience Atlas and catchment delineation was done in ArcGIS Pro. Details of process and references can be found in Sections 2.4.3 and 2.5.1.

Figure 3 Simplified bedrock geology of Newfoundland with the sampling location of six major rivers and delineated catchments up to the point of sampling. Bedrock was visualized using the 1:1 Million Bedrock Geology file from the Geoscience Atlas and catchment delineation was done in ArcGIS Pro. Details of process and references can be found in Sections 2.4.3 and 2.5.1.

Figure 4 (a) Vegetation overlay and (b) surficial geology map of western Newfoundland study site showing water sample locations and delineated catchments up until the point of sampling. Vegetation overlay extracted from CanVec "Wooded Area" files and surficial geology coverage, extracted from Geoscience Atlas "Detailed Surficial File". Details of process and references can be found in Section 2.4.3.

Figure 5 **Figure 5**: (a) Vegetation overlay and (b) surficial geology map of Burin Peninsula study site showing water sample locations and delineated catchments up until the point of sampling. Vegetation overlay extracted from CanVec "Wooded Area" files and surficial geology coverage, extracted from Geoscience Atlas "Detailed Surficial File". Details of process and references can be found in Section 2.4.3.

Figure 6 Major cation ternary diagram (Mg–Na+K–Ca) of waters and site-specific bedrock. All values are reported as molar proportions.

Figure 7 Stacked bar charts showing the relative proportions of dissolved major cations (Mg, Ca, Na, K) in the mean composition of small-catchment streams, after division into their target lithologic groupings: (a) monolithologic streams (granite, mafic, ultramafic) and (b) sub-monolithologic streams (granite, ultramafic). (c) Whole-rock major element data from bedrock presented in the same format as stream data for comparison. Bedrock compositions for the SLG in the Burin Peninsula from Magyarosi (2022). Bedrock compositions for rocks in the BOIC from western Newfoundland from Malpas (1976), divided into mafic and ultramafic groupings.

Figure 8 Principal component analysis (PCA) displaying major and trace element relationship of the monolithologic streams (granite, mafic, ultramafic). Element measurements below detection limit were taken at half the detection limit for PCA. Only Cr was affected by this.

Figure 9 Summary of the major cations (Mg, Ca, Na, K) in all stream/river samples from this study, categorized by their lithologic groupings. Data are presented (a) normalized by major cations (∑+) and (b) as measured abundances (µg/L).

Figure 10 Summary of the mafic and ultramafic rock-associated elements (Ni, Co, Cr) in all stream/river samples from this study, categorized by their lithologic groupings. Data are presented (a) normalized by major cations (∑+) and (b) as measured abundances (µg/L). Refer to Figure 9 for sample codes.

Figure 11 Summary of the felsic rock-associated elements (Li, Rb, Cs, Th, U) in all stream/river samples from this study, categorized by their lithologic groupings. Data are presented (a) normalized by major cations (∑+) and (b) as measured abundances (µg/L). Refer to Figure 9 for sample codes.

Figure 12 Stacked bar charts showing the relative proportions of dissolved major cations (Mg, Ca, Na, K) in the 6 Newfoundland major rivers sampled for this study.

Figure 13 Scatter plots of selected major cation ratios: (a) Ca/Mg vs K/Mg and (b) Ca/Na vs Mg/Na. Sample from this study are presented in their lithologic groupings (Section 2.5.1). Literature data from other studies of monolithologic catchments are compiled for comparison and includes: [1]granite catchments (as initially compiled from several localities by Oliva et al., 2003), [2]mafic catchments in Ireland (Gislason and Arnórsson, 1993), and [3,4]ultramafic catchments in California (McClain and Maher, 2016) and Philippines (Delina et al., 2020).

Figure 14 Slopes and anomalies calculated from normalized REE+Y patterns (Figure 15); see Section 2.4.4 for formulas): (a) ∑REE, (b) Y/Ho, (c) Eu_N/Eu_N^* (d) Ce_N/Ce_N^* (e) Pr_N/Er_N (f) Pr_N/Tb_N (g) Tb_N/Er_N. Samples are arranged by lithological grouping across the catchments (Table 2). Some samples are removed if analytical scatter skewed the calculation.

Figure 15 MuQ-normalized REE+Y patterns for water samples divided into: (a) major river samples, (b) heterolithologic/comparison streams at both sites (those in this group draining a catchment with sedimentary rocks are identified), (c) monolithologic granite streams, (d) sub-monolithologic granite streams, (e) monolithologic ultramafic streams, (f) sub-monolithologic ultramafic streams, (g) monolithologic mafic streams, and (h) rain-affected monolithologic mafic samples. Sample GM2206 removed due to very low REE-abundance with a pattern characterized by significant analytical scatter.

Figure 16 Scatter plots of the calculated % catchment coverage of ultramafic bedrock up to the point of sampling against stream water chemical characteristics: (a) Mg/∑+, (b) Ca/∑+, (c) Ni/∑+, (d) Cr/∑+, and (e) Co/∑+.

Figure 17 Scatter plots of the calculated % catchment coverage of granite bedrock up to the point of sampling against stream water chemical characteristics: (a) Na/∑+, (b) K/∑+, (c) Th/∑+, (d) U/∑+, (e) Li/∑+, (f) Rb/∑+, and (g) Cs/∑+. Two samples with anomalous chemistry are removed due to suspected influence from fluorite veins (Section 2.6.5).

Figure 18 Dissolved stream measurements of selected trace elements normalized by average world river compilation by Gaillardet et al. (2014). Data presented as mean from each group with error bars representing 1 standard deviation. Values below 3x higher than background equivalent concentration removed.

Figure 19 Principal component analysis (PCA) displaying major and trace element relationship of the ultramafic(-mafic) monolithologic and sub-monolithologic streams along with catchment attribute and physicochemical property relationships. Element measurements below detection limit were taken at half the detection limit for PCA. Only Cr was affected by this.

Figure 20 Principal component analysis (PCA) displaying major and trace element relationship of the granitic monolithologic and sub-monolithologic streams along with catchment attribute and physicochemical property relationships.

Figure 21 Scatter plot of calculated mean catchment slope against stream water U/∑+ and Th/∑+. Only stream samples falling into monolithological and sub-monolithogical granite groupings (>30% granite coverage in this case) are considered, with 2 anomalous samples (suspected vein influence) removed.

Figure 22 Location of known fluorite veins at the Burin Peninsula study site. Simplified bedrock geology as per Figure 2. Fluorite vein locations extracted from map data after Magyarosi (2022); Magyarosi et al. (2019); Strong et al. (1976, 1978); Wilson (2000).

Figure 23 Principle component analysis (PCA) displaying assumed diagnostic vein features (Ca, Cu, Ba, Sr, Pb, ∑REE, and Y/Ho) and diagnostic granitic rock signatures (Cs, Rb, and Li), as determined by 2.6.3 and other relevant elements (Na, K, EuN/EuN*) evaluated in 2.6.3 as variables for granite monolithologic and sub-monolithologic streams, including two determined anomalous samples.

Figure 24 Dissolved trace element abundances in roadside spring waters from 3 sites (see Section 2.3.4.) focused on 5 potentially toxic elements (PTEs): (a) U, (b) As, (c) Pb, (d) Cr, and (e) Cu. Inset plots with shaded background are an expanded abundance range in order to compare values to the Canadian drinking water guidelines (Health Canada, 2019) as represented by the solid (orange) line.

Organization of Thesis

This thesis is divided into two chapters. Chapter 1 is an introductory section that outlines the motivation of the study, a literature review of important topics of the study, and a summary of the thesis layout with a co-authorship statement. Chapter 2 is the original research component of the thesis, which is written in a manuscript format and includes a separate, more targeted, introduction and main conclusions of the project. Chapter 2 is not currently submitted to a journal as a manuscript to be considered for publication, but it was written with the Journal of Hydrology - Regional Studies in mind as an aimed publication venue. All original data collected for this research and all data compiled for comparative use in the study are available in thesis tables or appendices. Chapter 3 is a broader summary of the important contributions of the work and the use of the province as a natural laboratory for water research.

Chapter 1: Introduction and Background

1.1. Motivation of Study

Rivers are a vital component of Earth's surface systems, serving as important conduits of dissolved and suspended material from continents to oceans (Martin and Whitfield, 1983). Additionally major rivers place important global constraints on the biogeochemical cycles of elements (Meybeck, 1987; Suchet and Probst, 1993). The chemical composition of rivers is inherited primarily from surface processes within their terrestrial environments. Such controls range from bedrock interactions (mineralogy, weatherability, and physical properties controlling hydrologic flow), properties of soils, vegetation-type, inputs of surface runoff and groundwater discharge, anthropogenic point sources or modifications, and water parameters (e.g., Eh, pH). Through these dynamic and often interrelated controls, the mobilization of specific elements into the dissolved load (free elements/element complexes carried in a solution or elements bound to fine-colloidal material passing through a defined filter pore size) can differ across diverse climates, topographies, and land-use patterns, highlighting the need for further studies to fully understand the complexities that control river chemistry.

This is particularly true for trace (<1 mg/L) and ultra-trace (<1 μg/L) elements, where understanding of their terrestrial aquatic behavior is still developing. As freshwater systems face increasing susceptibility to multiple stressors (e.g., climate change, changing land-use, anthropogenic input), their water chemistry and ultimately transport of elements can be affected. Therefore, establishing baseline data and understanding the potential impacts on the behavior of certain elements becomes increasingly necessary.

Major rivers across the globe have often been the focus for studies due to their importance in mass transport of elements from terrestrial to marine environments (e.g., Dekov et al., 1998; Konhauser et al., 1994; Martin and Meybeck, 1979; Milliman and Meade, 1983). However, the catchments of major rivers cover wide areas and create challenges when attempting to isolate individual factors that control the chemical composition of these systems. Therefore, other studies have focused on element cycling of rivers or streams in small catchments that better allow for isolating primary factors that have the greatest influence on the dissolved chemical compositions (e.g., Gíslason et al., 1996; Jiang et al., 2018).

Headwaters, in particular, have been recognized for their significant influence on stream water chemistry, exerting a disproportionate influence across the entire river network (French et al., 2020; Temnerud and Bishop, 2005). Given that headwater streams can constitute a substantial portion of an overall stream network (Downing et al., 2012; Wohl, 2017), it is useful to characterize the spatial variability within a catchment and identify primary processes governing such streams across various scales.

Therefore, it is useful to investigate rivers with varying catchment size, land-use patterns, highly contrasting lithologies, and across different climate zones to create a more comprehensive understanding of the composition and cycling of elements in freshwater.

1.2. Project Overview and Key Objectives

This project uses two study sites from the island of Newfoundland (province of Newfoundland & Labrador), Canada to provide a comprehensive geochemical survey of the dissolved budget of streams draining endmember silicate lithology with the aim to establish the main catchment drivers

that control the water chemistry. More specifically, this project will define the dissolved element signatures of streams from two sites with contrasting endmember silicate bedrock: the ultramafic-mafic-dominated rocks of the Bay of Islands Complex (near Bay of Islands and Gros Morne, western Newfoundland) and the plutonic felsic-dominated rocks of Burin Peninsula (near St. Lawrence). Stream chemistry at both sites will be used to assess the primary watershed drivers that play important roles in regulating the dissolved composition within the ultramafic and granite catchments. This objective will specifically utilize geospatial data to define watershed attributes that contribute to variations in the dissolved composition of streams. These small catchment geochemical data observations will be compared to data from 6 major rivers across Newfoundland to assess how small catchment streams contribute to signatures in larger river catchments.

The aim of this study was not to address all factors that control the complex chemical dynamics of a watershed (seasonal variations, groundwater and meteoric water inputs, soil outputs, and steam flow, e.g., Chupakov et al., 2020; Ingri et al., 2000; Öhlander et al., 2013; Sun et al., 2019). Instead, the aim was to use a single-season and single-filtration sampling strategy to illustrate Newfoundland and Labrador's potential as an ideal natural laboratory to study element cycling in a temperate, boreal climate. This study contributes important baseline information to the province's freshwater system and outlines how the integration of multi-element datasets with geospatially constrained variables, such as specific bedrock lithology, vegetation coverage, surficial geology coverage, topographical data, can inform dominant controls on specific element signatures.

This introduction section reviews important factors in fluvial systems that are relevant to the project goals and will cover (1) advantage of multi-element aqueous geochemistry enabled by

inductively coupled plasma-mass spectrometry (ICP-MS) (Section 1.3), (2) current understanding between the links of lithologic controls on the dissolved fraction of freshwaters (Section 1.4), (3) reviews knowledge on selected major and trace element behavior that are of notable importance to this study (Section 1.5), and (4) finishes with advantage of employing integrated geospatial and geochemical datasets to study small-scale catchments (Section 1.6).

1.3. Advantage of multi-element aqueous geochemistry enabled by inductively coupled plasma-mass spectrometry (ICP-MS)

While major ion-forming elements (Mg^{2+}, Ca^{2+}, Na^{+}, K^{+}, SO_4^{2-}) within surface waters can reflect the mineralogy of source rocks in a catchment area, a full multi-element dataset can offer a more robust ability for proxy tracing and source fingerprinting (Gaillardet et al., 2014). Often, these elements are present at naturally low abundances in freshwater, referred to as trace (<1 mg/L) and ultra-trace (<1 μg/L) elements. However, comprehensive understanding of these naturally low-abundance elements are either emerging, evolving, or being refined through advancements in ICP-MS. Accompanying the advancement in instrument technology and sample preparation methodology (e.g., Fisher and Kara, 2016; Wysocka, 2021), ICP-MS is now a preferred instrument for low-abundance element determination in natural waters. As a result, there is more widely available data for the rare earth elements + yttrium (REE+Y) (e.g., Barrat and Bayon, 2024; Lawrence et al., 2006), extended alkali and alkaline earth elements (Li, Cs, Rb, Ba, Sr, Be) (e.g., Gou et al., 2020; Suhrhoff et al., 2019), and other transition metals (e.g., Colombo et al., 2019; Cuss et al., 2018). These elements serve as useful tracers of source weathering, redox state of waters, or anthropogenic or anomalous geogenic sources that can be used for environmental monitoring or mineral exploration purposes.

However, there is a range of ICP-MS instrument types and sample preparation methodologies that can introduce different strengths and weaknesses for natural water element abundance measurements.

Quadrupole ICP-MS instruments are advantageous due to their low cost relative to other types of ICP-MS, such as sector field instruments, while still retaining fast and full mass scanning and high sensitivity. A recent expansion of tandem ICP-MS/MS ("triple quad") instrument can offer advantages that overcome persistent issues encountered by traditional quadrupole ICP-MS when analyzing elements in natural waters. Specifically, quadrupole ICP-MS has limited ability to resolve species with the same mass/charge ratio (e.g., $ArCl^+$ on As mass; CaO^+ on Ni isotope mass), making accurate analysis a challenge. This is especially troublesome for analytes where traditional methods to remove interferences (e.g., He-based kinetic energy discrimination), or modification to sample matrices during sample preparation are not effective. ICP-MS/MS allows for greater flexibility in avoiding these polyatomic interferences by using different gases (O_2, N_2O, H_2) between the two quadrupoles that react or interfere with elements with different or same mass/charge ratio. This study has applied the Agilent Technologies Inc. 8800 ICP-MS/MS instrument (Agilent Technologies, (n.d.)) for sample analysis, undertaken by collaborators at Trent University Water Quality Centre (WQC).

Sample preparation strategies are also an important consideration, with the range of approaches typically depending on number of analytes, natural abundances in samples, or the type of instrument, laboratory, and reagents available. Most commonly used sample preparation strategies are pre-concentration or direct measurement approaches. Pre-concentration steps aim to increase the concentration of the analyte while reducing the overall volume of the sample. Often this

approach is used to improve measurement signals, including detection limits and precision (Hoang et al., 2019). However, this approach requires more initial sample volume, increased sample handling, and can amplify matrix interference effects. Other pre-concentration approaches focus on targeting specific elements or element groups (e.g., Ma et al., 2019; Sohrin et al., 2008; Stetzenbach et al., 1994; Wang et al., 2021), such as chromatography or coprecipitation but such strategies are often more time-consuming and don't provide a comprehensive multi-element analysis.

Direct measurement approaches prepare filtered and acidified water samples for ICP-MS analysis with only the addition of an internal standard (e.g., Babechuk et al., 2020; Dang et al., 2022; Lawrence et al., 2006b) and are often best at acquiring the most comprehensive multi-element suite. However, such approaches are limited by the instrument background and/or procedural blank and must mitigate sample matrix polyatomic interferences or employ mathematical correction strategies (e.g., oxide and hydroxide interference corrections; Aries et al. 2000). This study has adopted a direct measurement strategy using a single internal standard (In) as described and demonstrated in a previous study (Dang et al., 2022).

Reducing sample contamination is also a critical component of analytical methods. Sources of contamination can come through all stages of field sampling filtration, preservation and sample handing up to the point of measurement (Batley and Gardner, 1977; Kramer, 1994; Schulze et al., 2011). Contamination can come from residual elements in sample storage containers that are released upon interaction with the sample or acid used for preservation and from field equipment (e.g., high metal contents in nitrile gloves source of contamination during contact with a sample; Garçon et al., 2016). This study employed several strategies to mitigate or reduce such sources of

contamination which include: (1) multi-acid leaching and rinsing of all plastic sample containers; (2) purposeful use of Nylon filters that have low blank composition (based on experiential knowledge); (3) preparation of in-house triply distilled HNO_3 for sample preservations; and (4) use of "clean hand" and "dirty hands" in field whereby only "clean hands" undertakes filtration and acidification step (refer to EPA Method 1669 Field Sampling). Further sources of contamination can come from internal standards added to samples and washover from calibration or quality control standards during ICP-MS measurement. To assess the mitigation of all sources of contamination, a full procedural blank sample is created and analyzed, which represents all same steps and exposures of all other field samples.

1.4. Lithologic controls and dissolved trace element signatures in freshwater

Investigations into chemical composition of rivers reveal that lithology serves as a dominant control over the dissolved element composition of natural waters (e.g., Lyons et al., 2021) and entrance of elements into surface water is dependent on parent material, mineralogical properties, extent of water-rock interaction, and other physical parameters such as temperature and denudation rates (Gaillardet et al., 1999; Wilson, 2004). Therefore, enrichments of certain elements in freshwater would firstly reflect enrichment of the catchment source rock and secondly, the physical catchment properties that favor element solubility. These "geogenic" controls on surface waters have been the focus of many investigations into water chemistry. Such as sulfate deposits inducing high SO_4^{2-} within surface water (e.g., Fraser River; Cameron et al., 1995), or elevated Ca+Mg delivered to streams if highly weatherable carbonates are present in a catchment (Pande et al., 1994; Wadleigh et al., 1985). Understanding the control of specific lithology on water chemistry is relevant when investigating the role of weathering in Earth's surface system. Silicate rocks have been of particular focus (Dessert et al., 2003; Gaillardet et al., 1999; Meybeck, 1987), as

weathering of silicates is recognized as an important sink for atmospheric carbon dioxide (Berner, 2004; Berner and Berner, 1997). While weathering contribution of specific lithology can be evaluated through the major cation-forming elements (Mg, Na, Ca, K), there are also coupled geogenic links of trace and ultra-trace elements between lithology and surface water chemistry. However, the chemical signature of low-abundance elements can also be indicative of other environmental sources or processes. For example, localized contributions from mineral deposits can be detected in the trace element composition of rivers (Song et al., 2016). For elements such as Cr and U, inputs to water can track both contrasting geogenic sources (Cr is naturally concentrated in ultramafic rocks while U is concentrated in felsic rocks) and surface conditions since both have aqueous solubility enhanced in oxidizing environments (Astrom et al., 2009; Brugge and Buchner, 2011; D. Brugge et al., 2005; Izbicki et al., 2015; Post et al., 2017; Welch and Lico, 1998). Understanding the dynamics of trace element mobility is important as some can lead to concerns for public health. For example, the potentially toxic element As can be elevated above safe consumption limits (10 μg/L for Canada; Health Canada, 2019) in surface waters and groundwater when environmental conditions promote primary and secondary mineral dissolution of As-rich rocks (Chakraborty et al., 2015; Herath et al., 2016).

Accurately predicting water chemistry variations as a function of lithology still requires many additional considerations such as mineralogy, catchment hydrology, and climate zone. Nevertheless, chemical composition of bedrocks coupled with thermodynamic properties of elements and a long history of empirical and experimental studies can be combined towards making general hypotheses regarding relative element mobility. The general mobility of trace elements in aquatic systems has been estimated by relating the abundance of an element in the average upper continental crust to the average abundant of the same element in a global major

river compilation. Such a “mobility index” has been developed by Gaillardet et al. (2014) which separates elements with low chemical mobility (e.g., Nb, Ti, Zr, and Al) from elements with higher mobility (e.g., So, Mo, S, and Re). Rock types also contain unique chemical compositions. During igneous differentiation, the incompatibility of elements, controlled by ionic charge and size, result in predictable element compositions. As such, ultramafic rocks are most abundant in Mg and compatible trace elements Cr, V, Ni, Co, mafic rocks are abundant in Mg and Ca and other elements compatible in plagioclase and pyroxenes (Sr, Sc), and felsic rocks are most abundant in Na and K along with incompatible trace elements Li, Cs, Rb, Tl, U, Th and rare earth elements (REE). Despite the range of solubility of these elements and their host minerals, several studies have shown that small hydrologic catchments draining predominantly one silicate rock type show expected enrichments in freshwaters that reflect the igneous bedrock. Such studies have focused on catchments with primarily granitic rock (Aubert et al., 2001; García et al., 2007; Hinkley, 1976; Oliva et al., 2004, 2003; Porcelli et al., 1997; Sun et al., 2019), and ultramafic intrusive rocks (Binda et al., 2018; Kierczak et al., 2021; McClain and Maher, 2016; Vasileiou et al., 2021; Venturelli et al., 1997).

This study adopted a similar approach and pre-selected catchments across Newfoundland to sample streams with dominant catchment bedrock type. Specifically, areas of western Newfoundland draining an ophiolite (ultramafic-mafic rocks) were selected for comparison to an area of the Burin Peninsula draining granite. Both study sites are coastal, within the same climate zone, and outside of major urban influence, allowing for lithology, hydrology, and vegetation to be the primary controlling factors on stream chemistry. Additionally, 6 accessible major rivers across Newfoundland were also selected to allow the comparison of small stream chemistry to that of waters collecting drainage from much larger catchment areas and a wider range of bedrock.

1.5. Factors controlling the abundance and behavior of selected major and trace elements in freshwater

General focus for this study is given to the major cation-forming elements (Mg, Ca, Na, K; henceforth "major cations") as they are commonly used as water tracers with well-established aqueous behavior, and to selected trace elements based on the contrasting igneous bedrock types within the study areas. These trace elements include Li, Cs, Rb, Th, and U as elements enriched in felsic rocks relative to ultramafic-mafic rocks and Ni, Co, and Cr as elements enriched in ultramafic-mafic rocks relative to felsic rocks (Turekian and Wedepohl, 1961). The elemental abundance contrast in different rock types/Earth reservoirs is illustrated in Table 1 using values of the primitive mantle/bulk silicate Earth (proxy for ultramafic rocks), average mid-ocean ridge basalt (MORB) (proxy for mafic rocks), and estimated average upper continental crust (proxy for intermediate-to-felsic rocks). The rare earth elements + yttrium (REE+Y) are also included due to their contrasting abundances in the endmember silicate rock types (McLennan and Taylor, 2012) and their well-established use as aquatic tracers for processes in freshwater (Elderfield et al., 1990; Goldstein and Jacobsen, 1988; Lawrence et al., 2006a). This section provides a brief overview of key factors influencing the behavior of these elements within the hydrosphere and their key lithologic versus environmental controls. Dissolved elements can be broadly grouped into categories of (1) poorly mobile elements that will be preferentially retained within source minerals or secondary weathering products, (2) relatively mobile elements that are favorably released into the hydrosphere often from residence in easily weatherable material and high aqueous solubility, and (3) elements whose mobilities are dependent on redox and/or surface-sorption processes occurring in both the weathering and aquatic realms.

Table 1: Elemental abundance in different rock types/Earth reservoirs

mg/kg (ppm)	Primitive Mantle/Bulk Silicate Earth [1]	Global MORB average	Upper continental crust estimates
Li	1.6	5.1 [2]	21.0-28.2 [6-7]
Rb	0.6	1.5 [3]	79.5-112 [6-8]
Cs	0.021	0.019 [3]	4.6-5.4 [6-8]
Th	0.0795	0.219 [4]	10.5-11.1 [6-8]
U	0.0203	0.08 [4]	2.7-2.8 [6-7]
Ni	1960	200 [5]	31.6-47.0 [6-8]
Co	105	56 [5]	17.0-22.4 [6-8]
Cr	2625	326 [3]	64.5-92.0 [6-8]

Data sources: statistical screening and type of mean as per original studies, some reported as compiled in Arevalo and McDonough (2010); [1] McDonough and Sun (1995); [2] Ryan and Langmuir (1987); [3] Hofmann and White (1983); [4] Arevalo and McDonough (2010); [5] McDonough (1994); [6] Rudnick and Gao (2003); [7] Kamber et al. (2005); [8] McLennan (2001)

1.5.1. Major cations

The most abundant cations in surface water are ones with high aqueous solubility and are major elements in most common rock types: Mg, Ca, Na, and K. The weathering of evaporites and carbonates are only noted as a significant source of these ions when such rocks are present (e.g., Gaillardet et al., 1999; Lyons et al., 2021) and silicate rock weathering is the primary focus for this study. In the context of silicate rocks, Ca and Na enter the hydrosphere through weathering of plagioclase and to a lesser extent, Ca-bearing pyroxenes (Meybeck, 1987; Nesbitt and Wilson, 1992; Nesbitt and Young, 1989). Weathering products of plagioclase (kaolinite and gibbsite) have negligible retention capacity for Ca and Na (Eggleton et al., 1987; Kronberg et al., 1987; Nesbitt and Markovics, 1997; Schirrmeister and Störr, 1994), but weathering of clinopyroxenes to mixed-

layer clay minerals, such as smectite or chlorite can result in retention of Ca during early stages of weathering (Gíslason et al., 1996). Nevertheless, Ca is still considered highly mobile during chemical weathering of all silicate rock types (Nesbitt and Markovics, 1997; Nesbitt and Wilson, 1992). Sodium has limited retention capacity in all common secondary mineral phases and thus is considered one of the most mobile and conservative major cations in waters. Magnesium and K exhibit more complex weathering behavior. During the early stages of olivine weathering, Mg is observed to have significant mobility (Nesbitt and Wilson, 1992), but weathering of other mafic mineral phases, like pyroxenes, can produce clays that can retain Mg (Salil et al., 1997; Zeyen et al., 2022). Potassium is concentrated in K-feldspars or micas that are notably more resistant to chemical weathering than plagioclase and most mafic minerals (Banfield and Eggleton, 1990; Nesbitt and Markovics, 1997). The early weathering products of these K-bearing minerals (illite or vermiculite) also result in the appreciable retention of K (Nesbitt and Markovics, 1997). However, advanced weathering stages where kaolinite is developed from earlier-formed clays, result in enhanced release of Mg and K into the hydrosphere. In some weathering environments, the uptake of Mg and K into vegetation can contribute as a control on their flux to the hydrosphere (Choudhury et al., 1994; Uhlig et al., 2017). Additional sources of major ions can also include atmospheric deposition and ocean spray, an effect that can vary based on lithology, vegetation, altitude and proximity to the coast (Meybeck, 1983).

In general, the abundance and relative proportions of major cations in surface waters is expected to be controlled by bedrock, such that stream chemistry variations reflect lithologic variations. However, as discussed, they can still be susceptible to weathering reactions, additional sources, and other environmental factors such as vegetation.

1.5.2. Alkali trace elements

The alkali element group has broadly similar weathering behavior to each other and their abundance in surface waters reflect a combination of source rock enrichment/mineralogy, extent of weathering/water-rock interaction, and clay mineral type and abundance in the weathering profile.

Lithium is incompatible during magmatic differentiation with the highest concentrations generally associated with peraluminous granites (Chappell and White, 2001) and highly evolved granitic systems sometimes having extreme Li enrichment associated with pegmatites (Bradley et al., 2016; London, 2018; Martin and De Vito, 2005). Although an alkali element, Li^+ has a small ionic radius that is closer to Mg^{2+} and Al^{3+} than to the other alkali elements (Shannon, 1976), such that Li is often concentrated in different primary igneous and secondary minerals than the other alkali elements (Starkey, 1982). In surface waters, Li has been shown to have a similar behavior to Mg (Huh et al., 1998) despite its greater potential for uptake in secondary minerals formed during chemical weathering. Much of the environmental behavior of Li has been defined through measurement of stable Li isotope ratios in waters, weathering profiles, and river sediment. These studies reveal that most Li in rivers is sourced from silicate weathering (Dellinger et al., 2015; Huh et al., 2001; Kısakűrek et al., 2005; Lemarchand et al., 2010; Pogge von Strandmann et al., 2010) and that fractionation primarily through scavenging by secondary minerals with negligible biological uptake (Pogge von Strandmann et al., 2016) positions the isotopic ratio as an important silicate weathering proxy.

Of the alkali elements, Rb^+ has the closest ionic radius to K^+ (Shannon, 1976), resulting in closely coupled behavior during magmatic fractionation (Ahrens et al., 1952; Horstman, 1957) and K-

minerals (microcline or muscovite) becoming the main igneous hosts of Rb (e.g., Heier 1962). The weathering behavior of Rb is controlled by weathering of K-feldspar and micas and retention in secondary minerals such as illite and vermiculite (Nesbitt et al., 1980). During earlier stages of chemical weathering, Rb will be retained in secondary minerals via adsorption or incorporation preferentially to K, leading to decreasing K/Rb ratios within the weathering profile and eroded sediment (Middelburg et al., 1988; Nesbitt et al., 1980; Tanaka and Watanabe, 2015). The average K/Rb ratio of global river water is typically ~1000. However, higher K/Rb ratios in freshwater occur where dissolution of evaporite deposits contributes to water chemistry and the K taken into plants preferentially to Rb is recycled into surface waters by plant matter decay (Chaudhuri et al., 2007; Peltola et al., 2008).

Cesium^{+} has the largest ionic radii of the alkali elements and shows similar progressive enrichment during magmatic fraction as the rest of the alkali group (Horstman, 1957). Cesium is closest in behavior to Li in its ability to become extremely fractionated in pegmatite ore-forming processes (Bradley et al., 2016; London, 2018; Martin and De Vito, 2005). During chemical weathering, Cs exhibits behavior similar to the rest of the alkali element group but can have relatively higher adsorption capacity on secondary mineral surfaces (Fuller et al., 2015; Nesbitt et al., 1980; Tanaka and Watanabe, 2015; Wampler et al., 2012; Wu et al., 2022). Assessing the environmental behavior of Cs has also been a focus for understanding the distribution and residence time of radioactive Cs (^{137}Cs and ^{134}Cs) (Comans et al., 1989; de Koning and Comans, 2004; Mukai et al., 2016), especially after release during nuclear reactor accidents such as the Fukushima Daiichi Nuclear Power Plant (Taniguchi et al., 2019).

The primary control on the alkali element abundances for this study of Newfoundland stream waters is hypothesized to be source rock enrichment, with higher abundances being diagnostic of small catchments draining granite relative to those draining ultramafic-mafic rocks. The alkali elements have variable but generally high affinity for adsorption or incorporation into clay minerals, such as illite, vermiculite, and smectites and variations across catchments with the same bedrock type may reflect local changes in soil development that have variable reactive clay surfaces or variable vegetation type.

1.5.3. Thorium-Uranium

Thorium and U are the only actinide elements that occur naturally at appreciable levels within surface environments. The elements have closely coupled magmatic behavior but highly decoupled environmental behavior. Both elements are highly incompatible in magmatic systems due to their high charge relative to ionic radii (Shannon, 1976) and often are concentrated in accessary minerals such as apatite, zircon, monazite, allanite, uraninite, coffinite (e.g., Bea, 1996 and references therein).

Weathering behavior of Th- and U-bearing accessory minerals is an important control on the release of both actinides from rocks to the hydrosphere (e.g., Braun et al., 2018; Buriánek et al., 2022; Plasil, 2014). Typically, Th is immobile during silicate-rock weathering (albeit with some exceptions, see Chabaux et al., 2003), largely due to it being hosted in minerals resistant to weathering and/or becomes fixed by stable secondary minerals in weathering profiles (Babechuk et al., 2015; Kurtz et al., 2000; Nesbitt and Markovics, 1997). This retention in weathering resistant accessory minerals results in low concentration of Th in natural waters, with the main transport

mechanism of Th being through colloid and particulate transport (Degueldre and Kline, 2007; Langmuir and Herman, 1980; Short et al., 1988).

In contrast to Th, U can be oxidized from U^{4+} to U^{6+} during oxidative weathering, favouring the release and transport of soluble UO_2^{2+} or uranyl-carbonate species under oxidative and neutral to alkaline pH surface environments (Langmuir, 1978). These species of U can be immobilized by adsorption to mineral surfaces (Barnett et al., 2000; Jung et al., 2019) or when encountering reductive and/or organic-rich conditions (Campbell et al., 2015; Cumberland et al., 2016; Stetten et al., 2018). Dominant sources of U to freshwater are typically the natural weathering of marine sedimentary rocks if present, but U can also be anthropogenically elevated, most commonly through fertilizer sources (Gardner et al., 2023; Otero et al., 2005; Schnug and Haneklaus, 2016; Uchida et al., 2006). However, U in surface waters of silicate rock-dominated watersheds can also vary as a function of source-rock U enrichment with more felsic rocks exerting the strongest control (Palmer and Edmond, 1993; Sarin et al., 1990; Smedley and Kinniburgh, 2023). Since rivers are the primary source of U to the oceans, there is an advantage in studying U in freshwater systems to help understand its relationship with ocean waters. The activity ratio of U isotopes (^{234}U and ^{238}U) in ocean water indicates there is an excess of ^{234}U compared to what is expected from ^{238}U decay (Chen et al., 1986; Ku et al., 1977; Thurber et al., 1965). There is general agreement that the ^{234}U excess in the oceans is related to the terrestrial weathering of U-bearing minerals (Andersen et al., 2009; Anderson et al., 1989; Suhr et al., 2018), but rivers have highly variable dissolved $^{234}U/^{238}U$ activity ratios (Chabaux et al., 2003; Moore, 1967). This variability arises from varying weathering conditions across different regions (Andersen et al., 2009; Suhr et al., 2018), mixing of groundwater with surface waters prior to outflow into rivers (e.g., White et al., 2021; Zebracki et al., 2023), short- and long-term climate related changes on weathering (Chabaux et al.,

2001; Robinson et al., 2004), and exchanges between colloid-bound and dissolved U (e.g., Plater et al., 1992; Porcelli et al., 1997; Somayajulu, 1994; Swarzenski et al., 2004).

Overall, source rock enrichment, extent of water-rock interaction and weathering, and the redox state of the weathering environment and water all have important controls on abundance of Th and U in surface waters. The contrasting behavior of Th and U during weathering and aqueous transport can be tracked through Th/U ratios. Typically soils, river sediments, and colloids will inherit elevated Th/U ratios relative to source rocks while the dissolved load of waters will inherit lower Th/U ratios (Babechuk et al., 2020; Yu et al., 2019).

This study hypothesizes that variations in Th and U abundances will be predominantly controlled by source rock variations and weathering conditions but have potential for modifications through land-cover interactions that are present in the study sites. Specifically, slower moving steams and the onset of bogs will modify the mobility of Th-U through reactive surfaces (Lidman et al., 2012; Olivie-Lauquet et al., 2001) and/or complexation with organic matter (Viers et al., 1997).

1.5.4. Nickel-Chromium-Cobalt

The transition metals Ni, Co, and Cr have high compatibility in mafic minerals (spinel, olivine, clinopyroxene, orthopyroxene). Nickel^{2+} and Co^{2+} have a close ionic radii to Mg^{2+} and will partition mainly into olivine and pyroxenes, while Cr^{2+} and Cr^{3+} partition between spinel, olivine, and pyroxene (Barnes and Roeder, 2001; Carr and Turekian, 1961; Foley et al., 2013; Gülaçar and Delaloye, 1976). These properties result in peridotites having the highest abundance of these elements, followed by basalts (see Table 1). Serpentinization of ultramafic rocks, can transfer Ni, Co, and Cr into different low-T alteration phases, such as chrysotile and lizardite, but ultimately

serpentinization reactions do not result in extensive loss of these elements (Kierczak et al., 2021; Kodolányi et al., 2012). During initial chemical weathering, all three elements can be incorporated in or adsorbed to secondary clay minerals (e.g., Hao et al., 2022; Mitsis et al., 2018; Nahon et al., 1982; Putzolu et al., 2020), but advancement of chemical weathering can also lead to strong affinities for these elements to be adsorbed or incorporated into Fe- and Mn-(oxy)(hydr)oxides (e.g., Carvalho-E-Silva et al., 2003; Manceau et al., 2012; Wasylenki et al., 2015). The most advanced stages of chemical weathering can lead to extreme levels of Ni, Cr, and Co observed in laterite deposits (Golightly, 1981). However, Cr can have enhanced redox-induced mobilization after adsorption to Mn-(oxy)(hydr)oxide through oxidation of Cr^{3+} to Cr^{6+}, forming more soluble species of Cr (Fandeur et al., 2009; Liang et al., 2021). Cobalt can also be present in Co^{3+}, but this oxidation state is not common in surface systems (Pourret and Faucon, 2018).

Away from anthropogenic sources (e.g., Shtiza et al., 2005), high Ni abundances in rivers are documented in proximity to ultramafic-mafic source rocks (Binda et al., 2018; Vasileiou et al., 2021), despite the range of controls on Ni in weathering profiles (Cameron and Vance, 2014; Rinklebe and Shaheen, 2017; Sun et al., 2024). Nickel is also an essential nutrient, with observed uptake in biological systems (Price and Morel, 1991; Scheller et al., 2010). In fluvial systems, Ni is often transported as either a free ion (Ni^{2+}), $Ni(H_2O)_6^{2+}$, or complexed with OH^-, ($NiOH^+$), or CO_3^{2-} ($NiCO_3^0$) (Uren, 1992 and references therein) but can also be complexed with dissolved organic matter (Antić-Mladenović et al., 2017; Pokrovsky et al., 2006; Sekaly et al., 2003).

The weathering release of Co to the hydrosphere follows a similar pathway as Ni, primarily being transported as Co^{2+} species, although there are more uncertainties in the details of its speciation and complexation during transport (Collins and Kinsela, 2010; Pourret and Faucon, 2018). Similar

to Ni, Co also has capacity for biological uptake due to its biological utility (Collins and Kinsela, 2010). In boreal streams, Co is observed to be complexed to organic matter (Pokrovsky et al., 2006), have an association to colloids, and have higher abundances in streams draining forested areas (Lidman et al., 2012), reflecting complex interaction of source mineral weathering and variable adsorption on particulates in soils and in rivers.

The weathering and aqueous behavior of Cr has received the most attention of the three metals, despite their co-enrichment in ultramafic (and mafic) rocks (Kierczak et al., 2021) due to its much greater toxicity when in the form of Cr^{6+} (Shanker et al., 2005). Chromium hosted in silicate minerals can be released preferentially to the Cr hosted in chromite (Garnier et al., 2008; Oze, 2004) and silicate minerals are typically the most abundant in high-Cr source rocks. Upon release during weathering, Cr^{3+} is rapidly adsorbed or taken into secondary minerals. However, in the presence of Mn-(oxy)(hydr)oxides Cr^{3+} can be oxidized to Cr^{6+}, typically present as CrO_4^{2-} or $HCrO_4^-$ depending on pH, and thus more mobile in oxidized systems (Fendorf, 1995; Rai et al., 1989). However, Cr^{6+} but can be scavenged and/or back-reduced to Cr^{3+} if it encounters reductants or reactive surfaces (Richard and Bourg, 1991). Nonetheless, these conditions can result in high dissolved Cr concentrations in surface water when ultramafic rocks are exposed to high degrees of chemical weathering (Chrysochoou et al., 2016; Fantoni et al., 2002). McClain and Maher (2016) found important associations of Cr with ultramafic rock sources and noted that in some alkaline waters of ultramafic catchments, Cr can also be soluble as Cr^{3+} species ($CrOH(CO_3)^{2-}$ or $Cr(OH)_3$). Different inorganic or organic ligands can also aid in Cr^{3+} transport (Babechuk et al., 2018; Saad et al., 2017).

In this study, the abundances of Ni, Co, and Cr are only expected to be at appreciable levels in stream waters draining the ultramafic-mafic rocks in western Newfoundland. However, despite their high abundance in source rocks, release of these elements may be inhibited by the limited water interaction time with rocks and poorly developed or absent soil in several areas. Several groundwater seeps have been documented near the surface water sampling areas that have high pH developed during active continental serpentinization (Morrill et al., 2014; Szponar et al., 2013) and could locally promote Cr^{3+} mobility.

1.5.5. Rare Earth Elements

The rare earth element + yttrium (REE+Y) group are useful tracers in magmatic and environmental systems due to their identical 3+ charge (excluding Eu and Ce which have multiple redox states) and systematically decreasing ionic radii from La to Lu (McLennan and Taylor, 2012 and reference therein). Yttrium is often grouped with the REE due to its 3+ charge and near-identical ionic radii to Ho. The Y-Ho pair can also serve as a useful tracer due to their fractionation in fluid-rich magmatic systems or in low-T aqueous systems (Bau, 1996; Bau and Dulski, 1995). All of the REE+Y are incompatible, with increasing relative incompatibility of La through to Lu, during magmatic differentiation that results in felsic rocks having higher abundances and different patterns than ultramafic-mafic rocks. The REE+Y are often concentrated in accessory phases such as allanite, monazite, or apatite (Giere and Sorensen, 2004; O'Sullivan et al., 2020).

During most chemical weathering conditions, the REE are only sparingly soluble and fine-grained sediment and eroded heavy minerals are the main sedimentary reservoirs of the REE (see McLennan, 1989). However, the dissolved and colloid-bound REE fraction released into the hydrosphere during weathering is an important environmental tracer, despite the much lower

natural REE abundance in waters, as the changes in their pattern can reflect source rock differences, preferential mineral dissolution, and redox reactions in soils and waters. The REE+Y data are typically normalized to a reservoir composition, and for surface systems the normalizer typically represents an estimate of the average upper continental crust; in this study the MUQ (MUd from Queensland) composite, an alluvial sediment average from rivers in Queensland, Australia (Kamber et al., 2005) is used for normalization.

The REE+Y can be fractionated during weathering of different rock types (Babechuk et al., 2014; Nesbitt et al., 1980; Roy et al., 2024) and released or accumulated in specific weathering horizons where conditions are ideal for scavenging (Bao and Zhao, 2008). The fractionation of Ce from other light REE (LREE) and the fractionation of Y from Ho are some of the most useful inter-element fractionation patterns that occur during chemical weathering. Separation of Ce from the other LREE arises mainly due to the oxidation of Ce^{3+} to Ce^{4+} by (oxy)(hydr)oxide minerals, primarily Mn-(oxy)(hydr)oxides (Koppi et al., 1996; Laveuf et al., 2008 and references therein). This allows for the tracing of oxidative weathering in modern (e.g., Middelburg et al., 1988; Patino et al., 2003) and ancient (e.g., Pan and Stauffer, 2000; Panahi et al., 2000) surface environments. The fractionation of Y from Ho has also been documented in weathering environments and has been attributed to preferential adsorption of Ho>Y on secondary mineral surfaces (Babechuk et al., 2015; Thompson et al., 2013).

The REE+Y in the oceans, which record the most prominent inter-element REE+Y fractionation (Alibo and Nozaki, 1999; Nozaki et al., 1997), are sourced primarily from continental weathering and riverine delivery (Goldstein and Jacobsen, 1988). Prior to REE+Y delivery to the oceans, patterns in rivers can also reflect different fluvial processes such as the balance between organic

and inorganic complexation and between colloids and dissolved species (e.g., Davranche et al., 2004; Leybourne and Johannesson, 2008; Tang and Johannesson, 2003; Xu and Han, 2009) and source rock variations (e.g., Babechuk et al., 2020). Stream waters have also been shown to inherit an elevated Y>Ho compared to source rocks due to the aforementioned weathering effects, and selective variations in other elements such as Eu that may reflect differences in plagioclase abundance in source rocks.

In this study, the REE+Y dissolved in stream waters are hypothesized to most prominently reflect the difference in REE+Y abundance and normalized patterns between ultramafic-mafic and felsic rocks, while also potentially revealing different dynamics of the catchment through the fractionation of Y-Ho and Ce-LREE being inherited in waters.

1.6. Advantage of using geospatial data to study small-scale catchments

The drainage areas covered by the world's major rivers often include heterogenous land-type, topography, and lithology and therefore interpreting the controlling factors that govern dissolved load chemical signatures can be challenging. Despite small watersheds being more amenable to local fluctuations in chemistry alongside base flow changes, seasonality, and local environmental factors, they can more closely reflect local lithology and offer opportunities to better constrain environmental and temporal factors that control stream composition. As such, effort has been directed in many studies towards characterizing headwater streams. Headwater streams are classified as low-order streams that deliver source water down a river network and in some cases make up 70-80% of total channel length (Downing et al., 2012; Wohl, 2017). Headwaters have been documented to exert strong influence on the overall biogeochemical

composition downstream, despite the considerable variability in their stream chemistry (Wolock et al., 1997), even within areas with relatively uniform landscapes (Asano et al., 2009).

Given the complex interactions between lithology, topography, and land-type that influence water composition, there is utility in quantifying and characterizing these attributes alongside chemical composition measurements when investigating small-stream dynamics. Geographic information systems (GIS) allow for such spatial analysis of landscape characteristics within a watershed and has been commonly utilized for management purposes (Gracz and Glaser, 2017; Strager et al., 2010) or employed in conjunction with investigating the controlling factors of stream networks (Andersson and Nyberg, 2009; Liu et al., 2015; Walker et al., 2012). While GIS can be powerful in modeling and simulating hydrologic processes, this study focuses on characterizing watershed attributes that include topography, surficial geology, vegetation, and bedrock coverage.

The topography of landscape can influence hydrology, chemical weathering intensity, and erosion, dictating the direction and speed of water flow, which, in turn, influences the flow path and contact time water has with the subsurface and soils (McGuire et al., 2005; Wolock et al., 1997). Topography also plays crucial roles in soil distribution, which can lead to the mobilization and transfer of solutes, colloids, and particles. This has mostly been studied in the context of hillslopes (Chadwick and Asner, 2016; Khomo et al., 2013, 2011), where studies have shown that slope gradients promote chemical and physical weathering gradients. For example, areas upslope will incur higher rates of erosion that consistently expose fresh material (Chadwick and Asner, 2016). A chemical weathering gradient can also occur within the slope itself, where a hillslope has an upper eroding section, where rates of weathering are influenced by mineral supply, and transitions into a depositional area downslope where weathering rate is constrained by equilibrium between

water in the soil and present minerals (Yoo et al., 2009). Such processes have been shown to occur for gradients as small as 100 m (Vitousek et al., 2003). However, slope gradient, soil thickness, and presence of different land-coverage can all contribute to differences in physical and chemical processes.

One of the most important land-coverage changes is the presence of vegetation, which plays a role in regulating water availability, influencing mineral weathering processes and element complexation, and forming an important sink for bioavailable elements like K (Evans, 1964). Vegetation enhances release of elements by supplying organic acids that accelerate mineral weathering reactions and complex with elements (Drever, 1994; Griffiths et al., 1994; Riotte et al., 2014), and through decaying plant litter (Velbel and Price, 2007). For example, in Iceland, areas with dense vegetation exhibit enhanced release of Ca and Mg in streams compared to more barren ones (Moulton and Berner, 1998). The facilitation of element release can be dependent on vegetation-type, with a pronounced difference between coniferous verses deciduous trees. For example, coniferous trees, despite releasing leaves year-round where its decomposition can provide a more continuous element flux to the ecosystem (Thomas and Grigal, 1976), release nutrients more slowly than deciduous litter (Likens et al., 2013; Monk, 1966). Accordingly, deciduous vegetation type can often be a larger source of element release. Empirical evidence has supported this type-dependent variation on element release, such that in temperate regions, areas dominated by deciduous vegetation experienced higher fluxes of Mg, Ca, and K compared to those dominated by coniferous forests (Likens et al., 2013).

Vegetation can also decrease element fluxes through limiting the interaction of water with rocks and soils (Zhang et al., 2002), inhibiting chemical weathering that can limit export of elements to

streams. Wetlands, which are distinct ecosystems with plants saturated by water, also play important roles in element flux. These ecosystems are characterized by low-oxygenation water columns and abundant natural organic matter (Roux and Shotyk, 2006), which often leads to them serving as an important element sink (Cole, 1998; Lytle et al., 1998). However, seasonality, precipitation patterns, and biological activity can create dynamic cycles of oxidizing or more reducing periods that affect trace element release (McLatchey and Reddy, 1998; Olivie-Lauquet et al., 2001). Specifically, more reducing conditions can promote the dissolution of (oxy)(hydr)oxides and oxidizing conditions can more easily promote the decomposition of organic matter, both conditions that can release elements stored in these reservoirs (Trolard et al., 1995). Peatlands, a type of wetland, can export large amounts of dissolved organic matter to surface water (Aitkenhead et al., 1999; Dillon and Molot, 1997; Laudon et al., 2004; Worrall et al., 2002) and, despite filtering out many elements (Freeman et al., 1997; Palmer et al., 2015), the exported organic matter can also complex with major and trace elements and thus aid in their release (Broder and Biester, 2017).

For this project, the study sites are characterized by contrasting landscapes. The western Newfoundland site has steep hillslopes, coniferous vegetation when it is present, and large areas of exposed bedrock. In contrast, the Burin Peninsula site has gentler terrain and a persistent area of peatlands. Such sites offer contrasting conditions that will ultimately shape the transport of dissolved elements and help inform dynamics across variable landscapes. Specifically, the interrelated topography-vegetation-stream flow conditions of the Burin Peninsula study site is hypothesized to play a more prominent role in modifying stream chemistry than in the western Newfoundland site.

1.7. References

Agilent Technologies, (n.d.). Handbook of ICP-QQQ Applications using the Agilent 8800 and 8900.

Ahrens, L.H., Pinson, W.H., Kearns, M.M., 1952. Association of rubidium and potassium and their abundance in common igneous rocks and meteorites. Geochimica et Cosmochimica Acta 2, 229–242. https://doi.org/10.1016/0016-7037(52)90017-3

Aitkenhead, J.A., Hope, D., Billett, M.F., 1999. The relationship between dissolved organic carbon in stream water and soil organic carbon pools at different spatial scales. Hydrological Processes 13, 1289–1302. https://doi.org/10.1002/(SICI)1099-1085(19990615)13:8<1289::AID-HYP766>3.0.CO;2-M

Alibo, D.S., Nozaki, Y., 1999. Rare earth elements in seawater: particle association, shale-normalization, and Ce oxidation. Geochimica et Cosmochimica Acta 63, 363–372. https://doi.org/10.1016/S0016-7037(98)00279-8

Andersen, M.B., Erel, Y., Bourdon, B., 2009. Experimental evidence for 234U–238U fractionation during granite weathering with implications for 234U/238U in natural waters. Geochimica et Cosmochimica Acta 73, 4124–4141. https://doi.org/10.1016/j.gca.2009.04.020

Anderson, M.A., Bertsch, P.M., Miller, W.P., 1989. Exchange and apparent fixation of lithium in selected soils and clay minerals. Soil Science 148, 46.

Andersson, J.-O., Nyberg, L., 2009. Using official map data on topography, wetlands and vegetation cover for prediction of stream water chemistry in boreal headwater catchments. Hydrol. Earth Syst. Sci. 13, 537–549. https://doi.org/10.5194/hess-13-537-2009

Antić-Mladenović, S., Frohne, T., Kresović, M., Stärk, H.-J., Tomić, Z., Ličina, V., Rinklebe, J., 2017. Biogeochemistry of Ni and Pb in a periodically flooded arable soil: Fractionation and redox-induced (im)mobilization. Journal of Environmental Management, Biogeochemistry of trace elements in the environment 186, 141–150. https://doi.org/10.1016/j.jenvman.2016.06.005

Arevalo, R., McDonough, W.F., 2010. Chemical variations and regional diversity observed in MORB. Chemical Geology 271, 70–85. https://doi.org/10.1016/j.chemgeo.2009.12.013

Asano, Y., Uchida, T., Mimasu, Y., Ohte, N., 2009. Spatial patterns of stream solute concentrations in a steep mountainous catchment with a homogeneous landscape. Water Resources Research 45. https://doi.org/10.1029/2008WR007466

Astrom, M., Peltola, P., Rönnback, P., Lavergren, U., Bergbäck, B., Tarvainen, T., Backman, B., 2009. Uranium in surface and groundwaters in Boreal Europe. Geochemistry Exploration Environment Analysis 9, 51–62. https://doi.org/10.1144/1467-7873/08-185

Aubert, D., Stille, P., Probst, A., 2001. REE fractionation during granite weathering and removal by waters and suspended loads: Sr and Nd isotopic evidence. Geochimica et Cosmochimica Acta 65, 387–406. https://doi.org/10.1016/S0016-7037(00)00546-9

Babechuk, M.G., Kleinhanns, I.C., Reitter, E., Schoenberg, R., 2018. Kinetic stable Cr isotopic fractionation between aqueous Cr(III)-Cl-H2O complexes at 25 °C: Implications for Cr(III) mobility and isotopic variations in modern and ancient natural systems. Geochimica et Cosmochimica Acta 222, 383–405. https://doi.org/10.1016/j.gca.2017.10.002

Babechuk, M.G., O'Sullivan, E.M., McKenna, C.A., Rosca, C., Nägler, T.F., Schoenberg, R., Kamber, B.S., 2020. Ultra-trace Element Characterization of the Central Ottawa River Basin using a Rapid, Flexible, and Low-volume ICP-MS Method. Aquat Geochem 26, 327–374. https://doi.org/10.1007/s10498-020-09376-w

Babechuk, M.G., Widdowson, M., Kamber, B.S., 2014. Quantifying chemical weathering intensity and trace element release from two contrasting basalt profiles, Deccan Traps, India. Chemical Geology 363, 56–75. https://doi.org/10.1016/j.chemgeo.2013.10.027

Babechuk, M.G., Widdowson, M., Murphy, M., Kamber, B.S., 2015. A combined Y/Ho, high field strength element (HFSE) and Nd isotope perspective on basalt weathering, Deccan Traps, India. Chemical Geology 396, 25–41. https://doi.org/10.1016/j.chemgeo.2014.12.017

Banfield, J.F., Eggleton, R.A., 1990. Analytical Transmission Electron Microscope Studies of Plagioclase, Muscovite, and K-Feldspar Weathering. Clays Clay Miner. 38, 77–89. https://doi.org/10.1346/CCMN.1990.0380111

Bao, Z., Zhao, Z., 2008. Geochemistry of mineralization with exchangeable REY in the weathering crusts of granitic rocks in South China. Ore Geology Reviews 33, 519–535. https://doi.org/10.1016/j.oregeorev.2007.03.005

Barnes, S., Roeder, P., 2001. The Range of Spinel Compositions in Terrestrial Mafic and Ultramafic Rocks. Journal of Petrology - J PETROL 42, 2279–2302. https://doi.org/10.1093/petrology/42.12.2279

Barnett, M., Jardine, P., Brooks, S., Selim, H., 2000. Adsorption and Transport of Uranium(VI) in Subsurface Media. Soil Science Society of America Journal - SSSAJ 64. https://doi.org/10.2136/sssaj2000.643908x

Barrat, J.-A., Bayon, G., 2024. Practical guidelines for representing and interpreting rare earth abundances in environmental and biological studies. Chemosphere 352, 141487. https://doi.org/10.1016/j.chemosphere.2024.141487

Batley, G.E., Gardner, D., 1977. Sampling and storage of natural waters for trace metal analysis. Water Research 11, 745–756. https://doi.org/10.1016/0043-1354(77)90042-2

Bau, M., 1996. Controls on the fractionation of isovalent trace elements in magmatic and aqueous systems: evidence from Y/Ho, Zr/Hf, and lanthanide tetrad effect. Contributions to Mineralogy and Petrology 123, 323–333. https://doi.org/10.1007/s004100050159

Bau, M., Dulski, P., 1995. Comparative study of yttrium and rare-earth element behaviours in fluorine-rich hydrothermal fluids. Contr. Mineral. and Petrol. 119, 213–223. https://doi.org/10.1007/BF00307282

Bea, F., 1996. Residence of REE, Y, Th and U in Granites and Crustal Protoliths; Implications for the Chemistry of Crustal Melts. Journal of Petrology 37, 521–552. https://doi.org/10.1093/petrology/37.3.521

Berner, R.A., 2004. The Phanerozoic Carbon Cycle: CO2 and O2. Oxford University Press, USA.

Berner, R.A., Berner, E.K., 1997. Silicate Weathering and Climate, in: Tectonic Uplift and Climate Change. Springer, Boston, MA, pp. 353–365. https://doi.org/10.1007/978-1-4615-5935-1_15

Binda, G., Pozzi, A., Livio, F., Piasini, P., Zhang, C., 2018. Anomalously high concentration of Ni as sulphide phase in sediment and in water of a mountain catchment with serpentinite bedrock. Journal of Geochemical Exploration 190, 58–68. https://doi.org/10.1016/j.gexplo.2018.02.014

Bradley, D., Shea, E., Buchwaldt, R., Bowring, S., Benowitz, J., O'Sullivan, P., McCauley, A., 2016. Geochronology and Tectonic Context of Lithium-cesium-tantalum Pegmatites in the Appalachians. The Canadian Mineralogist 54, 945–969. https://doi.org/10.3749/canmin.1600035

Braun, J.-J., Riotte, J., Battacharya, S., Violette, A., Oliva, P., Prunier, J., Maréchal, J.-C., Ruiz, L., Audry, S., Subramanian, S., 2018. REY-Th-U Dynamics in the Critical Zone: Combined Influence of Reactive Bedrock Accessory Minerals, Authigenic Phases and Hydrological Sorting (Mule Hole Watershed, South India). Geochemistry, Geophysics, Geosystems 19. https://doi.org/10.1029/2018GC007453

Broder, T., Biester, H., 2017. Linking major and trace element concentrations in a headwater stream to DOC release and hydrologic conditions in a bog and peaty riparian zone. Applied Geochemistry 87, 188–201. https://doi.org/10.1016/j.apgeochem.2017.11.003

Brugge, D., Buchner, V., 2011. Health effects of uranium: new research findings 26, 231–249. https://doi.org/10.1515/REVEH.2011.032

Buriánek, D., Ivanov, M., Janderková, J., Patzel, M., 2022. Importance of accessory minerals for the vertical distribution of uranium and thorium in soil profiles: A case study of durbachite from the Třebíč Pluton (Czech Republic). CATENA 213, 106166. https://doi.org/10.1016/j.catena.2022.106166

Cameron, E.M., Hall, G.E.M., Veizer, J., Krouse, H.R., 1995. Isotopic and elemental hydrogeochemistry of a major river system: Fraser River, British Columbia, Canada. Chemical Geology 122, 149–169. https://doi.org/10.1016/0009-2541(95)00007-9

Cameron, V., Vance, D., 2014. Heavy nickel isotope compositions in rivers and the oceans. Geochimica et Cosmochimica Acta 128, 195–211. https://doi.org/10.1016/j.gca.2013.12.007

Campbell, K.M., Gallegos, T.J., Landa, E.R., 2015. Biogeochemical aspects of uranium mineralization, mining, milling, and remediation. Applied Geochemistry, Environmental Geochemistry of Modern Mining 57, 206–235. https://doi.org/10.1016/j.apgeochem.2014.07.022

Carr, M.H., Turekian, K.K., 1961. The geochemistry of cobalt. Geochimica et Cosmochimica Acta 23, 9–60. https://doi.org/10.1016/0016-7037(61)90087-4

Carvalho-E-Silva, M.L., Ramos, A.Y., Tolentino, H.C.N., Enzweiler, J., Netto, S.M., Alves, M.D.C.M., 2003. Incorporation of Ni into natural goethite: An investigation by X-ray absorption spectroscopy. American Mineralogist 88, 876–882. https://doi.org/10.2138/am-2003-5-617

Chabaux, F., Riotte, J., Clauer, N., France-Lanord, C., 2001. Isotopic tracing of the dissolved U fluxes of Himalayan rivers: implications for present and past U budgets of the Ganges-Brahmaputra system. Geochimica et Cosmochimica Acta 65, 3201–3217. https://doi.org/10.1016/S0016-7037(01)00669-X

Chabaux, F., Riotte, J., Dequincey, O., 2003. U-Th-Ra Fractionation During Weathering and River Transport. Reviews in Mineralogy and Geochemistry 52, 533–576. https://doi.org/10.2113/0520533

Chadwick, K.D., Asner, G.P., 2016. Tropical soil nutrient distributions determined by biotic and hillslope processes. Biogeochemistry 127, 273–289. https://doi.org/10.1007/s10533-015-0179-z

Chakraborty, M., Mukherjee, A., Ahmed, K.M., 2015. A Review of Groundwater Arsenic in the Bengal Basin, Bangladesh and India: from Source to Sink. Curr Pollution Rep 1, 220–247. https://doi.org/10.1007/s40726-015-0022-0

Chappell, B.W., White, A.J.R., 2001. Two contrasting granite types: 25 years later. Australian Journal of Earth Sciences 48.

Chaudhuri, S., Clauer, N., Semhi, K., 2007. Plant decay as a major control of river dissolved potassium: A first estimate. Chemical Geology 243, 178–190. https://doi.org/10.1016/j.chemgeo.2007.05.023

Chen, J.H., Lawrence Edwards, R., Wasserburg, G.J., 1986. 238U,234U and232Th in seawater. Earth and Planetary Science Letters 80, 241–251. https://doi.org/10.1016/0012-821X(86)90108-1

Choudhury, B.J., Ahmed, N.U., Idso, S.B., Reginato, R.J., Daughtry, C.S.T., 1994. Relations between evaporation coefficients and vegetation indices studied by model simulations. Remote Sensing of Environment 50, 1–17. https://doi.org/10.1016/0034-4257(94)90090-6

Chrysochoou, M., Theologou, E., Bompoti, N., Dermatas, D., Panagiotakis, I., 2016. Occurrence, Origin and Transformation Processes of Geogenic Chromium in Soils and Sediments. Curr Pollution Rep 2, 224–235. https://doi.org/10.1007/s40726-016-0044-2

Chupakov, A.V., Pokrovsky, O.S., Moreva, O.Y., Shirokova, L.S., Neverova, N.V., Chupakova, A.A., Kotova, E.I., Vorobyeva, T.Y., 2020. High resolution multi-annual riverine fluxes of organic carbon, nutrient and trace element from the largest European Arctic river, Severnaya Dvina. Chemical Geology 538, 119491. https://doi.org/10.1016/j.chemgeo.2020.119491

Cole, S., 1998. The Emergence of Treatment Wetlands. Environ. Sci. Technol. 32, 218A-223A. https://doi.org/10.1021/es9834733

Collins, R.N., Kinsela, A.S., 2010. The aqueous phase speciation and chemistry of cobalt in terrestrial environments. Chemosphere 79, 763–771. https://doi.org/10.1016/j.chemosphere.2010.03.003

Colombo, M., Brown, K.A., De Vera, J., Bergquist, B.A., Orians, K.J., 2019. Trace metal geochemistry of remote rivers in the Canadian Arctic Archipelago. Chemical Geology 525, 479–491. https://doi.org/10.1016/j.chemgeo.2019.08.006

Comans, R.N.J., Middelburg, J.J., Zonderhuis, J., Woittiez, J.R.W., Lange, G.J.D., Das, H.A., Weijden, C.H.V.D., 1989. Mobilization of radiocaesium in pore water of lake sediments. Nature 339, 367–369. https://doi.org/10.1038/339367a0

Cumberland, S.A., Douglas, G., Grice, K., Moreau, J.W., 2016. Uranium mobility in organic matter-rich sediments: A review of geological and geochemical processes. Earth-Science Reviews 159, 160–185. https://doi.org/10.1016/j.earscirev.2016.05.010

Cuss, C.W., Donner, M.W., Grant-Weaver, I., Noernberg, T., Pelletier, R., Sinnatamby, R.N., Shotyk, W., 2018. Measuring the distribution of trace elements amongst dissolved colloidal species as a fingerprint for the contribution of tributaries to large boreal rivers. Science of The Total Environment 642, 1242–1251. https://doi.org/10.1016/j.scitotenv.2018.06.099

D. Brugge, J. L. deLemos, B. Oldmixon, 2005. Exposure Pathways and Health Effects Associated with Chemical and Radiological Toxicity of Natural Uranium: A Review. Reviews on Environmental Health 20, 177–194. https://doi.org/10.1515/REVEH.2005.20.3.177

Dang, D.H., Ma, L., Ha, Q.K., Wang, W., 2022. A multi-tracer approach to disentangle anthropogenic emissions from natural processes in the St. Lawrence River and Estuary. Water Research 219, 118588. https://doi.org/10.1016/j.watres.2022.118588

Davranche, M., Pourret, O., Gruau, G., Dia, A., 2004. Impact of humate complexation on the adsorption of REE onto Fe oxyhydroxide. Journal of Colloid and Interface Science 277, 271–279. https://doi.org/10.1016/j.jcis.2004.04.007

de Koning, A., Comans, R.N.J., 2004. Reversibility of radiocaesium sorption on illite2. Geochimica et Cosmochimica Acta 68, 2815–2823. https://doi.org/10.1016/j.gca.2003.12.025

Degueldre, C., Kline, A., 2007. Study of thorium association and surface precipitation on colloids. Earth and Planetary Science Letters 264, 104–113. https://doi.org/10.1016/j.epsl.2007.09.012

Dekov, V.M., Araújo, F., Van Grieken, R., Subramanian, V., 1998. Chemical composition of sediments and suspended matter from the Cauvery and Brahmaputra rivers (India). Science of The Total Environment 212, 89–105. https://doi.org/10.1016/S0048-9697(97)00132-0

Dellinger, M., Gaillardet, J., Bouchez, J., Calmels, D., Louvat, P., Dosseto, A., Gorge, C., Alanoca, L., Maurice, L., 2015. Riverine Li isotope fractionation in the Amazon River basin controlled by the weathering regimes. Geochimica et Cosmochimica Acta 164, 71–93. https://doi.org/10.1016/j.gca.2015.04.042

Dessert, C., Dupré, B., Gaillardet, J., François, L.M., Allègre, C.J., 2003. Basalt weathering laws and the impact of basalt weathering on the global carbon cycle. Chemical Geology, Controls on Chemical Weathering 202, 257–273. https://doi.org/10.1016/j.chemgeo.2002.10.001

Dillon, P.J., Molot, L.A., 1997. Effect of landscape form on export of dissolved organic carbon, iron, and phosphorus from forested stream catchments. Water Resources Research 33, 2591–2600. https://doi.org/10.1029/97WR01921

Downing, J.A., Cole, J.J., Duarte, C.M., Middelburg, J.J., Melack, J.M., Prairie, Y.T., Kortelainen, P., Striegl, R.G., McDowell, W.H., Tranvik, L.J., 2012. Global abundance and size distribution of streams and rivers. Inland Waters 2, 229–236. https://doi.org/10.5268/IW-2.4.502

Drever, J.I., 1994. The effect of land plants on weathering rates of silicate minerals. Geochimica et Cosmochimica Acta 58, 2325–2332. https://doi.org/10.1016/0016-7037(94)90013-2

Eggleton, R.A., Foudoulis, C., Varkevisser, D., 1987. Weathering of Basalt: Changes in Rock Chemistry and Mineralogy. Clays and clay miner. 35, 161–169. https://doi.org/10.1346/CCMN.1987.0350301

Elderfield, H., Upstill-Goddard, R., Sholkovitz, E.R., 1990. The rare earth elements in rivers, estuaries, and coastal seas and their significance to the composition of ocean waters. Geochimica et Cosmochimica Acta 54, 971–991. https://doi.org/10.1016/0016-7037(90)90432-K

Evans, W.D., 1964. The organic solubilization of minerals in sediments, in: Advances in Organic Geochemistry. edited by Umberto Colombo, G. D. Hobson, pp. 263–270.

Fandeur, D., Juillot, F., Morin, G., Olivi, L., Cognigni, A., Webb, S.M., Ambrosi, J.-P., Fritsch, E., Guyot, F., Brown, Jr., Gordon E., 2009. XANES Evidence for Oxidation of Cr(III) to Cr(VI) by Mn-Oxides in a Lateritic Regolith Developed on Serpentinized Ultramafic Rocks of New Caledonia. Environ. Sci. Technol. 43, 7384–7390. https://doi.org/10.1021/es900498r

Fantoni, D., Brozzo, G., Canepa, M., Cipolli, F., Marini, L., Ottonello, G., Zuccolini, M., 2002. Natural hexavalent chromium in groundwaters interacting with ophiolitic rocks. Env Geol 42, 871–882. https://doi.org/10.1007/s00254-002-0605-0

Fendorf, S.E., 1995. Surface reactions of chromium in soils and waters. Geoderma 67, 55–71. https://doi.org/10.1016/0016-7061(94)00062-F

Fisher, A., Kara, D., 2016. Determination of rare earth elements in natural water samples – A review of sample separation, preconcentration and direct methodologies. Analytica Chimica Acta 935, 1–29. https://doi.org/10.1016/j.aca.2016.05.052

Foley, S.F., Prelevic, D., Rehfeldt, T., Jacob, D.E., 2013. Minor and trace elements in olivines as probes into early igneous and mantle melting processes. Earth and Planetary Science Letters 363, 181–191. https://doi.org/10.1016/j.epsl.2012.11.025

Freeman, C., Lock, M.A., Hughes, S., Reynolds, B., Hudson, J.A., 1997. Nitrous Oxide Emissions and the Use of Wetlands for Water Quality Amelioration. Environ. Sci. Technol. 31, 2438–2440. https://doi.org/10.1021/es9604673

French, D.W., Schindler, D.E., Brennan, S.R., Whited, D., 2020. Headwater Catchments Govern Biogeochemistry in America's Largest Free-Flowing River Network. Journal of Geophysical Research: Biogeosciences 125, e2020JG005851. https://doi.org/10.1029/2020JG005851

Fuller, A.J., Shaw, S., Ward, M.B., Haigh, S.J., Mosselmans, J.F.W., Peacock, C.L., Stackhouse, S., Dent, A.J., Trivedi, D., Burke, I.T., 2015. Caesium incorporation and retention in illite interlayers. Applied Clay Science 108, 128–134. https://doi.org/10.1016/j.clay.2015.02.008

Gaillardet, J., Dupré, B., Louvat, P., Allègre, C.J., 1999. Global silicate weathering and CO2 consumption rates deduced from the chemistry of large rivers. Chemical Geology 159, 3–30. https://doi.org/10.1016/S0009-2541(99)00031-5

Gaillardet, J., Viers, J., Dupré, B., 2014. Trace Elements in River Waters, Treatise on Geochemistry. https://doi.org/10.1016/B0-08-043751-6/05165-3

García, M.G., Lecomte, K.L., Pasquini, A.I., Formica, S.M., Depetris, P.J., 2007. Sources of dissolved REE in mountainous streams draining granitic rocks, Sierras Pampeanas (Córdoba, Argentina). Geochimica et Cosmochimica Acta 71, 5355–5368. https://doi.org/10.1016/j.gca.2007.09.017

Garçon, M., Sauzéat, L., Carlson, R., Shirey, S., Simon, M., Balter, V., Boyet, M., 2016. Nitrile, Latex, Neoprene and Vinyl Gloves: A Primary Source of Contamination for Trace Element and Zn Isotopic Analyses in Geological and Biological Samples. Geostandards and Geoanalytical Research 41. https://doi.org/10.1111/ggr.12161

Gardner, C.B., Wichterich, C., Calero, A.E., Welch, S.A., Widom, E., Smith, D.F., Carey, A.E., Lyons, W.B., 2023. Carbonate weathering, phosphate fertilizer, and hydrologic controls on dissolved uranium in rivers in the US Corn Belt: Disentangling seasonal geogenic- and fertilizer-derived sources. Science of The Total Environment 861, 160455. https://doi.org/10.1016/j.scitotenv.2022.160455

Garnier, J., Quantin, C., Guimarães, E., Becquer, T., 2008. Can chromite weathering be a source of Cr in soils? Mineralogical Magazine 72, 49–53. https://doi.org/10.1180/minmag.2008.072.1.49

Giere, R., Sorensen, S.S., 2004. Allanite and Other REE-Rich Epidote-Group Minerals. Reviews in Mineralogy and Geochemistry 56, 431–493. https://doi.org/10.2138/gsrmg.56.1.431

Gíslason, S.D.S.R., Arnórsson, S., Ármannsson, H., 1996. Chemical weathering of basalt in Southwest Iceland: Effects of runoff, age of rocks and vegetative/glacial cover. American Journal of Science 296, 837–907. https://doi.org/10.2475/ajs.296.8.837

Goldstein, S.J., Jacobsen, S.B., 1988. Rare earth elements in river waters. Earth and Planetary Science Letters 89, 35–47. https://doi.org/10.1016/0012-821X(88)90031-3

Golightly, J.P., 1981. Nickeliferous Laterite Deposits. Econ. Geology 75th Anniversary Volume 710–734.

Gou, L.-F., Jin, Z., Galy, A., Gong, Y.-Z., Nan, X.-Y., Jin, C., Wang, X.-D., Bouchez, J., Cai, H.-M., Chen, J.-B., Yu, H.-M., Huang, F., 2020. Seasonal riverine barium isotopic variation in the middle Yellow River: Sources and fractionation. Earth and Planetary Science Letters 531, 115990. https://doi.org/10.1016/j.epsl.2019.115990

Gracz, M., Glaser, P.H., 2017. Evaluation of a wetland classification system devised for management in a region with a high cover of peatlands: an example from the Cook Inlet Basin, Alaska. Wetlands Ecol Manage 25, 87–104. https://doi.org/10.1007/s11273-016-9504-0

Griffiths, R.P., Baham, J.E., Caldwell, B.A., 1994. Soil solution chemistry of ectomycorrhizal mats in forest soil. Soil Biology and Biochemistry 26, 331–337. https://doi.org/10.1016/0038-0717(94)90282-8

Gülaçar, O.F., Delaloye, M., 1976. Geochemistry of nickel, cobalt and copper in alpine-type ultramafic rocks. Chemical Geology 17, 269–280. https://doi.org/10.1016/0009-2541(76)90041-3

Hao, Y., Ma, H., Wang, Q., Zhu, C., He, A., 2022. Complexation behaviour and removal of organic-Cr(III) complexes from the environment: A review. Ecotoxicology and Environmental Safety 240, 113676. https://doi.org/10.1016/j.ecoenv.2022.113676

Health Canada, 2019. Guidelines for Canadian Drinking Water Quality—Summary Table.

Heier, K.S., 1962. Trace elements in feldspars, a review. Nor. Geol. Tidski 42, 415–455.

Herath, I., Vithanage, M., Bundschuh, J., Maity, J.P., Bhattacharya, P., 2016. Natural Arsenic in Global Groundwaters: Distribution and Geochemical Triggers for Mobilization. Curr Pollution Rep 2, 68–89. https://doi.org/10.1007/s40726-016-0028-2

Hinkley, T., 1976. Pathways and mass balance of natural cesium compared with some related metals in a rock-soil-water system, sierra nevada, california. Environmental Chemistry and Cycling Process.

Hoang, Q.D., Kunihiro, T., Sakaguchi, C., Yamanaka, M., Kitagawa, H., Nakamura, E., 2019. Determination of Abundances of Fifty-Two Elements in Natural Waters by ICP-MS with Freeze-Drying Pre-concentration. Geostandards and Geoanalytical Research 43, 147–161. https://doi.org/10.1111/ggr.12245

Hofmann, A.W., White, W.M., 1983. Ba, Rb and Cs in the Earth's Mantle. Zeitschrift für Naturforschung A 38, 256–266. https://doi.org/10.1515/zna-1983-0225

Horstman, E.L., 1957. The distribution of lithium, rubidium and caesium in igneous and sedimentary rocks. Geochimica et Cosmochimica Acta 12, 1–28. https://doi.org/10.1016/0016-7037(57)90014-5

Huh, Y., Chan, L.-H., Edmond, J.M., 2001. Lithium isotopes as a probe of weathering processes: Orinoco River. Earth and Planetary Science Letters 194, 189–199. https://doi.org/10.1016/S0012-821X(01)00523-4

Huh, Y., Chan, L.-H., Zhang, L., Edmond, J.M., 1998. Lithium and its isotopes in major world rivers: implications for weathering and the oceanic budget. Geochimica et Cosmochimica Acta 62, 2039–2051. https://doi.org/10.1016/S0016-7037(98)00126-4

Ingri, J., Widerlund, A., Land, M., Gustafsson, Ö., Andersson, P., Öhlander, B., 2000. Temporal variations in the fractionation of the rare earth elements in a boreal river; the role of colloidal particles. Chemical Geology 166, 23–45. https://doi.org/10.1016/S0009-2541(99)00178-3

Izbicki, J.A., Wright, M.T., Seymour, W.A., McCleskey, R.B., Fram, M.S., Belitz, K., Esser, B.K., 2015. Cr(VI) occurrence and geochemistry in water from public-supply wells in California. Applied Geochemistry 63, 203–217. https://doi.org/10.1016/j.apgeochem.2015.08.007

Jiang, H., Liu, W., Xu, Z., Zhou, X., Zheng, Z., Zhao, T., Zhou, L., Zhang, X., Xu, Y., Liu, T., 2018. Chemical weathering of small catchments on the Southeastern Tibetan Plateau I: Water sources, solute sources and weathering rates. Chemical Geology 500, 159–174. https://doi.org/10.1016/j.chemgeo.2018.09.030

Jung, H.B., Xu, H., Roden, E.E., 2019. Long-term sorption and desorption of uranium in saprolite subsoil with nanoporous goethite. Applied Geochemistry 102, 129–138. https://doi.org/10.1016/j.apgeochem.2019.01.017

Kamber, B.S., Greig, A., Collerson, K.D., 2005. A new estimate for the composition of weathered young upper continental crust from alluvial sediments, Queensland, Australia. Geochimica et Cosmochimica Acta 69, 1041–1058. https://doi.org/10.1016/j.gca.2004.08.020

Khomo, L., Bern, C.R., Hartshorn, A.S., Rogers, K.H., Chadwick, O.A., 2013. Chemical transfers along slowly eroding catenas developed on granitic cratons in southern Africa. Geoderma 202–203, 192–202. https://doi.org/10.1016/j.geoderma.2013.03.023

Khomo, L., Hartshorn, A.S., Rogers, K.H., Chadwick, O.A., 2011. Impact of rainfall and topography on the distribution of clays and major cations in granitic catenas of southern Africa. CATENA 87, 119–128. https://doi.org/10.1016/j.catena.2011.05.017

Kierczak, J., Pietranik, A., Pędziwiatr, A., 2021. Ultramafic geoecosystems as a natural source of Ni, Cr, and Co to the environment: A review. Science of The Total Environment 755, 142620. https://doi.org/10.1016/j.scitotenv.2020.142620

Kısakűrek, B., James, R.H., Harris, N.B.W., 2005. Li and δ7Li in Himalayan rivers: Proxies for silicate weathering? Earth and Planetary Science Letters 237, 387–401. https://doi.org/10.1016/j.epsl.2005.07.019

Kodolányi, J., Pettke, T., Spandler, C., Kamber, B., Gméling, K., 2012. Geochemistry of Ocean Floor and Fore-arc Serpentinites: Constraints on the Ultramafic Input to Subduction Zones. Journal of Petrology 53, 235–270. https://doi.org/10.1093/petrology/egr058

Konhauser, K.O., Fyfe, W.S., Kronberg, B.I., 1994. Multi-element chemistry of some Amazonian waters and soils. Chemical Geology 111, 155–175. https://doi.org/10.1016/0009-2541(94)90088-4

Koppi, A.J., Edis, R., Field, D.J., Geering, H.R., Klessa, D.A., Cockayne, D.J.H., 1996. Rare earth element trends and cerium-uranium-manganese associations in weathered rock from Koongarra, Northern Territory, Australia. Geochimica et Cosmochimica Acta 60, 1695–1707. https://doi.org/10.1016/0016-7037(96)00047-6

Kramer, K.J.M., 1994. What about quality assurance before the laboratory analysis? Marine Pollution Bulletin 29, 222–227. https://doi.org/10.1016/0025-326X(94)90413-8

Kronberg, B.I., Nesbitt, H.W., Fyfe, W.S., 1987. Mobilities of alkalis, alkaline earths and halogens during weathering. Chemical Geology, Proceedings of an International Seminar on Laterite 60, 41–49. https://doi.org/10.1016/0009-2541(87)90108-2

Ku, T.-L., Mathieu, G.G., Knauss, K.G., 1977. Uranium in open ocean: concentration and isotopic composition. Deep Sea Research 24, 1005–1017. https://doi.org/10.1016/0146-6291(77)90571-9

Kurtz, A.C., Derry, L.A., Chadwick, O.A., Alfano, M.J., 2000. Refractory element mobility in volcanic soils. Geology 28, 683–686. https://doi.org/10.1130/0091-7613(2000)28<683:REMIVS>2.0.CO;2

Langmuir, D., 1978. Uranium solution-mineral equilibria at low temperatures with applications to sedimentary ore deposits. Geochimica et Cosmochimica Acta 42, 547–569. https://doi.org/10.1016/0016-7037(78)90001-7

Langmuir, D., Herman, J.S., 1980. The mobility of thorium in natural waters at low temperatures. Geochimica et Cosmochimica Acta 44, 1753–1766. https://doi.org/10.1016/0016-7037(80)90226-4

Laudon, H., Köhler, S., Buffam, I., 2004. Seasonal TOC export from seven boreal catchments in northern Sweden. Aquat. Sci. 66, 223–230. https://doi.org/10.1007/s00027-004-0700-2

Laveuf, C., Cornu, S., Juillot, F., 2008. Rare earth elements as tracers of pedogenetic processes. Comptes Rendus Geoscience 340, 523–532. https://doi.org/10.1016/j.crte.2008.07.001

Lawrence, M.G., Greig, A., Collerson, K.D., Kamber, B.S., 2006a. Rare Earth Element and Yttrium Variability in South East Queensland Waterways. Aquat Geochem 12, 39–72. https://doi.org/10.1007/s10498-005-4471-8

Lawrence, M.G., Greig, A., Collerson, K.D., Kamber, B.S., 2006b. Direct quantification of rare earth element concentrations in natural waters by ICP-MS. Applied Geochemistry, Frontiers in Analytical Geochemistry–An IGC 2004 Perspective 21, 839–848. https://doi.org/10.1016/j.apgeochem.2006.02.013

Lemarchand, E., Chabaux, F., Vigier, N., Millot, R., Pierret, M.-C., 2010. Lithium isotope systematics in a forested granitic catchment (Strengbach, Vosges Mountains, France). Geochimica et Cosmochimica Acta 74, 4612–4628. https://doi.org/10.1016/j.gca.2010.04.057

Leybourne, M.I., Johannesson, K.H., 2008. Rare earth elements (REE) and yttrium in stream waters, stream sediments, and Fe–Mn oxyhydroxides: Fractionation, speciation, and controls over REE + Y patterns in the surface environment. Geochimica et Cosmochimica Acta 72, 5962–5983. https://doi.org/10.1016/j.gca.2008.09.022

Liang, J., Huang, X., Yan, J., Li, Y., Zhao, Z., Liu, Y., Ye, J., Wei, Y., 2021. A review of the formation of Cr(VI) via Cr(III) oxidation in soils and groundwater. Science of The Total Environment 774, 145762. https://doi.org/10.1016/j.scitotenv.2021.145762

Lidman, F., Mörth, C.M., Laudon, H., 2012. Landscape control of uranium and thorium in boreal streams – spatiotemporal variability and the role of wetlands. Biogeosciences 9, 4773–4785. https://doi.org/10.5194/bg-9-4773-2012

Likens, G.E., Bormann, F.H., Pierce, R.S., Eaton, J.S., Johnson, N.M., 2013. Biogeochemistry of a Forested Ecosystem. Springer-Verlag, New York.

Liu, Y., Guo, Y., Li, Yurui, Li, Yuheng, 2015. GIS-based effect assessment of soil erosion before and after gully land consolidation: A case study of Wangjiagou project region, Loess Plateau. Chin. Geogr. Sci. 25, 137–146. https://doi.org/10.1007/s11769-015-0742-5

London, D., 2018. Ore-forming processes within granitic pegmatites. Ore Geology Reviews 101, 349–383. https://doi.org/10.1016/j.oregeorev.2018.04.020

Lyons, W.B., Carey, A.E., Gardner, C.B., Welch, S.A., Smith, D.F., Szynkiewicz, A., Diaz, M.A., Croot, P., Henry, T., Flynn, R., 2021. The geochemistry of Irish rivers. Journal of Hydrology: Regional Studies 37, 100881. https://doi.org/10.1016/j.ejrh.2021.100881

Lytle, C.M., Lytel, F.W., Yang, N., Qian, J.-H., Hansen, D., Zayed, A., Terry, N., 1998. Reduction of Cr(VI) to Cr(III) by Wetland Plants: Potential for In Situ Heavy Metal Detoxification. Environmental Science & Technology 32, 3087–3093.

Ma, Q., Evans, N.J., Ling, X.-X., Yang, J.-H., Wu, F.-Y., Zhao, Z.-D., Yang, Y.-H., 2019. Natural Titanite Reference Materials for In Situ U-Pb and Sm-Nd Isotopic Measurements by LA-(MC)-ICP-MS. Geostandards and Geoanalytical Research 43, 355–384. https://doi.org/10.1111/ggr.12264

Manceau, A., Marcus, M.A., Grangeon, S., 2012. Determination of Mn valence states in mixed-valent manganates by XANES spectroscopy. American Mineralogist 97, 816–827. https://doi.org/10.2138/am.2012.3903

Martin, J.-M., Meybeck, M., 1979. Elemental mass-balance of material carried by major world rivers. Marine Chemistry 7, 173–206. https://doi.org/10.1016/0304-4203(79)90039-2

Martin, J.-M., Whitfield, M., 1983. The Significance of the River Input of Chemical Elements to the Ocean, in: Wong, C.S., Boyle, E., Bruland, K.W., Burton, J.D., Goldberg, E.D. (Eds.), Trace Metals in Sea Water. Springer US, Boston, MA, pp. 265–296. https://doi.org/10.1007/978-1-4757-6864-0_16

Martin, R.F., De Vito, C., 2005. The patterns of enrichment in felsic pegmatites ultimately depend on tectonic setting. The Canadian Mineralogist 43, 2027–2048. https://doi.org/10.2113/gscanmin.43.6.2027

McClain, C.N., Maher, K., 2016. Chromium fluxes and speciation in ultramafic catchments and global rivers. Chemical Geology 426, 135–157. https://doi.org/10.1016/j.chemgeo.2016.01.021

McDonough, W., 1994. Chemical and isotopic systematics of continental lithospheric mantle. Kimberlites, Related Rocks and Mantle Xenoliths 5, 478–485. https://doi.org/10.29173/ikc2536

McDonough, W.F., Sun, S. -s., 1995. The composition of the Earth. Chemical Geology, Chemical Evolution of the Mantle 120, 223–253. https://doi.org/10.1016/0009-2541(94)00140-4

McGuire, K.J., McDonnell, J.J., Weiler, M., Kendall, C., McGlynn, B.L., Welker, J.M., Seibert, J., 2005. The role of topography on catchment-scale water residence time. Water Resources Research 41. https://doi.org/10.1029/2004WR003657

McLatchey, G.P., Reddy, K.R., 1998. Regulation of Organic Matter Decomposition and Nutrient Release in a Wetland Soil. Journal of Environmental Quality 27, 1268–1274. https://doi.org/10.2134/jeq1998.00472425002700050036x

McLennan, S.M., 2001. Relationships between the trace element composition of sedimentary rocks and upper continental crust. Geochemistry, Geophysics, Geosystems 2. https://doi.org/10.1029/2000GC000109

McLennan, S.M., 1989. Rare earth elements in sedimentary rocks: influence of provenance and sedimentary processes, in: Geochemistry and Mineralogy of Rare Earth Elements. De Gruyter, pp. 169–200. https://doi.org/10.1515/9781501509032-010

McLennan, S.M., Taylor, S.R., 2012. Geology, Geochemistry and Natural Abundances, in: Encyclopedia of Inorganic and Bioinorganic Chemistry. John Wiley & Sons, Ltd. https://doi.org/10.1002/9781119951438.eibc2004

Meybeck, M., 1987. Global chemical weathering of surficial rocks estimated from river dissolved loads. American Journal of Science 287, 401–428. https://doi.org/10.2475/ajs.287.5.401

Meybeck, M., 1983. Atmospheric inputs and river transport of dissolved substances, in: Proceedings of the Hamburg Symposium.

Middelburg, J.J., van der Weijden, C.H., Woittiez, J.R.W., 1988. Chemical processes affecting the mobility of major, minor and trace elements during weathering of granitic rocks. Chemical Geology 68, 253–273. https://doi.org/10.1016/0009-2541(88)90025-3

Milliman, J.D., Meade, R.H., 1983. World-Wide Delivery of River Sediment to the Oceans. The Journal of Geology 91, 1–21. https://doi.org/10.1086/628741

Mitsis, I., Godelitsas, A., Göttlicher, J., Steininger, R., Gamaletsos, P.N., Perraki, M., Abad-Ortega, M.M., Stamatakis, M., 2018. Chromium-bearing clays in altered ophiolitic rocks from Crommyonia (Soussaki) volcanic area, Attica, Greece. Applied Clay Science 162, 362–374. https://doi.org/10.1016/j.clay.2018.06.016

Monk, C.D., 1966. An Ecological Significance of Evergreenness. Ecology 47, 504–505. https://doi.org/10.2307/1932995

Moore, W.S., 1967. Amazon and Mississippi river concentrations of uranium, thorium, and radium isotopes. Earth and Planetary Science Letters 2, 231–234. https://doi.org/10.1016/0012-821X(67)90134-3

Morrill, P.L., Brazelton, W.J., Kohl, L., Rietze, A., Miles, S.M., Kavanagh, H., Schrenk, M.O., Ziegler, S.E., Lang, S.Q., 2014. Investigations of potential microbial methanogenic and carbon monoxide utilization pathways in ultra-basic reducing springs associated with present-day continental serpentinization: the Tablelands, NL, CAN. Front. Microbiol. 5. https://doi.org/10.3389/fmicb.2014.00613

Moulton, K.L., Berner, R.A., 1998. Quantification of the effect of plants on weathering: Studies in Iceland. Geology 26, 895–898. https://doi.org/10.1130/0091-7613(1998)026<0895:QOTEOP>2.3.CO;2

Mukai, H., Motai, S., Yaita, T., Kogure, T., 2016. Identification of the actual cesium-adsorbing materials in the contaminated Fukushima soil. Applied Clay Science 121–122, 188–193. https://doi.org/10.1016/j.clay.2015.12.030

Nahon, D., Colin, F., Tardy, Y., 1982. Formation and distribution of Mg, Fe, Mn-smectites in the first stages of the lateritic weathering of forsterite and tephroite. Clay Minerals 17, 339–348. https://doi.org/10.1180/claymin.1982.017.3.06

Nesbitt, H., Markovics, G., 1997. Weathering of granodioritic crust, long-term storage of elements in weathering profiles, and petrogenesis of siliciclastic sediments. Geochimica et Cosmochimica Acta 61, 1653–1670. https://doi.org/10.1016/S0016-7037(97)00031-8

Nesbitt, H.W., Markovics, G., Price, R.C., 1980. Chemical processes affecting alkalis and alkaline earths during continental weathering. Geochimica et Cosmochimica Acta 44, 1659–1666. https://doi.org/10.1016/0016-7037(80)90218-5

Nesbitt, H.W., Wilson, R.E., 1992. Recent chemical weathering of basalts. American Journal of Science 292, 740–777. https://doi.org/10.2475/ajs.292.10.740

Nesbitt, H.W., Young, G.M., 1989. Formation and Diagenesis of Weathering Profiles. The Journal of Geology 97, 129–147. https://doi.org/10.1086/629290

Nozaki, Y., Zhang, J., Amakawa, H., 1997. The fractionation between Y and Ho in the marine environment. Earth and Planetary Science Letters 148, 329–340. https://doi.org/10.1016/S0012-821X(97)00034-4

Öhlander, B., Land, M., Ingri, J., Widerlund, A., 2013. Mobility and Transport of Nd Isotopes in the Vadose Zone During Weathering of Granitic Till in a Boreal Forest. Aquatic Geochemistry 20, 1–17. https://doi.org/10.1007/s10498-013-9203-x

Oliva, P., Dupré, B., Martin, F., Viers, J., 2004. The role of trace minerals in chemical weathering in a high-elevation granitic watershed (Estibère, France): chemical and mineralogical evidence1. Geochimica et Cosmochimica Acta 68, 2223–2243. https://doi.org/10.1016/j.gca.2003.10.043

Oliva, P., Viers, J., Dupré, B., 2003. Chemical weathering in granitic environments. Chemical Geology 202, 225–256. https://doi.org/10.1016/j.chemgeo.2002.08.001

Olivie-Lauquet, G., Gruau, G., Dia, A., Riou, C., Jaffrezic, A., Henin, O., 2001. Release of Trace Elements in Wetlands: Role of Seasonal Variability. Water Research 35, 943–952. https://doi.org/10.1016/S0043-1354(00)00328-6

O'Sullivan, G., Chew, D., Kenny, G., Henrichs, I., Mulligan, D., 2020. The trace element composition of apatite and its application to detrital provenance studies. Earth-Science Reviews 201, 103044. https://doi.org/10.1016/j.earscirev.2019.103044

Otero, N., Vitòria, L., Soler, A., Canals, A., 2005. Fertiliser characterisation: Major, trace and rare earth elements. Applied Geochemistry 20, 1473–1488. https://doi.org/10.1016/j.apgeochem.2005.04.002

Oze, C., 2004. Chromium geochemistry in serpentinized ultramafic rocks and serpentine soils from the Franciscan complex of California. American Journal of Science - AMER J SCI 304, 67–101. https://doi.org/10.2475/ajs.304.1.67

Palmer, K., Ronkanen, A.-K., Kløve, B., 2015. Efficient removal of arsenic, antimony and nickel from mine wastewaters in Northern treatment peatlands and potential risks in their long-term use. Ecological Engineering 75, 350–364. https://doi.org/10.1016/j.ecoleng.2014.11.045

Palmer, M.R., Edmond, J.M., 1993. Uranium in river water. Geochimica et Cosmochimica Acta 57, 4947–4955. https://doi.org/10.1016/0016-7037(93)90131-F

Pan, Y., Stauffer, M.R., 2000. Cerium anomaly and Th/U fractionation in the 1.85 Ga Flin Flon Paleosol: Clues from REE- and U-rich accessory minerals and implications for paleoatmospheric reconstruction. American Mineralogist 85, 898–911. https://doi.org/10.2138/am-2000-0703

Panahi, A., Young, G.M., Rainbird, R.H., 2000. Behavior of major and trace elements (including REE) during Paleoproterozoic pedogenesis and diagenetic alteration of an Archean granite near Ville Marie, Québec, Canada. Geochimica et Cosmochimica Acta 64, 2199–2220. https://doi.org/10.1016/S0016-7037(99)00420-2

Pande, K., Sarin, M.M., Trivedi, J.R., Krishnaswami, S., Sharma, K.K., 1994. The Indus river system (India-Pakistan): Major-ion chemistry, uranium and strontium isotopes. Chemical Geology 116, 245–259. https://doi.org/10.1016/0009-2541(94)90017-5

Patino, L.C., Velbel, M.A., Price, J.R., Wade, J.A., 2003. Trace element mobility during spheroidal weathering of basalts and andesites in Hawaii and Guatemala. Chemical Geology, Controls on Chemical Weathering 202, 343–364. https://doi.org/10.1016/j.chemgeo.2003.01.002

Peltola, P., Brun, C., Åström, M., Tomilina, O., 2008. High K/Rb ratios in stream waters — Exploring plant litter decay, ground water and lithology as potential controlling mechanisms. Chemical Geology 257, 92–100. https://doi.org/10.1016/j.chemgeo.2008.08.009

Plasil, J., 2014. Oxidation-hydration weathering of uraninite: the current state-of-knowledge. J Geosci 59, 99–114. https://doi.org/10.3190/jgeosci.163

Plater, A.J., Ivanovich, M., Dugdale, R.E., 1992. Uranium series disequilibrium in river sediments and waters: the significance of anomalous activity ratios. Applied Geochemistry 7, 101–110. https://doi.org/10.1016/0883-2927(92)90029-3

Pogge von Strandmann, P.A.E., Burton, K.W., Opfergelt, S., Eiríksdóttir, E.S., Murphy, M.J., Einarsson, A., Gislason, S.R., 2016. The effect of hydrothermal spring weathering processes and primary productivity on lithium isotopes: Lake Myvatn, Iceland. Chemical Geology 445, 4–13. https://doi.org/10.1016/j.chemgeo.2016.02.026

Pogge von Strandmann, P.A.E.P., Burton, K.W., James, R.H., van Calsteren, P., Gislason, S.R., 2010. Assessing the role of climate on uranium and lithium isotope behaviour in rivers draining a basaltic terrain. Chemical Geology 270, 227–239. https://doi.org/10.1016/j.chemgeo.2009.12.002

Pokrovsky, O.S., Schott, J., Dupré, B., 2006. Trace element fractionation and transport in boreal rivers and soil porewaters of permafrost-dominated basaltic terrain in Central Siberia. Geochimica et Cosmochimica Acta 70, 3239–3260. https://doi.org/10.1016/j.gca.2006.04.008

Porcelli, D., Andersson, P.S., Wasserburg, G.J., Ingri, J., Baskaran, M., 1997. The importance of colloids and mires for the transport of uranium isotopes through the Kalix River watershed and Baltic Sea. Geochimica et Cosmochimica Acta 61, 4095–4113. https://doi.org/10.1016/S0016-7037(97)00235-4

Post, V.E.A., Vassolo, S.I., Tiberghien, C., Baranyikwa, D., Miburo, D., 2017. High Uranium Concentrations in Groundwater in Burundi. Procedia Earth and Planetary Science, 15th Water-Rock Interaction International Symposium, WRI-15 17, 524–527. https://doi.org/10.1016/j.proeps.2016.12.132

Pourret, O., Faucon, M.-P., 2018. Cobalt, in: Encyclopedia of Earth Sciences Series. pp. 291–294.

Price, N.M., Morel, F.M.M., 1991. Colimitation of phytoplankton growth by nickel and nitrogen. Limnol. & Oceanogr. 36, 1071–1077. https://doi.org/10.4319/lo.1991.36.6.1071

Putzolu, F., Abad, I., Balassone, G., Boni, M., Cappelletti, P., Graziano, S.F., Maczurad, M., Mondillo, N., Najorka, J., Santoro, L., 2020. Parent rock and climatic evolution control on the genesis of Ni-bearing clays in Ni-Co laterites: New inferences from the Wingellina deposit (Western Australia). Ore Geology Reviews 120, 103431. https://doi.org/10.1016/j.oregeorev.2020.103431

Rai, D., Eary, L.E., Zachara, J.M., 1989. Environmental chemistry of chromium. Science of The Total Environment, The Chromium Paradox in Modern Life 86, 15–23. https://doi.org/10.1016/0048-9697(89)90189-7

Richard, F.C., Bourg, A.C.M., 1991. Aqueous geochemistry of chromium: A review. Water Research 25, 807–816. https://doi.org/10.1016/0043-1354(91)90160-R

Rinklebe, J., Shaheen, S.M., 2017. Redox chemistry of nickel in soils and sediments: A review. Chemosphere 179, 265–278. https://doi.org/10.1016/j.chemosphere.2017.02.153

Riotte, J., Maréchal, J.C., Audry, S., Kumar, C., Bedimo Bedimo, J.P., Ruiz, L., Sekhar, M., Cisel, M., Chitra Tarak, R., Varma, M.R.R., Lagane, C., Reddy, P., Braun, J.J., 2014. Vegetation impact on stream chemical fluxes: Mule Hole watershed (South India). Geochimica et Cosmochimica Acta 145, 116–138. https://doi.org/10.1016/j.gca.2014.09.015

Robinson, L., Henderson, G., Hall, L., Matthews, I., 2004. Climatic Control of Riverine and Seawater Uranium-Isotope Ratios. Science (New York, N.Y.) 305, 851–4. https://doi.org/10.1126/science.1099673

Roux, G.L., Shotyk, W., 2006. Chapter 9 Weathering of inorganic matter in bogs, in: Martini, I.P., Martínez Cortizas, A., Chesworth, W. (Eds.), Developments in Earth Surface Processes, Peatlands. Elsevier, pp. 197–215. https://doi.org/10.1016/S0928-2025(06)09009-2

Roy, S., Acharya, S.S., Chakrabarti, R., 2024. Mobilization of rare earth elements during extreme weathering of basalt. Geochemistry 84, 126086. https://doi.org/10.1016/j.chemer.2024.126086

Rudnick, R., Gao, S., 2003. Composition of the Continental Crust. Treatise Geochem 3:1-64. Treatise on Geochemistry 3, 1–64. https://doi.org/10.1016/B0-08-043751-6/03016-4

Ryan, J.G., Langmuir, C.H., 1987. The systematics of lithium abundances in young volcanic rocks. Geochimica et Cosmochimica Acta 51, 1727–1741. https://doi.org/10.1016/0016-7037(87)90351-6

Saad, E., Wang (王相力）, X., Planavsky, N., Reinhard, C., Tang, Y., 2017. Redox-independent chromium isotope fractionation induced by ligand-promoted dissolution. Nature Communications 8. https://doi.org/10.1038/s41467-017-01694-y

Salil, M.S., Shrivastava, J.P., Pattanayak, S.K., 1997. Similarities in the mineralogical and geochemical attributes of detrital clays of Maastrichtian Lameta Beds and weathered Deccan basalt, Central India. Chemical Geology 136, 25–32. https://doi.org/10.1016/S0009-2541(96)00128-3

Sarin, M.M., Krishnaswami, S., somayajulu, B.L.K., Moore, W.S., 1990. Chemistry of uranium, thorium, and radium isotopes in the Ganga-Brahmaputra river system: Weathering

processes and fluxes to the Bay of Bengal. Geochimica et Cosmochimica Acta 54, 1387–1396. https://doi.org/10.1016/0016-7037(90)90163-F

Scheller, S., Goenrich, M., Boecher, R., Thauer, R.K., Jaun, B., 2010. The key nickel enzyme of methanogenesis catalyses the anaerobic oxidation of methane. Nature 465, 606–608. https://doi.org/10.1038/nature09015

Schirrmeister, L., Störr, M., 1994. The weathering of basaltic rocks in Burundi and Vietnam. CATENA 21, 243–256. https://doi.org/10.1016/0341-8162(94)90015-9

Schnug, E., Haneklaus, S.H., 2016. The Enigma of Fertilizer Phosphorus Utilization, in: Schnug, E., De Kok, L.J. (Eds.), Phosphorus in Agriculture: 100 % Zero. Springer Netherlands, Dordrecht, pp. 7–26. https://doi.org/10.1007/978-94-017-7612-7_2

Schulze, T., Streck, G., Paschke, A., 2011. Sampling and Conservation, in: Treatise on Water Science. pp. 131–152. https://doi.org/10.1016/B978-0-444-53199-5.00054-3

Sekaly, A.L.R., Murimboh, J., Hassan, N.M., Mandal, R., Ben Younes, M.E., Chakrabarti, C.L., Back, M.H., Grégoire, D.C., 2003. Kinetic Speciation of Co(II), Ni(II), Cu(II), and Zn(II) in Model Solutions and Freshwaters: Lability and the d Electron Configuration. Environ. Sci. Technol. 37, 68–74. https://doi.org/10.1021/es025805g

Shanker, A.K., Cervantes, C., Loza-Tavera, H., Avudainayagam, S., 2005. Chromium toxicity in plants. Environment International 31, 739–753. https://doi.org/10.1016/j.envint.2005.02.003

Shannon, R.D., 1976. Revised effective ionic radii and systematic studies of interatomic distances in halides and chalcogenides. Acta Cryst A 32, 751–767. https://doi.org/10.1107/S0567739476001551

Short, S.A., Lowson, R.T., Ellis, J., 1988. 234U238U and 240Th234U activity ratios in the colloidal phases of aquifers in lateritic weathered zones. Geochimica et Cosmochimica Acta 52, 2555–2563. https://doi.org/10.1016/0016-7037(88)90026-9

Shtiza, A., Swennen, R., Tashko, A., 2005. Chromium and nickel distribution in soils, active river, overbank sediments and dust around the Burrel chromium smelter (Albania). Journal of Geochemical Exploration 87, 92–108. https://doi.org/10.1016/j.gexplo.2005.07.005

Smedley, P.L., Kinniburgh, D.G., 2023. Uranium in natural waters and the environment: Distribution, speciation and impact. Applied Geochemistry 148, 105534. https://doi.org/10.1016/j.apgeochem.2022.105534

Sohrin, Y., Urushihara, S., Nakatsuka, S., Kono, T., Higo, E., Minami, T., Norisuye, K., Umetani, S., 2008. Multielemental Determination of GEOTRACES Key Trace Metals in Seawater by ICPMS after Preconcentration Using an Ethylenediaminetriacetic Acid Chelating Resin. Anal. Chem. 80, 6267–6273. https://doi.org/10.1021/ac800500f

Somayajulu, B.L.K., 1994. Uranium isotopes in the Hooghly estuary, India. Marine Chemistry, Chemistry of the Northern Indian Ocean 47, 291–296. https://doi.org/10.1016/0304-4203(94)90027-2

Song, S., Mathur, R., Ruiz, J., Chen, D., Allin, N., Guo, K., Kang, W., 2016. Fingerprinting two metal contaminants in streams with Cu isotopes near the Dexing Mine, China. Science of The Total Environment 544, 677–685. https://doi.org/10.1016/j.scitotenv.2015.11.101

Starkey, H.C., 1982. The Role of Clays in Fixing Lithium. U.S. Government Printing Office.

Stetten, L., Mangeret, A., Brest, J., Seder-Colomina, M., Le Pape, P., Ikogou, M., Zeyen, N., Thouvenot, A., Julien, A., Alcalde, G., Reyss, J.L., Bombled, B., Rabouille, C., Olivi, L., Proux, O., Cazala, C., Morin, G., 2018. Geochemical control on the reduction of U(VI) to mononuclear U(IV) species in lacustrine sediments. Geochimica et Cosmochimica Acta 222, 171–186. https://doi.org/10.1016/j.gca.2017.10.026

Stetzenbach, K., Amano, M., Kreamer, D., Hodge, V., 1994. Testing the Limits of ICP-MS: Determination of Trace Elements in Ground Water at the Part-Per-Trillion Level. Ground Water 32, 976–985. https://doi.org/10.1111/j.1745-6584.1994.tb00937.x

Strager, M.P., Fletcher, J.J., Strager, J.M., Yuill, C.B., Eli, R.N., Todd Petty, J., Lamont, S.J., 2010. Watershed analysis with GIS: The watershed characterization and modeling system software application. Computers & Geosciences 36, 970–976. https://doi.org/10.1016/j.cageo.2010.01.003

Suchet, P.A., Probst, J.L., 1993. Modelling of atmospheric CO2 consumption by chemical weathering of rocks: Application to the Garonne, Congo and Amazon basins. Chemical Geology, Third International Symposium on the Geochemistry of the Earth Surface 107, 205–210. https://doi.org/10.1016/0009-2541(93)90174-H

Suhr, N., Widdowson, M., McDermott, F., Kamber, B., 2018. Th/U and U series systematics of saprolite: Importance for the oceanic 234U excess. Geochemical Perspectives 6. https://doi.org/10.7185/geochemlet.1803

Suhrhoff, T.J., Rickli, J., Crocket, K., Bura-Nakic, E., Vance, D., 2019. Behavior of beryllium in the weathering environment and its delivery to the ocean. Geochimica et Cosmochimica Acta 265, 48–68. https://doi.org/10.1016/j.gca.2019.08.017

Sun, M., Wu, W., Ji, X., Wang, X., Qu, S., 2019. Silicate weathering rate and its controlling factors: A study from small granitic watersheds in the Jiuhua Mountains. Chemical Geology 504, 253–266. https://doi.org/10.1016/j.chemgeo.2018.11.019

Sun, S.-S., Deng, T.-H.-B., Ao, M., Yang, W.-J., Liu, X.-R., Liu, T., Zhu, J.-M., Morel, J.L., Tang, Y.-T., Qiu, R.-L., 2024. Nickel isotope fractionation during intense weathering of basalt: Implications for Ni output from continental weathering. Geochimica et Cosmochimica Acta 367, 107–122. https://doi.org/10.1016/j.gca.2023.12.023

Swarzenski, P., Campbell, P., Porcelli, D., McKee, B., 2004. The estuarine chemistry and isotope systematics of 234,238U in the Amazon and Fly Rivers. Continental Shelf Research, Tropical River-Ocean Processes in Coastal Settings 24, 2357–2372. https://doi.org/10.1016/j.csr.2004.07.025

Szponar, N., Brazelton, W.J., Schrenk, M.O., Bower, D.M., Steele, A., Morrill, P.L., 2013. Geochemistry of a continental site of serpentinization, the Tablelands Ophiolite, Gros Morne National Park: A Mars analogue. Icarus 224, 286–296. https://doi.org/10.1016/j.icarus.2012.07.004

Tanaka, K., Watanabe, N., 2015. Size distribution of alkali elements in riverbed sediment and its relevance to fractionation of alkali elements during chemical weathering. Chemical Geology 411, 12–18. https://doi.org/10.1016/j.chemgeo.2015.05.025

Tang, J., Johannesson, K.H., 2003. Speciation of rare earth elements in natural terrestrial waters: assessing the role of dissolved organic matter from the modeling approach. Geochimica et Cosmochimica Acta 67, 2321–2339. https://doi.org/10.1016/S0016-7037(02)01413-8

Taniguchi, K., Onda, Y., Smith, H.G., Blake, W., Yoshimura, K., Yamashiki, Y., Kuramoto, T., 2019. Transport and Redistribution of Radiocesium in Fukushima Fallout through Rivers. Environ. Sci. Technol. 53, 12339–12347.

Temnerud, J., Bishop, K., 2005. Spatial Variation of Streamwater Chemistry in Two Swedish Boreal Catchments: Implications for Environmental Assessment. Environ. Sci. Technol. 39, 1463–1469. https://doi.org/10.1021/es040045q

Thomas, W.A., Grigal, D.F., 1976. Phosphorus Conservation by Evergreenness of Mountain Laurel. Oikos 27, 19–26. https://doi.org/10.2307/3543426

Thompson, A., Amistadi, M.K., Chadwick, O.A., Chorover, J., 2013. Fractionation of yttrium and holmium during basaltic soil weathering. Geochimica et Cosmochimica Acta 119, 18–30. https://doi.org/10.1016/j.gca.2013.06.003

Thurber, D.L., Broecker, W.S., Blanchard, R.L., Potratz, H.A., 1965. Uranium-Series Ages of Pacific Atoll Coral. Science 149, 55–58. https://doi.org/10.1126/science.149.3679.55

Trolard, F., Bourrie, G., Jeanroy, E., Herbillon, A.J., Martin, H., 1995. Trace metals in natural iron oxides from laterites: A study using selective kinetic extraction. Geochimica et Cosmochimica Acta 59, 1285–1297. https://doi.org/10.1016/0016-7037(95)00043-Y

Turekian, K.K., Wedepohl, K.H., 1961. Distribution of the Elements in Some Major Units of the Earth's Crust. GSA Bulletin 72, 175–192. https://doi.org/10.1130/0016-7606(1961)72[175:DOTEIS]2.0.CO;2

Uchida, S., Tagami, K., Tabei, K., Hirai, I., 2006. Concentrations of REEs, Th and U in river waters collected in Japan. Journal of Alloys and Compounds, Proceedings of Rare Earths'04 in Nara, Japan 408–412, 525–528. https://doi.org/10.1016/j.jallcom.2004.12.104

Uhlig, D., Schuessler, J.A., Bouchez, J., Dixon, J.L., von Blanckenburg, F., 2017. Quantifying nutrient uptake as driver of rock weathering in forest ecosystems by magnesium stable isotopes. Biogeosciences 14, 3111–3128. https://doi.org/10.5194/bg-14-3111-2017

Uren, N.C., 1992. Forms, Reactions, and Availability of Nickel in Soils, in: Sparks, D.L. (Ed.), Advances in Agronomy. Academic Press, pp. 141–203. https://doi.org/10.1016/S0065-2113(08)60937-2

Vasileiou, E., Papazotos, P., Dimitrakopoulos, D., Perraki, M., 2021. Hydrogeochemical Processes and Natural Background Levels of Chromium in an Ultramafic Environment. The Case Study of Vermio Mountain, Western Macedonia, Greece. Water 13, 2809. https://doi.org/10.3390/w13202809

Velbel, M.A., Price, J.R., 2007. Solute geochemical mass-balances and mineral weathering rates in small watersheds: Methodology, recent advances, and future directions. Applied Geochemistry, Metal interactions with natural organic matter and Watershed-scale geochemistry 22, 1682–1700. https://doi.org/10.1016/j.apgeochem.2007.03.029

Venturelli, G., Contini, S., Bonazzi, A., Mangia, A., 1997. Weathering of ultramafic rocks and element mobility at Mt. Prinzera, Northern Apennines, Italy. Mineral. mag. 61, 765–778. https://doi.org/10.1180/minmag.1997.061.409.02

Viers, J., Dupré, B., Polvé, M., Schott, J., Dandurand, J.-L., Braun, J.-J., 1997. Chemical weathering in the drainage basin of a tropical watershed (Nsimi-Zoetele site, Cameroon) : comparison between organic-poor and organic-rich waters. Chemical Geology 140, 181–206. https://doi.org/10.1016/S0009-2541(97)00048-X

Vitousek, P., Chadwick, O., Matson, P., Allison, S., Derry, L., Kettley, L., Luers, A., Mecking, E., Monastra, V., Porder, S., 2003. Erosion and the Rejuvenation of Weathering-derived Nutrient Supply in an Old Tropical Landscape. Ecosystems 6, 762–772. https://doi.org/10.1007/s10021-003-0199-8

Wadleigh, M.A., Veizer, J., Brooks, C., 1985. Strontium and its isotopes in Canadian rivers: Fluxes and global implications. Geochimica et Cosmochimica Acta 49, 1727–1736. https://doi.org/10.1016/0016-7037(85)90143-7

Walker, C.M., King, R.S., Whigham, D.F., Baird, S.J., 2012. Landscape and Wetland Influences on Headwater Stream Chemistry in the Kenai Lowlands, Alaska. Wetlands 32, 301–310. https://doi.org/10.1007/s13157-011-0260-x

Wampler, J.M., Krogstad, E.J., Elliott, W.C., Kahn, B., Kaplan, D.I., 2012. Long-Term Selective Retention of Natural Cs and Rb by Highly Weathered Coastal Plain Soils. Environ. Sci. Technol. 46, 3837–3843. https://doi.org/10.1021/es2035834

Wang, W., Evans, R.D., Newman, K., Khokhar, R., 2021. Automated separation, preconcentration and measurement of 90Sr in liquid samples with complex matrices by online ion exchange chromatography coupled with inductively coupled plasma mass spectrometry (ICP-MS). Talanta 222, 121488. https://doi.org/10.1016/j.talanta.2020.121488

Wasylenki, L.E., Howe, H.D., Spivak-Birndorf, L.J., Bish, D.L., 2015. Ni isotope fractionation during sorption to ferrihydrite: Implications for Ni in banded iron formations. Chemical Geology 400, 56–64. https://doi.org/10.1016/j.chemgeo.2015.02.007

Welch, A.H., Lico, M.S., 1998. Factors controlling As and U in shallow ground water, southern Carson Desert, Nevada. Applied Geochemistry 13, 521–539. https://doi.org/10.1016/S0883-2927(97)00083-8

White, A., Ma, L., Moravec, B., Chorover, J., McIntosh, J., 2021. U-series and Sr isotopes as tracers of mineral weathering and water routing from the deep Critical Zone to streamflow in a high-elevation volcanic catchment. Chemical Geology 570, 120156. https://doi.org/10.1016/j.chemgeo.2021.120156

Wilson, M.J., 2004. Weathering of the primary rock-forming minerals: processes, products and rates. Clay Minerals 39, 233–266. https://doi.org/10.1180/0009855043930133

Wohl, E., 2017. The significance of small streams. Front. Earth Sci. 11, 447–456. https://doi.org/10.1007/s11707-017-0647-y

Wolock, D.M., Fan, J., Lawrence, G.B., 1997. Effects of basin size on low-flow stream chemistry and subsurface contact time in the Neversink River watershed, New York. Hydrological Processes 11, 1273–1286. https://doi.org/10.1002/(SICI)1099-1085(199707)11:9<1273::AID-HYP557>3.0.CO;2-S

Worrall, F., Burt, T.P., Jaeban, R.Y., Warburton, J., Shedden, R., 2002. Release of dissolved organic carbon from upland peat. Hydrological Processes 16, 3487–3504. https://doi.org/10.1002/hyp.1111

Wu, K., Liu, S., Shi, X., Colin, C., Bassinot, F., Lou, Z., Zhang, H., Zhu, A., Fang, X., Mohamed, C.Abd.R., 2022. The Effect of Size Distribution on the Geochemistry and Mineralogy of Tropical River Sediments and Its Implications regarding Chemical Weathering and Fractionation of Alkali Elements. Lithosphere 2022, 8425818. https://doi.org/10.2113/2022/8425818

Wysocka, I., 2021. Determination of rare earth elements concentrations in natural waters – A review of ICP-MS measurement approaches. Talanta 221, 121636. https://doi.org/10.1016/j.talanta.2020.121636

Xu, Z., Han, G., 2009. Rare earth elements (REE) of dissolved and suspended loads in the Xijiang River, South China. Applied Geochemistry 24, 1803–1816. https://doi.org/10.1016/j.apgeochem.2009.06.001

Yoo, K., Mudd, S.M., Sanderman, J., Amundson, R., Blum, A., 2009. Spatial patterns and controls of soil chemical weathering rates along a transient hillslope. Earth and Planetary Science Letters 288, 184–193. https://doi.org/10.1016/j.epsl.2009.09.021

Yu, C., Berger, T., Drake, H., Song, Z., Peltola, P., Åström, M.E., 2019. Geochemical controls on dispersion of U and Th in Quaternary deposits, stream water, and aquatic plants in an area with a granite pluton. Science of The Total Environment 663, 16–28. https://doi.org/10.1016/j.scitotenv.2019.01.293

Zebracki, M., Marlin, C., Gaillard, T., Gorny, J., Diez, O., Durand, V., Lafont, C., Jardin, C., Monange, V., 2023. Elevated uranium concentration and low activity ratio (234U/238U) in the Œuf river as the result of groundwater–surface water interaction (Essonne river valley, South of Paris Basin, France). Science of The Total Environment 876, 162537. https://doi.org/10.1016/j.scitotenv.2023.162537

Zeyen, N., Wang, B., Wilson, S., Paulo, C., Stubbs, A.R., Power, I.M., Steele-Maclnnis, M., Lanzirotti, A., Newville, M., Paterson, D.J., Hamilton, J.L., Jones, T.R., Turvey, C.C., Dipple, G.M., Southam, G., 2022. Cation Exchange in Smectites as a New Approach to Mineral Carbonation. Front. Clim. 4. https://doi.org/10.3389/fclim.2022.913632

Zhang, P.-C., Krumhansl, J.L., Brady, P.V., 2002. Introduction to Properties, Sources and Characteristics of Soil Radionuclides, in: Geochemistry of Soil Radionuclides. John Wiley & Sons, Ltd, pp. 1–20. https://doi.org/10.2136/sssaspecpub59.c1

Co-Authorship Statement

The design and structure of this research was conceived by Michael Babechuk. All aspects of this project, apart from the laboratory analysis, were led by Gabrielle Ledesma. Laboratory field preparation work was carried out by Gabrielle Ledesma and Inês Garcia Nobre Silva. Sample collection and field work was carried out by Gabrielle Ledesma, Michael Babechuk, and Ajatshatru Balaji. Gabrielle Ledesma led the selection of specific sampling locations at all study sites and handled filtration and acidification of sampling of waters. Laboratory analysis work was handled by Huy Duc Dang and Wei Wang, collaborators from Trent University. The work presented in this thesis was written by Gabrielle Ledesma with edits by Michael Babechuk, apart from laboratory methods of Chapter 2, which was written by Michael Babechuk, Huy Duc Dang and Wei Wang.

Chapter 2 is written in a manuscript format and is intended to be submitted to a journal to be considered for publication and was written with the Journal of Hydrology – Regional Studies in mind. When this work is submitted as a manuscript, Michael Babechuk, Huy Duc Dang, and Wei Wang will be listed as co-authors.

Chapter 2: Integrated geospatial-geochemical catchment analysis of Newfoundland stream waters draining endmember silicate bedrock types (ultramafic-mafic rocks vs. granite)

Ledesma, G[1]., Babechuk, MG[1]., Wang W[2]., Dang DH[2].
[1]Memorial University of Newfoundland
[2]Trent University

To be submitted to Journal of Hydrology - Regional Studies

2.1. Abstract

Studies of small hydrological catchments draining a singular or restricted range of bedrock type(s) reveal the first-order control of geology on the dissolved element composition of stream waters. However, this geologic control competes with other physicochemical and environmental factors. Better understanding these catchment dynamics is important from a local scale (e.g., constraining ties of potentially toxic element inputs to specific lithology and processes) to a regional scale (e.g., deciphering how major rivers that transport dissolved elements to the oceans may inherit their signatures). This study assesses dissolved major, trace, and rare earth element data from streams at two coastal study sites within the same (boreal) climate zone that drain silicate-endmember bedrock compositions: (1) Bay of Islands in western Newfoundland draining an ophiolite sequence of ultramafic-mafic bedrock, and (2) Burin Peninsula draining a granite pluton (St. Lawrence granite) that hosts fluorite mineralization. By quantifying physical properties of catchments with geospatial data (bedrock geology, surficial geology, topography, vegetative cover) and integrating this with geochemical data, this study was able to constrain the primary catchment drivers on the dissolved composition of different elements/element groups in the streams draining ultramafic rock and granite. Specifically, this study has isolated elements strongly to moderately controlled by: bedrock geology (Mg, Cr, Ni in ultramafic rock streams; Rb, Cs in granite streams; contrasting REE abundances and Eu anomalies); weathering/soil/vegetation effects and associated flux of

dissolved organic matter to streams (K, Ni, Co, Ce anomalies); and short temporal events or local geological features such as the fluorite mineralization (elevated element flux, high Y/Ho). Several of these more local water chemical features were traceable into larger catchment areas of Newfoundland major rivers. The low-abundance trace element data presented here are the first to be reported for any Newfoundland surface water and results confirm that these data are useful to trace boreal catchment dynamics.

2.2. Introduction

Rivers are important transport mechanisms for mobile (dissolved and colloid-affiliated) elements, but the processes that govern the release, transport, and fractionation of such elements are complex and often require the assessment of several chemical, biological, and hydrological proxies to untangle (e.g., Andersson and Nyberg, 2009; Bluth and Kump, 1994; Dillon and Molot, 1997; Mora et al., 2020).

For some elements, bedrock geology is an important first-order control on the composition of rivers, but for other elements factors such as surficial geology, topography, hydrology, soil interaction, and vegetation can modify and heavily influence dissolved element budgets. Elucidating such controls is critical when constraining the role of the hydrosphere in modern and ancient surface element cycling and when isolating the impacts of anthropogenic influences (such as agricultural and urban run-off) from natural factors (e.g., geologically anomalous bedrock enrichment).

Major rivers have expansive drainage networks that often interact with diverse geology and topography over long transport distances, making it challenging to determine element-specific controls. Studying smaller catchments with singular or restricted range of bedrock type(s) has been invoked to better isolate details of geologic controls and how they compete with other physicochemical and environmental factors (Krám et al., 2012; Lidman et al., 2012; McClain and Maher, 2016; Mistikawy et al., 2020; Négrel, 1999; Oliva et al., 2004; Yu et al., 2019). This study uses a multi-element approach to investigate streams from small catchments within in a boreal climate zone from two study sites on the island of Newfoundland (Newfoundland & Labrador, Canada). Targeted stream waters were selected based on the contrasting, endmember igneous silicate bedrock composition (ultramafic-mafic vs. felsic) of the catchments. By adopting an integrated geochemical and geospatial information approach, this study informs the catchments dynamics and controls on element budgets.

Understanding aquatic geochemistry of boreal ecosystems is an important component of predicting how such environments may adjust to a warming climate. Newfoundland lies within the eastern-most section of Canada's boreal zone, a water-rich ecozone that supplies 50% of the Canadian freshwater with outflow to the oceans (Webster et al., 2015). It is predicted that the boreal zone is especially susceptible to climate change and will warm quicker than any other biozone (Price et al., 2013). Thus, it has become more prevalent to assess the current compositional state of freshwater with the boreal zone and how it might shift with a changing ecosystem as well as establish environmental baseline data within these geographic and climatic zones.

The island of Newfoundland has abundant geologic diversity, minimal anthropogenic modification, and vast network of streams that make it an advantageous place to examine regional

geological controls on surface water chemistry. At present, however, there are limited data on most of Newfoundland's surface waters, especially for low-abundance trace elements and for areas outside of the capital city, St. John's. Such trace elements are especially sensitive to aqueous processes and can be utilized as powerful fingerprints that can evaluate element sources and catchment-scale weathering and aquatic processes (Babechuk et al., 2020; Chabaux et al., 2003; Steinmann and Stille, 2008).

This study is the first to report a comprehensive low-abundance dataset from the dissolved load (defined as <0.45 μm, which includes colloidal materials in their defined size of <0.45 μm – 1 nm) of stream waters within the province using clean handling protocols from field to analysis and determination through inductively coupled plasma mass spectrometry (ICP-MS), showcasing low-level, high-precision geochemical analyses of freshwater. Stream samples were characterized with a comprehensive geochemical dataset that includes major cations, trace elements, and dissolved organic and inorganic carbon, alongside on-site measurement of pH, E_h, conductivity, and temperature. The samples measured here include 30 rivers and streams that come from low-population catchment areas targeted due to the specific bedrock geology (ultramafic-mafic bedrock within the Bay of Islands and Gros Morne areas and crystalline felsic bedrock within the Burin Peninsula) and 6 Newfoundland major rivers. Additionally, 3 roadside springs that are used as present day and/or historical drinking water sources were sampled for an evaluation of the dissolved abundances of potential toxic elements. Integrating the geochemical data with geospatially quantified catchment properties is demonstrated as effective in revealing important controls within small catchments of singular lithology (monolithologic) across a diverse set of landscape, topography, and vegetation.

2.3. Sample sites

2.3.1. Western Newfoundland site

A total of 19 streams were sampled from western Newfoundland across an area of ~3985 km^2 (Figure 1). The hydrological catchment size, up to the point of stream sampling, ranged from 0.8 km^2 to 278 km^2 with an average catchment size of 45 km^2. Annual precipitation for the west coast ranges between 1100-1400 mm/year with the driest season in spring and early summer and wettest in fall early winter (Ullah, 1992). The Long Range Mountains dominate the landscape in western Newfoundland with high relief areas reaching over 700 m above sea level. At higher elevations, vegetation is sparse and characterized by abundant rock outcrops while balsam firs are the dominant forest cover at lower elevation (Woodrow and Heringa, 1987). This study focused on sampling streams draining the well-preserved 488 ± 1.5 Ma (Yan and Casey, 2020) Bay of Islands ophiolite complex (BOIC).

The BOIC was emplaced by an arc-continent collision during the Ordovician Taconic orogeny (Williams and Smyth, 1973) and comprises a full ophiolite transect that is exposed between four main massifs on the west coast of Newfoundland. This study primarily sampled streams draining the southern Blow Me Down Mountain massif and the northern Table Mountain massif. Within these massifs, primary focus was given to targeted streams draining the basal ultramafic and associated cumulate rocks and the overlying intrusive and extrusive mafic packages.

The ultramafic section of the BOIC contains primarily harzburgite with lower volumes of clinopyroxenite gradually decreasing in abundance down unit and coarse-grained lherzolite present at the base of the mantle sequence (Church and Riccio, 1977; Malpas et al., 1978; Suen et al., 1979). The Table Mountain massif preserves the thickest ultramafic section of the BOIC (~6-

7.5 km) (Suhr, 1993). Massive dunite is present at the top of the ultramafic section and is up to several km thick on the Blow Me Down Mountain massif (Malpas, 1976; Suhr and Robinson, 1994). Layered and massive gabbro makes up the overlying mafic section of the BOIC with increasing abundance of diabase dykes towards the top and a transition to overlying pillowed basalt (Suen et al., 1979).

2.3.2. Burin Peninsula site

A total of 11 streams were sampled from the Burin Peninsula across an area of ~689 km^2 (Figure 2). The hydrological catchment size, up to the point of stream sampling, ranged from 1 km^2 to 166 km^2 with an average catchment size of 27 km^2. Annual precipitation is slightly higher on the Burin Peninsula than the west coast, ranging between 1200-1500 mm per year with a dry season in spring and early summer and wet season in fall and early winter (Ullah, 1992; Woodrow and Heringa, 1987). The Burin Peninsula has much lower relief than the west coast and is characterized by blanket bogs and moss with sporadic forests containing balsam fir and black spruce growing on wet lowlands (Woodrow and Heringa, 1987). The area is abundant in glacial tills that range from a few centimeters to a meter thick. Most till in the area geochemically reflects the underlying bedrock geology (Batterson and Taylor, 2009), which consists mostly of Neoproterozoic submarine and non-marine volcanic and sedimentary rocks overlain with similar aged shallow marine sediments and intrusions of Devonian granite (O'Brien et al., 1977). This study focused on sampling rivers draining the St. Lawrence Granite (SLG), a Devonian pluton that outcrops across a 30 km by 10 km area on the Burin Peninsula (Teng and Strong, 1976).

The SLG is a highly evolved, peralkaline granite with slight compositional variations that subdivide the granite into an east- and west-lobe, and an associated porphyry (Winterland

porphyry) in the northern section of the granite (Magyarosi, 2022; Teng and Strong, 1976). The granite is primarily made up of quartz, orthoclase, and albite with minor riebeckite, aegirine, biotite, fluorite, magnetite, and hematite (Teng, 1974). The Winterland porphyry and east-lobe have similar mineralogy but differ in texture (Miller, 1994). The west lobe is dated at 374 ± 2 Ma (Kerr et al., 1993) and is more granodioritic in composition, containing a higher proportion of plagioclase to orthoclase with increased hornblende (Teng and Strong, 1976). The SLG is also known for association of extensive fluorite veins which are mostly located within the east lobe (Magyarosi, 2022; Magyarosi et al., 2019; Van Alstine, 1944). Fluorite veins range from centimeters to 30 meters wide in size and up to 3 km long (Magyarosi, 2022).

2.3.3. Major rivers

Newfoundland comprises 4 major drainage basins that drain towards the northeast or south into the Atlantic Ocean or drain west into the Gulf of St. Lawrence (Ullah, 1992). In this study, 6 major rivers were sampled (Figure 3), representing drainage from 3 of the 4 major basins. Major rivers within Newfoundland were defined following the Water Resources Atlas of Newfoundland (Ullah, 1992) as rivers with the largest gauged basins. Rivers sampled included the Terra Nova River, Gander River, and Exploits River (Northeast Coast Drainage Basin), Humber River (West Coast Drainage Basin), and Garnish River and Piper's Hole River (South Coast Drainage Basin). These major river samples were collected within the same sampling excursion as the main study site localities (Sections 2.3.1 and 2.3.2) to offer a provincial comparison to other major rivers globally and to contrast the smaller Newfoundland catchment streams with larger regional signatures.

2.3.4. Roadside spring water sites

Three roadside sites were sampled across Newfoundland where spring water is either actively or previously collected for consumption or other domestic use. The spring water sites were selected from areas of contrasting geology to develop a one-off baseline of geochemical data, with emphasis on trace elements of potential health concern (Health Canada, 2019). The two actively used sites were a spring off Highway 430 near Wiltondale, NL draining through sedimentary rocks and one off Highway 450 near York Harbour, NL draining through mainly ultramafic-mafic rocks. The formerly used site (no longer used for drinking water) was sampled in Winterland at the Heritage Well site near Winterland, NL draining mainly granite. The specific locations are reported in Appendix 1.

2.4. Materials and methods

2.4.1. Field sampling

Between the 2 study sites a total of 30 locations were sampled within 1 week of field work in July 2022, along with the 6 major rivers. Of the 30 samples, 25 are hydrologically independent streams and are non-nested (not hydrologically connected). All sampled water was collected in acid-leached high-density polyethylene (HDPE) bottles. Acid leaching of sample bottles involved 1 week of soaking in a cold-water soap bath, followed by 2 weeks of bottles sitting in 10% hydrochloric acid (HCl) + 1% hydrofluoric acid (HF), followed by an additional 2 weeks sitting in 10% HNO_3. After acid-leaching was completed, all sample bottles were filled with ultra-pure ($\geq$ 18.2 MΩ) water from a Millipore Milli-Q IQ7000 unit and sealed until use in the field.

When sampling at each site, water was retrieved in a collection bottle from visibly flowing areas of the stream or river approximately 10 cm below the water surface and well above the bedload. All samples were filtered in-field using a vacuum-aided polysulfone ThermoFisher Nalgene filter unit, loaded with Nalgene membrane filters (47 mm diameter; 0.45 μm pore size; nylon). Filters were pre-wetted by filtering a small amount of sample water through the filter, which was then discarded prior to final sample filtration. Filtered samples were immediately transferred to two HDPE bottles (125 mL and 250 mL). Samples in 125 mL HDPE bottles were acidified immediately in-field to ~2% HNO_3 using in-house prepared triply distilled concentrated HNO_3. The acidified and unacidified sample bottles were sealed and kept cold and away from light until analysis at Trent University. Overall, sampling followed cleanliness protocols utilizing the "clean hands, dirty hands" approach, with one person designated 'clean hands' for all contact with sample bottles to minimize contamination while a separate 'dirty hands' person handled equipment (e.g., field probes) while sampling (Lurry and Kolbe, 2000).

At each sample location, pH, ORP, conductivity, and temperature measurements were taken using Oakton® ORPTestr® and PCTSTestrTM pocket testers (Appendix 1). ORP values are reported as the standard hydrogen electrode redox values (E_h), which were converted from ORP values. Field observations of each river were also noted, such as flow conditions and bedload material (Appendix 2).

2.4.2. Sample analysis & quality assurance/quality control

Filtered and acidified samples were measured within 1 month of field collection for element abundances at the Trent Water Quality Centre (WQC). Samples were combined with a pure solution of In (ICP-standard, PlasmaCAL) to serve as an internal standard (concentration of ~10

ng/g) for drift correction, resulting in negligible dilution, and measured directly using an Agilent 8800 inductively coupled plasma tandem mass spectrometer (ICP-MS/MS, colloquially "triple quadrupole ICP-MS"). The experimental method followed the procedure described in detail in previous studies (Dang et al., 2022b, 2022a). In brief, all analytes were measured in He-gas mode with the exception of Li and Be (no-gas mode) and V, As, Mo, Sb and all of the rare earth elements and Y (in O_2-mass shift mode). Samples reported in this study were measured in one experiment session. For quality assurance/quality control (QA/QC) purposes, two natural water reference materials (AQUA-1 and SLRS-6, n=6) were used to bracket every ten samples to assess within-experimental run analyte "recovery" after internal standard correction and to permit accuracy and long-term precision assessment. In terms of recovery, all repeat measurements were within 5% of the initial reference material measurements for individual experiments. For accuracy assessment, elements were compared to certified values when available (i.e., NRC-CNRC certificates for SLRS-6 and AQUA-1); however most trace elements in these reference materials were not certified as part of initial development, such that data confidence is instead built through inter-laboratory comparisons. The reference material measurements from this study are compared to previously published SLRS-6 means at the WQC (Dang et al., 2022a), and selected published values for SLRS-6 (Babechuk et al., 2020; Yeghicheyan et al., 2019) and AQUA-1 (Yeghicheyan et al., 2021). Repeat measurements of the reference materials throughout the experiment also provides an estimation of precision at two different element abundance levels. Reference material values from this study and comparison studies are reported in Appendix 3.

Filtered but unacidified samples were measured for dissolved organic and inorganic C (DOC and DIC) using a Total Organic Carbon (TOC) analyzer (TOC-VCPH, Shimadzu). Calibration solutions were prepared from potassium hydrogen phthalate (reagent ACS, Acros organics) for

DOC and sodium carbonate (99+% extra pure, Acros organics) for DIC. An organic carbon standard at 10 mg/L C, prepared from a certified standard (1000 mg/L C, LabChemTM), was used to bracket every 10 samples to monitor instrument stability; the measured concentrations were 10.06±0.07 mg/L C (n=5). A river water certified reference material PERADE-09 (Environment Canada) was used to validate the QA/QC; the measured DIC and DOC concentrations were 2.5±0.2 mg/L C and 4.3±0.3 mg/L C (n=3), in agreement with the certified values (2.4±0.4 mg/L C and 3.6±0.4 mg/L C, respectively).

2.4.3. Spatial analysis

Watershed boundaries of all sample locations were delineated in ArcGIS Pro 2.8.0 using a 5 m digital elevation model (DEM) created from 1:20,000 scale aerial photo (accuracy of 2 m). Processing was done using the Spatial Analyst Hydrology function to fill sinks, calculate flow directions and flow accumulation to determine contributing area above each sampling location.

To evaluate percent coverage of major lithology types and surficial geology within each watershed, this study used GIS files of bedrock geology downloaded from the Government of Newfoundland & Labrador Geology Survey Branch (Open File GS# NFLD/2192) and surficial geology downloaded from the Geological Survey's Newfoundland and Labrador GeoScience Atlas Online. Major lithologic units of each study area were categorized using the bedrock files as described in Section 2.5.1 (Figure 1 and 2). Surficial geology was divided into the three categories of till, exposed or partially concealed rock, and bog coverage (Figure 4 and 5). Vegetation data were extracted from the CanVec series (Wooded Areas, Saturated Soils and Landscape in Canada) under an open government license. Using attributes listed in this file, this study created a new layer labeled "Dense/Open Forest Coverage" which included polygons representing dense and open

broadleaf-type, coniferous-type, and mixed wood-type. Dense forest represents more than 40% canopy coverage and open forest represents canopy coverage between 20-40%. This new layer was to visualize where significant forest presence occurred within each study area (Figure 4 and 5). For further details about these descriptors see "Wooded Area" in Canvec metadata catalogue: NVCP 2018.

Calculations of spatial coverage of these layers within each catchment were accomplished using overlap analyses tool in QGIS 3.22.3. Mean slope values were calculated for each catchment area using the slope tool of the raster terrain analysis plugin. The slope tools calculates the slope of each cell in the 5 m DEM raster and is expressed in a degree, which represents change in elevation from horizontal. Mean slope values were computed using the zonal statistics raster analysis tool, producing the average of all slope values within the defined catchment areas (Appendix 1).

2.4.4. Data analysis

Principal component analyses (PCA) were done in R version 1.4.1717 using the built-in function 'prcomp', with all variables scaled for comparability. When introduced in text, active variables and individuals are denoted along with their principle component contribution values.

When reporting variance from data sets in this study, collectively or sub-divided by lithologic groupings, a mean or median was selected based on the specific variable distribution, and in the case of using a mean it was reported alongside 1 standard deviation.

Major cation-forming elements (Mg, Ca, Na, K; henceforth "major cations") were examined either as abundance variations or individually normalized to the sum of these elements (on a mass-based

abundance basis), denoted as Element/∑+, where ∑+ = Mg+Ca+Na+K, when comparing geochemical data across all streams. This approach is useful to compare data when there are wider concentration gradients and to account for hydrological effects such as dilution or runoff that can change with catchment and stream size. Where appropriate, major cation data was also examined using selected element ratios and relative proportion ternary plots. Notably, anion (e.g., Cl^-, SO_4^{2-}) data were not collected as part of this study, preventing the ability to use some traditional water-type classifications as well as to correct major cation data for any possible inputs from marine/atmospheric sources.

Trace element data were reported either as their measured abundance, as Element/∑+ (see above), or as individual inter-element mass ratio or normalized abundance ratio. Of the full trace element suite collected for this study, Ni, Co, and Cr were selected as the elements with the potential to make the closest links between waters and bedrock in the ultramafic-mafic catchments, whereas Li, Rb, Cs, Th, and U were selected for the same reason for the felsic rock catchments. The sum of rare earth elements (∑REE) was calculated as the sum of non-anomalous elements where: ∑REE=Pr+Nd+Sm+Tb+Dy+Ho+Er+Tm+Yb. All rare earth element+Y (REE+Y) patterns were normalized to the Mud from Queensland (MuQ) composite, an estimation of the upper continental crust (Kamber et al., 2005). Normalized REE+Y are denoted as REE_N. To evaluate the slope of the REE+Y pattern, ratios of a light REE (LREE), middle REE (MREE), or heavy REE (HREE) are used, typically Pr_N/Er_N (LREE/HREE), Pr_N/Tb_N (LREE/MREE), and Tb_N/Er_N (MREE/HREE). Anomalies of Ce (Ce_N/Ce_N^*) and Eu (Eu_N/Eu_N^*) were calculated using a geometric mean for REE_N^* (Lawrence et al., 2006a) where:

$$\boldsymbol{Ce_N^* = Pr_N^* \left(\frac{Pr_N}{Nd_N}\right)}$$

$$Eu_N^* = \left(Sm_N^2 * Tb_N\right)^{1/3}$$

In cases where one of the elements used in an anomaly calculation showed analytical scatter in a normalized pattern, an adjacent proxy element was used to project to where the element would be in a smooth pattern (also denoted REE_N*). When analytical scatter exerted too much influence on ratio-ratio plots, samples were sometimes excluded. The Y anomaly was calculated using the mass ratio of Y/Ho.

2.5. Results

2.5.1. Lithology and sample watershed classification

The bedrock geology of the BOIC in western Newfoundland was grouped into two major units: (1) an ultramafic unit that encompasses the mantle and melt-residual rocks of the ophiolite sequence, consisting of variable proportions of lherzolite, harzburgite, dunite, websterite, and orthopyroxenite and (2) a mafic layer that encompasses the intrusive and extrusive mafic rocks of the ophiolite sequence, consisting of layered gabbro, diabase dikes, and pillow basalt (Figure 1). The St. Lawrence Granite in the Burin Peninsula was considered as one unit (Figure 2). The percent coverage of each lithologic grouping within individual catchment areas was calculated up until the point of sampling (Table 2). From these calculations, sampled streams were categorized into groups based on relative coverage of a lithologic grouping as: (1) monolithologic catchments, (2) sub-monolithologic catchments, or (3) heterolithic/comparison catchments. Monolithologic catchments are defined as having dominant coverage (>60%) of one silicate lithology/lithologic group (granite, intrusive/extrusive mafic rocks, or intrusive ultramafic rocks). Sub-monolithologic catchments are defined as those that drain a significant proportion of a target lithologic groups

when it does not constitute the spatial coverage majority (between 18-60%). Heterolithic/comparison samples are those not draining the target lithology/lithologic groups, including those that drain either a mixture of several lithology-types or sedimentary units that were not targeted for this study.

Of the 19 streams sampled in western Newfoundland, 9 streams have been attributed to monolithologic catchments, (6 draining ultramafic units, 3 draining mafic units), 4 have been attributed to sub-monolithologic catchments, and 6 streams were considered heterolithic/comparison catchments. One of the 3 monolithologic mafic streams has been isolated from the others in many cases throughout this study due to its sampling shortly after a rain event that had an affect on the stream chemistry. Of the 11 streams sampled in Burin Peninsula, 5 streams were attributed to monolithologic catchments (all draining the SLG), 5 streams were attributed to sub-monolithologic catchments, and 1 was considered a heterolithic/comparison catchment (Table 2).

A lithologic categorization of the bedrock geology in the major river catchments was also undertaken based on the high-level subdivisions of Colman-Sadd et al. (1990) using the Open File GS# NFLD/2192, as shown in Figure 3 and in Table 2. As expected, the major river catchments contain a higher diversity of bedrock types relative to the smaller catchments.

2.5.2. Watershed characteristics – size, surficial coverage, topography, and vegetation

The catchment size, topography (evaluated as mean slope), surficial coverage (divided into % of till, exposed/concealed rock, and bog), and vegetation (% of dense/open forest) for all catchments is available in Appendix 1 and summarized in Table 3 by study site and by lithologic classification

(Section 2.5.1). Due to large gaps in available data and the larger catchment size, surficial geology and mean slope were not calculated for the major river catchments.

Across the two main study sites, sampled streams (n=30) drain catchments ranging in size from 0.8 km^2 to 278 km^2 (median: 6.8 km^2). The 6 Newfoundland major rivers sampled for this study drain catchments ranged in size from 203.9 km^2 (Garnish River) to 9579.6 km^2 (Humber River).

The catchments in western Newfoundland (n=19) have more variability in surficial coverage, topography, and vegetation compared to those in Burin Peninsula (n=11). Most notably, however, the western Newfoundland catchments include a high percentage of the surficial coverage that is exposed or partially concealed rock (median: 66%) compared to those in Burin Peninsula (median: 1%). Conversely, the Burin Peninsula catchments have more bog coverage (median: 22%) than those in western Newfoundland (median: 3%).

Mean slope refers to the average steepness of the land within the catchments, providing small indications of the hydrologic processes within the area. It is assumed that higher mean slope values would lead to faster runoff and increased erosion while lower mean slope values can indicate slower runoff and allow more water-rock interaction time and/or soil development. The topography of western Newfoundland is more mountainous, resulting in catchments with steeper terrains, (mean slope; median: 10%), larger elevation ranges (median: 581 m), and visibly fast-flowing water in the sampled streams. In contrast, the topography of the Burin Peninsula includes more extensive barrens, resulting in smaller average elevation ranges (median: 581 m), more low-lying terrain (mean slope: median: 3%), and slower-moving streams.

The coverage of dense/open vegetation type was slightly higher in catchments of western Newfoundland (median: 14%) compared to those in Burin Peninsula (median: 3%), reflecting an inverse relationship with bog coverage (Figure 4 and Figure 5). The vegetation was calculated and ranged between 15% to 76% coverage across the major river catchments.

2.5.3. Physicochemical properties and DIC/DOC of streams

The physicochemical properties and DIC/DOC of all samples are available in Appendix 1.

The streams sampled in western Newfoundland (n=19) were generally more oxidizing (E_h: 404-478 mV; median: 437 mV), more basic (pH 7.20-8.40; median: 7.95), and had higher conductivity (µS/cm 32.6-250.0; median: 85.8) compared to those sampled in Burin Peninsula that were overall less oxidizing (E_h: 350-509; median: 401 mV), more acidic (pH 6.28-8.11; median: 6.81), and had lower conductivity (µS/cm 34.1-252.0; median: 47.7). The DOC and DIC also varied between the two study sites, with streams in western Newfoundland having lower DOC (0.86-16.26; median: 3.15 mg/L) but higher DIC (1.32-19.29; median: 7.54 mg/L) than streams in Burin Peninsula with higher DOC (4.94-11.51; median: 7.94 mg/L) and lower DIC (0.49-16.36; median: 0.81 mg/L). Excluded from the western Newfoundland samples above was sample GM2207, a rain-affected sample that was distinct from all others measured with the highest DOC of 16.26 mg/L.

The major rivers had minimal variation in their E_h (397.4-426.6 mV) and a slim range in conductivity (17.5-40.0 µS/cm). Excluding the Garnish River with its slightly lower pH of 6.89, variations in the pH were minimal across the remaining major rivers (7.08-7.45). The DIC was consistently low across major rivers (0.59-1.21 mg/L) excluding the Humber River with a higher

value of 2.55 mg/L. Excluding the Garnish River with its higher DOC (8.56 mg/L), variations in DOC were minimal across the remaining major rivers (4.88-6.84 mg/L).

2.5.4. Lithologic compositions

Bedrock major element and trace element (when available) compositions from the catchments were compiled for comparison to the stream water and are available in Appendix 4. Data from rock units of the BOIC were compiled from Malpas (1976). The BOIC compilation includes data from dunite (including "critical zone" rocks) (n=18), harzburgite (n=18), and lherzolite (n=5), as well as diabase (n=13), gabbro (n=29), and basalt (typically pillow basalt) (n=6), representing the ultramafic and mafic groups, respectively. Data from the St. Lawrence Granite (n=6) were taken from Magyarosi (2022).

The relative differences in bedrock major element composition most relevant to the major cations in stream waters (Mg, Ca, Na, K) are illustrated in a molar ternary plot (Figure 6) and a scaled total% bar graph (Figure 7). The BOIC ultramafic rocks have the highest MgO wt% abundance, with mean MgO wt.% values of 30.56 ± 12.4 (dunite), and 35.49 ± 2.4 (lherzolite), and 38.38 ± 6.0 (harzburgite), followed by the BOIC mafic rocks with mean values of, 8.38 ± 1.9 (gabbro), 7.91 ± 1.12 (diabase), and 7.17 ± 1.32 (volcanic rocks). The SLG has the lowest MgO (0.01-0.74 wt.%). The BOIC mafic rocks have the highest CaO, with mean CaO wt.% of 13.06 ± 1.8 (gabbro), and 9.97 ± 1.4 (diabase) and 9.88 ± 2.2 (volcanic rocks), compared to the generally low values in the BOIC ultramafic rocks apart from some high values in dunite (up to 17.5 wt.%) and an anomalous harzburgite (19.05 wt.%). The CaO is consistently low in the SLG (0.11-1.12 wt.%). The Na_2O abundances are similar between the SLG (3.15-4.22 wt.%) and BOIC volcanic rocks (2.81-4.90 wt.%), but low in BOIC ultramafic rocks (<1.32 wt.%). The SLG has the highest K_2O

(mean: 4.94 ± 0.7; range: 4.19-6.47 wt.%) compared to the mafic and ultramafic rocks of BOIC where the K_2O is consistently less than 1.8 wt.% and 0.6 wt.%, respectfully.

Of the trace elements selected as proxies for ultramafic-mafic (Ni, Cr, Co) or felsic (Li, Rb, Cs, Th, U) bedrock, available data are sparse overall and/or below detection for the contrasting rock type expected to be depleted in the elements. The highest Ni and Cr are in the BOIC mafic (Ni: 28-548 mg/kg, median 3050; Cr: 24-833, median 197.5) and ultramafic (Ni: 90-4200 mg/kg, median 3050; Cr: 320-5800, median 197.50) rocks, where the highest Ni and Cr values are typically in harzburgite and dunite, respectively. The SLG has the lowest Ni (3-9 mg/kg) and Cr (1-4 mg/kg). Data for Co are more sparse and show higher values in the ultramafic rocks (33-158 mg/kg) relative to the SLG (2-5 mg/kg) albeit with less relative contrast in abundance. In contrast, the SLG has a higher Rb (247-416 mg/kg; median 321.5 mg/kg) compared to the mafic (3-18 mg/kg; median 8 mg/kg) and ultramafic (1-16 mg/kg; median 8 mg/kg) rocks of the BOIC. Lithium (21.5-145.1 mg/kg; median 37.4 mg/kg), Cs (1.5-6.2 mg/kg; median 4.2 mg/kg), Th (12.5-36.9 mg/kg; median 25.1 mg/kg), and U (4-10.9 mg/kg; median 7.1 mg/kg) in the SLG are also expected to be much higher than in the BOIC rocks, especially the ultramafic rocks; however, no data for these elements were available in the studies used in the compilation.

2.5.5. Stream geochemistry

The physicochemical properties (e.g., redox potential, conductivity, water temperature) of the streams were overall similar, indicating all waters were oxidized with minor differences between the geological endmember catchments. The conductivity is well-explained by a strong correlation with the sum of the major cations, with Ca or Ca+Mg being the dominant conductive ions. The stream geochemical differences are revealed with more detailed breakdown of their major and

trace element composition. To evaluate the compositional difference between streams that drain highly contrasting bedrock lithology, a PCA was used to illustrate element groupings between the endmember silicate monolithologic streams (Figure 8). The PCA explained 70.9% of the data variance (PC1: 54.5%, PC2: 16.4%) and captures: (1) groupings near the ultramafic streams (n=6) that include Mg, Ni, and Cr (but not Co despite it being more abundant in ultramafic bedrock relative to other bedrock types); (2) groupings near the mafic streams (n=2) that includes Ca; and (3) groupings near the granitic streams (n=5) that include Cs, Rb, Th, U, and Li. These groupings reveal the strong bedrock compositional association in the stream waters for several elements. In sub-monolithologic and heterolithologic/comparative streams, chemical association between stream water and bedrock is typically less apparent, and several other factors influencing the stream chemistry become more prominent.

Here, the major cations (Mg, Ca, Na, K) and the selection of elements showing strong correspondence between the stream water and respective dominant bedrock in the catchment (Ni, Cr, Co, Li, Cs, Rb, U, Th, REE+Y) are summarized in more detail, divided first by study site and then by their assigned lithologic categorization (Section 2.5.1). The major cation data are plotted alongside bedrock compositions in a relative proportion ternary plot (Figure 6) and separately in scaled % bar graphs divided by catchment and lithologic grouping (Figure 7). The major and trace element data are presented in several plots with a similar division by catchment and by lithology (Figure 9-11). The major river data are included in most of the aforementioned plots and considered separately in Figure 12.

Western Newfoundland

Major cations: The 6 ultramafic monolithologic streams are distinct in their major cation chemistry with their consistently high Mg abundance (6.37-8.60 mg/L; median: 6.81 mg/L) and highest relative proportion of Mg (Mg/∑+: 0.56-0.75) out of all stream waters (Figure 9). These streams show major cation variation in both Mg and Ca as indicated by a spread in Mg/Na ratios (2.14-3.90) and Ca/Na ratios (0.21-0.65) and also by a greater spread in Ca/Mg ratios (0.06-0.30) relative to K/Mg ratios (0.01-0.03) (Figure 13). The 3 mafic monolithologic streams are separated from the ultramafic monolithologic streams mainly by their lower abundance and relative proportion of Mg and higher relative proportion of Ca with 1 of the 3 samples (BI2205) being distinctly higher in Ca than the others (Figure 9). Such differences are captured well by the separation in Ca/Mg (1.47-4.71) and Mg/Na (0.34-0.42) relative to the ultramafic monolithologic streams which have lower ratio ranges of Ca/Mg (0.06-0.30) but higher ranges of Mg/Na (2.14-3.90) (Figure 13). The ultramafic sub-monolithologic streams (n=4) include the sample with the highest Mg abundance of all streams (9.5 mg/L in BI2207), 2 samples that overlap in Mg abundance with the ultramafic monolithologic streams (6.1-8.2 mg/L; sample GM2202 and BI2208), and 1 sample (GM2201) with lower Mg closer to the mafic monolithologic streams (Figure 9). The ultramafic sub-monolithologic sample with the highest Mg proportion has similar major cation proportions as the ultramafic monolithologic streams (Mg/∑+: 0.61; Ca/Mg: 0.21), whereas the remaining 3 have a major cation composition with Ca/Mg intermediate (0.34-1.27) between the mafic and ultramafic monolithologic streams (Figure 9). Other than Ca, a contrasting relative Na abundance separates the ultramafic monolithologic (Ca/Na: 0.21-0.65; median: 0.32) from sub-monolithologic (Ca/Na: 0.50-1.29; median: 0.76) streams. In the heterolithologic/comparison streams sampled in western NL (n=6), 3 of the samples (BI2203, BI2209, GM2211) have the highest Ca abundance of all measured streams, 2 of which have highest relative Ca proportion of all samples (Ca/∑+: 0.72-

0.83; Figure 9, Figure 6). These 3 samples are ones where the heterolithologic component includes sedimentary rocks. The major element composition of the remaining 3 heterolithologic/comparison samples is close to that of the monolithologic mafic samples (Figure 9, Figure 6), and have a higher component of igneous rock in their catchments (Figure 1).

Trace elements: The geochemical trends of Ni and Cr are similar to those of Mg. The highest abundance (Ni: 2412-9937 ng/L; median: 6887 ng/L; Cr: 946.5-1938 ng/L; median: 1556 ng/L) and relative proportions (Ni/∑+: 24 $x10^{-5}$ - 93$x10^{-5}$, median: 62 $x10^{-5}$; Cr/∑+: 8.5 $x10^{-5}$ - 19 $x10^{-5}$, median: 16 $x10^{-5}$) are found in the monolithologic ultramafic streams (Figure 10). Of the 3 mafic monolithologic streams, 2 have very low Ni abundances (76.0-570.8 ng/L) and Cr abundances below detection, whereas the rain-influenced sample (GM2207) has distinctly higher Ni and Cr abundances (Ni: 3096 ng/L; Cr: 1102 ng/L) and relative proportions (Ni/∑+: 46 $x10^{-5}$; Cr/∑+: 17 $x10^{-5}$) (Figure 10). The ultramafic sub-monolithologic streams are intermediate in Ni (1632-5636 ng/L; median: 2803 ng/L) and Cr (508.0-986.9 ng/L; median: 784.5 ng/L) abundances between the latter two groups, but are closer in composition to the ultramafic monolithologic streams. The heterolithologic/comparison streams show generally low Ni and Cr (when above detection) with 2 samples from the group having distinctly higher Ni (BI2202 and GM2210; 2450.3-1963.0 ng/L) and Cr (BI2202 and BI2203; 1121.7-1926.5 ng/L) than the others (Figure 10). Cobalt did not show much variation across the ultramafic monolithologic (16.9-45.8 ng/L; median: 34.3 ng/L), mafic monolithologic (12.3-23.8 ng/L; excluding GM2207), ultramafic sub-monolithologic (16.0-42.6 ng/L; median: 21.8 ng/L), and heterolithologic/comparison (10.3-54.6 ng/L; median: 31.2 ng/L) groupings. The rain-affected mafic monolithologic sample was distinct relative to all other streams with its high Co (70.7 ng/L; Co/∑+: 1.06 $x10^{-5}$). The Li, Rb, Cs, Th, and U abundances were very low across all of the ultramafic (monolithologic and sub-monolithologic) and mafic streams and

most of the heterolithologic/comparative streams in western Newfoundland (Figure 11); only 2 samples of the heterolithologic/comparative streams (GM2210 and BP2210) showed slightly elevated proportions of Li (Li/∑+: 4.2 $x10^{-5}$- 4.9 $x10^{-5}$) and Rb (Rb/∑+: 2.8 $x10^{-5}$-4.0 $x10^{-5}$).

REE+Y: Two clusters of REE+Y data are apparent between the ultramafic monolithologic (n=6) and sub-monolithologic (n=4) groupings. Of the monolithologic streams, 4 streams (GM2203-06) have lower ∑REE (2.0-9.1 ng/g) that match closely with 1 of the streams from the sub-monolithologic streams (BI2207) with similarly low ∑REE (5.8 ng/g) (Figure 14). These samples show a high degree of analytical scatter due to the abundance of REE being closer to the detection limit, especially sample GM2206 (Figure 15). The remaining samples from both ultramafic groupings plot at higher ∑REE (44.2-159.7 ng/g) with near-parallel normalized REE+Y patterns (Figure 15) defined by a relatively flat pattern across the MREE to HREE (Tb_N/Er_N: 1.15-1.33) and LREE>MREE depletion (Pr_N/Tb_N: 0.49-0.75) and generally correspond to the samples with a higher proportion of Ca relative to Mg (Ca/Mg: 0.21-1.27). The mafic monolithologic samples are split by REE abundance with 2 samples at lower ∑REE (34.8-42.5 ng/g) separated from the 1 rain-affected sample with much higher ∑REE (228.7 ng/g), but all 3 samples have parallel normalized REE+Y patterns that include a greater selective LREE>MREE (Pr_N/Tb_N: 0.30-0.58) depletion compared to the ultramafic groupings. All of the mafic and ultramafic groupings have negative Ce anomalies (Ce_N/Ce_N*: 0.20-0.90; median: 0.58; excluding GM2206) and most have minor positive Eu anomalies (Eu_N/Eu_N* 0.68-1.70; median: 1.25) as well as slightly superchondritic Y/Ho ratios (24.6-32.4; median: 29.2; excluding the 3 samples with lowest ∑REE) (Figure 14). The heterolithologic/comparative samples show a wider spread in ∑REE (13.9-277.3), but also identifiable sub-groups. Most notably, the 4 samples with the highest ∑REE (183.3-277.3) are those with major cation proportions similar to the mafic monolithologic streams (Figure 6) and

REE+Y patterns (Figure 15) similar to the mafic and ultramafic streams. The remaining heterolithologic samples have lower ∑REE and more pattern diversity.

Burin Peninsula

Major Cations: The 5 granite monolithologic streams have major cation chemistry that is generally high in Na relative proportion (Na/∑+: 0.34-0.74; median: 0.61 mg/L) compared to other sampled streams (Figure 9). Aside from the major rivers and some of the heterolithologic/comparison samples, the monolithologic granite streams have a higher relative proportion of K (K/∑+: 0.02-0.06; median: 0.02) compared to mafic-ultramafic streams, but this is not as distinct as for Na. One sample (BP2206) of the monolithologic streams has anomalously higher Ca abundance (19.29 mg/L) and relative proportion of Ca (Ca/∑+: 0.60) and is among the highest Ca of all the measured samples. The 5 sub-monolithologic granite streams also have one anomalous sample (BP2207) that measured distinctly high Na, K, and Ca abundance (Na: 45.25 mg/L; K: 3.39 mg/L; Ca: 7.16 mg/L) out of all measured stream waters (Figure 9). The two samples (BP2206 and BP2207) are identified as anomalous based on these major cation and other trace element characteristics. With these samples excluded, the sub-monolithologic granite streams have similar major cation composition to the monolithologic samples, as indicated by their scaled % bar graphs (Figure 7) and their similar major cation ratios (Figure 13).

Trace elements: The geochemical trends of the trace elements have greater diversity than the major cations within the monolithologic granite streams compared to all the other sampled streams. The highest abundance of Li (717.2-2246 ng/L; median: 1245 ng/L), Rb (454.1-1273 ng/L; median: 799.4 ng/L), and Cs (93.3-165.6 ng/L; median: 116.5 ng/L) are found in the monolithologic granite streams (Figure 11). The anomalous monolithologic granite stream (BI2206) has elevated

abundance of Li (2777 ng/L), Rb (18550 ng/L), and Cs (174.5 ng/L). Of the 5 monolithologic granite streams, 3 (BP2201, BP2205, BP2212) have elevated U (193.8-1038 ng/L) and Th (75.5-140.6 ng/L) abundance above all other streams, while the other 2 have lower abundance of U (10.3-32.9 ng/L) and Th (11.3-12.1 ng/L). Of the granite sub-monolithologic streams, the 1 anomalous stream (BI2207) contains an extremely elevated abundance of Li (9644 ng/L), Rb (6389 ng/L), and Cs (372.4 ng/L) over all other measured streams. The other 4 sub-monolithologic granite streams are generally lower in abundance of Li (601.4-1064 ng/L; median: 910.2 ng/L), Rb (301.9-535.7 ng/L; median: 390.8 ng/L), and Cs (25.3-63.7 ng/L; median: 39.5 ng/L) compared to the monolithologic group, but still contain somewhat elevated values relative to those in western NL. The sub-monolithologic granite streams contain similar U (47.4-226.0 ng/L; median: 84.3 ng/L) and Th (12.6-24.2 ng/L; median: 21.0 ng/L) abundances to that of the lower U and Th abundances measured in the monolithologic streams. The Ni and Cr abundances were either very low or below detection for the monolithologic and sub-monolithologic granite streams while Co was at slightly elevated abundance (7.2-105.4 ng/L) and elevated relative proportion (Co/∑+: 0.08 $x10^{-5}$ – 0.9 $x10^{-5}$) in the monolithologic granite streams compared to those in western NL.

REE+Y: Similar to the western NL, the REE+Y data in Burin Peninsula can be split into two clusters among the monolithologic (n=5) and sub-monolithologic (n=5) granite groupings. Two streams (BP2208 and BP2212) from the monolithologic category have lower ∑REE (581.6-597.3 ng/g) that match closely with 4 sub-monolithologic streams that have similarly low ∑REE (379.3-413.0 ng/g), while 1 sub-monolithologic stream (BP2207) has higher ∑REE (1722 ng/g) that matches with the higher ∑REE of 3 of the monolithologic streams. The two anomalous samples (BP2206 and BP227), as determined above, are included in the higher group. This latter group of higher ∑REE are defined by deeply negative Eu anomalies (Eu/Eu*: 0.15-0.32), LREE>MREE

depletion (Pr_N/Tb_N: 0.38-0.57) but flatter MREE to HREE patterns (Tb_N/Er_N: 0.68-1.08). The group of lower measured ∑REE samples have parallel normalized REE+Y patterns that include some with a slightly greater selective LREE>HREE (Pr_N/Tb_N: 0.56-1.16) depletion, albeit less extreme than the higher ∑REE cluster. All of the granite samples show minimal to slightly negative Ce (Ce_N/Ce_N*: 0.75-1.13; median: 0.89), negative Eu anomalies (Eu_N/Eu_N*: 0.15-0.98; median: 0.47), and super-chondritic Y/Ho ratio (32.01-41.06; median: 36.02) (Figure 14).

2.6. Discussion

2.6.1. Geologic controls on stream water chemistry revealed by monolithologic and sub-monolithologic streams and application to larger catchments

Several small-catchment studies have previously demonstrated the utility of selecting water sampling locations draining a restricted catchment geology (often labeled "monolithologic"). This study used geospatial data to more specifically define the bedrock division in small catchments up to the point of sampling (Section 2.4.3), allowing for independent comparison to the geochemical data (Section 2.5.4). Connecting these two data sets is demonstrably useful in defining geologically controlled differences in stream water chemistry.

Plotting the specific % of ultramafic bedrock in the monolithologic (>60%) and sub-monolithologic (18%-60%) catchment water samples of western Newfoundland against the proportion of elements (Element/∑+) with expected links to ultramafic bedrock (Mg, Ni, and Cr) reveals moderate to strong positive correlations (Figure 16). This co-variation emphasizes the control on the stream water chemistry mainly from the interaction of waters with the weatherable mafic minerals in the ultramafic rocks. In this case, the control is likely due to olivine with

secondary contributions from pyroxenes, potentially chromite for Cr, and the alteration minerals developed during seafloor serpentinization such as Mg-bearing carbonate. The correlation between the % of ultramafic bedrock and element proportion in stream waters decreases for Ni and Cr, and for Co is not well defined, indicating that the geology/mineralogy has only a moderate control on stream chemistry with other factors emerging (further discussed in Section 2.6.2 and 2.6.3). The proportion of Ca in the monolithologic and sub-monolithologic streams is also plotted against the % of ultramafic bedrock and shows a lower proportion of Ca in the ultramafic streams relative to the mafic streams, but without a strong inverse correlation. These can be explained as reflecting the inverse geological relationship of ultramafic-mafic rock proportion in the catchments, as illustrated by the lithologic trends seen if combining all ultramafic rock types (lherzolite, dunite, harzburgite) from the ultramafic lithologic grouping (Section 2.5.1) relative to the combined mafic rock types (gabbro, diabase, and volcanic rocks). In this case, the greater weatherability of plagioclase, which has less capacity for Ca-retention in secondary weathering products, would likely dominate the Ca supply over clinopyroxene, which has more capacity for Ca-retention in smectites formed during earlier weathering stages. However, other local effects related to specific water-interaction pathways in the ultramafic streams seems to also be important (Section 2.6.2).

Plotting the specific % of granite bedrock in the monolithologic and sub-monolithologic catchment water samples of Burin Peninsula against the proportion of elements with expected links to granite bedrock (Na, K, Li, Rb, Cs, Th, U) (Figure 17) reveals a positive correlation only for Rb and Cs, presumably tracking their coupled enrichment in K-bearing minerals such as K-feldspar and micas (Heier, 1962; Horstman, 1957). The lack of correlation of the remaining elements indicates that other controls (e.g., mineral host, uptake in vegetation, particle reactivity) all play a more important

role than geology in the flatter, more bog-covered catchment of Burin Peninsula (further discussed in Section 2.6.3).

To emphasize the strongly contrasting and geologically controlled geochemical signatures of the small ultramafic and granite catchment streams, it is useful to compare these data from Newfoundland waters to other small catchment monolithologic studies to place them in a more global context. For this purpose, the focus is on major cations (Mg, Ca, Na, K) due to the greater availability of data, and ratio-ratio plots of Ca/Mg-K/Mg and Ca/Na-Mg/Na (Figure 13; see figure caption for data sources) are useful for comparison as they can level hydrological factors such as flux (climate/weathering) and dilution on element abundances. The greatest relative contrast between the ultramafic and granite streams is seen by the highly contrasting Mg abundances in the source rocks, such that both the K/Mg and Ca/Mg ratios are effective in separating the two groups from each other (Figure 13). Compared to other ultramafic streams, there is generally good overlap in these ratios, with the Newfoundland stream samples plotting to slightly higher K/Mg and Ca/Mg values. The Newfoundland granite streams plot on the lower end of K/Mg and Ca/Mg values relative to other granite streams. While the ratio comparison indicates a similar overall geologic control on the Newfoundland streams, the lower K/Mg may be due to the local climate being less conducive to K release from the K-rich SLG granites during chemical weathering and/or more efficient K retention under slower stream flow through bog cover that is prevalent at the study site.

The Ca/Mg ratio also distinctly separates the ultramafic samples from the mafic monolithologic samples, granite samples (monolithologic and sub-monolithologic), and heterolithologic samples. This separation between the ultramafic samples from the higher Ca/Mg ratios measured in the mafic and granitic stream samples likely arises due to the greater contribution from plagioclase

within the granite and mafic catchments, but in the latter case could also include contributions from fluorite or other Ca-bearing minerals in altered areas of the granite. The additional contributions from sedimentary sources (including carbonate) are likely driving the higher Ca/Mg ratios in the heterolithologic/comparison streams (Figure 13).

When comparing the endmember granite and ultramafic streams from Newfoundland to other areas with Ca/Na and Mg/Na a different story emerges. The ultramafic monolithologic streams are offset from the majority of comparison streams towards a coupled lower Mg/Na and Ca/Na (Figure 13). Given the very low Na in the source rocks, this offset is better explained by atmospheric input of cations, which is known to affect primarily Na (e.g., Fernández-Martínez et al., 2019), compared to the comparison sites. All data from other streams were compiled without any correction for atmospheric contributions, but most of the study sites examined previously are from more continental areas further removed from the sea than the Newfoundland samples. All ratios involving Na are likely to be influenced by this contribution, which is seemingly evident in the very low Mg/Na of the ultramafic sub-monolithologic samples, although these samples likely record the combined effects of Na released from plagioclase and atmospheric Na contributions. Based on similar plotting location of the comparison granite samples compared to the Newfoundland granite (monolithologic and sub-monolithologic) samples, there seem to be less influence from atmospheric Na contribution, likely due to the greater relative contribution of Na from the source rock compared to ultramafic streams. Nevertheless, the behavior of Na is not considered further in this study.

Most of the selected low-abundance tracer elements (Li, Rb, Cs, Th, U, Cr, Co, and Ni) show strong geochemical contrast between the monolithologic ultramafic and granite streams. Taking

the mean value from the monolithologic ultramafic and granite streams (excluding sample BP2206 from the latter), the ultramafic streams are 62 times higher in Ni (Cr cannot be directly compared due to being below detection in all granite streams), and the granite streams are 10, 5, 97, 48, and 98 times higher in Li, Rb, Cs, Th, and U, respectively. Cobalt is noted to show a narrower spread in abundances between the geologically contrasting streams, overlapping within the uncertainty of their means, but with the granite streams generally having higher Co abundances. The contrast of these elements between the small endmember catchments is further emphasized through a comparison of the Newfoundland monolithologic (granite, ultramafic) streams to a world major river average trace element abundance (Gaillardet et al., 2014) (Figure 18). When normalized to the world major river average, the Ni and Cr in the ultramafic streams is 2 and 8 times higher than the compiled world average, and the Cs and Th in the granite streams are 11 times and 1.5 times higher, respectively while the Li, Rb, and U overlap within uncertainty of the compiled world average.

Establishing the key geochemical patterns of small streams draining endmember silicate bedrock compositions (monolithologic ultramafic and granite) also provides useful comparison to the chemistry of the larger rivers within the province, as represented by the 6 major rivers sampled for this study (Table 4). In general, with the exception of Co being lower in abundance in major rivers relative to the small catchment streams, the mean values of the major rivers are intermediate between the chemistry of the endmember small catchments for Li, Rb, Cs, Th, U, Cr (taking 3 times the detection limit as a proxy for granite streams), and Ni (Figure 18). However, Rb and Ni abundances overlap between major rivers and granite monolithologic streams. Although not the focus of this study, there are also geospatial and geochemical links that can be seen within major river data. Most notably, the major river catchments that drain >20% intrusive granitoid lithology

(Terra Nova, Gander, and Piper's Hole) show separation in their Li, Cs, Rb, and U abundances relative to other major rivers and are closer to the granite monolithologic streams. In the case of Terra Nova and Piper's Hole, it is especially notable that the headwaters of the catchment are preferentially dominated by the granitoid rocks (Figure 3) and indicate that signatures inherited in small catchments survive downstream collected into a larger river system even when the downstream catchment contains a diversity of geology. This effect is presumably most prominent for elements that have both strong source enrichment and higher aqueous solubility, but nonetheless suggests the importance of bedrock contribution upstream, relevant to applications such as mineral exploration and environmental management practices.

2.6.2. Assessing interrelated controls on stream chemistry in small, ultramafic-mafic catchments of western Newfoundland

Moderate to strong correlations in the western Newfoundland stream water proportional abundances and % ultramafic bedrock was demonstrated for Mg, Ni, and Cr, but not Co, in Section 2.6.1 (Figure 17). Elements Mg, Ni, and Cr in the stream chemistry are most prominently related to bedrock element abundances. However, other factors related to the geology or vegetation/soils are also inferred to play important secondary roles, even for Mg where the clearest and strongest correlation exists with % of ultramafic bedrock.

The ultramafic rocks are part of an obducted ophiolite that often defines mountainous terrain where surface runoff and groundwater discharge contribute to stream input. Within the ultramafic streams, the high proportion of Mg in waters relative to Ca, could be the result of Ca removal at hyper-alkaline spring sites (Morrill et al., 2014; Szponar et al., 2013), several of which are present in the area of stream sampling. The groundwater draining from upland areas rapidly develops high

pH and upon emanation at springs, mixes with meteoric water and precipitates Ca-carbonate. This effect would drive up the relative proportion of Mg>Ca in surface waters; however, since the groundwater reactions are unique to the (continental) serpentinization in ultramafic rocks, there is still an expected strong correlation of the Mg proportion with % ultramafic bedrock.

Beyond the lack of correlation observed for Co, there was also appreciable scatter and variation in abundance for Ni and Cr within the ultramafic streams, which point to additional factors that are contributing to the stream water chemistry for these elements. This section takes a deeper analysis of potentially important factors for Ni, Cr, and Co that includes consideration of probable element speciation, weathering/soil effects, and redox effects. This evaluation is developed partly from a study site-specific PCA (using only monolithologic and sub-monolithologic ultramafic-mafic data and considering all chemical, geospatial, and physicochemical variables) as well as a comparison with other studies that look at streams draining similar bedrock.

A PCA, explaining 33.7% (PC1) and 22.5% (PC2) of the data variability, confirms the grouping of Mg and Ni with ultramafic bedrock coverage (Figure 19) atop of the strong correlation of Mg (r^2=0.86) and moderate correlation of Ni (r^2=0.39). Despite the generally poor vegetation cover in the western Newfoundland study site, there is modest secondary correlation of Ni with Fe (r^2=0.29; graph not shown), that becomes much stronger (r^2=0.73; graph not shown) when considering only the monolithologic ultramafic samples. Further, there is a strong positive correlation between Ni abundance and DOC (r^2=0.75; graph not shown) in the latter ultramafic sample group. These results are best explained by Fe and Ni being transported in streams as organo-metallic complexes, likely originating from surficial runoff from areas with soil and vegetation present, such as the

marshy areas atop plateaus of ultramafic rock massifs. Plant uptake through upper soil horizons is also known to be an important control on the budget of Ni exported to streams in ultramafic catchments (Estrade et al., 2015) and other small-stream studies have demonstrated an association of Ni with dissolved organic matter, implying the importance of complexation processes within the active weathering environment of soils prior to export to streams (Antić-Mladenović et al., 2017; Pokrovsky et al., 2006; Sekaly et al., 2003). Weathering processes are important controls on the Ni export and its isotopic ratio in major river systems (Cameron and Vance, 2014). Such effects are further supported by weathering profile studies linking Ni behavior to the extent of primary mineral degradation and its incorporation and adsorption in secondary minerals, citing Fe-(oxy)(hydr)oxides as an important control (Sun et al., 2024). Streams in other catchments draining Ni-rich ultramafic bedrock, but within a warmer climate and/or better developed vegetation/soil cover, have higher Ni abundances than those in western Newfoundland, as evident from those in California (Ni µg/L: mean: 3.8, range: 0.9-21.2) (McClain and Maher, 2016) and Italy (Ni µg/L mean: 8.43, range: 1.1-20.4) (Binda et al., 2018). Collectively, these observations suggest that, beyond the source rock Ni abundance, influences from both weathering effects and other processes that promote the release of Ni are important in the western Newfoundland catchments. As Ni is concentrated in a weathering zone prior to release, it is expected to have a stronger association and coherent trends with its main secondary mineral hosts (e.g., Fe-(oxy)(hydr)oxides). The release of Ni is then aided by rainfall events, which, through the addition of meteoric water, facilitate the export of dissolved Ni bound to organic matter.

The association of Cr with Mg and ultramafic rock coverage in western Newfoundland is evident with the moderate correlation in Figure 16, and the association of high Cr with ultramafic rocks in other catchments globally is well-established. However, the dependence of climate, which

influences weathering and subsequent processes within weathering profiles and Cr host mineralogy, are the most probable secondary controls on dissolved Cr abundances in stream waters. For example, studies have reported relatively low stream Cr abundances in a temperate climates in mountainous terrain (mean 1.17 µg/L; range: 0.13-2.86) (Binda et al., 2018), but elevated abundances in temperate coastal (Cr µg/L mean: 10.47, range: 0.77-30.26) (McClain and Maher, 2016) and tropical climates (Cr µg/L mean: 47.0, range: 5.3-162.8) (Delina et al., 2020). The Cr abundances measured in this study are most similar to those from temperate climate in a mountains terrain. The primary control from the weathering environment on Cr is the oxidation of Cr^{3+} to the more soluble aqueous species of Cr^{6+} (Fendorf, 1995; Rai et al., 1989). However, even under tropical weathering conditions the majority of the Cr budget in weathered ultramafic rocks can remain locked in chemically resistant minerals, such as Cr-spinel, or be strongly adsorbed and/or structurally incorporated into secondary minerals, such as Fe-(oxy)(hydr)oxides (e.g., Delina et al., 2020). Considering the limited soil development within the western Newfoundland study site and that the release of Cr^{3+} from bedrock minerals is an essential prerequisite step to forming soluble Cr^{6+}, the low Cr abundance in ultramafic stream waters from Newfoundland is not surprising, even with very high Cr in source rocks. However, as investigated by McClain and Maher (2016), complexed soluble Cr^{3+} species may also be an important contribution to Cr budgets within alkaline ultramafic stream environments, providing an additional pathway for elevated dissolved Cr levels in streams through reducing the rate of Cr^{3+} oxidation and adsorption to particulates at high pH. The hyper-alkaline groundwater springs identified in the ultramafic bedrock of the western Newfoundland study area (Morrill et al., 2014; Szponar et al., 2013) were hypothesized to play a role in aiding aqueous Cr mobility; however, a lack of correlation between

dissolved Cr with Ca or DIC suggests that Cr^{3+}-carbonate species were not a major component of the stream waters.

Among the selected tracer elements that are known to be enriched in ultramafic rocks and soils (Kierczak et al., 2021), Co was unique in not exhibiting any association with % of ultramafic bedrock, and also in showing lower abundances in the ultramafic streams relative to other streams from this study. Other studies across climates but with similar ultramafic bedrock report low Co abundances (Binda et al., 2018; Delina et al., 2020; McClain and Maher, 2016). A moderate correlation of Co with Fe across the ultramafic streams (r^2=0.43; graph not shown) is apparent and, if isolating just the ultramafic monolithologic streams, a strong correlation with DOC (r^2=0.86; graph not shown) and stronger correlation with Fe (r^2=0.73; graph not shown) is revealed. These trends form close parallels with the secondary effects identified for Ni. Specifically, a close association with organic matter in weathering environments followed by continued close association in waters (likely with organic matter complexes) predominate as the main controls in the western Newfoundland catchments. The decoupling of Co from ultramafic rock abundance indicates that the element remains closely associated with all secondary minerals until conditions in soils, independent of source rock variations, aid the element's export to streams. This observation is supported by other studies noting linked Ni-Co-organic matter associations in streams (Pokrovsky et al., 2006) and increased Co abundance in boreal catchments specifically linked to streams draining more heavily forested areas with developed soils (Wällstedt et al., 2017). Further, the slightly higher Co documented in the Burin Peninsula granite catchments relative to the western Newfoundland ultramafic catchments (Figure 10) despite the higher Co in the ultramafic bedrock emphasizes that environmental controls outweigh geological controls.

2.6.3. Assessing interrelated controls on stream chemistry in small, granite catchments of Burin Peninsula

Moderate correlations in the Burin Peninsula stream water proportional abundances and % granite bedrock was demonstrated for Rb and Cs, but not the other elements enriched in the bedrock (Li, Th, U, K) (Figure 17). Such observations reflect the range of more complex element behavior coupled with the increased influence of various environmental factors within the study site, including indirect relationships with slower stream flow through more bog-covered and vegetated terrain. Here, a deeper analysis of the interrelated controls on these elements is considered similar to the approach in Section 2.6.2, with the exclusion of the anomalous samples identified in the monolithologic and sub-monolithogic groupings (BP2206 and BP2207). Although sampled streams drained areas of the East lobe, West lobe, and Winterland porphyry of the SLG (Section 2.3.2), the compositional variation of the granite itself (Section 2.5.4) does not vary enough to likely produce a difference in the stream waters, so was not considered further as a factor.

A PCA, explaining 35.5% (PC1) and 23.3% (PC2) of the data variability, for the granite streams (monolithologic and sub-monolithologic) (Figure 20) affirms the grouping of bedrock with Rb, although less with Cs. A close association between K, Rb, and Cs is expected in felsic igneous bedrock where all elements are commonly present in K-feldspar and micas (Heier, 1962; Horstman, 1957). However, during weathering and through interaction within the aqueous environment, fractionation of these elements from each other is expected. Specifically secondary clay minerals in soils and fluvial sediments will preferentially scavenge Cs>Rb>K (Nesbitt et al., 1980; Tanaka and Watanabe, 2015; Wu et al., 2022) along with preferential uptake of K over Rb and Cs in vegetation (Chaudhuri et al., 2007; Peltola et al., 2008). The stronger positive correlation

of % granite abundance with the proportion of Rb relative to Cs is consistent with the higher relative adsorption potential of Cs on secondary minerals. Nonetheless, the close association of % granite bedrock with both increasing Rb and Cs is important in revealing that bedrock geological control on these elements persists even through secondary mineral effects. In contrast, the lack of correlation of K with % granite bedrock is unexpected as K has generally greater weathering mobility relative to Cs and Rb. The other factors that influence K fluxes to the hydrosphere are inputs from atmospheric sources (e.g., Chang et al., 2020) or uptake within vegetation (e.g., Choudhury et al., 1994; Uhlig et al., 2017). The ratio K/Rb can be a useful indicator to track differences in weathering effects and plant litter decay. Global average ratio of river waters have an average K/Rb ratio of ~1000 (Chaudhuri et al., 2007). While the mean ultramafic (monolithologic/sub-monolithologic) and mafic streams (excluding rain-affected sample GM2207) is similar to this global average (mean: 1210 ± 230; range: 795-1540), the mean K/Rb of granite (monolithologic/sub-monolithologic) streams is much lower (mean: 330±110; range: 200-500). These lower granite stream K/Rb ratios are comparable to those also found in the 6 Newfoundland major rivers (mean: 530 ± 270; range: 310-910). It is unlikely that atmospheric deposition of K would preferentially influence the granite catchments over the ultramafic-mafic catchments given both sites have similar proximity to the coast. It is also unlikely that atmospheric inputs have a selective influence on much larger river systems further removed from the coast. The clear variations of K/Rb between the small-catchment study sites suggest that the abundance of vegetation in the Burin Peninsula plays an important role in the greater uptake of K relative to Rb. Similarly, the larger major river catchments extend predominantly through boreal forest ecosystems with greater development of vegetation that bear more similarity to the Burin Peninsula site than the western Newfoundland ultramafic site. Such observations have two important

implications. First, vegetation in boreal climate zones appears to efficiently fractionate K/Rb, and that this fractionation is traceable in streams. Second, using K to track inputs from the weathering of felsic bedrock to streams may be less effective than with Rb and Cs, as the lack of relative uptake of these latter elements by vegetation results in a stronger geochemical signature linked to bedrock, despite their higher affinity for clay adsorption.

Lithium exhibits a notably higher abundance in granite streams compared to all others in this study, indicating a geological control. However, at the catchment scale, there is no clear association between Li and the other selected granite tracer elements (K, Rb, Cs, Th, U) and the Li abundances do not show an association with Na, which would imply atmospheric sources as a dominant control. Lithium is also decoupled from K and is not established as having any significant biological function/uptake (Pogge von Strandmann et al., 2010), such that any uptake in vegetation would only be passive. Isolating only monolithologic granite streams, Li shows strong positive correlations with DIC (r^2=0.85), Ca (r^2=0.78), Sr (r^2=0.82), and Mo (r^2=0.89). While the latter elements were not the focus of the study, these trends establish a separate geological control independent of the other alkali elements. In general, the decoupled behavior of Li from other alkalis is not surprising, as its behavior is largely driven by its smaller ionic radii and association with other mineral phases (Huh et al., 1998). Such mineral phases could be related to the potential Ca-rich mineral phase among the granite catchments, where more plagioclase-rich rocks may be contributing to streams. The E lobe of the SLG has also been documented to show extensive alteration, where quartz and potassium feldspar have been replaced by albite and calcite (Strong, 1982), which could be an additional potential source. Further assessment of Li sources is not undertaken here.

Thorium and U are both enriched in granite and typically associated with accessory minerals (Bea, 1996 and references therein) and the co-enrichment of both elements in surface waters has established links to felsic plutonic rocks (e.g., Frengstad et al., 2000). In this study, the granite stream waters show an expected overall enrichment, linked to bedrock, relative to other streams (Figure 11). However, the variations of Th and U in granite monolithologic streams are decoupled from % of granite bedrock and most other variables. Instead, PCA helped to identify the catchment mean slope variable as having an association with Th and U. This association is also shown independently through strong correlations between mean slope and $Th/\sum^{+}$ ($r=0.82$) and $U/\sum^{+}$ ($r=0.65$) (Figure 21). Individual correlations are also apparent for Th-U abundances and those of the REE ($Th/\sum^{+}$ ($r^2=0.92$) and $U/\sum^{+}$ ($r^2=0.73$)). Together, these observations indicate a distinction between catchments with higher elevation gradients, where there is more preferential release of Th and U from granite and catchments with lower elevation gradients, where the removal of such elements after release to waters begins to dominate. The combined supply of Th, U, and REE is evident primarily in catchment streams with more direct runoff from the granite, likely recording surface water and groundwater fluxes. The link to REE suggests that accessory mineral weathering is important to Th-U release. Some studies have shown an association between Th-U enrichment and waters high in dissolved organic matter (Olivie-Lauquet et al., 2001; Viers et al., 1997), often linked to wetland-dominated areas. However no direct correlation between $Th/\sum^{+}$ and $U/\sum^{+}$ with DOC or percent bog coverage (between 8%-38%) was found in the Burin Peninsula catchments, emphasizing that the dominant role of the vegetation was Th-U uptake.

Thorium-U fluxes also have contrasting relative solubility and redox-controlled mobility, resulting in decoupled aqueous behavior. Thorium is less soluble and almost exclusively colloid-bound (Degueldre and Kline, 2007; Langmuir and Herman, 1980; Short et al., 1988). In contrast, U can

form soluble species upon oxidation of U^{4+} in host rock minerals to soluble U^{6+} and has a greater proportion in the truly dissolved load relative to colloid-bound U (Plater et al., 1992; Porcelli et al., 1997; Somayajulu, 1994; Swarzenski et al., 2004). The contrasting Th-U behavior can be monitored through changes in Th/U ratios in waters relative to source rocks. In this study all of the granite waters (mean: 0.38±0.29; 0.10-1.1) are lower than the ratios of whole-rock granite (3.0-4.3) and indicate an expected preferential transfer of U>Th overall during weathering and aqueous transport.

2.6.4. REE+Y as tracers of both source rock input and catchment processes

The REE+Y abundances, patterns, and anomalies of stream waters have established utility for tracing variation controlled by source rock, as well as the effects of weathering and aqueous geochemical processes in surface environments (e.g., Babechuk et al. 2020; Ingri et al. 2000; Lawrence et al. 2006; Steinmann and Stille 2008). As such, assessing the key differences and commonalities in the dissolved REE chemistry of waters, within their constrained geological context, can isolate source-rock from process-related controls.

Several REE+Y features display prominent bedrock controls. Western Newfoundland streams draining ultramafic rocks measure the lowest overall REE abundances and samples with the greatest contribution from Mg-ultramafic bedrock (defined by lower Ca/Mg ratios) have the lowest REE. The increase in Ca contribution, accompanied by a corresponding increase in REE concentrations across the ultramafic monolithologic and sub-monolithologic streams, likely indicates a contribution shift from the highly REE-depleted ultramafic rocks to Ca-bearing source rock with higher REE, as seen through higher Ca/Mg ratio. This association is further reflected in the corresponding subtle LREE/MREE depletion of the samples with higher Ca and elevated REE

contributions. This MuQ-normalized pattern pattern closely parallels those documented in some pillowed basalt, diabase, and gabbroic rocks from the BOIC (Suen et al., 1979), suggesting a potential link of these streams with increased weathering contribution from minor mafic rock sources. However, it is recognized that such contribution could originate from ultramafic rocks with higher clinopyroxene abundance.

The two streams associated with mafic monolithologic catchments (excluding the rain-affected sample GM2207) have REE abundances similar to those of the higher-Ca ultramafic streams described above. However, their patterns have a distinct positive Eu anomaly that is absent in samples from all other lithologically grouped streams. This Eu feature is likely related to the greater abundance of plagioclase in the mafic bedrock, which can be preferentially weathered compared to other common basalt minerals, such as pyroxene, during early stages of weathering (Eggleton et al., 1987; Nesbitt and Wilson, 1992; Wilson, 2004). The LREE>MREE depletion in the basalt streams is also suggested to be primarily bedrock controlled since LREE-depleted basalts are documented in the BOIC (Suen et al., 1979), but this feature could be amplified by preferential LREE retention in basaltic weathering profiles (Babechuk et al., 2014).

In contrast to the mafic-ultramafic streams, the granite streams have much higher REE abundances, greater variability in MREE/HREE and LREE/MREE slopes, consistently positive Y anomalies, and variable but generally negative to highly negative Eu anomalies. With the exception of the Y anomaly (discussed further in Section 2.6.5), these features reflect the normalized REE+Y patterns of the SLG (Magyarosi, 2022); however, the variability in the MREE/HREE could point to an association with variable accessory mineral weathering.

Overall, across the two sites and three bedrock types, there is strong coherence of stream water REE+Y features with the associated catchment bedrock, suggesting bedrock dominates as a control on REE abundance and pattern. Such observation is notable as aquatic fractionation and colloid exchange process, rather than lithology, is shown to have stronger control on dissolved REE+Y abundances and patterns in larger rivers. Often such controls are tied with stream pH, where higher REE abundances and LREE>HREE enrichment correspond to decreasing pH (Byrne and Sholkovitz, 1996; Elderfield et al., 1990; Lawrence et al., 2006a).

The data from this study show an association of higher REE with lower pH that separates the samples of the two endmember catchment lithologies. However, this association is better explained as indirect rather than causal, with the bedrock composition controlling the REE abundance and the bedrock-associated terrain and hydrological and vegetation conditions controlling the pH. The lower pH observed for granite streams is generated by the granite terrain favoring flatter and boggier areas with greater organic acid flux. Conversely, the more alkaline pH of the western Newfoundland streams is generated through increased flux of the Mg-rich minerals that release hydroxide ions, raising the pH of the waters (McClain and Maher, 2016; Neal and Shand, 2002) and the lack of well-developed soils/vegetation.

Overprinted on the bedrock-controlled REE features is a consistent negative Ce anomaly present across nearly all streams (Figure 14, Figure 15). Cerium anomalies are well-established as a tracer of redox conditions from weathering profiles (e.g., Middelburg et al., 1988; Patino et al., 2003) through to aquatic systems (e.g., Koppi et al., 1996; Laveuf et al., 2008), reflecting the oxidation of Ce^{3+} to Ce^{4+} by soil or sediment Mn-(oxy)(hydr)oxides followed by preferential retention of Ce on particles compared to the remaining REE^{3+}. The presence of the negative Ce anomalies within

streams of this study, persisting even near their headwater sources with limited time for water to interact with fluvial particles, suggest that soil processes exert a greater influence over aquatic processes on the anomaly development. The pervasive nature of the negative Ce anomaly from the small stream waters to the major rivers in Newfoundland indicates that boreal soil systems (even with various stages of soil development) are effective in oxidizing and retaining Ce. Dissolved organic matter in soil and aquatic systems and their relationship to topography are also known to be important to the magnitude of the Ce anomaly when transferred to surface waters (Gruau et al., 2004; Pédrot et al., 2015). Specifically, organic matter can inhibit the particle interactions of Ce^{3+} that ultimately result in Ce oxidation (Davranche et al., 2008, 2005). The results of this study reveal supporting evidence for these interrelated effects of topography and organic matter influencing the Ce anomaly. When considering all stream and major river data (excluding the 4 heterolithologic/comparison samples with sedimentary rock in the catchment to avoid pre-existing Ce anomalies transferred into streams), there is a strong correlation between DOC and Ce_N/Ce_N^* (r^2=0.67). In effect, the ultramafic-mafic streams, characterized by higher pH, lower DOC and draining more mountainous terrain, had the most negative Ce anomalies, whereas granite streams draining terrain with lower elevation gradients measured less negative Ce anomalies that coincided with increasing DOC levels and lower pH.

The final observation of note within the REE+Y data is the supercrustal Y/Ho ratios that are most prevalent in the granite streams. While slightly supercrustal Y/Ho ratios are a common feature reported in river waters (e.g., Babechuk et al., 2020; Lawrence et al., 2006b), the values observed in Burin Peninsula granite streams reach values higher than typically reported (>35). Often, such high Y/Ho ratios are only seen in estuary settings where freshwater mixes within seawater and fractionation is most efficient (Lawrence and Kamber, 2006; Nozaki et al., 2000) or in areas with

anthropogenic input involving runoff interacting with fertilizers (Hu et al., 1998). However, there is no agricultural land in the granite catchment that could result in anthropogenic modification of stream Y/Ho ratios. The much lower REE abundance of seawater compared to that of the streams leaves Y/Ho changes from atmospheric deposition of marine materials (e.g. sea spray or aerosols) improbable. Further, there are no apparent correlations of Y/Ho with Na (assuming Na as the best proxy for marine input). Therefore, the high Y/Ho ratios must be generated from source and/or weathering effects that are unique to the granite catchments compared to the ultramafic-mafic and major river catchments.

The Y/Ho ratios of the SLG are typical for crustal rocks (25.0-27.8; Magyarosi, 2022). It is conceivable that supercrustal Y/Ho ratios could be generated from granite weathering by more efficient Ho>Y scavenging during chemical weathering compared to other systems where supercrustal Y/Ho ratios have been reported, or that preferential dissolution of accessory minerals with more Y than Ho contributed disproportionately to stream waters. However, the higher DOC concentrations and suppressed Ce anomalies within the streams provide evidence for inhibited REE-particle interaction, where Y/Ho fractionation would occur. Further, previous studies evaluating Y/Ho fractionation in the weathering environment (Babechuk et al., 2015; Thompson et al., 2013) identified the abundance of (oxy)(hydr)oxides as an important driver of Y/Ho fractionation. The lower Fe/Mn abundance in the granite bedrock would result in less (oxy)(hydr)oxide development and less efficient Y/Ho fractionation in granite soils relative to soils developed on more mafic bedrock.

With regard to selective accessory mineral dissolution controlling the high Y/Ho, there is no easy way to support or refute the possibility. However, the fluorite mineralization observed throughout

the SLG granite (Section 2.3.2) is noteworthy. The fluorite veins have a high Y/Ho (>90; Collins, 1992), typical of the hydrothermal-magmatic conditions that drive Y/Ho fractionation in such systems (Bau, 1996; Bau and Dulski, 1995). With the lack of direct evidence that can explain the supracrustal Y/Ho values in the Burin granite streams, contributions from the weathering of fluorite mineralization is the suggested explanation. While it is challenging to directly establish this link, the two anomalous samples from the monolithologic and sub-monolithologic groupings seem to offer some support, as discussed in more depth in Section 2.6.5.

2.6.5. Anomalous samples and their geological and temporal influences at a localized scale

Three samples in this study were identified as "anomalous" (distinct in chemistry relative to others in the grouping), with 2 from Burin Peninsula (one each from the granite monolithologic and sub-monolithologic groupings) and 1 from western Newfoundland (mafic monolithologic). The 2 Burin Peninsula samples (BP2206 and BP2207) have much higher element concentrations (e.g., Rb, Cs, Th, U) relative to the remaining samples in the area. Since sampling occurred during the same day with minimal weather pattern changes, the unusual features are not attributed to changes in hydrology. Instead, the specific geochemical features of these streams, which includes much higher Ca than the other samples, coupled with their close proximity to fluorite veins (Figure 22) seems to suggest that localized weathering of the veins was the dominant influence. The SLG and other volcanic rocks in the area are generally very low in Ca (Magyarosi, 2022), therefore suggesting that the fluorite veins would be a probable additional source of Ca to the streams. The 2 anomalous streams also have the highest concentrations of Ca, Cu, Sr, Pb, and ∑REE, and the first and third highest Ba (several elements with capacity to substitute into fluorite; Collins, 1992). The 2 anomalous streams have the most elevated Y/Ho ratios. The high Y/Ho of the other streams

in the catchment was already hypothesized to be related to the fluorite veins (Section 2.6.4), but the highest Y/Ho in these 2 streams with the closest proximity to fluorite veins is not likely to be coincidental. To further evaluate the fluorite-stream water chemistry association, a PCA was conducted using only the Burin Peninsula streams (Figure 23). The PCA used the assumed diagnostic vein features (Ca, Cu, Ba, Sr, Pb, ∑REE, and Y/Ho), diagnostic granite signatures (Cs, Rb, and Li), and other relevant elements evaluated in 2.6.3. (Na, K, Eu_N/Eu_N^*) as variables. The resulting PCA describes 81.1% of the data variance with two principal components, PC1 explaining 61.1% and PC2 explaining 20.2% of the variance. The analysis revealed 2 distinct groups, one comprising the assumed diagnostic vein features and the other consisting of negative Eu_N/Eu_N* anomalies. While not the focus of the study, these observations lay interesting groundwork for the potential application for mineral exploration and as an area for further investigation in terms of potential health/environmental impacts.

The 1 western Newfoundland sample (GM2207) from a monolithologic mafic catchment collected shortly after a significant rain event was distinct from the 2 other mafic monolithologic streams (Section 2.5.4). This sample was visibly more orange-hued in water color and measured the highest DOC of all samples collected (Section 2.5.3), including those draining through bog area in the Burin Peninsula. This rain-affected sample was similar in its major cation chemistry to the other mafic monolithologic samples, but was distinct in its enrichment of specific trace elements, most notably REE abundances and Fe-Mn-Ni-Co. The normalized REE+Y pattern was similar to the other mafic monolithologic streams but had a less negative Ce anomaly (Figure 14, Figure 15). As discussed across Section 2.6.2 to 2.6.4, all of these trace element features are linked via their association with organic matter. Finally, the K/Rb ratio of the rain-affected sample (GM2207) is lower than the other 2 mafic monolithologic samples, suggesting a Rb>K flux, which can be

explained as export from soil waters where more K is retained in vegetation. Although the anomalous sample tracks only a single point in time after one rain event, it provides good evidence that such events generate more surface runoff that can flush elements out of soils, specifically those with a strong affinity for complexation with dissolved organic matter.

2.6.6. Evaluation of trace elements in groundwater tapped for present day or historical drinking water

Roadside springs are visited across Newfoundland and other Atlantic provinces for drinking water use, but these springs are often not routinely monitored for trace elements to evaluate for potentially toxic elements (PTEs) such as As, U, Cd, Co, Cr, Cu, Hg, Ni, Pb, Sb, and Zn (Nieder and Benbi, 2023; Pourret and Hursthouse, 2019). Variation in natural bedrock compositional are liable to influence groundwater chemistry in a similar way as documented for the stream waters in this study (e.g., Frengstad et al., 2000). The three spring samples taken from distinct lithologic zones (granitic, mafic, and sedimentary) were screened for PTE abundance levels (As, U, Pb, Cr, Cu) and compared to Canadian drinking water guidelines (Health Canada, 2019).

All PTE abundances were generally low and none exceeded guideline values of concern (Figure 24). However, when evaluated against each other, concentrations of PTEs align with expected enrichments of surrounding rock. The granite spring water measured slightly acidic and more reducing waters relative to the mafic or sedimentary spring waters and measured the highest abundance of Zn, Cd, As, and Pb (Appendix 1). Conversely the mafic spring water measured the

highest abundance of Cr, Cu, and Ni relative to the other spring samples, and the sedimentary spring water measured the highest levels of U.

Although measured values of PTEs were not within levels that would pose general concern, some research suggests that even low levels can pose health risks (e.g., Ahmad and Bhattacharya, 2019). Further, these results are from one-off sampling from only a small number of springs used across the province. Of particular concern within Newfoundland and Labrador are U and As and risk maps have been developed for these elements to indicate areas that may be of potential concern in well water (https://www.gov.nl.ca/mpa/files/waterres-cycle-groundwater-well-arsenic4a.pdf, https://www.gov.nl.ca/ecc/files/waterres-cycle-groundwater-well-uranium.pdf). The province monitors many community water supplies, but often these services are not available within rural communities. This study underscores the dimension imposed from natural lithology variations in Newfoundland. By linking element enrichments to specific bedrock and processes, it offers additional potential to better understand the natural controls and pathways of PTEs.

2.7. Conclusions

This study undertook a multi-element analysis of the dissolved load (<0.45 µm) of small catchment stream waters draining a restricted range of bedrock lithology (ultramafic rock, mafic rock, and granite) at two sites (western Newfoundland and Burin Peninsula) across the island of Newfoundland (Newfoundland & Labrador, Canada). The small catchment streams were compared to 6 major rivers across the island (Terra Nova, Gander, Exploits, Humber, Piper's Hole, and Garnish Rivers) and 3 roadside spring sites used for active or past local community consumption were sampled to screen for any elevated element abundances of potential health concern. This is the first study to report an element dataset with a wide suite of elements in the

trace (<1 mg/L) to ultra-trace (<1 µg/L) abundance range from any freshwater in this Canadian province. A primary goal of this study was to separate the geologically controlled variations in streams expected to be linked to the highly contrasting bedrock mineralogy/geochemistry, (mainly ultramafic rock vs. granite) from other natural catchment parameters that can directly or indirectly influence stream chemistry (elevation gradient, vegetation cover, surficial geology). A subset of elements was selected for focus (major cations; ultramafic elements: Ni, Co, Cr; felsic elements: Li, Cs, Rb, Th, U; REE+Y) and all other catchment parameters were quantitatively assessed via publicly available geospatial data for comparison to the geochemical data. This integrated geochemical-geospatial approach was useful in isolating the bedrock geological controls by enabling the separation of monolithologic streams, defined as those draining >60% of the target lithology, from those with decreasing amount of the target lithology. Additionally, it allowed for more confident identification of the elements influenced by interrelated catchment controls. In most cases, further insight into the dominant non-lithologic control could be identified based on correlations with other parameters that aligned with current knowledge from research at other sites across the globe. The key findings of this study were:

- The major cation chemistry of the small, lithologically restricted catchments resembles that of other regions worldwide draining the same rock types, exhibiting distinct separation of Mg-Ca-K, with the exception of modifications from uncorrected marine atmospheric influence (notably Na in all catchments; potentially more prominent in Newfoundland due to its proximity to the ocean) and some K-retention by vegetation (observed in granite streams only).

- The chemistry of Mg, Ni, and Cr are moderately to strongly controlled by the abundance of ultramafic rock in the western Newfoundland catchments, but also have secondary factors

associated with groundwater vs. surface runoff and the dissolved organic matter generated in areas of poorly developed soil and vegetation.

- The chemistry of Rb and Cs is most strongly controlled by the abundance of granite in the Burin Peninsula catchments despite their strong affinity for clay adsorption; K was revealed as less diagnostic of felsic bedrock despite its greater mobility and is likely due to its preferential association with vegetation in this catchment relative Rb and Cs.

- Thorium and U showed evidence for more complicated cycling out of bedrock with likely export from the weathering of accessory minerals in granite (with expected U>Th export due to its greater solubility) in streams closer to hilly areas of granite followed by strong uptake into other environmental reservoirs during transport through slow-flowing streams through bog and vegetative areas.

- Cobalt was completely decoupled from enrichment in bedrock and exhibited higher values in granite streams relative to mafic and ultramafic streams, despite inverse enrichment in the bedrock compositions. Cobalt's primary control seems to be the stronger influence of weathering processes and organic complexation in soils, aiding its transport to streams.

- REE+Y abundances, normalized pattern slopes, and Eu anomalies were most strongly controlled by bedrock composition rather than direct aqueous controls, such as stream pH.

- Cerium anomalies are prominent throughout all streams and rivers, reflecting efficient Ce oxidation and scavenging in boreal climate weathering systems, but also show an important secondary association with DOC that supports organic matter complexation as a further important role in controlling the magnitude of the anomaly.

- The highly superchondritic Y/Ho ratios in the granite stream waters of the Burin Peninsula are suggested to arise from the weathering of fluorite mineralization. Such elevated Y/Ho ratios of the Burin Peninsula are among the highest measured for freshwaters.

- Roadside spring waters show chemical variations reflective of the surrounding bedrock, but did not contain any elements (of the measured suite) that were near levels of health concern.

2.8.References

Ahmad, A., Bhattacharya, P., 2019. Arsenic in Drinking Water: Is 10 µg/L a Safe Limit? Curr Pollution Rep 5, 1–3. https://doi.org/10.1007/s40726-019-0102-7

Andersson, J.-O., Nyberg, L., 2009. Using official map data on topography, wetlands and vegetation cover for prediction of stream water chemistry in boreal headwater catchments. Hydrol. Earth Syst. Sci. 13, 537–549. https://doi.org/10.5194/hess-13-537-2009

Antić-Mladenović, S., Frohne, T., Kresović, M., Stärk, H.-J., Tomić, Z., Ličina, V., Rinklebe, J., 2017. Biogeochemistry of Ni and Pb in a periodically flooded arable soil: Fractionation and redox-induced (im)mobilization. Journal of Environmental Management, Biogeochemistry of trace elements in the environment 186, 141–150. https://doi.org/10.1016/j.jenvman.2016.06.005

Babechuk, M.G., O'Sullivan, E.M., McKenna, C.A., Rosca, C., Nägler, T.F., Schoenberg, R., Kamber, B.S., 2020. Ultra-trace Element Characterization of the Central Ottawa River Basin using a Rapid, Flexible, and Low-volume ICP-MS Method. Aquat Geochem 26, 327–374. https://doi.org/10.1007/s10498-020-09376-w

Babechuk, M.G., Widdowson, M., Kamber, B.S., 2014. Quantifying chemical weathering intensity and trace element release from two contrasting basalt profiles, Deccan Traps, India. Chemical Geology 363, 56–75. https://doi.org/10.1016/j.chemgeo.2013.10.027

Babechuk, M.G., Widdowson, M., Murphy, M., Kamber, B.S., 2015. A combined Y/Ho, high field strength element (HFSE) and Nd isotope perspective on basalt weathering, Deccan Traps, India. Chemical Geology 396, 25–41. https://doi.org/10.1016/j.chemgeo.2014.12.017

Batterson, M.J., Taylor, D.M., 2009. Till geochemistry of the Burin Peninsula, Newfoundland (NTS map areas 1L/13, 1L/14, 1M/2,1M/3, 1M/4, 1M/6, 1M/7, 1M/10 and 1M/11) (No. NFLD/3043). Government of Newfoundland and Labrador, Department of Natural Resources, Geological Survey.

Bau, M., 1996. Controls on the fractionation of isovalent trace elements in magmatic and aqueous systems: evidence from Y/Ho, Zr/Hf, and lanthanide tetrad effect. Contributions to Mineralogy and Petrology 123, 323–333. https://doi.org/10.1007/s004100050159

Bau, M., Dulski, P., 1995. Comparative study of yttrium and rare-earth element behaviours in fluorine-rich hydrothermal fluids. Contr. Mineral. and Petrol. 119, 213–223. https://doi.org/10.1007/BF00307282

Bea, F., 1996. Residence of REE, Y, Th and U in Granites and Crustal Protoliths; Implications for the Chemistry of Crustal Melts. Journal of Petrology 37, 521–552. https://doi.org/10.1093/petrology/37.3.521

Binda, G., Pozzi, A., Livio, F., Piasini, P., Zhang, C., 2018. Anomalously high concentration of Ni as sulphide phase in sediment and in water of a mountain catchment with serpentinite bedrock. Journal of Geochemical Exploration 190, 58–68. https://doi.org/10.1016/j.gexplo.2018.02.014

Bluth, G.J.S., Kump, L.R., 1994. Lithologic and climatologic controls of river chemistry. Geochimica et Cosmochimica Acta 58, 2341–2359. https://doi.org/10.1016/0016-7037(94)90015-9

Byrne, R.H., Sholkovitz, E.R., 1996. Chapter 158 Marine chemistry and geochemistry of the lanthanides, in: Handbook on the Physics and Chemistry of Rare Earths. Elsevier, pp. 497–593. https://doi.org/10.1016/S0168-1273(96)23009-0

Cameron, V., Vance, D., 2014. Heavy nickel isotope compositions in rivers and the oceans. Geochimica et Cosmochimica Acta 128, 195–211. https://doi.org/10.1016/j.gca.2013.12.007

Chabaux, F., Riotte, J., Dequincey, O., 2003. U-Th-Ra Fractionation During Weathering and River Transport. Reviews in Mineralogy and Geochemistry 52, 533–576. https://doi.org/10.2113/0520533

Chang, C.-T., Shih, Y.-T., Lee, L.-C., Lee, J.-Y., Lee, T.-Y., Lin, T.-C., Huang, J.-C., 2020. Effects of Land Cover and Atmospheric Input on Nutrient Budget in Subtropical Mountainous Rivers, Northeastern Taiwan. Water 12, 2800. https://doi.org/10.3390/w12102800

Chaudhuri, S., Clauer, N., Semhi, K., 2007. Plant decay as a major control of river dissolved potassium: A first estimate. Chemical Geology 243, 178–190. https://doi.org/10.1016/j.chemgeo.2007.05.023

Choudhury, B.J., Ahmed, N.U., Idso, S.B., Reginato, R.J., Daughtry, C.S.T., 1994. Relations between evaporation coefficients and vegetation indices studied by model simulations. Remote Sensing of Environment 50, 1–17. https://doi.org/10.1016/0034-4257(94)90090-6

Church, W.R., Riccio, L., 1977. Fractionation trends in the Bay of Islands ophiolite of Newfoundland: polycyclic cumulate sequences in ophiolites and their classification. Can. J. Earth Sci. 14, 1156–1165. https://doi.org/10.1139/e77-105

Collins, C.J., 1992. A fluid inclusion and trace element geochemical study of the granite-hosted, St. Lawrence fluorspar deposits and related host rocks (masters). Memorial University of Newfoundland.

Colman-Sadd, S., Hayes, J., Knight, I., 1990. The Geology of the Island of Newfoundland: Government of Newfoundland and Labrador, Department of Mines and Energy. GL#NFLD/2192.

Dang, D.H., Ma, L., Ha, Q.K., Wang, W., 2022a. A multi-tracer approach to disentangle anthropogenic emissions from natural processes in the St. Lawrence River and Estuary. Water Research 219, 118588. https://doi.org/10.1016/j.watres.2022.118588

Dang, D.H., Wang, W., Sikma, A., Chatzis, A., Mucci, A., 2022b. The contrasting estuarine geochemistry of rare earth elements between ice-covered and ice-free conditions. Geochimica et Cosmochimica Acta 317, 488–506. https://doi.org/10.1016/j.gca.2021.10.025

Davranche, M., Pourret, O., Gruau, G., Dia, A., Jin, D., Gaertner, D., 2008. Competitive binding of REE to humic acid and manganese oxide: Impact of reaction kinetics on development of cerium anomaly and REE adsorption. Chemical Geology 247, 154–170. https://doi.org/10.1016/j.chemgeo.2007.10.010

Davranche, M., Pourret, O., Gruau, G., Dia, A., Le Coz-Bouhnik, M., 2005. Adsorption of REE(III)-humate complexes onto MnO2: Experimental evidence for cerium anomaly and lanthanide tetrad effect suppression. Geochimica et Cosmochimica Acta 69, 4825–4835. https://doi.org/10.1016/j.gca.2005.06.005

Degueldre, C., Kline, A., 2007. Study of thorium association and surface precipitation on colloids. Earth and Planetary Science Letters 264, 104–113. https://doi.org/10.1016/j.epsl.2007.09.012

Delina, R.E., Arcilla, C., Otake, T., Garcia, J.J., Tan, M., Ito, A., 2020. Chromium occurrence in a nickel laterite profile and its implications to surrounding surface waters. Chemical Geology 558, 119863. https://doi.org/10.1016/j.chemgeo.2020.119863

Dillon, P.J., Molot, L.A., 1997. Effect of landscape form on export of dissolved organic carbon, iron, and phosphorus from forested stream catchments. Water Resources Research 33, 2591–2600. https://doi.org/10.1029/97WR01921

Ebeling, P., Kumar, R., Lutz, S.R., Nguyen, T., Sarrazin, F., Weber, M., Büttner, O., Attinger, S., Musolff, A., 2022. QUADICA: water QUAlity, DIscharge and Catchment Attributes for large-sample studies in Germany. Earth System Science Data 14, 3715–3741. https://doi.org/10.5194/essd-14-3715-2022

Eggleton, R.A., Foudoulis, C., Varkevisser, D., 1987. Weathering of Basalt: Changes in Rock Chemistry and Mineralogy. Clays and clay miner. 35, 161–169. https://doi.org/10.1346/CCMN.1987.0350301

Elderfield, H., Upstill-Goddard, R., Sholkovitz, E.R., 1990. The rare earth elements in rivers, estuaries, and coastal seas and their significance to the composition of ocean waters. Geochimica et Cosmochimica Acta 54, 971–991. https://doi.org/10.1016/0016-7037(90)90432-K

Estrade, N., Cloquet, C., Echevarria, G., Sterckeman, T., Deng, T., Tang, Y., Morel, J.-L., 2015. Weathering and vegetation controls on nickel isotope fractionation in surface ultramafic environments (Albania). Earth and Planetary Science Letters 423, 24–35. https://doi.org/10.1016/j.epsl.2015.04.018

Fendorf, S.E., 1995. Surface reactions of chromium in soils and waters. Geoderma 67, 55–71. https://doi.org/10.1016/0016-7061(94)00062-F

Fernández-Martínez, M., Margalef, O., Sayol, F., Asensio, D., Bagaria, G., Corbera, J., Sabater, F., Domene, X., Preece, C., 2019. Sea spray influences water chemical composition of Mediterranean semi-natural springs. CATENA 173, 414–423. https://doi.org/10.1016/j.catena.2018.10.035

Frengstad, B., Midtgård Skrede, A.K., Banks, D., Reidar Krog, J., Siewers, U., 2000. The chemistry of Norwegian groundwaters: III. The distribution of trace elements in 476 crystalline bedrock groundwaters, as analysed by ICP-MS techniques. Science of The Total Environment 246, 21–40. https://doi.org/10.1016/S0048-9697(99)00413-1

Gaillardet, J., Viers, J., Dupré, B., 2014. Trace Elements in River Waters, Treatise on Geochemistry. https://doi.org/10.1016/B0-08-043751-6/05165-3

Gruau, G., Dia, A., Olivié-Lauquet, G., Davranche, M., Pinay, G., 2004. Controls on the distribution of rare earth elements in shallow groundwaters. Water Research 38, 3576–3586. https://doi.org/10.1016/j.watres.2004.04.056

Health Canada, 2019. Guidelines for Canadian Drinking Water Quality—Summary Table.

Heier, K.S., 1962. Trace elements in feldspars, a review. Nor. Geol. Tidski 42, 415–455.

Horstman, E.L., 1957. The distribution of lithium, rubidium and caesium in igneous and sedimentary rocks. Geochimica et Cosmochimica Acta 12, 1–28. https://doi.org/10.1016/0016-7037(57)90014-5

Hu, Y., Vanhaecke, F., Moens, L., Dams, R., del Castilho, P., Japenga, J., 1998. Determination of the aqua regia soluble content of rare earth elements in fertilizer, animal fodder phosphate and manure samples using inductively coupled plasma mass spectrometry. Analytica Chimica Acta 373, 95–105. https://doi.org/10.1016/S0003-2670(98)00399-7

Huh, Y., Chan, L.-H., Zhang, L., Edmond, J.M., 1998. Lithium and its isotopes in major world rivers: implications for weathering and the oceanic budget. Geochimica et Cosmochimica Acta 62, 2039–2051. https://doi.org/10.1016/S0016-7037(98)00126-4

Ingri, J., Widerlund, A., Land, M., Gustafsson, Ö., Andersson, P., Öhlander, B., 2000. Temporal variations in the fractionation of the rare earth elements in a boreal river; the role of colloidal particles. Chemical Geology 166, 23–45. https://doi.org/10.1016/S0009-2541(99)00178-3

Kamber, B.S., Greig, A., Collerson, K.D., 2005. A new estimate for the composition of weathered young upper continental crust from alluvial sediments, Queensland, Australia. Geochimica et Cosmochimica Acta 69, 1041–1058. https://doi.org/10.1016/j.gca.2004.08.020

Kerr, A., Dunning, G.R., Tucker, R.D., 1993. The youngest Paleozoic plutonism of the Newfoundland Appalachians: U–Pb ages from the St. Lawrence and François granites. Can. J. Earth Sci. 30, 2328–2333. https://doi.org/10.1139/e93-202

Kierczak, J., Pietranik, A., Pędziwiatr, A., 2021. Ultramafic geoecosystems as a natural source of Ni, Cr, and Co to the environment: A review. Science of The Total Environment 755, 142620. https://doi.org/10.1016/j.scitotenv.2020.142620

Koppi, A.J., Edis, R., Field, D.J., Geering, H.R., Klessa, D.A., Cockayne, D.J.H., 1996. Rare earth element trends and cerium-uranium-manganese associations in weathered rock from Koongarra, Northern Territory, Australia. Geochimica et Cosmochimica Acta 60, 1695–1707. https://doi.org/10.1016/0016-7037(96)00047-6

Krám, P., Hruška, J., Shanley, J.B., 2012. Streamwater chemistry in three contrasting monolithologic Czech catchments. Applied Geochemistry, 13th International Symposium on Water-Rock Interaction (WRI -13) 27, 1854–1863. https://doi.org/10.1016/j.apgeochem.2012.02.020

Langmuir, D., Herman, J.S., 1980. The mobility of thorium in natural waters at low temperatures. Geochimica et Cosmochimica Acta 44, 1753–1766. https://doi.org/10.1016/0016-7037(80)90226-4

Laveuf, C., Cornu, S., Juillot, F., 2008. Rare earth elements as tracers of pedogenetic processes. Comptes Rendus Geoscience 340, 523–532. https://doi.org/10.1016/j.crte.2008.07.001

Lawrence, M.G., Greig, A., Collerson, K.D., Kamber, B.S., 2006a. Rare Earth Element and Yttrium Variability in South East Queensland Waterways. Aquat Geochem 12, 39–72. https://doi.org/10.1007/s10498-005-4471-8

Lawrence, M.G., Jupiter, S.D., Kamber, B.S., 2006b. Aquatic geochemistry of the rare earth elements and yttrium in the Pioneer River catchment, Australia. Mar. Freshwater Res. 57, 725. https://doi.org/10.1071/MF05229

Lawrence, M.G., Kamber, B.S., 2006. The behaviour of the rare earth elements during estuarine mixing—revisited. Marine Chemistry 100, 147–161. https://doi.org/10.1016/j.marchem.2005.11.007

Lidman, F., Mörth, C.M., Laudon, H., 2012. Landscape control of uranium and thorium in boreal streams – spatiotemporal variability and the role of wetlands. Biogeosciences 9, 4773–4785. https://doi.org/10.5194/bg-9-4773-2012

Lurry, D.L., Kolbe, C.M., 2000. Interagency Field Manual for the Collection of Water-Quality Data (Open-File Report No. 00–213), Open-File Report. USGS.

Magyarosi, Z., 2022. Late-magmatic processes in the St. Lawrence Granite: Implications for fluorite mineralization. Journal of Geochemical Exploration 239, 107014. https://doi.org/10.1016/j.gexplo.2022.107014

Magyarosi, Z., Sparkes, B.A., Conliffe, J., Dunning, G.R., 2019. The AGS fluorite deposit, St. Lawrence: paragenetic sequence, fluid-inclusion analysis, structural control, host rock geochronology and implications for ore genesis (No. 19–1). Newfoundland and Labrador Department of Natural Resources Geological Survey.

Malpas, J., Bottinga, Y., Francis, T.J.G., Brown, G.M., O'Hara, M.J., Oxburgh, E.R., 1978. Magma generation in the upper mantle, field evidence from ophiolite suites, and application to the generation of oceanic lithosphere. Philosophical Transactions of the Royal Society of London. Series A, Mathematical and Physical Sciences 288, 527–546. https://doi.org/10.1098/rsta.1978.0032

Malpas, J.G., 1976. The petrology and petrogenesis of the Bay of Islands Ophiolite Suite, Western Newfoundland (Thesis (Doctoral (PhD))). Memorial University of Newfoundland.

McClain, C.N., Maher, K., 2016. Chromium fluxes and speciation in ultramafic catchments and global rivers. Chemical Geology 426, 135–157. https://doi.org/10.1016/j.chemgeo.2016.01.021

Middelburg, J.J., van der Weijden, C.H., Woittiez, J.R.W., 1988. Chemical processes affecting the mobility of major, minor and trace elements during weathering of granitic rocks. Chemical Geology 68, 253–273. https://doi.org/10.1016/0009-2541(88)90025-3

Miller, R.R., 1994. Rare-metal metallogeny in Newfoundland and Labrador. In: Geological Survey Branch, Newfoundland Department of Mines and Energy, Final Report. Geoscience Contract Project NC.1.2.1, Canada-Newfoundland Cooperation Agreement on Mineral Development.

Mistikawy, J.A., Mackowiak, T.J., Butler, M.J., Mischenko, I.C., Cernak, R.S., Richardson, J.B., 2020. Chromium, manganese, nickel, and cobalt mobility and bioavailability from mafic-to-ultramafic mine spoil weathering in western Massachusetts, USA. Environ Geochem Health 42, 3263–3279. https://doi.org/10.1007/s10653-020-00566-7

Mora, A., Moreau, C., Moquet, J.-S., Gallay, M., Mahlknecht, J., Laraque, A., 2020. Hydrological control, fractionation, and fluxes of dissolved rare earth elements in the lower Orinoco River, Venezuela. Applied Geochemistry 112, 104462. https://doi.org/10.1016/j.apgeochem.2019.104462

Morrill, P.L., Brazelton, W.J., Kohl, L., Rietze, A., Miles, S.M., Kavanagh, H., Schrenk, M.O., Ziegler, S.E., Lang, S.Q., 2014. Investigations of potential microbial methanogenic and carbon monoxide utilization pathways in ultra-basic reducing springs associated with present-day continental serpentinization: the Tablelands, NL, CAN. Front. Microbiol. 5. https://doi.org/10.3389/fmicb.2014.00613

Neal, C., Shand, P., 2002. Spring and surface water quality of the Cyprus ophiolites. Hydrology and Earth System Sciences 6, 797–817. https://doi.org/10.5194/hess-6-797-2002

Négrel, P., 1999. Geochemical Study of a Granitic Area – The Margeride Mountains, France: Chemical Element Behavior and 87Sr/86Sr Constraints. Aquatic Geochemistry 5, 125–165. https://doi.org/10.1023/A:1009625412015

Nesbitt, H.W., Markovics, G., Price, R.C., 1980. Chemical processes affecting alkalis and alkaline earths during continental weathering. Geochimica et Cosmochimica Acta 44, 1659–1666. https://doi.org/10.1016/0016-7037(80)90218-5

Nesbitt, H.W., Wilson, R.E., 1992. Recent chemical weathering of basalts. American Journal of Science 292, 740–777. https://doi.org/10.2475/ajs.292.10.740

Nieder, R., Benbi, D.K., 2023. Potentially toxic elements in the environment – a review of sources, sinks, pathways and mitigation measures. Reviews on Environmental Health. https://doi.org/10.1515/reveh-2022-0161

Nozaki, Y., Lerche, D., Alibo, D.S., Snidvongs, A., 2000. The estuarine geochemistry of rare earth elements and indium in the Chao Phraya River, Thailand. Geochimica et Cosmochimica Acta 64, 3983–3994. https://doi.org/10.1016/S0016-7037(00)00473-7

O'Brien, S.J., Strong, P.G., Evans, J.L., 1977. Geology of the Grand Bank and Lamaline map areas; in Report of Activities for 1976 (No. 77–1). Newfoundland Department of Hines and Energy, Mineral Development Division, Newfoundland Department of Hines and Energy, Mineral Development Division.

Oliva, P., Dupré, B., Martin, F., Viers, J., 2004. The role of trace minerals in chemical weathering in a high-elevation granitic watershed (Estibère, France): chemical and mineralogical evidence1. Geochimica et Cosmochimica Acta 68, 2223–2243. https://doi.org/10.1016/j.gca.2003.10.043

Olivie-Lauquet, G., Gruau, G., Dia, A., Riou, C., Jaffrezic, A., Henin, O., 2001. Release of Trace Elements in Wetlands: Role of Seasonal Variability. Water Research 35, 943–952. https://doi.org/10.1016/S0043-1354(00)00328-6

Patino, L.C., Velbel, M.A., Price, J.R., Wade, J.A., 2003. Trace element mobility during spheroidal weathering of basalts and andesites in Hawaii and Guatemala. Chemical Geology, Controls on Chemical Weathering 202, 343–364. https://doi.org/10.1016/j.chemgeo.2003.01.002

Pédrot, M., Dia, A., Davranche, M., Gruau, G., 2015. Upper soil horizons control the rare earth element patterns in shallow groundwater. Geoderma 239–240, 84–96. https://doi.org/10.1016/j.geoderma.2014.09.023

Peltola, P., Brun, C., Åström, M., Tomilina, O., 2008. High K/Rb ratios in stream waters — Exploring plant litter decay, ground water and lithology as potential controlling mechanisms. Chemical Geology 257, 92–100. https://doi.org/10.1016/j.chemgeo.2008.08.009

Plater, A.J., Ivanovich, M., Dugdale, R.E., 1992. Uranium series disequilibrium in river sediments and waters: the significance of anomalous activity ratios. Applied Geochemistry 7, 101–110. https://doi.org/10.1016/0883-2927(92)90029-3

Pogge von Strandmann, P.A.E.P., Burton, K.W., James, R.H., van Calsteren, P., Gislason, S.R., 2010. Assessing the role of climate on uranium and lithium isotope behaviour in rivers draining a basaltic terrain. Chemical Geology 270, 227–239. https://doi.org/10.1016/j.chemgeo.2009.12.002

Pokrovsky, O.S., Schott, J., Dupré, B., 2006. Trace element fractionation and transport in boreal rivers and soil porewaters of permafrost-dominated basaltic terrain in Central Siberia. Geochimica et Cosmochimica Acta 70, 3239–3260. https://doi.org/10.1016/j.gca.2006.04.008

Porcelli, D., Andersson, P.S., Wasserburg, G.J., Ingri, J., Baskaran, M., 1997. The importance of colloids and mires for the transport of uranium isotopes through the Kalix River watershed and Baltic Sea. Geochimica et Cosmochimica Acta 61, 4095–4113. https://doi.org/10.1016/S0016-7037(97)00235-4

Pourret, O., Hursthouse, A., 2019. It's Time to Replace the Term "Heavy Metals" with "Potentially Toxic Elements" When Reporting Environmental Research. International Journal of Environmental Research and Public Health 16, 4446. https://doi.org/10.3390/ijerph16224446

Price, D.T., Alfaro, R.I., Brown, K.J., Flannigan, M.D., Fleming, R.A., Hogg, E.H., Girardin, M.P., Lakusta, T., Johnston, M., McKenney, D.W., Pedlar, J.H., Stratton, T., Sturrock, R.N., Thompson, I.D., Trofymow, J.A., Venier, L.A., 2013. Anticipating the consequences of climate change for Canada's boreal forest ecosystems. Environ. Rev. 21, 322–365. https://doi.org/10.1139/er-2013-0042

Rai, D., Eary, L.E., Zachara, J.M., 1989. Environmental chemistry of chromium. Science of The Total Environment, The Chromium Paradox in Modern Life 86, 15–23. https://doi.org/10.1016/0048-9697(89)90189-7

Sekaly, A.L.R., Murimboh, J., Hassan, N.M., Mandal, R., Ben Younes, M.E., Chakrabarti, C.L., Back, M.H., Grégoire, D.C., 2003. Kinetic Speciation of Co(II), Ni(II), Cu(II), and Zn(II) in Model Solutions and Freshwaters: Lability and the d Electron Configuration. Environ. Sci. Technol. 37, 68–74. https://doi.org/10.1021/es025805g

Short, S.A., Lowson, R.T., Ellis, J., 1988. 234U238U and 240Th234U activity ratios in the colloidal phases of aquifers in lateritic weathered zones. Geochimica et Cosmochimica Acta 52, 2555–2563. https://doi.org/10.1016/0016-7037(88)90026-9

Somayajulu, B.L.K., 1994. Uranium isotopes in the Hooghly estuary, India. Marine Chemistry, Chemistry of the Northern Indian Ocean 47, 291–296. https://doi.org/10.1016/0304-4203(94)90027-2

Steinmann, M., Stille, P., 2008. Controls on transport and fractionation of the rare earth elements in stream water of a mixed basaltic–granitic catchment basin (Massif Central, France). Chemical Geology 254, 1–18. https://doi.org/10.1016/j.chemgeo.2008.04.004

Strong, D.F., 1982. Carbothermal metasomatism of alaskitic granite, St. Lawrence, Newfoundland, Canada. Chemical Geology 35, 97–114. https://doi.org/10.1016/0009-2541(82)90021-3

Suen, C.J., Frey, F.A., Malpas, J., 1979. Bay of Islands ophiolite suite, Newfoundland: Petrologic and geochemical characteristics with emphasis on rare earth element geochemistry. Earth and Planetary Science Letters 45, 337–348. https://doi.org/10.1016/0012-821X(79)90134-1

Suhr, G., 1993. Evaluation of upper mantle microstructures in the Table Mountain massif (Bay of Islands ophiolite). Journal of Structural Geology 15, 1273–1292. https://doi.org/10.1016/0191-8141(93)90102-G

Suhr, G., Robinson, P.T., 1994. Origin of mineral chemical stratification in the mantle section of the Table Mountain massif (Bay of Islands Ophiolite, Newfoundland, Canada). Lithos 31, 81–102. https://doi.org/10.1016/0024-4937(94)90002-7

Sun, S.-S., Deng, T.-H.-B., Ao, M., Yang, W.-J., Liu, X.-R., Liu, T., Zhu, J.-M., Morel, J.L., Tang, Y.-T., Qiu, R.-L., 2024. Nickel isotope fractionation during intense weathering of basalt: Implications for Ni output from continental weathering. Geochimica et Cosmochimica Acta 367, 107–122. https://doi.org/10.1016/j.gca.2023.12.023

Swarzenski, P., Campbell, P., Porcelli, D., McKee, B., 2004. The estuarine chemistry and isotope systematics of 234,238U in the Amazon and Fly Rivers. Continental Shelf Research, Tropical River-Ocean Processes in Coastal Settings 24, 2357–2372. https://doi.org/10.1016/j.csr.2004.07.025

Szponar, N., Brazelton, W.J., Schrenk, M.O., Bower, D.M., Steele, A., Morrill, P.L., 2013. Geochemistry of a continental site of serpentinization, the Tablelands Ophiolite, Gros Morne National Park: A Mars analogue. Icarus 224, 286–296. https://doi.org/10.1016/j.icarus.2012.07.004

Tanaka, K., Watanabe, N., 2015. Size distribution of alkali elements in riverbed sediment and its relevance to fractionation of alkali elements during chemical weathering. Chemical Geology 411, 12–18. https://doi.org/10.1016/j.chemgeo.2015.05.025

Teng, H.C., 1974. A lithogeochemical study of the St. Lawrence granite, Newfoundland (masters). Memorial University of Newfoundland.

Teng, H.C., Strong, D.F., 1976. Geology and geochemistry of the St. Lawrence peralkaline granite and associated fluorite deposits, southeast Newfoundland. Can. J. Earth Sci. 13, 1374–1385. https://doi.org/10.1139/e76-142

Thompson, A., Amistadi, M.K., Chadwick, O.A., Chorover, J., 2013. Fractionation of yttrium and holmium during basaltic soil weathering. Geochimica et Cosmochimica Acta 119, 18–30. https://doi.org/10.1016/j.gca.2013.06.003

Uhlig, D., Schuessler, J.A., Bouchez, J., Dixon, J.L., von Blanckenburg, F., 2017. Quantifying nutrient uptake as driver of rock weathering in forest ecosystems by magnesium stable isotopes. Biogeosciences 14, 3111–3128. https://doi.org/10.5194/bg-14-3111-2017

Ullah, W., 1992. Water resources Atlas of Newfoundland. Water Resources Division, St. John's.

Van Alstine, R.E., 1944. The fluorspar deposits of Saint Lawrence, Newfoundland. Economic Geology 39, 109–132. https://doi.org/10.2113/gsecongeo.39.2.109

Viers, J., Dupré, B., Polvé, M., Schott, J., Dandurand, J.-L., Braun, J.-J., 1997. Chemical weathering in the drainage basin of a tropical watershed (Nsimi-Zoetele site, Cameroon) : comparison between organic-poor and organic-rich waters. Chemical Geology 140, 181–206. https://doi.org/10.1016/S0009-2541(97)00048-X

Wällstedt, T., Björkvald, L., Laudon, H., Borg, H., Mörth, C.-M., 2017. Landscape control on the hydrogeochemistry of As, Co and Pb in a boreal stream network. Geochimica et Cosmochimica Acta 211, 194–213. https://doi.org/10.1016/j.gca.2016.08.030

Webster, K.L., Beall, F.D., Creed, I.F., Kreutzweiser, D.P., 2015. Impacts and prognosis of natural resource development on water and wetlands in Canada's boreal zone. Environ. Rev. 23, 78–131. https://doi.org/10.1139/er-2014-0063

Williams, H., Smyth, W.R., 1973. Metamorphic aureoles beneath ophiolite suites and alpine peridotites; tectonic implications with west Newfoundland examples. American Journal of Science 273, 594–621. https://doi.org/10.2475/ajs.273.7.594

Wilson, M.J., 2004. Weathering of the primary rock-forming minerals: processes, products and rates. Clay Minerals 39, 233–266. https://doi.org/10.1180/0009855043930133

Woodrow, E.F., Heringa, P.K., 1987. Pedoclimatic zones of the island of Newfoundland (No. 32). Canada Soil Survey.

Wu, K., Liu, S., Shi, X., Colin, C., Bassinot, F., Lou, Z., Zhang, H., Zhu, A., Fang, X., Mohamed, C.Abd.R., 2022. The Effect of Size Distribution on the Geochemistry and Mineralogy of Tropical River Sediments and Its Implications regarding Chemical Weathering and Fractionation of Alkali Elements. Lithosphere 2022, 8425818. https://doi.org/10.2113/2022/8425818

Yan, W., Casey, J., 2020. A new concordia age for the'forearc'Bay of Islands Ophiolite complex, Western Newfoundland utilizing spatially-resolved LA-ICP-MS U-Pb analyses of zircon. Gondwana Res 86, 1–22. https://doi.org/10.1016/j.gr.2020.05.007

Yeghicheyan, D., Aubert, D., Bouhnik-Le Coz, M., Chmeleff, J., Delpoux, S., Djouraev, I., Granier, G., Lacan, F., Piro, J.-L., Rousseau, T., Cloquet, C., Marquet, A., Menniti, C., Pradoux, C., Freydier, R., Vieira da Silva-Filho, E., Suchorski, K., 2019. A New Interlaboratory Characterisation of Silicon, Rare Earth Elements and Twenty-Two Other Trace Element Concentrations in the Natural River Water Certified Reference Material SLRS-6 (NRC-CNRC). Geostandards and Geoanalytical Research 43, 475–496. https://doi.org/10.1111/ggr.12268

Yu, C., Berger, T., Drake, H., Song, Z., Peltola, P., Åström, M.E., 2019. Geochemical controls on dispersion of U and Th in Quaternary deposits, stream water, and aquatic plants in an area with a granite pluton. Science of The Total Environment 663, 16–28. https://doi.org/10.1016/j.scitotenv.2019.01.293

Table 2: Detailed catchment bedrock geology used to derive the lithologic groupings of streams for this study.

Samples	Catchment Coverage
Major River	
Terra Nova River	48% metasedimentary rocks and migmatite (Gander Zone)
(MR2201)	27% intrusive granitoid rocks
	6% sedimentary, volcanic, and intrusive rocks (Avalon Zone)
	7% clastic and volcanic rock (Dunnage Zone)
Gander River	35% clastic and volcanic rock (Dunnage Zone)
(MR2202)	26% metasedimentary rocks and migmatite (Gander Zone)
	20% intrusive granitoid rocks
	8% sedimentary and volcanic rocks (Overlap Sequences)
	2% intrusive mafic rocks
Humber River	28% sedimentary and volcanic rocks (Overlap Sequences)
(MR2203)	17% intrusive granitoid rocks
	15% clastic and volcanic rock (Dunnage Zone)
	15% quartzo-feldspathic gneiss and schist (Humber Zone)
	9% sedimentary, metasedimentary, and volcanic rock (Humber Zone)
	3% intrusive mafic rocks
	1% ophiolitic rocks (Dunnage Zone)
Exploits River	51% clastic and volcanic rock (Dunnage Zone)
(MR2204)	14% intrusive granitoid rocks
	9% metasedimentary rocks and migmatite (Gander Zone)
	6% sedimentary and volcanic rocks (Overlap Sequences)
	4% ophiolitic rocks (Dunnage Zone)
	4% intrusive mafic rocks
	2% sedimentary, volcanic, and intrusive rocks (Avalon Zone)
Garnish River	92% sedimentary, volcanic, and intrusive rocks (Avalon Zone)
(MR2205)	
Piper's Hole River	64% sedimentary, volcanic, and intrusive rocks (Avalon Zone)
(MR2206)	24% intrusive granitoid rocks
	3% metasedimentary rocks and migmatite (Gander Zone)
Heterolithic/Comparison	
BI2201	55% sedimentary, metasedimentary, and volcanic rock (Humber Zone)
	45% unseperated plutonic and volcanic rocks (Little Port Complex)
BI2202	93% unseperated plutonic and volcanic rocks (Little Port Complex)
	7% sedimentary, metasedimentary, and volcanic rock (Humber Zone)
BI2203	100% sedimentary, metasedimentary, and volcanic rocks (Humber Zone)
BI2209	97% sedimentary, metasedimentary, and volcanic rock (Humber Zone)
GM2210	84% sedimentary, metasedimentary, and volcanic rock (Humber Zone)
	9% ultramafic unit (Bay of Islands Ophiolite Complex)*
GM2211	84% sedimentary, metasedimentary, and volcanic rock (Humber Zone)
	7% quartzo-feldspathic gneiss and schist (Humber Zone)
BP2210	62% Acidic to mafic volcanic rocks(Marystown Group)
	39% Felsic plutonic and volcanics (Anchor Drogue Granodiorite, Grand Beach Complex, Rocky Ridge Formation)

*Ultramafic unit includes lherzolites, harzburgites, dunites, websterite, and orthopyroxenites

**Mafic unit includes layered gabbro, diabase dikes, and pillow basalts

Table 2 cont: Detailed catchment bedrock geology used to derive the lithologic groupings of streams for this study.

Samples	Catchment Coverage
Monolithological Granite	
BP2201	79% Granite (St. Lawrence Granite)
	21% Acidic to mafic volcanic rocks(Marystown Group)
BP2203	60% Granite (St. Lawrence Granite)
	40% Siliciclastic Marine Shales (Inlet Group)
BP2206	100% Granite (St. Lawrence Granite)
BP2208	100% Granite (St. Lawrence Granite)
	4% Acidic to mafic volcanic rocks(Marystown Group)
BP2212	73% Granite (St. Lawrence Granite)
	27% Acidic to mafic volcanic rocks(Marystown Group)
Sub-monolithological Granite	
BP2202	
	48% Granite (St. Lawrence Granite)
	41% Acidic to mafic volcanic rocks(Marystown Group)
	4% Plutonic Mafic/Volcanic Mafic Marine (Loughlins Hill Gabbro/Burin Group)
	1% Siliciclastic Marine Shales (Inlet Group)
BP2204	51% Acidic to mafic volcanic rocks(Marystown Group)
	36% Granite (St. Lawrence Granite)
	13% Siliciclastic Marine Shales (Inlet Group)
BP2205	38% Acidic to mafic volcanic rocks(Marystown Group)
	36% Granite (St. Lawrence Granite)
	27% Siliciclastic Marine Shales (Inlet Group)
BP2207	45% Granite (St. Lawrence Granite)
	44% Siliciclastic Marine Shales (Inlet Group)
	7% Acidic to mafic volcanic rocks(Marystown Group)
BP2209	43% Granite (St. Lawrence Granite)
	40% Acidic to mafic volcanic rocks(Marystown Group)
	10% Felsic plutonic and volcanics (Anchor Drogue Granodiorite, Grand Beach Complex, Rocky Ridge Formation)
Monolithological Mafic	
BI2205	100% mafic unit (Bay of Islands Ophiolite Complex)**
BI2206	93% mafic unit (Bay of Islands Ophiolite Complex)**
	1% ultramafic unit (Bay of Islands Ophiolite Complex)*
Monolithological Ultramafic	
GM2203	86% ultramafic unit (Bay of Islands Ophiolite Complex)*
	14% mafic unit (Bay of Islands Ophiolite Complex)**
	1% sedimentary, metasedimentary, and volcanic rock (Humber Zone)
GM2204	100% ultramafic unit (Bay of Islands Ophiolite Complex)*
GM2205	100% ultramafic unit (Bay of Islands Ophiolite Complex)*
GM2206	100% ultramafic unit (Bay of Islands Ophiolite Complex)*
GM2208	66% ultramafic unit (Bay of Islands Ophiolite Complex)*
	23% unseperated plutonic and volcanic rocks (Little Port Complex)
	11% sedimentary, metasedimentary, and volcanic rock (Humber Zone)
GM2209	75% ultramafic unit (Bay of Islands Ophiolite Complex)*
	17% sedimentary, metasedimentary, and volcanic rock (Humber Zone)

*Ultramafic unit includes lherzolites, harzburgites, dunites, websterite, and orthopyroxenites

**Mafic unit includes layered gabbro, diabase dikes, and pillow basalts

Table 2 cont: Detailed catchment bedrock geology used to derive the lithologic groupings of streams for this study.

Samples	Catchment Coverage
Sub-monolithological Ultramafic	
BI2207	49% ultramafic unit (Bay of Islands Ophiolite Complex)*
	41% mafic unit (Bay of Islands Ophiolite Complex)**
	9% sedimentary, metasedimentary, and volcanic rock (Humber Zone)
BI2208	73% sedimentary, metasedimentary, and volcanic rock (Humber Zone)
	26% ultramafic unit (Bay of Islands Ophiolite Complex)*
GM2201	53% sedimentary, metasedimentary, and volcanic rock (Humber Zone)
	18% ultramafic unit (Bay of Islands Ophiolite Complex)*
	18% mafic unit (Bay of Islands Ophiolite Complex)**
	2% unseperated plutonic and volcanic rocks (Little Port Complex)
GM2202	52% mafic unit (Bay of Islands Ophiolite Complex)**
	36% ultramafic unit (Bay of Islands Ophiolite Complex)*
	12% sedimentary, metasedimentary, and volcanic rock (Humber Zone)

*Ultramafic unit includes lherzolites, harzburgites, dunites, websterite, and orthopyroxenites

**Mafic unit includes layered gabbro, diabase dikes, and pillow basalts

Table 3: Summary of watershed attributes and physicochemical properties of streams divided into their lithologic groupings.

	%	%	%	%	km2	degrees (0 to 90)	mV		µS/cm	C	mg/L	mg/L
	Till	**Exposed/Concealed Rock**	**Bog**	**Dense/Open Forest**	**Size**	**Mean Slope**	**Eh**	**pH**	**Conductivity**	**Temperature**	**DOC**	**DIC**
Major Rivers(n=6)												
Mean	*Not calculated*	*Not calculated*	*Not calculated*	*49.0*	4039.4	*Not calculated*	408.8	7.30	28.2	20.0	5.99	1.17
Median	*Not calculated*	*Not calculated*	*Not calculated*	*57.0*	3036.3	*Not calculated*	408.5	7.38	25.3	20.4	5.56	1.00
Min	*Not calculated*	*Not calculated*	*Not calculated*	*15.0*	203.9	*Not calculated*	389.8	6.89	17.5	16.6	4.53	0.59
Max	*Not calculated*	*Not calculated*	*Not calculated*	*76.0*	9579.6	*Not calculated*	426.6	7.62	40.0	22.4	8.56	2.55
Western NL Study Site (n=18*)												
Mean	14	62	7	18	33	11	442	7.89	106.5	15.6	4.34	8.53
Median	11	65	4	11	9	10	438	7.94	93.4	16.4	3.38	7.57
Min	0	0	0	0	2	6	404	7.20	32.6	7.5	1.20	1.32
Max	47	96	45	46	243	16	478	8.40	250.0	18.9	16.26	19.29
Burin Peninsula Study Site (n=11)												
Mean	71	7	19	6	27	4	413	6.93	76.3	21.6	7.71	3.31
Median	71	1	22	4	3	3	401	6.81	47.7	23.5	7.94	0.81
Min	50	0	0	0	1	1	350	6.28	34.1	7.7	4.94	0.49
Max	100	45	38	26	166	7	509	8.11	252.0	27.3	11.51	16.36
Granitic Monolithologic(n=5)												
Mean	77	6	16	7	1.9	3.7	416.4	6.90	74.9	18.4	8.26	3.05
Median	80	0	20	7	1.3	3.4	401.8	6.72	64.7	18.5	8.31	1.94
Min	50	0	0	3	1.0	1.4	349.6	6.28	37.5	7.7	5.42	0.49
Max	100	27	26	10	3.0	6.6	509.5	7.68	160.5	23.8	10.57	9.40
Granitic Sub-Monolithologic(n=5)												
Mean	68	1	26	2	57.3	3.2	414.5	6.96	81.6	24.1	7.03	3.78
Median	70	1	23	1	22.9	3.0	400.5	6.81	38.4	24.3	5.64	0.68
Min	59	0	13	0	4.5	2.9	382.6	6.34	34.1	20.7	4.94	0.50
Max	72	2	38	11	166.1	3.9	478.0	8.11	252.0	27.3	11.51	16.36
Ultramafic Monolithologic(n=6)												
Mean	9	68	6	4	6.6	12.3	431.0	7.98	75.0	15.0	2.27	7.25
Median	0	66	5	0	6.4	11.9	427.2	7.99	74.7	14.4	1.86	7.16
Min	0	47	0	0	0.8	9.2	417.6	7.91	63.2	13.2	0.86	6.34
Max	37	92	18	21	13.7	16.2	454.9	8.03	94.9	17.5	4.03	8.95
Ultramafic Sub-Monolithologic(n=4)												
Mean	12	66	5	18	89.4	9.2	448.7	7.97	91.7	17.4	3.08	7.76
Median	11	67	3	12	46.4	9.3	446.9	7.99	92.8	17.0	3.09	8.18
Min	0	42	0	4	21.4	8.9	431.5	7.82	65.6	16.5	1.20	4.33
Max	24	87	15	46	243.4	9.5	469.8	8.08	115.4	18.9	4.93	10.37
Mafic Monolithologic(n=2)												
Mean	1	86	6	22	9.9	11.5	471.8	7.51	72.1	15.3	2.40	4.53
Median	1	86	6	22	9.9	11.5	471.8	7.51	72.1	15.3	2.40	4.53
Min	0	77	1	7	6.3	8.0	465.3	7.32	32.6	15.3	1.89	1.41
Max	1	95	11	37	13.5	15.0	478.3	7.70	111.6	15.3	2.91	7.66
Heterolithic/Comparison Catchments (n=7*)												
Mean	33	50	10	38	64.9	9.8	433.8	7.92	160.5	16.5	5.67	12.43
Median	27	49	1	37	5.3	8.0	441.2	7.94	176.8	16.4	4.99	11.84
Min	18	25	0	26	2.4	5.6	385.3	6.98	57.1	7.5	1.72	2.23
Max	55	66	45	58	278.0	16.4	463.5	8.40	250.0	25.5	9.71	19.29

**Sample BI2203, classified as heterolithic/comparison sample had difficulty in delineating boundaries of drainage basin was therefore excluded from coverage values.*
Spatial analysis was not calculated and is excluded from summary table for % Till, % Exposed/concealed rock, % bog, % vegetation, size, and % mean slope.
Sample GM2207 was excluded from these summarized values

Table 4: Summary of selected geochemical data of streams divided into their lithologic groupings.

	mg/L	mg/L	mg/L	mg/L	ng/L	ng/L	ng/L	ng/L	ng/L	ng/L	ng/L	ng/L				
	Mg	**Ca**	**Na**	**K**	**Li**	**Rb**	**Cs**	**Th**	**U**	**Cr**	**Co**	**Ni**	**Ca/Na**	**Mg/Na**	**Ca/Mg**	**K/Mg**
Major Rivers																
n	6	6	6	6	6	6	6	6	6	0	6	6	6	6	6	6
Mean	0.5217	2.075	2.438	0.2513	305.1	540.6	18.6	16.13	69.01		17.60	198.4	0.9215	0.2305	4.009	0.4923
Median	0.4979	1.897	2.059	0.2009	294.4	585.0	17.2	15.66	65.81		16.07	137.1	0.7788	0.2312	4.095	0.4610
Min	0.3544	1.125	1.603	0.1473	93.99	210.3	2.1	9.572	19.33		11.14	58.13	0.4286	0.1275	2.300	0.3196
Max	0.8079	3.901	4.566	0.4941	521.5	873.8	44.9	26.19	140.1		31.11	495.7	1.496	0.3157	5.419	0.7720
Granitic Monolithologic (excludes anomalous sample)																
n	4	4	4	4	4	4	4	4	4	0	4	4	4	4	4	4
Mean	0.9386	2.332	6.275	0.2071	1363	831.4	123.0	60.87	213.9		59.60	103.4	0.3541	0.1446	2.383	0.2151
Median	0.9301	2.281	6.429	0.1912	1245	799.4	116.5	45.78	113.4		45.94	95.73	0.3337	0.1382	2.405	0.1907
Min	0.5055	1.096	4.871	0.0994	717.2	454.1	93.3	11.30	10.30		41.07	93.92	0.2249	0.1038	2.017	0.1841
Max	1.389	3.670	7.372	0.3465	2246	1273	165.6	140.6	618.7		105.4	128.3	0.5240	0.1983	2.706	0.2948
Granitic Sub-Monolithologic (excludes anomalous sample)																
n	4	4	4	4	4	4	4	4	4	0	4	4	4	4	4	4
Mean	0.5538	1.532	4.948	0.1738	871.5	404.8	42.0	19.69	110.5		16.06	54.24	0.3134	0.1116	2.823	0.3085
Median	0.5270	1.518	4.792	0.1495	910.2	390.8	39.5	20.98	84.25		14.24	46.38	0.3103	0.1129	2.819	0.3069
Min	0.4546	1.445	4.228	0.1297	601.4	301.9	25.3	12.62	47.42		7.214	38.98	0.2753	0.1014	2.329	0.2428
Max	0.7066	1.646	5.979	0.2665	1064	535.7	63.7	24.17	226.0		28.54	85.22	0.3577	0.1192	3.326	0.3772
Ultramafic Monolithologic																
n	6	6	6	6	6	6	6	6	6	6	6	6	6	6	6	6
Mean	7.070	1.001	2.345	0.1337	120.7	130.6	1.253	1.250	2.172	1475	33.83	6559	0.3825	3.161	0.1376	0.0185
Median	6.815	0.6745	2.123	0.1021	77.16	77.87	0.7320	0.7590	0.7870	1556	34.32	6887	0.3156	3.289	0.0964	0.0149
Min	6.375	0.3713	1.664	0.0784	64.80	68.26	0.4700	0.4180	0.4600	946.5	16.86	2412	0.2117	2.139	0.0572	0.0121
Max	8.602	2.060	3.194	0.2398	238.1	301.5	2.706	2.452	6.200	1938	45.93	9937	0.6450	3.902	0.3015	0.0279
Ultramafic Sub-Monolithologic																
n	4	4	4	4	4	4	4	4	4	3	4	4	4	4	4	4
Mean	6.687	3.423	4.039	0.2057	322.1	176.9	2.447	5.130	8.958	794.5	25.58	3219	0.8298	1.645	0.6320	0.0378
Median	7.134	2.937	3.893	0.2094	265.0	157.5	1.709	4.633	7.449	888.7	21.85	2803	0.7635	1.686	0.5281	0.0279
Min	3.014	1.952	3.830	0.1526	118.4	130.5	1.174	2.562	0.6600	508.0	16.00	1632	0.4994	0.7869	0.2062	0.0204
Max	9.466	5.868	4.539	0.2516	639.8	262.0	5.194	8.692	20.27	986.9	42.62	5636	1.293	2.422	1.266	0.0750
Mafic Monolithologic (excludes anomalous sample)																
	2	2	2	2	2	2	2	2	2	0	2	2	2	2	2	2
Mean	1.658	6.304	4.725	0.1897	62.60	134.3	1.467	1.343	4.259		18.05	323.4	1.107	0.3484	3.149	0.1216
Median	1.658	6.304	4.725	0.1897	62.60	134.3	1.467	1.343	4.259		18.05	323.4	1.107	0.3484	3.149	0.1216
Min	0.962	1.532	2.813	0.1336	53.04	108.3	1.266	0.9360	2.266		12.29	75.97	0.5446	0.3421	1.592	0.1044
Max	2.353	11.08	6.637	0.2457	72.15	160.4	1.668	1.750	6.252		23.81	570.8	1.669	0.3546	4.707	0.1388
Heterolithic/Comparison Catchments																
	7	7	7	7	7	7	7	7	7	3	7	7	7	7	7	7
Mean	4.600	16.12	9.627	0.5011	489.0	395.1	3.277	7.082	50.05	1166	30.29	854.1	2.808	0.5929	4.443	0.1406
Median	4.532	12.95	6.333	0.6147	383.7	404.5	2.620	7.734	26.27	1122	31.16	222.8	1.573	0.5520	2.804	0.1219
Min	1.129	3.165	3.621	0.2721	210.4	290.1	0.8940	0.9000	10.45	450.9	10.27	50.55	0.4998	0.1783	1.935	0.0574
Max	9.352	31.89	19.99	0.6878	897.4	479.0	6.486	11.43	122.7	1926	54.57	2450	7.934	1.502	14.29	0.2568
Anomalous Granite Monolithologic																
	1.353	19.29	10.72	0.5788	2777	1853	174.5	75.53	1038		35.64	173.7	1.799	0.1262	14.26	0.4278
Anomalous Granite Sub-Monolithologic																
	1.065	7.164	45.25	3.395	9644	6388	372.4	83.21	4272	242.7	165.2	288.3	0.1583	0.0235	6.724	3.186
Anomalous Mafic Monolithologic																
	1.352	1.993	3.211	0.1164	82.14	123.1	1308	7998	5778	1102	70.76	3096	0.6207	0.4210	1.474	0.0861

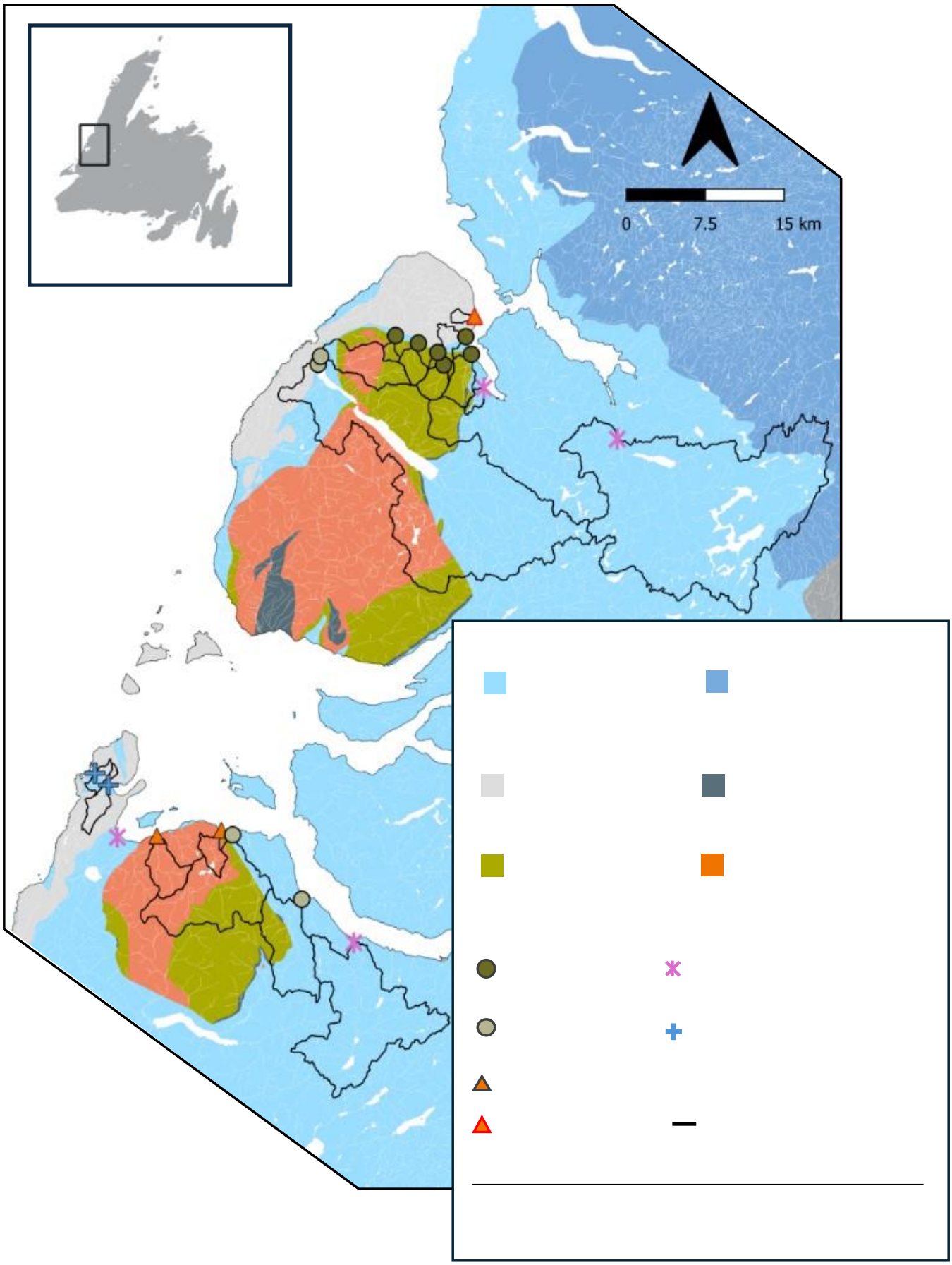

Figure 1: Simplified bedrock geology of western Newfoundland study site showing water sample locations and delineated catchments up until the point of sampling. Bedrock was visualized using the 1:1 Million Bedrock Geology file from the Geoscience Atlas and catchment delineation was done in ArcGIS Pro. Details of process and references can be found in Sections 2.4.3 and 2.5.1.

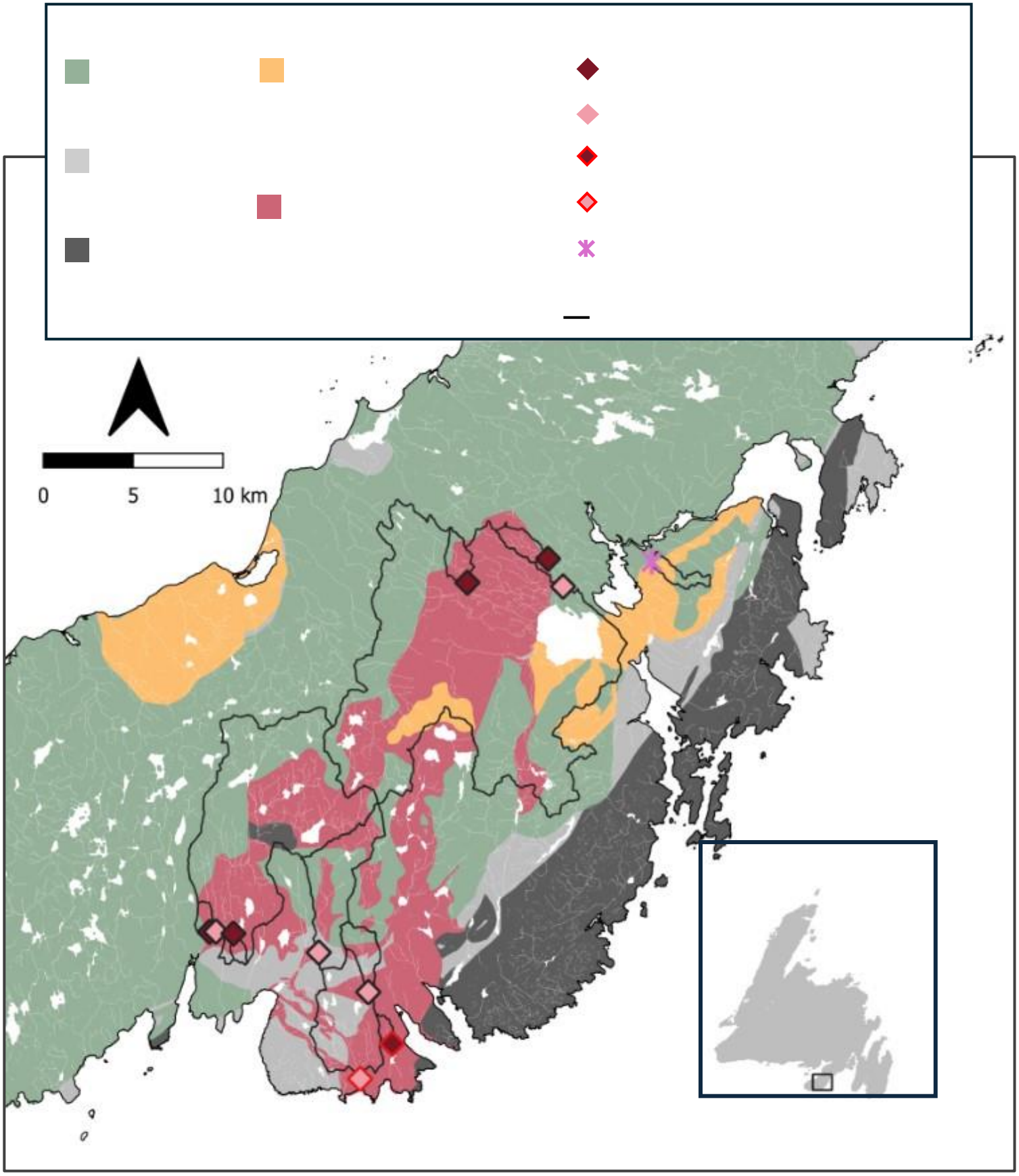

Figure 2: Simplified bedrock geology of Burin Peninsula study site showing water sample locations and delineated catchments up until the point of sampling. Bedrock was visualized using the 1:1 Million Bedrock Geology file from the Geoscience Atlas and catchment delineation was done in ArcGIS Pro. Details of process and references can be found in Sections 2.4.3 and 2.5.1.

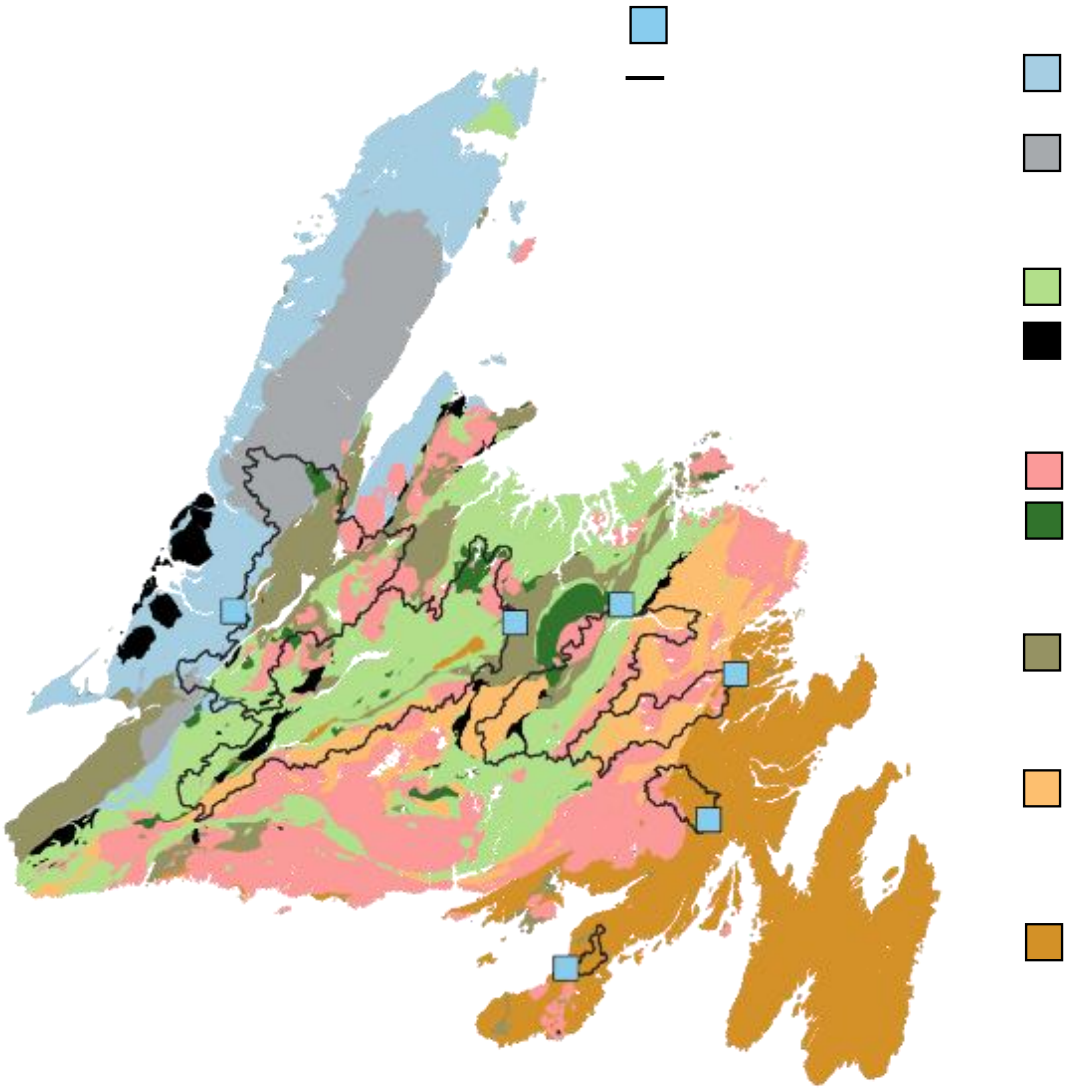

Figure 3: Simplified bedrock geology of Newfoundland with the sampling location of six major rivers and delineated catchments up to the point of sampling. Bedrock was visualized using the 1:1 Million Bedrock Geology file from the Geoscience Atlas and catchment delineation was done in ArcGIS Pro. Details of process and references can be found in Sections 2.4.3 and 2.5.1.

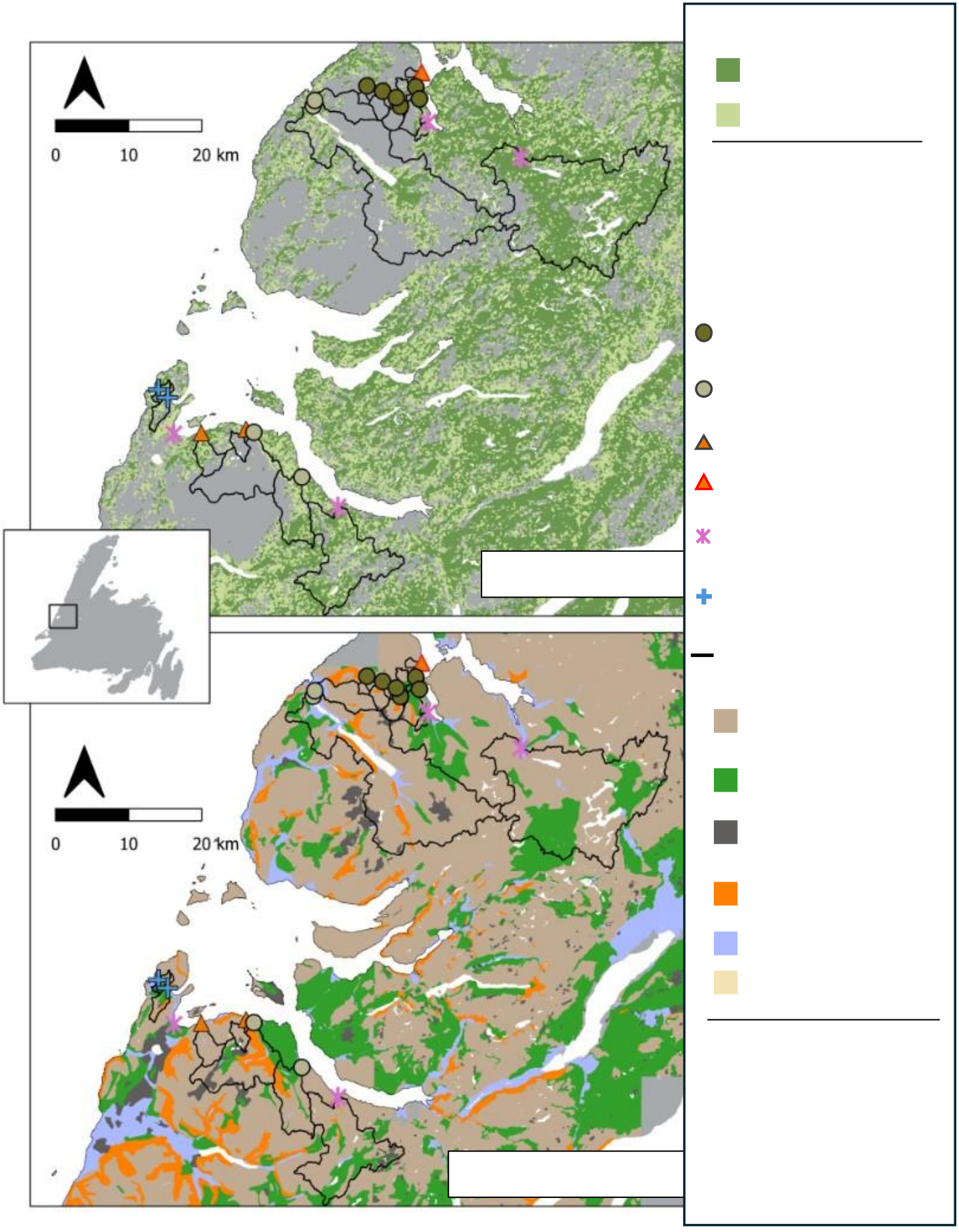

Figure 4: (a) Vegetation overlay and (b) surficial geology map of western Newfoundland study site showing water sample locations and delineated catchments up until the point of sampling. Vegetation overlay extracted from CanVec “ ” “ ”

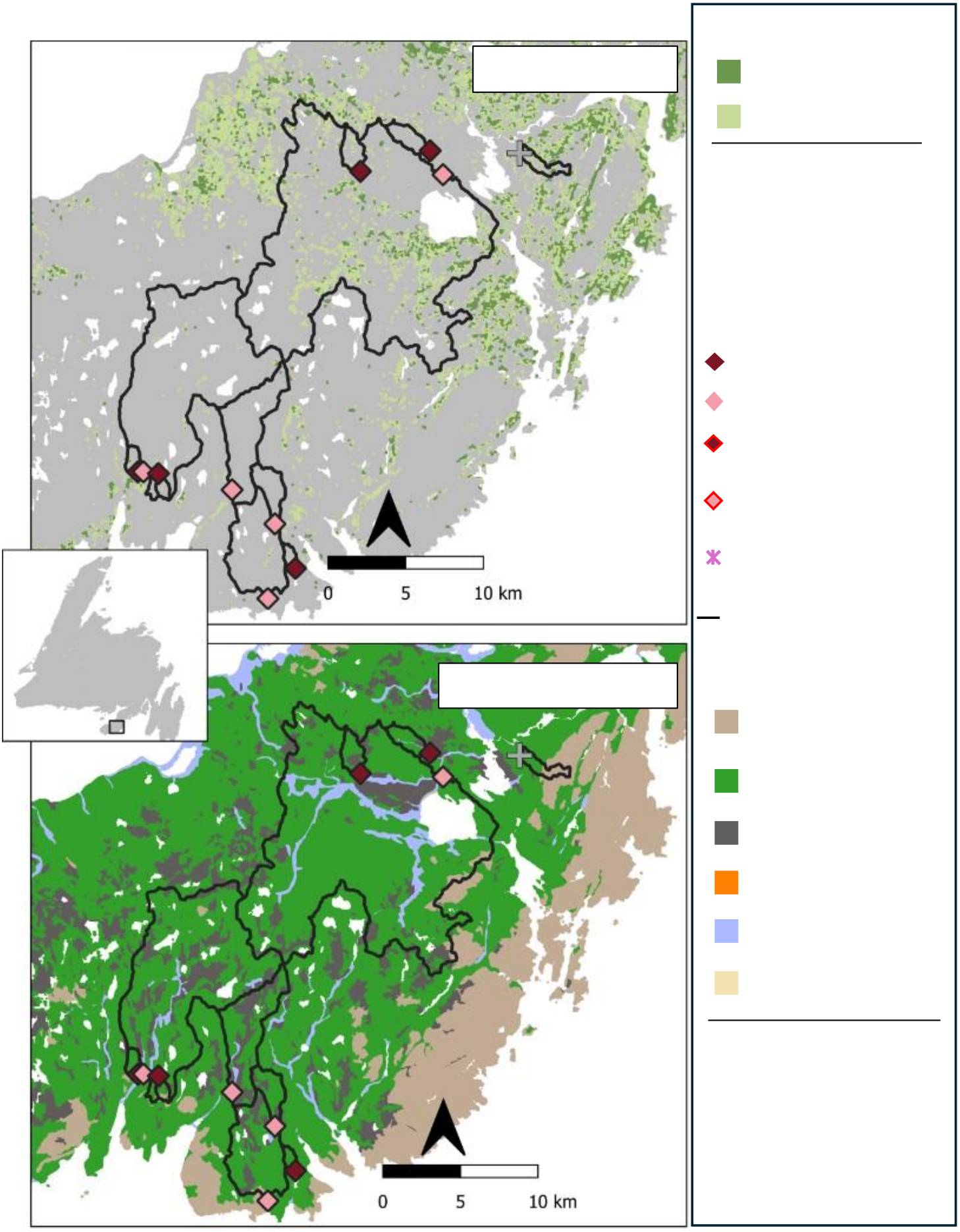

Figure 5: (a) Vegetation overlay and (b) surficial geology map of Burin Peninsula study site showing water sample locations and delineated catchments up until the point of sampling. Vegetation overlay extracted from CanVec " " " "

Details of process and references can be found in Section 2.4.3.

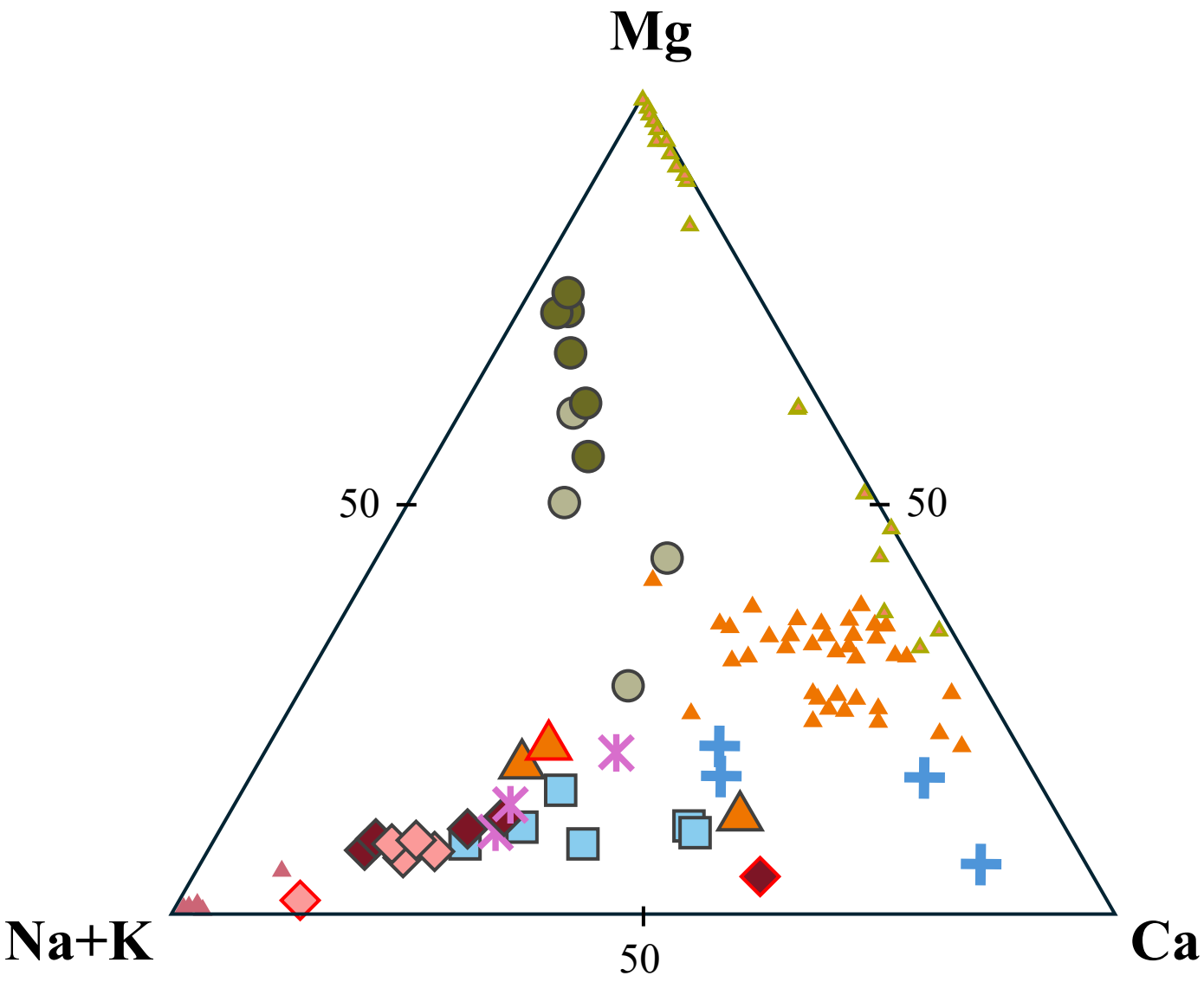

Monolithologic Streams

- Ultramafic Monolithologic
- Granite Monolithologic
- Mafic Monolithologic

Sub-Monolithologic Streams

- Ultramafic Sub-monolithologic
- Granite Sub-Monolithologic

- Major River

Anomalous Streams

- Anomalous Granite Monolithologic
- Anomalous Granite Sub-Monolithologic
- Anomalous Mafic Monolithologic

Heterolithologic/Comparison Streams

- Heterolithologic/Comparison Samples (Igneous and Sedimentary)
- Heterolithologic/Comparison Samples (Predominantly Sedimentary)

Bedrock Compositions

- Ultramafic Unit[1] ***Bay of Islands Complex***
- Mafic Unit[2] ***Bay of Islands Complex***
- Granite ***St. Lawrence Granite***

Figure 6: Major cation ternary diagram (Mg–Na+K–Ca) of waters and site-specific bedrock. All values are reported as molar proportions.
[1,2]Values of ultramafic and mafic units can be found in Appendix 4. Details of process and references can be found in Sections 2.4.3 and 2.5.1.

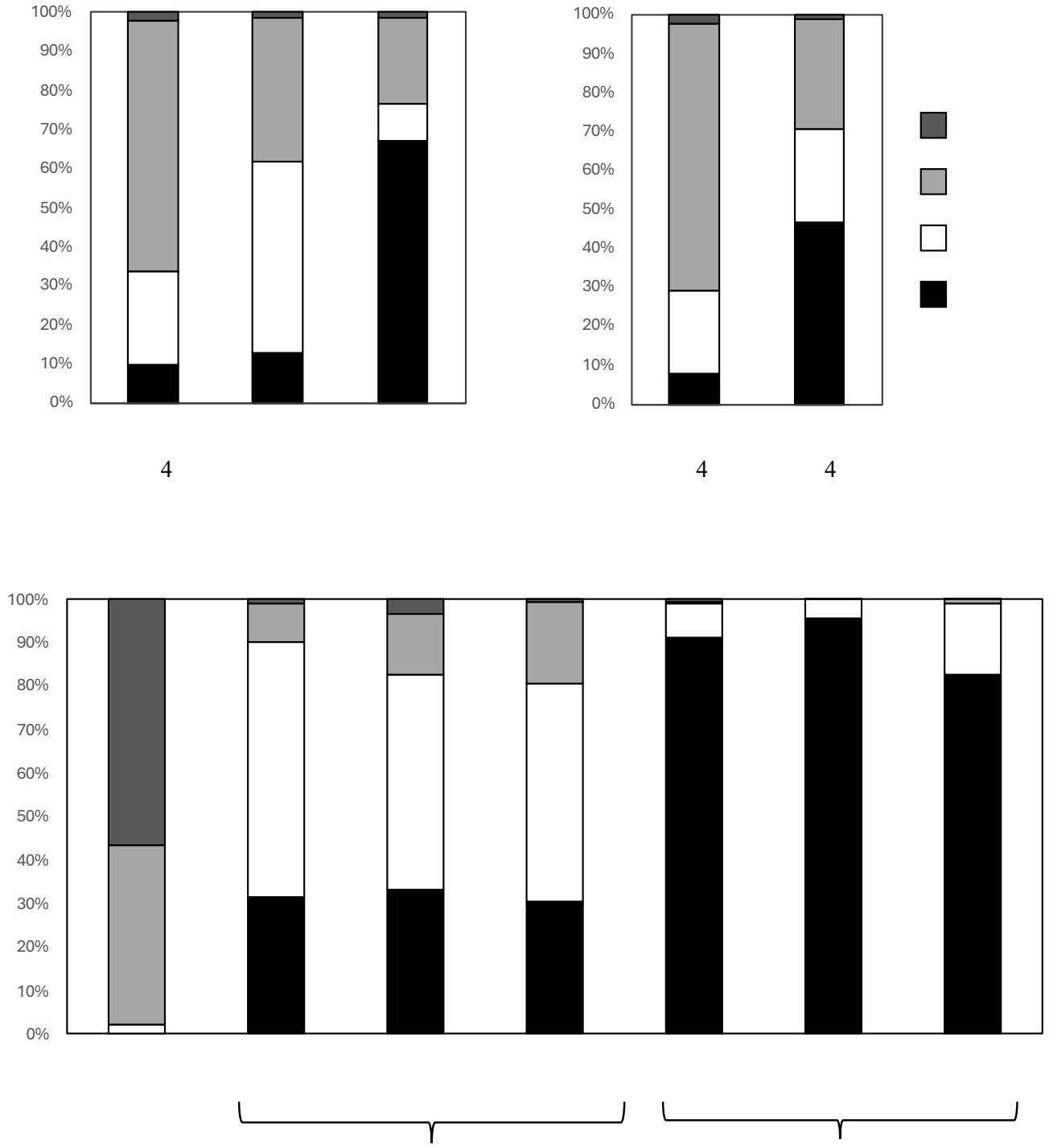

Figure 7: Stacked bar charts showing the relative proportions of dissolved major cations (Mg, Ca, Na, K) in the mean composition of small-catchment streams, after division into their target lithologic groupings: (a) monolithologic streams (granite, mafic, ultramafic) and (b) sub-monolithologic streams (granite, ultramafic). (c) Whole-rock major element data from bedrock presented in the same format as stream data for comparison. Bedrock compositions for the SLG in the Burin Peninsula from Magyarosi (2022). Bedrock compositions for rocks in the BOIC from western Newfoundland from Malpas (1976), divided into mafic and ultramafic groupings.

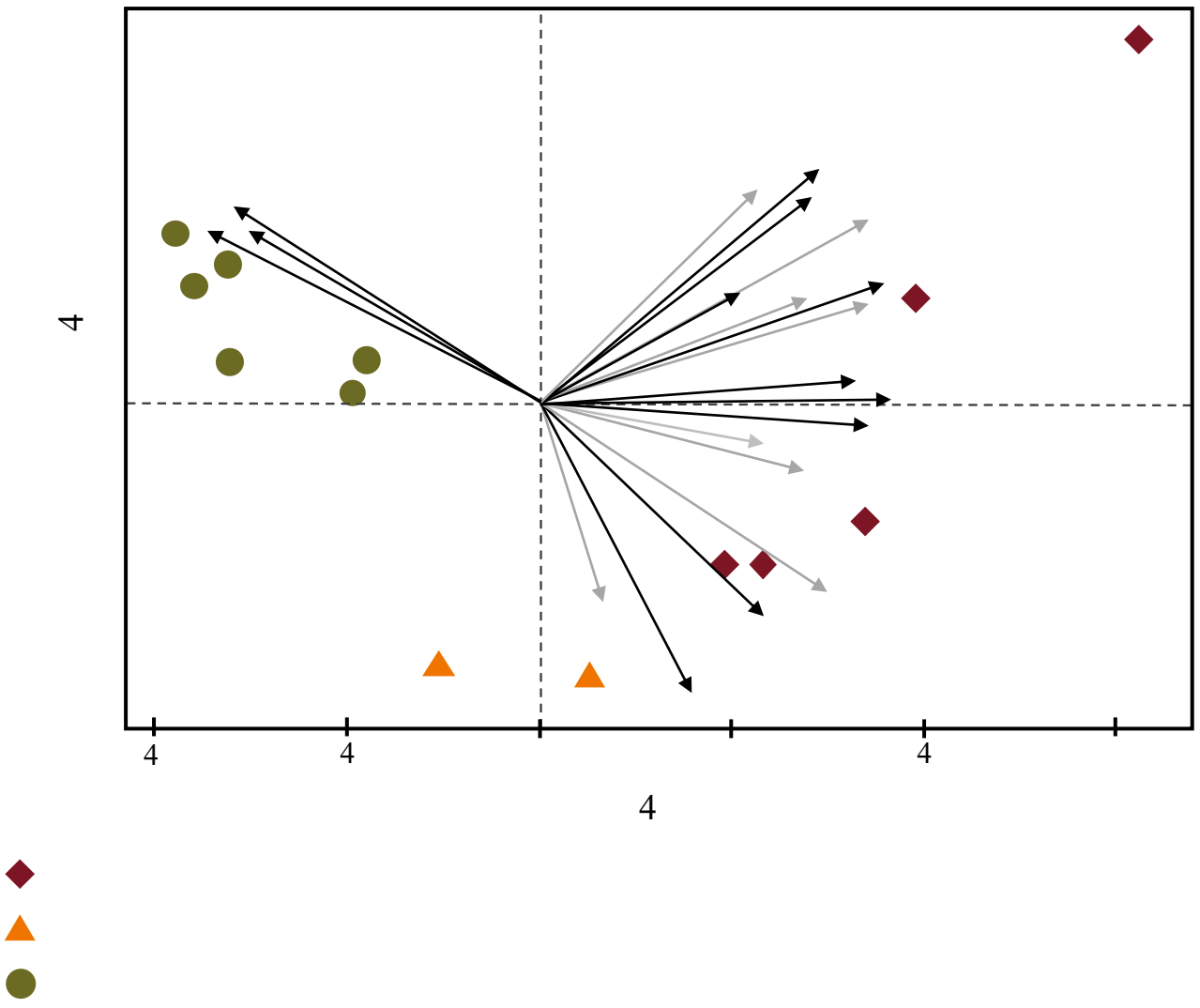

Figure 8: Principal component analysis (PCA) displaying major and trace element relationship of the monolithologic streams (granite, mafic, ultramafic). Element measurements below detection limit were taken at half the detection limit for PCA. Only Cr was affected by this.

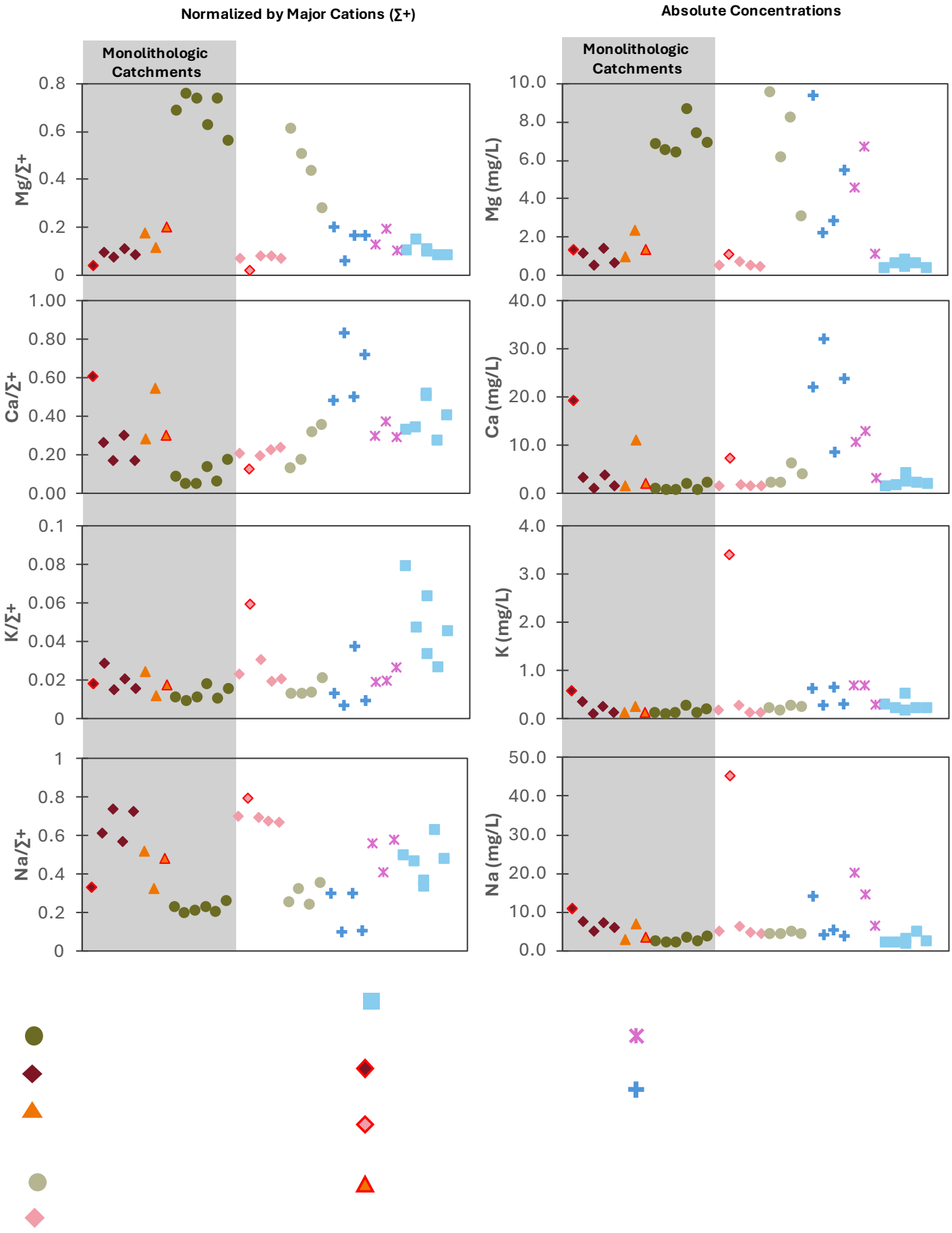

Figure 9: Summary of the major cations (Mg, Ca, Na, K) in all stream/river samples from this study, as measured abundances (µg/L).

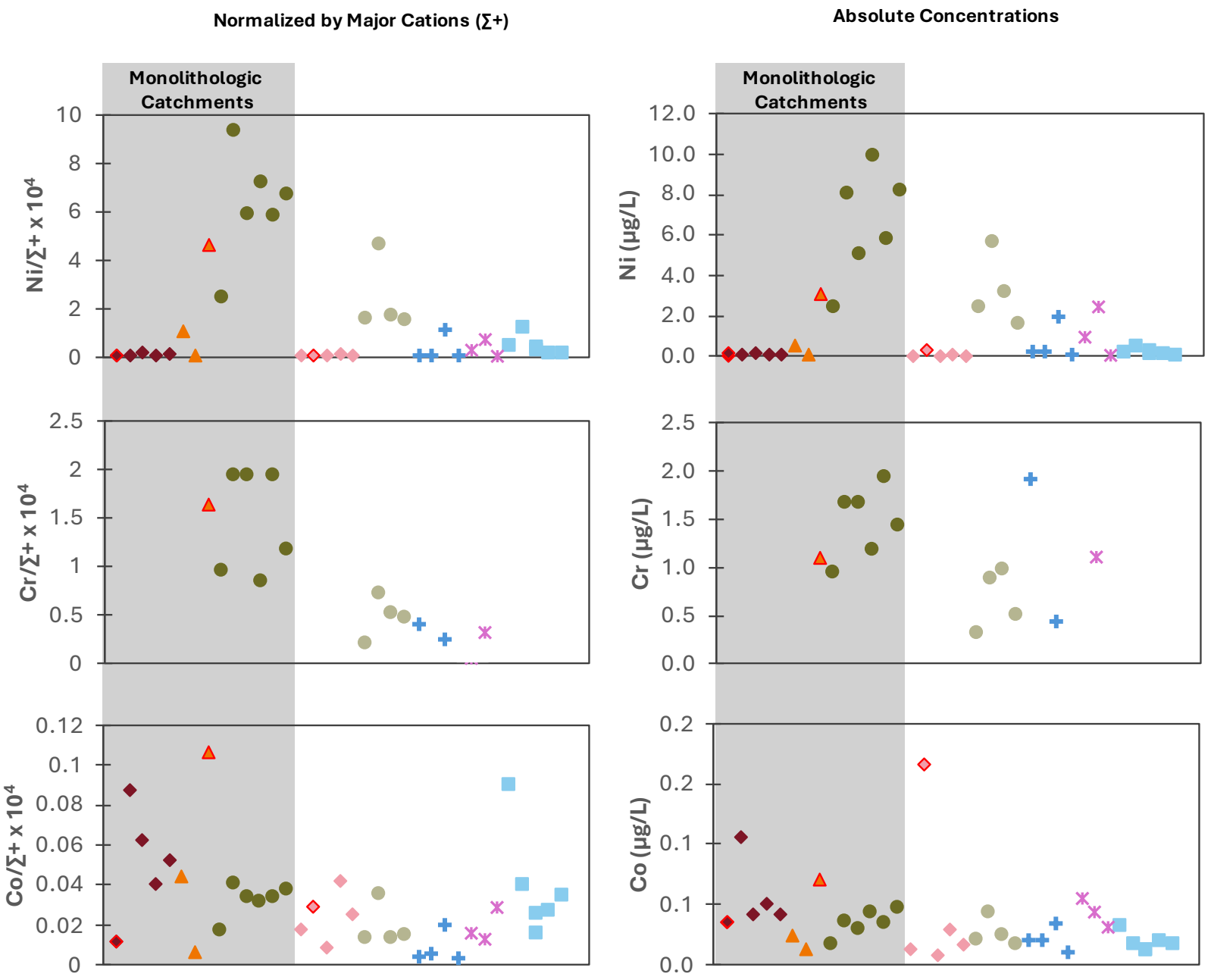

Figure 10: Summary of the mafic and ultramafic rock-associated elements (Ni, Co, Cr) in all stream/river samples from this study, categorized by their lithologic groupings. Data are presented (a) normalized by

∑ µ

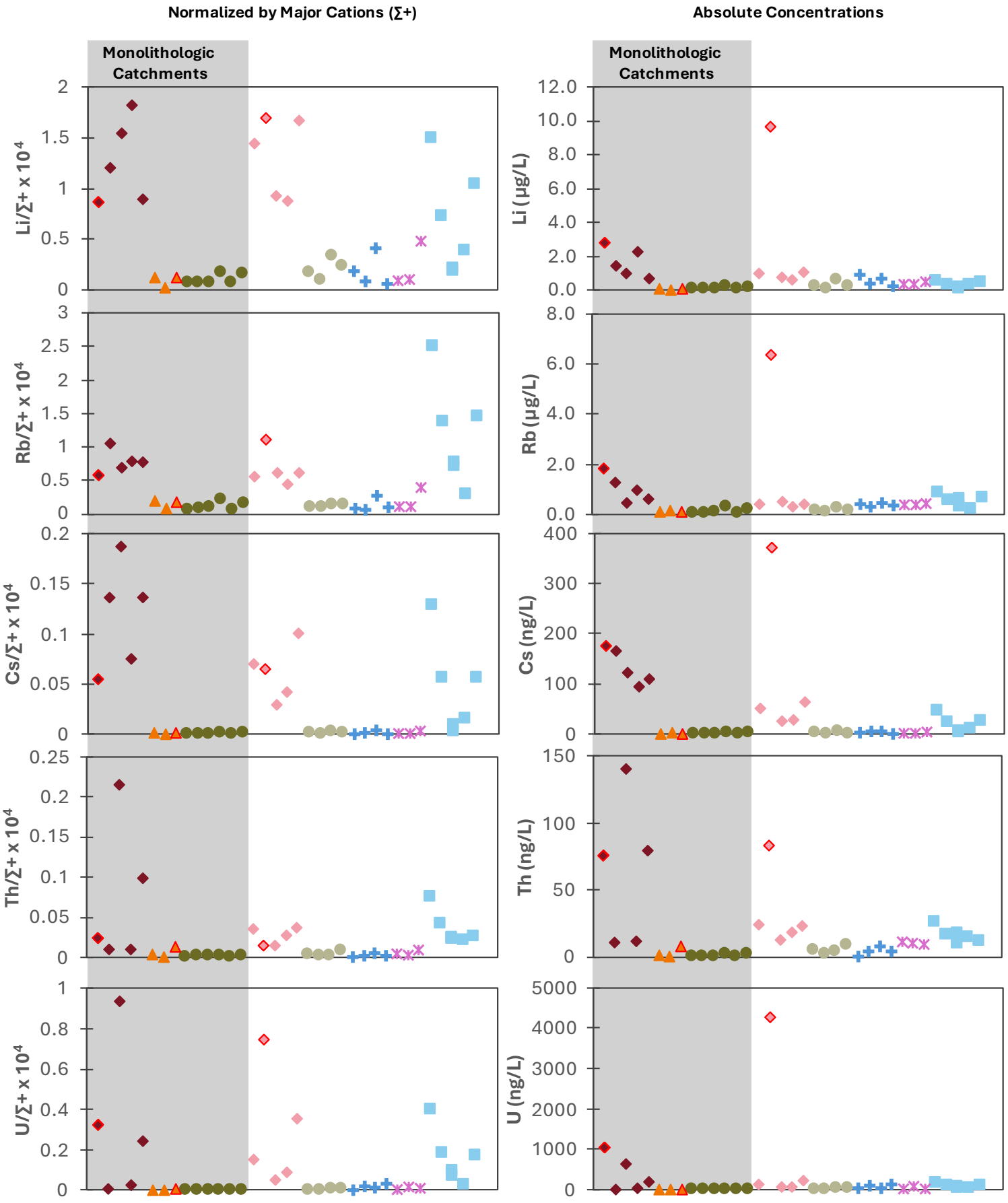

Figure 11: Summary of the felsic rock-associated elements (Li, Rb, Cs, Th, U) in all stream/river samples from this study, categorized by their lithologic groupings. Data are presented (a) normalized by major

Σ µ

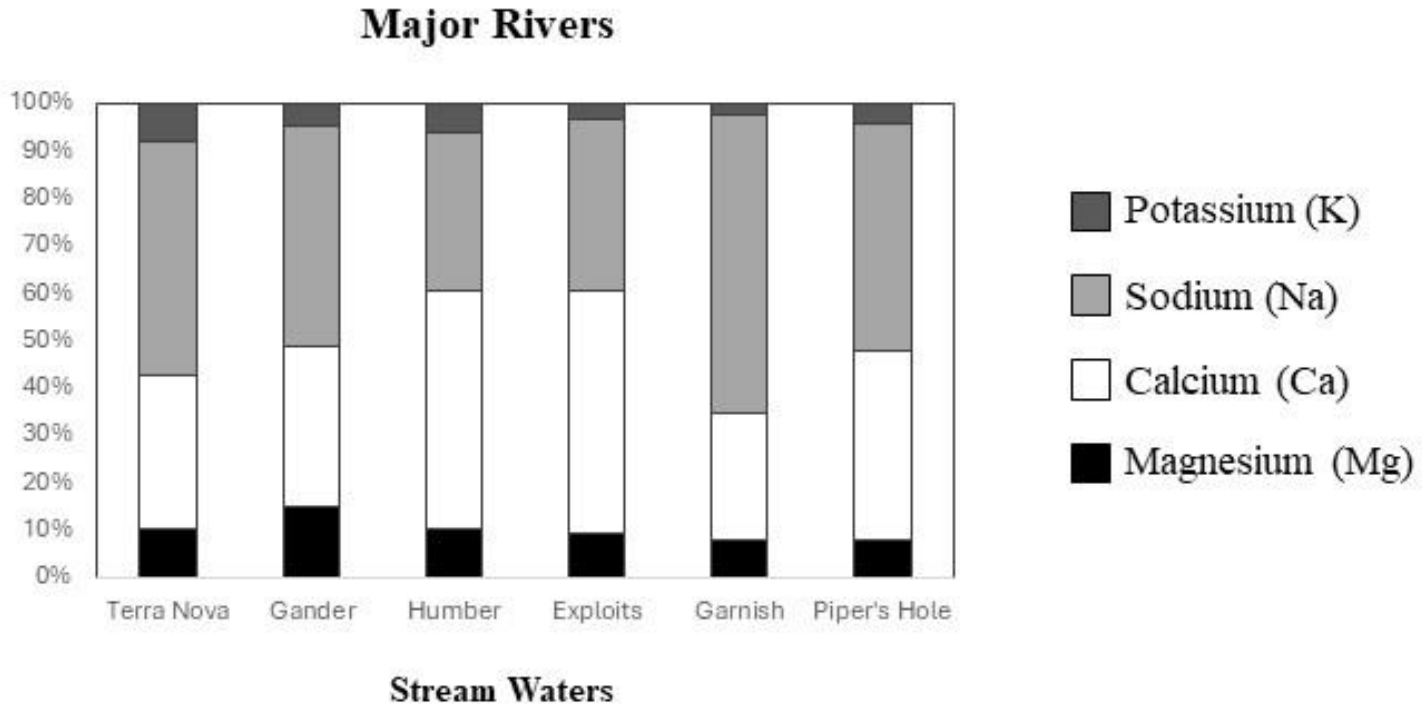

Figure 12: Stacked bar charts showing the relative proportions of dissolved major cations (Mg, Ca, Na, K) in the 6 Newfoundland major rivers sampled for this study.

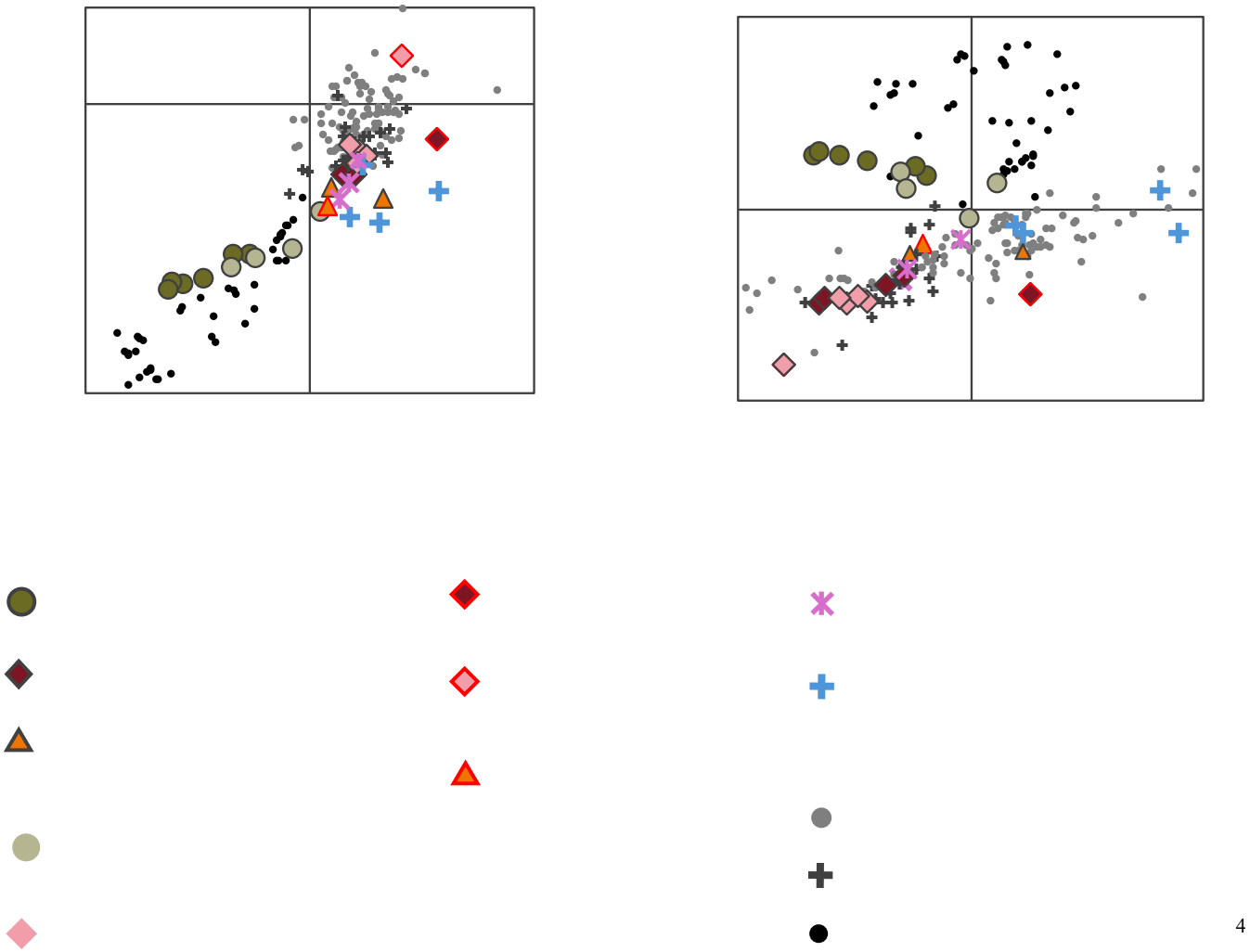

Figure 13: Scatter plots of selected major cation ratios: (a) Ca/Mg vs K/Mg and (b) Ca/Na vs Mg/Na. Sample from this study are presented in their lithologic groupings (Section 2.5.1). Literature data from other studies of monolithologic catchments are compiled for comparison and includes: [1]granite catchments (as initially compiled from several localities by Oliva et al., 2003), [2]mafic catchments in Ireland (Gislason and Arnórsson, 1993), and [3,4]ultramafic catchments in California (McClain and Maher, 2016) and Philippines (Delina et al., 2020).

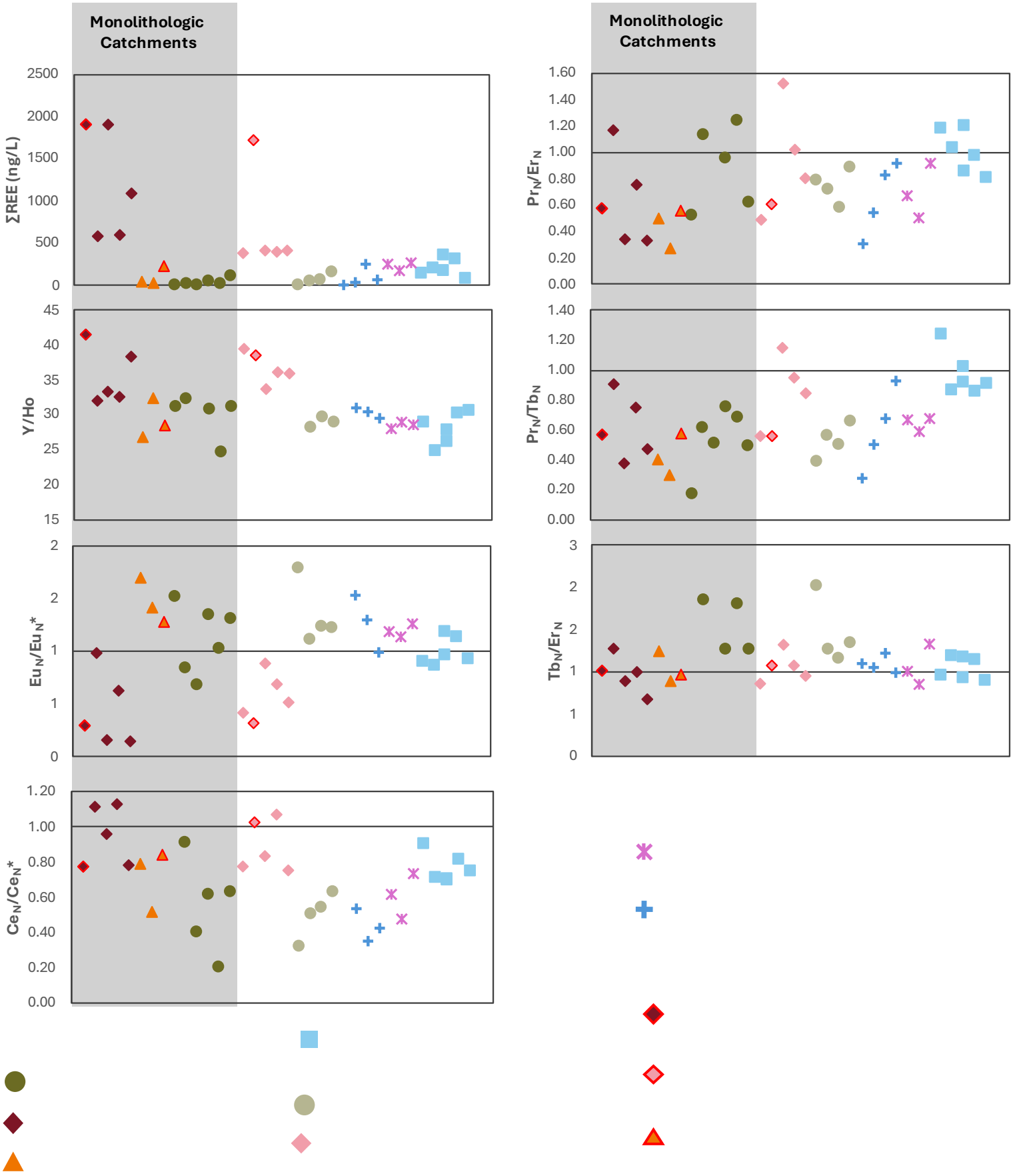

Figure 14: Slopes and anomalies calculated from normalized REE+Y patterns (Figure 15); see Section 2.4.4 ∑ Y Eu_N/Eu_N^* (d) Ce_N/Ce_N^* (e) Pr_N/Er_N (f) Pr_N/Tb_N (g) Tb_N/Er_N. Samples are arranged by lithological grouping across the catchments (Table 2). Some samples are removed if analytical scatter skewed the calculation.

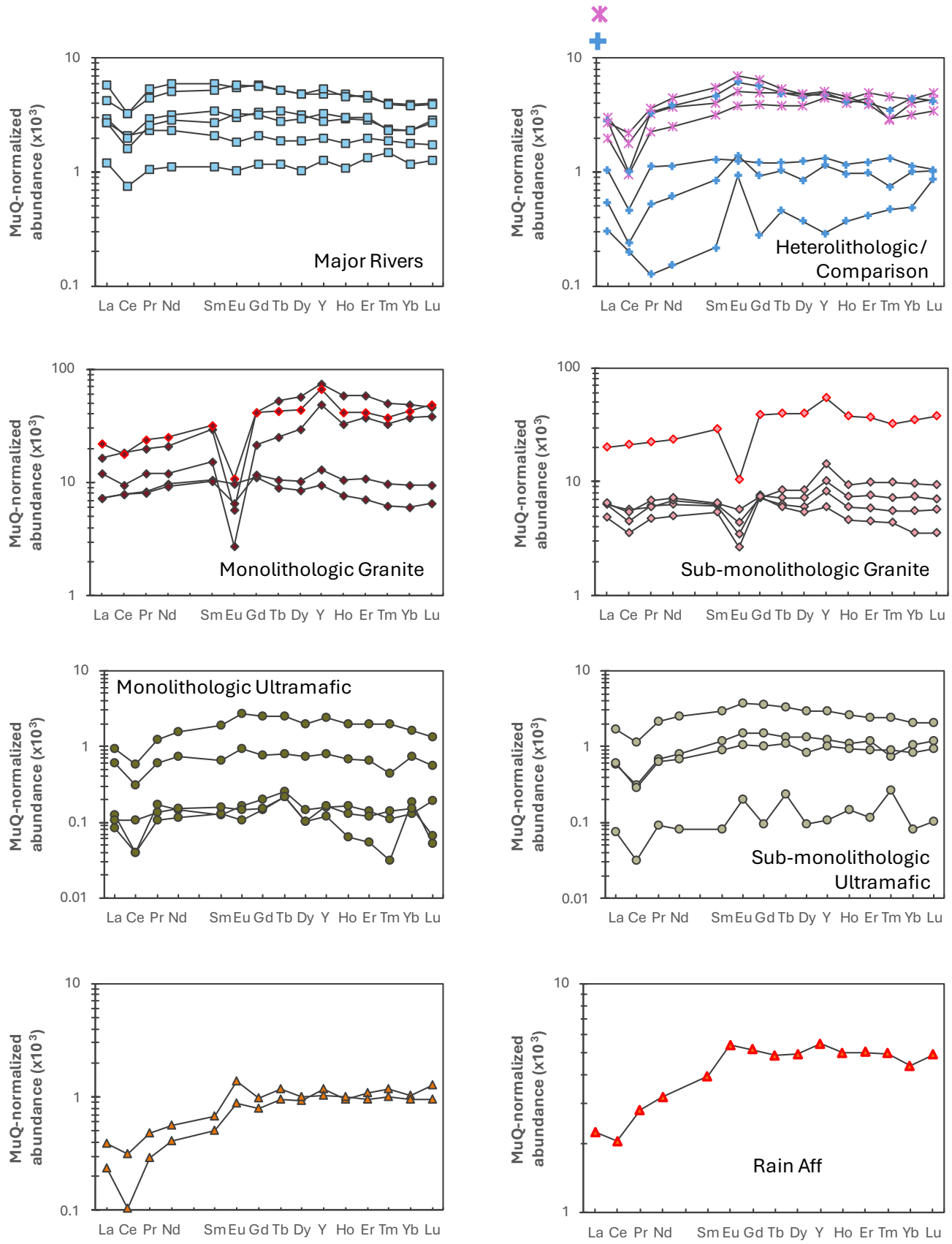

Figure 15: MuQ-normalized REE+Y patterns for water samples divided into: (a) major river samples, (b) heterolithologic/comparison streams at both sites (those in this group draining a catchment with sedimentary rocks are identified), (c) monolithologic granite streams, (d) sub-monolithologic granite streams, (e) monolithologic ultramafic streams, (f) sub-monolithologic ultramafic streams, (g) monolithologic mafic streams, and (h) rain-affected monolithologic mafic samples. Sample GM2206 removed due to very low REE-abundance with a pattern characterized by significant analytical scatter.

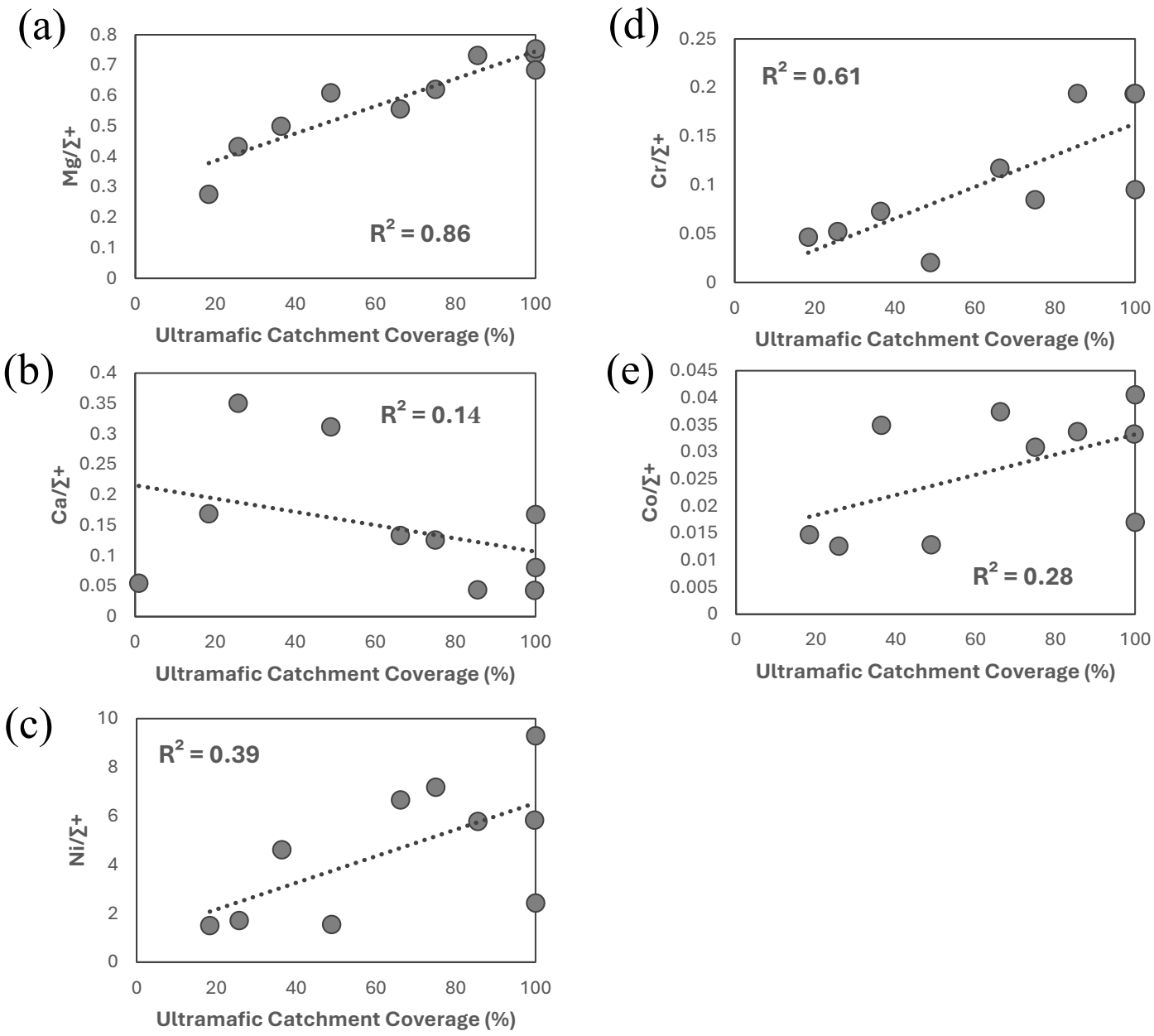

Figure 16: Scatter plots of the calculated % catchment coverage of ultramafic bedrock up to the point of Σ Σ Σ Σ Σ

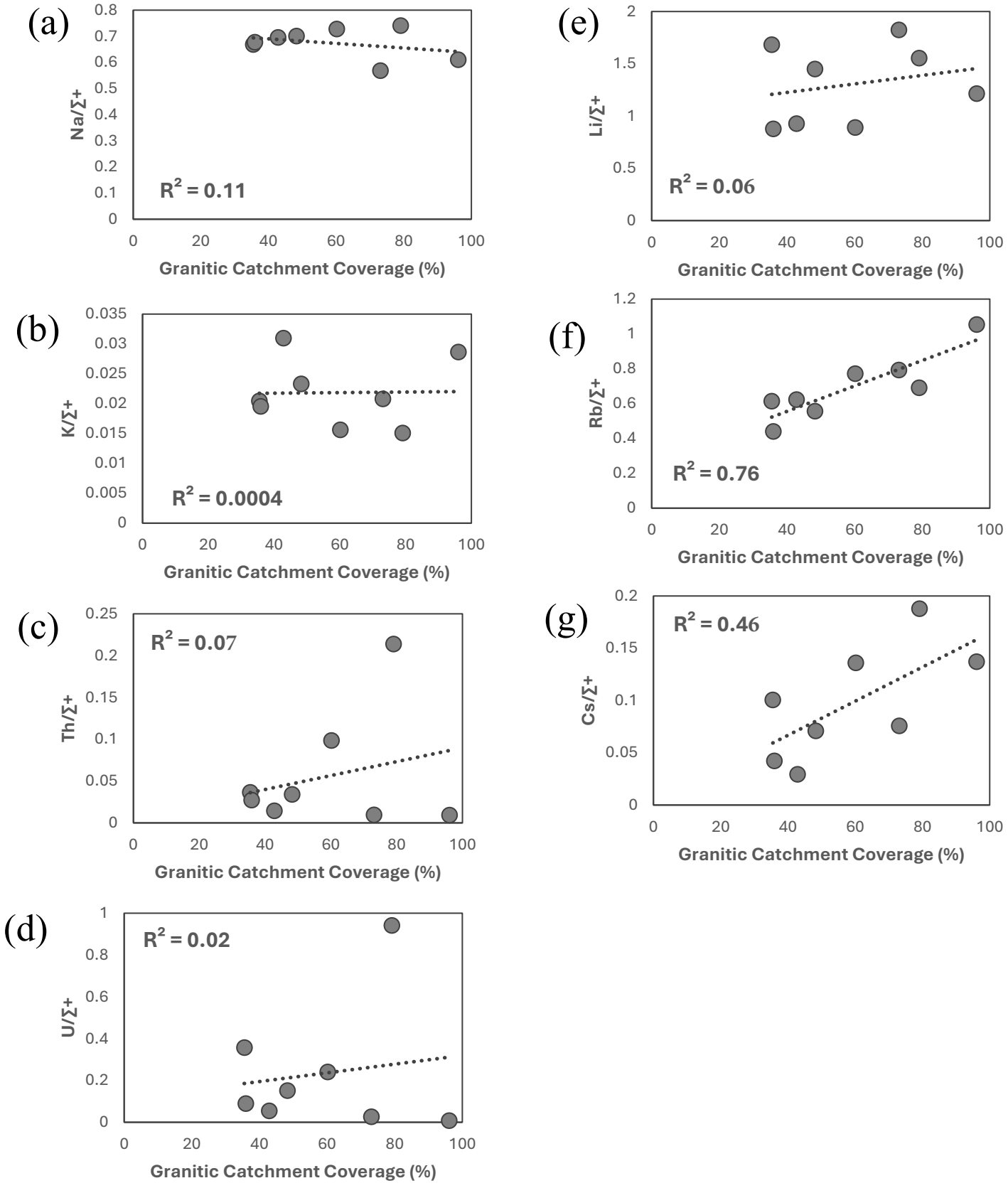

Figure 17: Scatter plots of the calculated % catchment coverage of granite bedrock up to the point of ∑ ∑ ∑ ∑ ∑ ∑ ∑ influence from fluorite veins (Section 2.6.5).

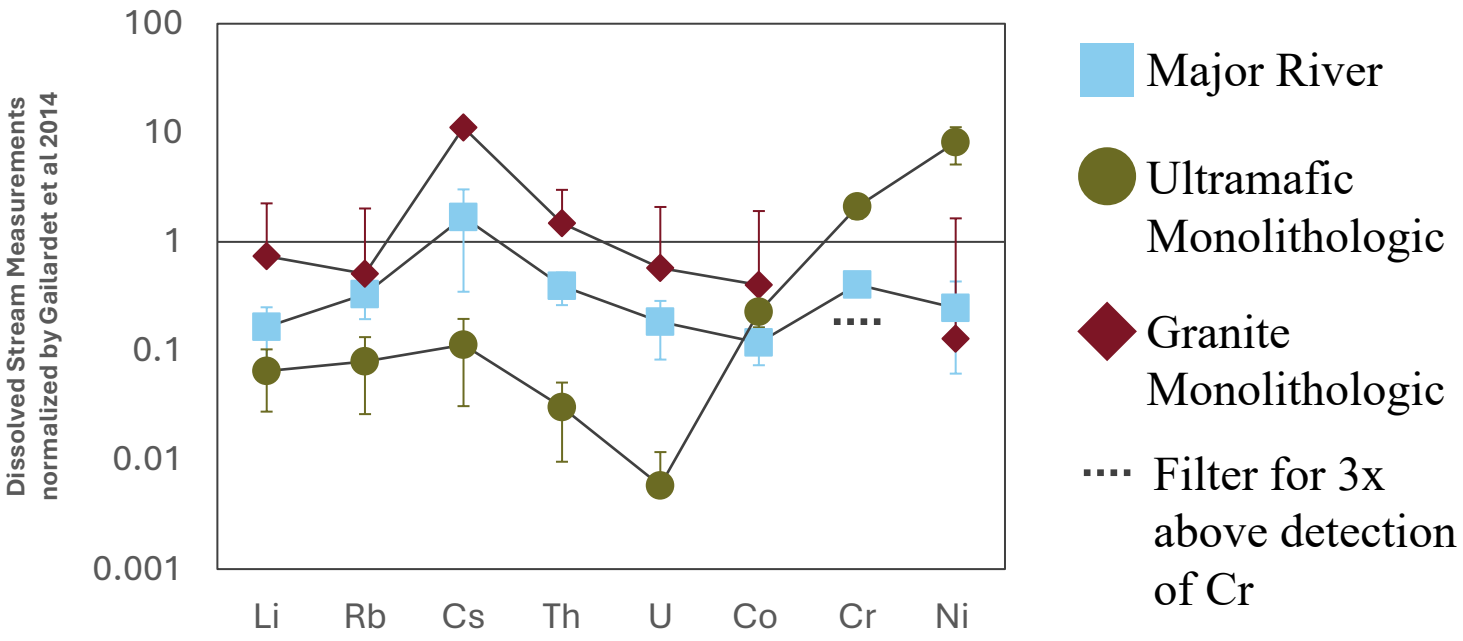

Figure 18: Dissolved stream measurements of selected trace elements normalized by avg world river compilation by Gaillardet et al. (2014). Data presented as mean from each group with error bars representing 1 standard deviation. Values below 3x higher than background equivalent concentration removed.

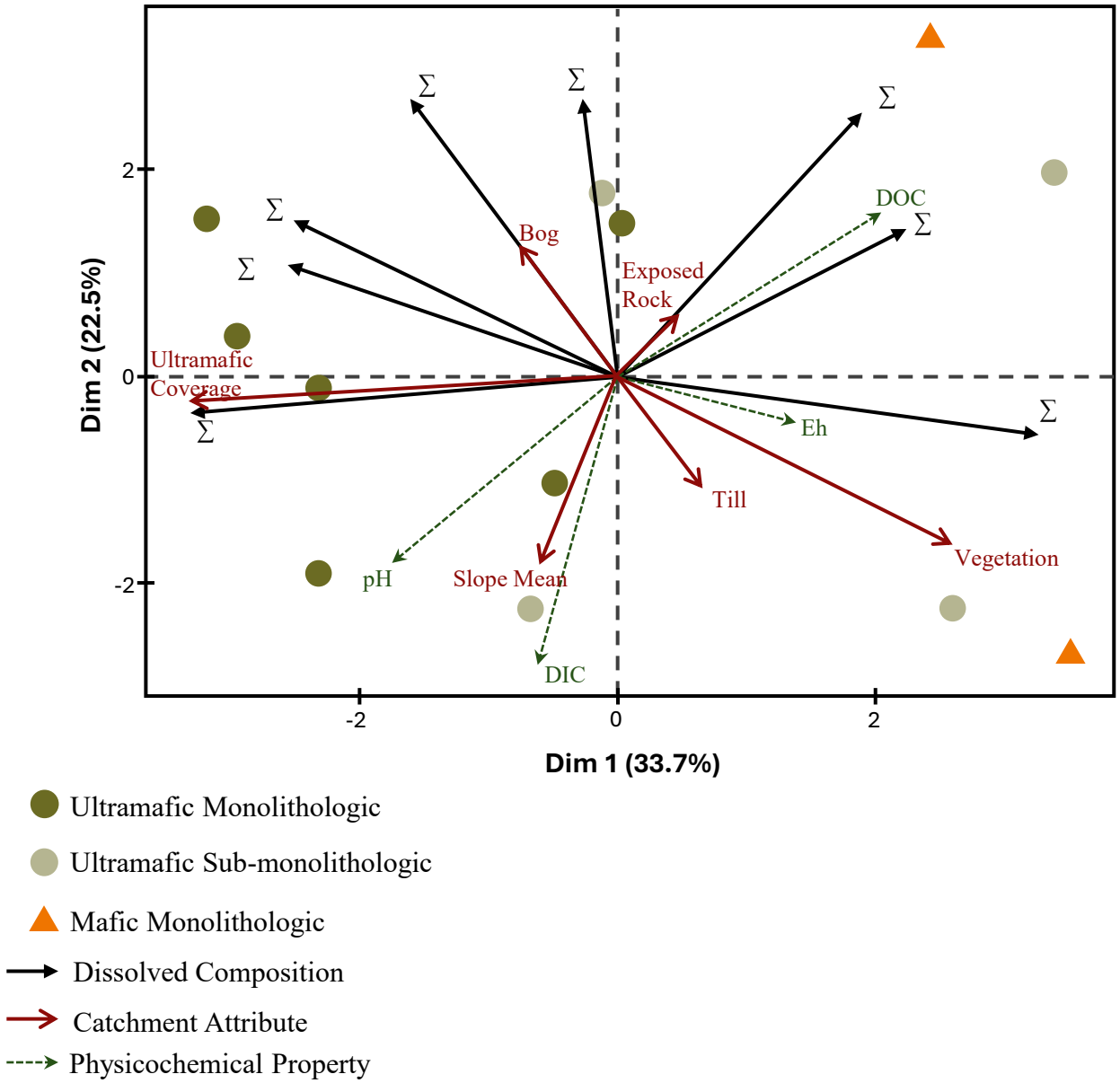

Figure 19: Principal component analysis (PCA) displaying major and trace element relationship of the ultramafic(-mafic) monolithologic and sub-monolithologic streams along with catchment attribute and physicochemical property relationships. Element measurements below detection limit were taken at half the detection limit for PCA. Only Cr was affected by this.

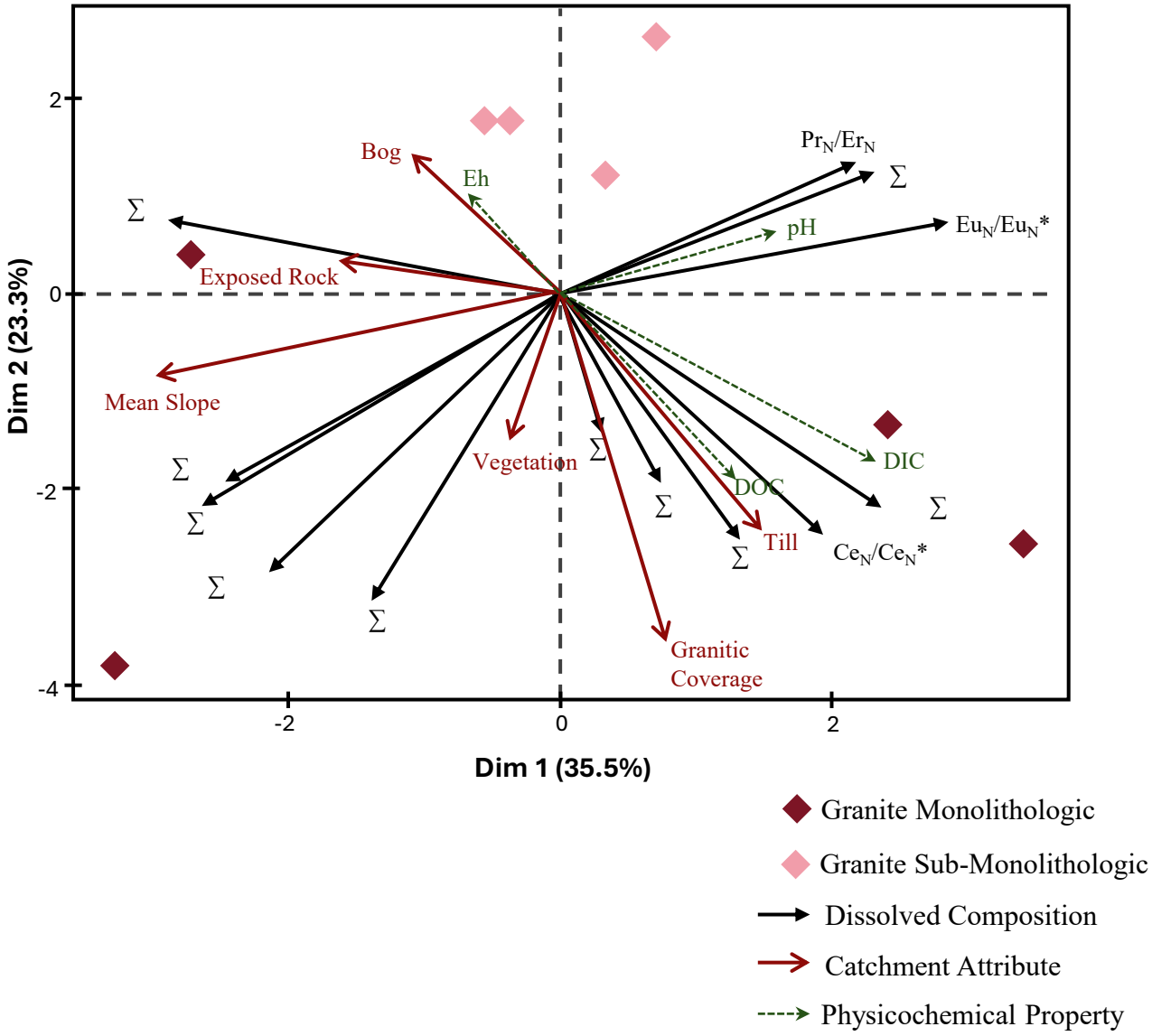

Figure 20: Principal component analysis (PCA) displaying major and trace element relationship of the granitic monolithologic and sub-monolithologic streams along with catchment attribute and physicochemical property relationships.

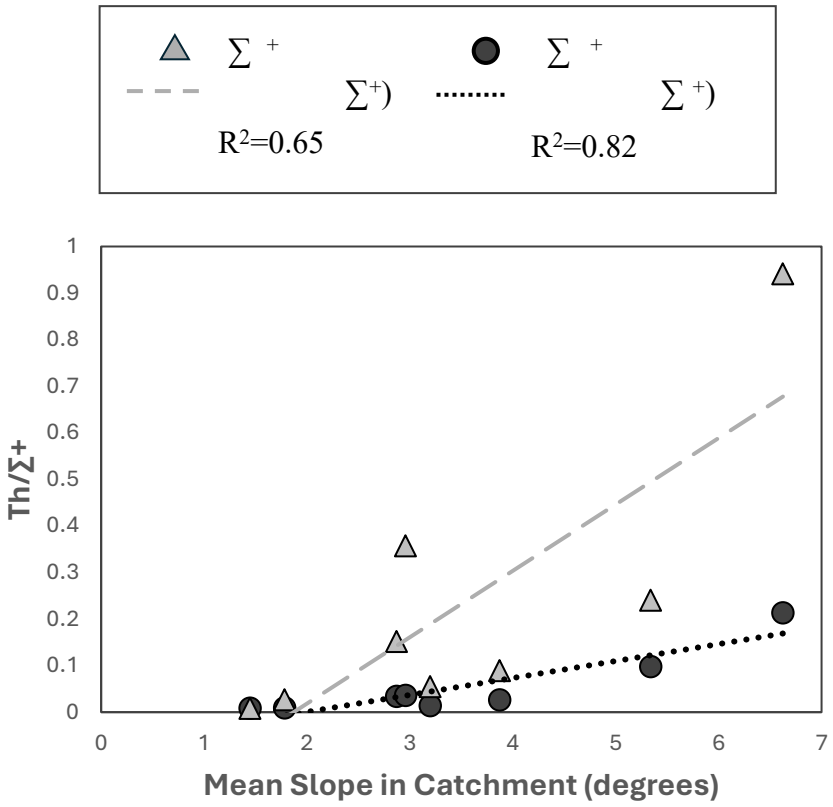

Figure 21 ∑ ∑
stream samples falling into monolithological and sub-monolithogical granite groupings (>30% granite coverage in this case) are considered, with 2 anomalous samples (suspected vein influence) removed.

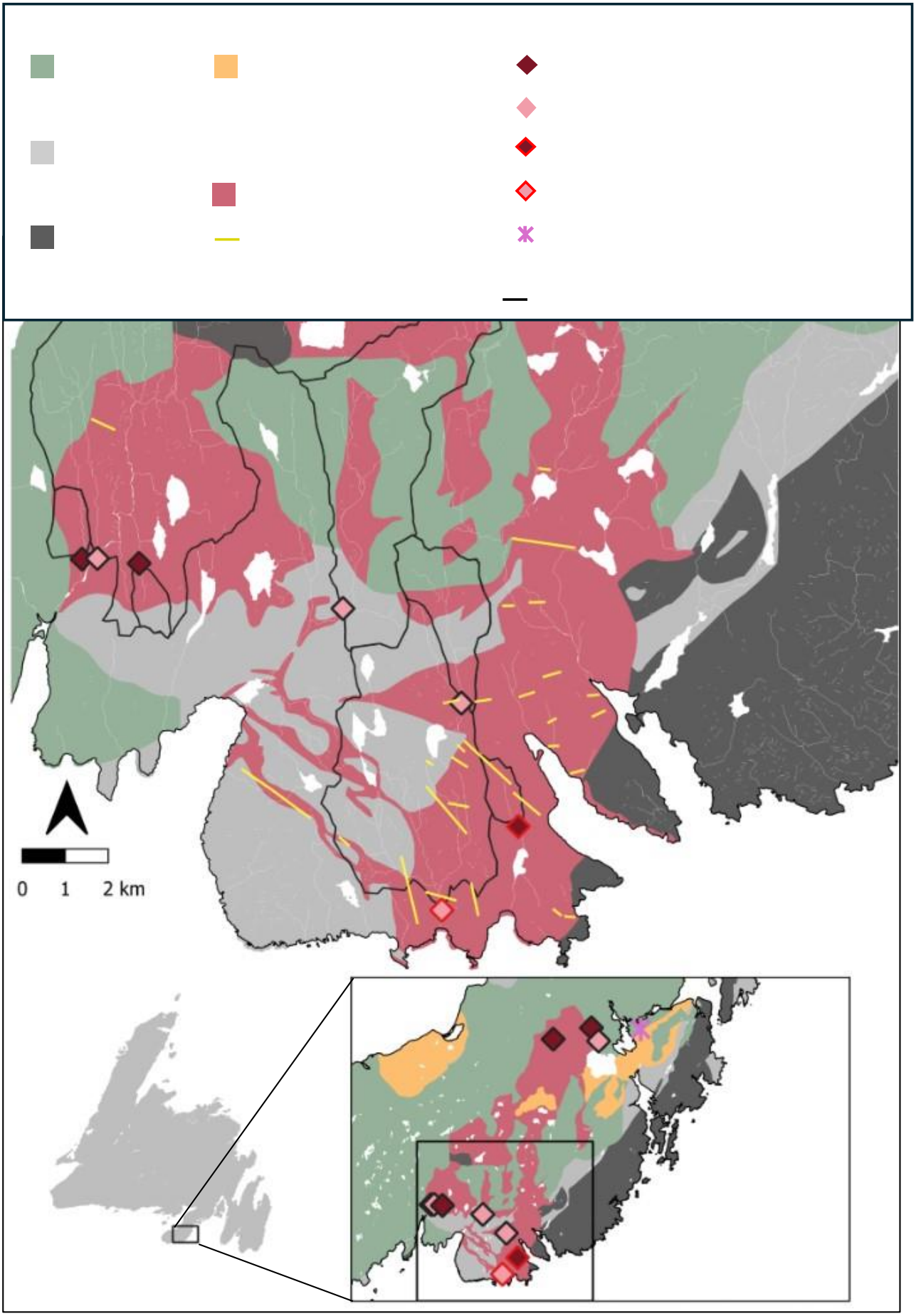

Figure 22: Location of known fluorite veins at the Burin Peninsula study site. Simplified bedrock geology as per Figure 2. Fluorite vein locations extracted from map data after Magyarosi (2022), Magyarosi et al. (2019), Strong et al. (1976, 1978), Wilson (2000).

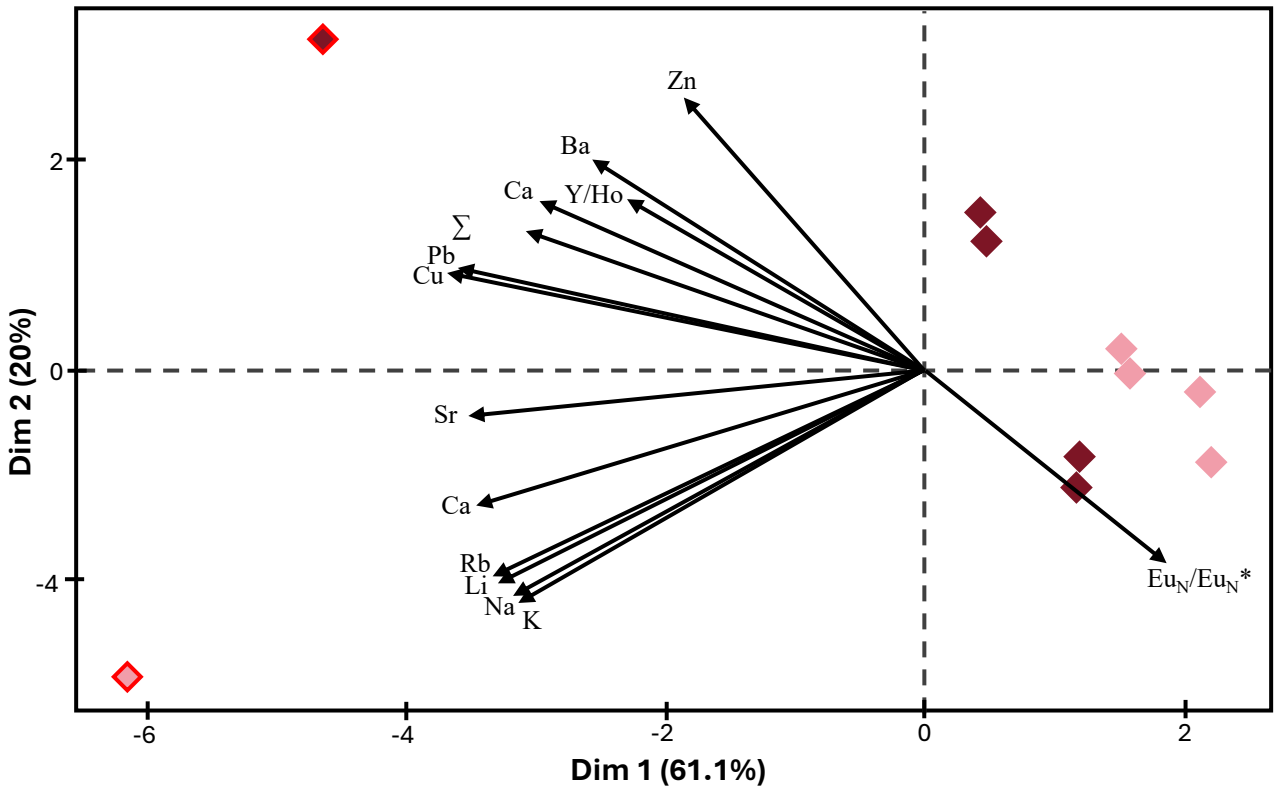

Figure 23: Principal component analysis (PCA) displaying assumed diagnostic vein features (Ca, Cu, Ba, ∑ Y by Section 2.6.3 and other relevant elements (Na, K, EuN/EuN*) evaluated in 2.6.3 as variables for granite monolithologic and sub-monolithologic streams, including two determined anomalous samples.

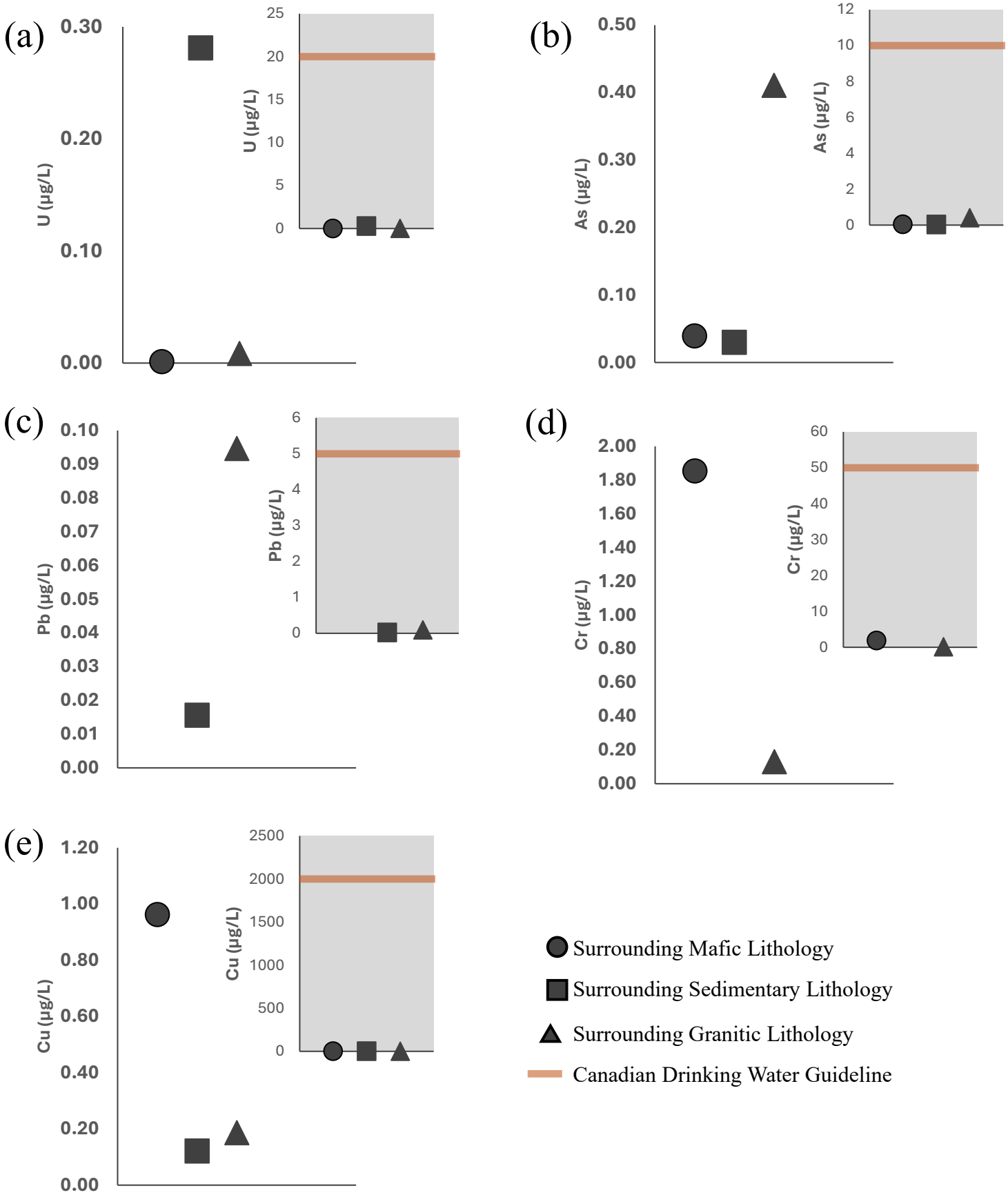

Figure 24: Dissolved trace element abundances in roadside spring waters from 3 sites (see Section 2.3.4.) focused on 5 potentially toxic elements (PTEs): (a) U, (b) As, (c) Pb, (d) Cr, and (e) Cu. Inset plots with shaded background are an expanded abundance range in order to compare values to the Canadian drinking water guidelines (Health Canada, 2019) as represented by the solid (orange) line.

Chapter 3: Conclusions

Rivers have been a focus for research due to their biogeochemical importance at Earth's surface and ability to record information of surface processes; however, the recent and rapid advancement in inductively coupled plasma-mass spectrometry (ICP-MS) technology, along with controlled conditions offered by clean laboratories, has allowed multi-element characterization of the dissolved load of freshwaters systems covering a range of abundances from "major cations" (>1 mg/L) down to ultra-trace elements (<1 μg/L). Canada hosts 28% of the global boreal climate zone area (Brandt et al., 2013) and the rivers in this zone serve as important pathways for studying the fluxes of elements from land into waters, several of which are essential to supporting aquatic life (Cuss et al., 2020) and regulating carbon exchange at the surface (Kohl et al., 2018). This thesis focuses on the island of Newfoundland, situated on the eastern edge of Canada's boreal climate zone, and demonstrates how studying the geochemical cycling of low-abundance trace elements dissolved in waters can offer valuable insights into surface dynamics within Newfoundland, adding important information to similar approaches taken in other boreal climate regions (e.g., Cuss et al., 2020; Pokrovsky et al., 2022).

The first important contribution of this study was a comparative approach between small streams draining contrasting bedrock to emphasize the important role that bedrock geochemical composition and mineralogy play in driving the fluxes of specific elements to small streams and, ultimately, into larger river systems. This study found that major cation and selected trace element chemistry of lithologically restricted catchment streams resembles catchment source rock. While this connection was expected, this study was important in providing new insights of where stream water element abundances were lower than expected based on their source rock enrichment (e.g.,

Co being controlled by dissolved organic matter), emphasizing the need to better understand these complexities across other boreal climate zones with different levels of soil development and vegetation cover. More broadly, research focusing on the geological factors influencing water chemistry is valuable for identifying areas where specific elements are expected to be higher, as well as anticipating areas that could be potential concerns for toxicity (e.g., Cr in areas rich in ultramafic rocks vs. U in areas rich in felsic rocks). While this study evaluated only a small transect of the province's streams and larger rivers, there is more work to be done to fully represent the full diversity in geology, landscape, and vegetation. Studying more of these variations will help to understand the province's freshwater systems and broader boreal catchment dynamics. The Newfoundland study sites for this study lie in coastal locations that resulted in more prominent addition of atmospherically derived elements, evident with the Na proportional abundance. Most of the elements evaluated for this study had clear links to terrestrial catchment control, but further evaluation using major cation/anion and trace element data in streams and precipitation can provide refined insight and accuracy into the element inputs into boreal streams. Specifically, it was apparent from this study that Cl^- is essential to monitor ocean-derived aerosols, and thus provide accurate corrections to stream water data to isolate rock weathering signatures. Other anions such as SO_4^{2-} are predicted to be important in understanding the weathering of sulfide-rich source rocks across the province alongside their contribution of metals to stream waters.

The second important contribution of this study was the quantitative integration of geochemical and geospatial data (% coverage of specific bedrock, elevation gradient, vegetation cover, surficial geology), an approach not commonly undertaken in geochemical-focused studies. This approach allowed for the direct link between bedrock element enrichments and enrichment in stream water, but also revealed where other catchment parameters exerted a greater control on element

abundance in waters rather than the bedrock geology. The close connection of these independent datasets also provided an interesting form of groundtruthing the accuracy of these datasets.

The third important contribution of this study was newfound recognition of more localized geological controls on stream chemistry unique to the research sites. Most prominently, this study provided the first evidence that fluorite mineralization may impart a locally high dissolved Y/Ho ratio to surface waters (reaching levels higher than documented in other low-ionic strength streams globally) – an effect not documented elsewhere prior to this study, to the best of thesis author's knowledge. Further, the rain event documented to drive enhanced organic and inorganic flux to streams emphasized the importance of such events on the surface cycling of dissolved element loads, but also in recognizing the role it can play in potentially toxic element inputs to streams. This input can have implications for aquatic life and human health. For example, further investigation should be undertaken to better understand when it is advisable to avoid the collection of water for personal consumption. This investigation would benefit from addressing the specific organic-inorganic element associations in different areas of the province with varying bedrock, surficial geology, and vegetation.

While this study collected the first multi-element analysis of streams and rivers and Newfoundland, including elements down to ultra-trace levels, it only represents a snapshot of information within the constantly shifting dynamics of boreal systems. It remains an ongoing challenge to assess all the complex and interrelated factors that control the chemical dynamics of a watershed. Some of the factors include seasonal variations that influence weathering rate, runoff, and associated soil outputs and stream flow. To better predict element concentrations, speciation models can be advantageous but often require data that is not common or readily available. Greater

emphasis and investment should be placed on acquiring such data (e.g., trace element data in rocks, organics, groundwater composition, soil environment) to aid in these types of analysis (e.g., equilibrium thermodynamics or kinetics-based approach). Further, this study only measured the dissolved budget of elements at a singular filtration size (water passing through a 0.45 μm filter). There are increasing levels of knowledge to be gained regarding the details of element transport upon further budgeting between truly dissolved species and colloids smaller than common filter pore sizes. Assessing more of these factors require significant allocation of time, funding, and dedicated instrument time and resources as well as ability to revisit sample points across different seasons. This study could not dissect all the established factors of known complexity as part of a single-season and single filtration sampling strategy.

Despite some of the limitations and restrictions associated with this study, this research has set a foundation for future studies to apply similar approaches demonstrated here within the province and beyond. Newfoundland and Labrador's abundant freshwater running throughout its diverse geology and landscapes positions the province as an ideal location for further work on investigating geochemical dynamics in surface boreal systems. Such work should include: further refinement in understanding fundamental Earth surface processes such as chemical weathering in boreal climate zones; exploiting the connection between water chemistry and geology as a mineral deposit exploration tool, and; assessing the terrestrial and aqueous conditions leading to the release and transport of potentially toxic elements into freshwater systems.

3.1. References

Brandt, J.P., Flannigan, M.D., Maynard, D.G., Thompson, I.D., Volney, W.J.A., 2013. An introduction to Canada's boreal zone: ecosystem processes, health, sustainability, and environmental issues. Environ. Rev. 21, 207–226. https://doi.org/10.1139/er-2013-0040

Cuss, C.W., Glover, C.N., Javed, M.B., Nagel, A., Shotyk, W., 2020. Geochemical and biological controls on the ecological relevance of total, dissolved, and colloidal forms of trace elements in large boreal rivers: review and case studies. Environ. Rev. 28, 138–163. https://doi.org/10.1139/er-2019-0014

Kohl, L., Philben, M., Edwards, K.A., Podrebarac, F.A., Warren, J., Ziegler, S.E., 2018. The origin of soil organic matter controls its composition and bioreactivity across a mesic boreal forest latitudinal gradient. Global Change Biology 24, e458–e473. https://doi.org/10.1111/gcb.13887

Pokrovsky, O.S., Manasypov, R.M., Chupakov, A.V., Kopysov, S., 2022. Element transport in the Taz River, western Siberia. Chemical Geology 614, 121180. https://doi.org/10.1016/j.chemgeo.2022.121180

Appendix 1: Full watershed attributes and physicochemical properties of all streams/rivers

	Latitude	Longitude	BOIC Ultramafic Bedrock	BOIC Mafic Bedrock	St. Lawrence Granite	Till	Exposed/Concealed Rock
	N	W	%	%	%	%	%
Major Rivers							
MR2201 (Terra Nova)	48˚ 38' 25.9"	054˚ 02' 10.5"	*N.A*	*N.A*	*N.A*	*Not calculated*	*Not calculated*
MR2202 (Gander)	48˚ 59' 53.8"	056˚51'58.6"	*N.A*	*N.A*	*N.A*	*Not calculated*	*Not calculated*
MR2203 (Humber)	48˚59'00.6"	057˚45'37.4"	*N.A*	*N.A*	*N.A*	*Not calculated*	*Not calculated*
MR2204 (Exploits)	48˚55'23.5"	055˚39'44.4"	*N.A*	*N.A*	*N.A*	*Not calculated*	*Not calculated*
MR2205 (Garnish)	47˚13'21.7"	055˚20'23.6"	*N.A*	*N.A*	*N.A*	*Not calculated*	*Not calculated*
MR2206 (Piper's Hole)	47˚55'49.7"	54˚16'23.0"	*N.A*	*N.A*	*N.A*	*Not calculated*	*Not calculated*
Western NL Samples							
BI2201	49˚06'39.1"	058˚24'18.8"	0	0	*N.A*	18	25
BI2202	49˚06'03.6"	058˚23'14.3"	0	0	*N.A*	27	48
BI2203*	49˚03'23.9"	058˚22'29.7"	0	0	*N.A*	~100*	0
BI2205	49˚03'29.7"	058˚19'23.8"		100	*N.A*		
BI2206	49˚03'50.5"	058˚14'23.0"	0	93	*N.A*	0	95
BI2207	49˚03'37.1"	058˚13'29.6"	1	41	*N.A*	1	77
BI2208	49˚00'22.1"	058˚08'02.1"	49	0	*N.A*	15	42
BI2209	48˚58'11.2"	058˚03'56.1	26	0	*N.A*	24	65
GM2201	49˚27'46.7"	058˚07'22.4"	0	18	*N.A*	26	66
GM2202	49˚28'11.0"	058˚07'11.5"	36	52	*N.A*	7	69
GM2203	49˚29'13.3"	058˚01'02.1"	86	14	*N.A*	0	87
GM2204	49˚28'55.8"	057˚59'30.8"	100	0	*N.A*	0	92
GM2205	49˚27'50.2"	057˚57'36.1"	100	0	*N.A*	0	79
GM2206	49˚28'28.3"	057˚57'57.9"	100	0	*N.A*	0	65
GM2207**	49˚30'20.9"	057˚55'07.1"	0	0	*N.A*	0	67
GM2208	49˚29'17.4"	057˚55'47.4"	66	0	*N.A*	0	96
GM2209	49˚28'23.8	057˚55'20.6"	75	0	*N.A*	17	58
GM2210	49˚26'41.1"	057˚54'18.6"	9	0	*N.A*	37	47
GM2211	49˚24'08.2"	057˚43'48.4"	0	0	*N.A*	47	50
Burin Peninsula Samples							
BP2201	46˚57'31.2"	055˚31'41.0"	*N.A*	*N.A*	79	80	1
BP2202	46˚57'31.5"	055˚31'24.3"	*N.A*	*N.A*	48	69	1
BP2203	46˚57'27.2"	055˚30'38.4"	*N.A*	*N.A*	60	50	27
BP2204	46˚56'50.2"	055˚26'54.7"	*N.A*	*N.A*	36	59	0
BP2205	46˚55'37.3"	055˚24'46.6"	*N.A*	*N.A*	36	70	0
BP2206	46˚54'3.8"	055˚23'46.8"	*N.A*	*N.A*	100	100	0
BP2207	46˚53'02.8"	055˚25'13.5"	*N.A*	*N.A*	45	72	2
BP2208	47˚08'29.0"	055˚16'28.8"	*N.A*	*N.A*	96	82	0
BP2209	47˚07'38.3"	055˚15'50.9"	*N.A*	*N.A*	43	71	2
BP2210	47˚08'19.3"	055˚11'55.3"	*N.A*	*N.A*	0	55	45
BP2212	47˚07'49.2"	55˚20'03.3"	*N.A*	*N.A*	73	75	0
Spring Waters							
BI2204	49˚03'24.1"	058˚20'00.8"					
GM2212	49˚30'19.8"	057˚48'11.4"					
BP2211	47˚09'39.4"	55˚18'37.1"					

*Difficulty in delineating sample catchment boundaries and was therefore excluded from coverage values, except where files overlapped completely and value of 100% could be used.

**Sample catchment is classified as monolithologic mafic but does not contain mafic rocks from the Bay of Island Complex and contains 100% Little Port Complex.

Appendix 1 cont.: Full watershed attributes and physicochemical properties of all streams/rivers

		Bog	Dense/Open Forest	Size	Mean Slope	Eh	pH	Conductivity	Temperature	DOC	DIC
		%	%	km2	degrees (0 to 90)	mV		µS/cm	C	mg/L	mg/L
Major Rivers											
	MR2201 (Terra Nova)	*Not calculated*	63	1875.1	*Not calculated*	397.4	7.33	17.5	21.3	5.59	0.59
	MR2202 (Gander)	*Not calculated*	76	4197.5	*Not calculated*	399.7	7.08	22.0	18.4	6.84	0.66
	MR2203 (Humber)	*Not calculated*	59	7588.2	*Not calculated*	417.3	7.62	40.0	16.6	5.53	2.55
	MR2204 (Exploits)	*Not calculated*	55	9579.6	*Not calculated*	422.1	7.45	24.8	19.5	4.88	1.19
	MR2205 (Garnish)	*Not calculated*	27	203.9	*Not calculated*	426.6	6.89	39.0	21.9	8.56	0.81
	MR2206 (Piper's Hole)	*Not calculated*	15	791.8	*Not calculated*	389.8	7.42	25.8	22.4	4.53	1.21
Western NL Samples											
	BI2201	45	29	3.4	7.3	413.0	7.70	176.8	15.5	9.71	9.11
	BI2202	9	27	7.1	14.4	431.6	7.94	186.1	16.4	4.99	11.84
	BI2203*	0	0			454.7	8.26	250.0	7.5	1.72	19.29
	BI2205					465.3	7.70	111.6	15.3	1.89	7.66
	BI2206	1	37	13.5	15.0	478.3	7.32	32.6	15.3	2.91	1.41
	BI2207	11	7	6.3	8.0	469.8	8.07	107.4	17.0	1.20	9.67
	BI2208	15	4	56.9	9.5	457.0	8.08	115.4	18.9	3.38	10.37
	BI2209	0	46	35.8	9.1	441.2	8.40	184.7	16.7	4.98	19.20
	GM2201	3	45	95.9	6.2	436.8	7.82	65.6	17.0	4.93	4.33
	GM2202	6	17	243.4	9.4	431.5	7.91	78.2	16.5	2.80	6.69
	GM2203	0	6	21.4	8.9	421.6	8.02	75.8	13.7	1.58	7.42
	GM2204	0	0	2.1	9.2	426.3	7.91	64.1	13.2	1.47	6.38
	GM2205	6	0	5.9	10.2	437.8	7.96	63.2	13.6	2.13	6.34
	GM2206	18	0	6.8	11.8	417.6	8.03	73.5	15.1	0.86	6.91
	GM2207**	0	0	0.8	16.2	404.4	7.20	33.2	17.9	16.26	1.32
	GM2208	0	11	1.8	10.7	428.0	7.98	78.2	17.5	4.03	7.51
	GM2209	9	4	13.7	11.9	454.9	7.99	94.9	16.9	3.57	8.95
	GM2210	4	21	10.0	14.7	463.5	7.94	93.4	15.8	6.18	7.57
	GM2211	0	45	2.4	16.4	447.0	8.22	175.6	18.2	3.70	17.75
Burin Peninsula Samples											
	BP2201	20	10	1.3	6.6	401.8	6.28	37.5	18.3	8.31	0.49
	BP2202	23	1	75.5	2.9	393.3	6.94	38.4	20.7	5.62	0.54
	BP2203	26	4	1.1	5.3	392.2	6.64	43.4	23.5	5.42	0.75
	BP2204	38	0	17.6	3.0	400.5	6.81	35.9	26.0	5.64	0.81
	BP2205	32	0	4.5	3.9	382.6	6.34	34.1	27.3	11.51	0.68
	BP2206	0	9	1.0	3.4	509.5	7.68	160.5	7.7	7.94	9.40
	BP2207	22	1	22.9	2.9	478.0	8.11	252.0	22.3	7.42	16.36
	BP2208	9	3	3.0	1.4	349.6	6.72	64.7	18.5	9.07	1.94
	BP2209	13	11	166.1	3.2	418.0	6.59	47.7	24.3	4.94	0.50
	BP2210	0	26	2.4	5.6	385.3	6.98	57.1	25.5	8.40	2.23
	BP2212	26	7	3.0	1.8	428.8	7.18	68.2	23.8	10.57	2.67
Spring Waters											
	BI2204					460.2	7.83	142.5	7.8	2.08	5.74
	GM2212					491.7	7.83	328.0	8.2	1.21	31.17
	BP2211					389.5	7.18	68.2	23.8	5.93	3.37

*Difficulty in delineating sample catchment boundaries and was therefore excluded from coverage values, except where files overlapped completely and value of 100% could be used.

**Sample catchment is classified as monolithologic mafic but does not contain mafic rocks from the Bay of Island Complex and contains 100% Little Port Complex.

Appendix 2: Field observations for all streams/rivers

Sample ID	Flow Conditions and Field Observations	Bedload Observations
Western NL Sites		
BI2201	Small stream draining flat, vegetative valley between mafic-ultramafic mountains, took long to filter	Pebbles to boulders but banks and low flow areas have sand to mud and more organic-rich
BI2202	Filtered easily, adjacent to dark/grey alluvium very muddy, water flowing at medium pace, banks mostly till, grass and trees well stabilized	Mostly pebbles to boulders with areas of sand to minor mud
BI2203	Gentleflow, in forest vegetation, young deciduous trees, shrub on banks	Mostly pebble bedload with sand on banks
BI2204	Sample spring water at a roadside point where water flows rapidly from plastic tubing at the end of a steep rocky slope covered in moss, with trees above	NA
BI2205	Relatively fast-flowing 'mountainous' stream	Large boulder load, only sand-sized sediment in small pockets of slower flow and on some banks, boulder contain many mafic rock (volc-pillows, flow-top breccias with hematite) possible ultra-mafic, some felsic
BI2206	Brook similar to BI2205, can see headwaters (waterfall) up the mountain, fast flowing stream, elevation climbs quickly, started to rain during sampling	Large boulder bedload dominates with pebble/cobbles in slower-flowing areas, coarse sand in banks, mostly mafic boulder
BI2207	Blow Me Down Brook, fast-flowing book, actively raining, filtered in car, downstream of swimming area	Large boulder bedload, pebbles and rare sand-sized on some banks, many mafic-ultramafic rocks
BI2208	Fast-flowing river/brook, upstream of St. Peter's Academy, actively raining during sampling, filtered in car, can see waterfall upstream of sampling point	Bedload similar to BI2207
BI2209	Sampled day after heavy rain, relatively fast-flowing stream, can see waterfall upstream	Rounded boulders as major bedload but metamorphosed sed rocks in outcrop nearby, breaks into blocks and is in bedload near outcrop
GM2201	Trout River - river flowing at medium pace, wide but shallow	Bedload rocky, pebbles to boulders, with finer seds in low areas with some vegetation
GM2202	Tributary to Trout River, upstream to town, just upstream from town water supply with area under construction for upgrades, fast-flowing stream, shallow	Very coarse bedload, large boulder to pebble, only sand sed noted in very small, bank areas, mixture of rock types in banks boulders but many ultra-mafic-mafic, minor seds (cherty rocks), human-added pebble crushed construction rock in some areas around sampling site. High bouldery bank possibly man-made
GM2203	Tablelands stream, fast-flowing high elevation climb, stream fed from top of tablelands, carving down valley	Rounded boulder bed, coarse with sand at finest, some clay coatings on banks, some shrubby areas growing on more stable banks.
GM2204	Fast-flowing tablelands stream, similar to GM2203	Rounded pebble dominated bedload, typical tablelands variably serpentinized ultra-mafic rock, orange-oxide-coated, sediment distribution similar to GM2203
GM2205	Winterhouse Canyon Brook in Tablelands, up from board walk near stream split/juncture, fast-flowing	Bedload similar to GM2204, boulders rounded and ultra-mafic
GM2206	Tablelands stream, fast-flowing stream downslope large boulder bedload	Large boulder bedload, very little fine sediment, lots of serpentinized rocks in bedloads and around bank
GM2207	Fast-flowing brook, assumed to be a low-level, gentle-flow before rain on previous day and less colored, water looks red-to-orange, some anthropogenic influence to stream (tires, scrap metal)	Generally large boulder bedload but some pockets of pebbly areas and rarer fines on banks, bedload geology is mixed in composition but mafic-ultramafic still noticeable, high banks of boulders with shrubs and trees - more pines upstream
GM2208	Winterhouse Brook after traverse through other rock types and pine forest (much different color of water), sampled at point just before concrete dam in area where there is an artificial bank built with foreign rocks	
GM2209	Brook draining pine tree area, sampled upstream of property, relatively fast-flowing, bouldery river, very few fine sediment in sample area, water not as organic-looking as GM2208	
GM2210	Brook draining metasedimentary rock, artificial bank of massive limestone blocks, sampled upstream from this, brook draining high elevation of bedrock/outcrop is metamorphosed fine-grained siliclastic rock	Bedload is coarse, some small ponds, along waterfall stretch and at some banks near trees, above outcrop bank vegetation is trees (mixed deciduous and pines) and shrubs
GM2211	Large river in area, wider, relatively fast-flowing	Observations not taken
GM2212	Sampled directly from a rock groundwater spring via a pipe adjacent to a highway, consistent to slow trickle flow	NA

Appendix 2 cont.: Field observations for all streams/rivers

Sample ID	Flow Conditions and Field Observations	Bedload Observations
Burin Peninsula Sites		
BP2201	Sampled in very foggy weather, small - very slow flowing stream, low elevation through flat grassy marsh wetland area, higher up gentle banks, young pine trees, water anticipated to be high in organics, required 2 filters	Bedload largely blocky boulders despite low stream flow, organic scum and some small aquatic plants covering boulders
BP2202	Larger stream/brook near BP2201, samples with bucket from bridge, fast-flowing brook, still colored water with clear organic load present, sed could have anthropogenic influence from road/bridge grit	Granite block bedload, variably rounded but blockier than western NL samples, banks rocky and transitioned to wetland grass/shrubs, pine on some inner banks.
BP2203	Small Stream, slow-flowing stream, took 2 filters	Large granite boulders, organic-crud covered, banks low-lying relatively flat granite base covered by bog/marsh
BP2204	Larger stream draining granite, sampled ~30 m upstream of road/culvert after short through boggy marsh area, foggy, relatively fast-flowing stream but ponds before road culvert, small aquatic plants in sandy areas, took 2 filters.	Bedload mostly cobbles to pebbles with some areas of boulders, variably rounded to blocky, sandy sed trapped between some of the boulders, pebbles and boulders all look pink but most is pinky-orange coating on different rock types
BP2205	Small stream just near limit of St Lawrence, near Bell Aliant hut/Lions club sign, gentle but consistent flow up to a bit of ponding at the culvert, very dark-colored water compared to previous samples, bit of aquatic plants life and bugs, small fish, bull frogs in area but mostly in the ponds, wind mills in distance upstream, same pine trees in upstream of banks, took 3 filters	Boulder to pebble bedload, not much sand to mud, banks build of boulders but quickly turns to flanking marsh with many still ponds
BP2206	Small stream draining down from fluorspar mine in St Lawrence, sampled between two manmade rock dams, can see biofilms, gentle but 'babbling' stream, good constant flow, only took 1 filter	Bedload angular boulders, minimal sediment
BP2207	Brook under the St Lawrence miner's memorial bridge leading to Camber Cove, sampled from bridge with bucket, fast-flowing, only took 1 filter	Rocky, boulder bedload, possible sand to pebbles in slower moving bank areas, outcrop visible under bridge but banks are coarse boulders often covered in shrubs to pine trees
BP2208	Small stream off Kimberley Farm, gentle but consistent flow in stream, very organic-y colored water, took 3 filters	Banks are muddy and organic-y, stabilized by pine tree and moss almost right up to the stream, stream bedload, at center bobble to pebble with some trapped sand and lesser mud
BP2209	Larger brook/river in area (BP2208 drains into it), relatively fast flowing, filtered easily, relatively clean/pure-looking water, some aquatic plant life near banks	Bedload boulders to pebbles with pebbles trapped between boulders with some fines, green 'moss' covered boulders in some areas, banks build of rock boulders that quickly transition to marsh and pine
BP2210	Small stream draining into a pond and intersecting walking trail, water is shallow and appears relatively clear	Bedload mostly pebbles with some boulders, sand on banks but banks are manmade with grass on one side and other side more natural (pine and minor deciduous trees and shrubs)
BP2211	Natural spring in winterland at Heritage Well site, small stream that was sampled close to where it started (seemingly) in small clearing in trees, water seems to interact a bit with pine forest soil, gentle consistent trickle, no tube or piping evident	Mostly pine but some deciduous trees in area of spring, spring moving through grassy area over boulders.
BP2212	Stream off of gravel road sampled using bucket from bridge, relatively medium-paced flowing stream, highly vegetated area with pine and deciduous trees, shrubs at lower levels	Relatively coarse bedload with high banks filled with vegetation

Appendix 3: Summary of measured AQUA-1 and SLRS-6 reference material values compared to certified and literature values.

	SLRS-6 This Study		SLRS-6 NRC-CNRC[1]			SLRS-6 Yeghicheyan et al. (2019)		
	Measured Concentration	**sd**	**Certified concentration**	**sd**	**% Bias[2]**	**Certified concentration**	**sd**	**% Bias[2]**
Li (pg/g)	442	17				531	25	-16.8
Be (pg/g)	5.3	0.9	6.6*	2.2*	-19.2	6.6	1.1	-19.2
Na (ng/g)	2864	108	2770	220	3.4	2740	128	4.5
Mg (ng/g)	2175	79	2137	58	1.8	2135	72	1.9
Al (ng/g)	32.77	1.53	33.9	2.2	-3.3	33.4	1	-1.9
Ga (pg/g)	16.3	2.1						
As (pg/g)	567.0	16.2						
K (ng/g)	651	21	652	54	-0.1	630	24	3.4
Ca (ng/g)	8750	293	8770	200	-0.2	8624	206	1.5
Sn (pg/g)	12.3	1.4						
V (pg/g)	350	14	352	6	-0.5	361	14	-3.0
Cr (pg/g)	81	35	252	12	-68.0	247	12	-67.3
Fe (ng/g)	78.0	2.0	84.5	3.6	-7.7	82.2	2.7	-5.1
Mn (ng/g)	2.1	0.1	2.12	0.1	0.5	2.14	0.06	-0.5
Co (pg/g)	50.7	2.5	53*	12*	-4.4	55	3	-7.9
Ni (pg/g)	570	30	617	22	-7.6	609	28	-6.4
Cu (pg/g)	23449	966				24700	600	-5.1
Zn (pg/g)	1804	109	1760	120	2.5	1780	110	1.3
Re (pg/g)	15.7	1.4						
Sr (ng/g)	40.4	0.7	40.7	0.3	-0.7	41	1	-1.6
Rb (ng/g)	1.4	0.0				1.41	0.05	-2.5
Y (pg/g)	124.3	1.8				128	6	-2.9
Mo (pg/g)	184	10	215	18	-14.4	196	18	-6.1
Cd (pg/g)	9.7	0.7	6.3	1.4	53.4	7.4	1.7	30.6
Sb (pg/g)	343.7	21.2	337.7	5.8	1.8	335	10	2.6
Cs (pg/g)	4.3	0.7				4.6	0.5	-5.8
Ba (pg/g)	14717	839	14300	480	2.9	14120	400	4.2
La (pg/g)	252.00	3.06				248.7	12.1	1.3
Ce (pg/g)	295.67	3.54				293.1	15.1	0.9
Pr (pg/g)	59.00	1.00				59.2	1.9	-0.3
Nd (pg/g)	231.33	5.25				228.1	9.4	1.4
Sm (pg/g)	39.00	1.91				39.5	1.7	-1.3
Eu (pg/g)	8.00	0.00				7.27	0.35	10.0
Tb (pg/g)	4.00	0.00				4.07	0.27	-1.7
Gd (pg/g)	31.33	0.94				31.6	2.5	-0.8
Dy (pg/g)	21.67	1.37				21.9	1.1	-1.1
Ho (pg/g)	4.00	0.00				4.3	0.3	-7.0
Er (pg/g)	12.33	0.75				12.4	0.7	-0.5
Tm (pg/g)	2.00	0.00				1.79	0.18	11.7
Yb (pg/g)	11.00	1.00				11.2	0.7	-1.8
Lu (pg/g)	2.00	0.00				1.91	0.23	4.7
Tl (pg/g)	8.00	1.15				8.5	2.9	-5.9
Pb (pg/g)	163	6	170	26	-3.9	166	13	-1.6
Th (pg/g)	15.7	4.5				16	7	-2.1
U (pg/g)	73.7	2.4	69.9	3.4	5.4	67	3	10.0

[1]National Research Council Canada

*Reference Values (not certified)

[2] % Bias calculated as (Measured - Certified Value) / Certified Value *100

Appendix 3 cont.: Summary of measured AQUA-1 and SLRS-6 reference material values compared to certified and literature values.

	SLRS-6 Babechuk et al. (2020)			SLRS-6 Dang et al. (2022)		
	Certified concentration	**sd**	**% Bias[2]**	**Certified concentration**	**sd**	**% Bias[2]**
Li (pg/g)	551	8	-19.8	490	20	-9.9
Be (pg/g)	7.21	0.5	-26.0	7	2	-23.8
Na (ng/g)	2720	140	5.3	3352	255	-14.6
Mg (ng/g)	2140	39	1.6	2186	125	-0.5
Al (ng/g)				31.3	1.6	4.7
Ga (pg/g)						
As (pg/g)						
K (ng/g)	650	25	0.2	636	54	2.4
Ca (ng/g)	8750	178	0.0	8161	276	7.2
Sn (pg/g)						
V (pg/g)				350	10	0.1
Cr (pg/g)				270		-70.1
Fe (ng/g)				89	2.9	-12.4
Mn (ng/g)				2.2	300	-3.2
Co (pg/g)				50	5	1.3
Ni (pg/g)				200	10	185.0
Cu (pg/g)				27400	1000	-14.4
Zn (pg/g)				1700	200	6.1
Re (pg/g)						
Sr (ng/g)	40.45	0.91	0.0	41.8	1.0	-3.3
Rb (ng/g)	1.435	0.03	-4.2	1.45	0.1	-5.2
Y (pg/g)	130.7	2.9	-4.9	129	2	-3.6
Mo (pg/g)	198.4	5.5	-7.3	200	10	-8.0
Cd (pg/g)	5.5	0.5	75.8	30	10	-67.8
Sb (pg/g)	340	25	1.1	320	20	7.4
Cs (pg/g)	4.69	0.1	-7.6	10	7	-56.7
Ba (pg/g)	14300	160	2.9	14900	300	-1.2
La (pg/g)	250.6	1.6	0.6	246	6	2.4
Ce (pg/g)	300.1	2	-1.5	291	4	1.6
Pr (pg/g)	60.69	0.6	-2.8	58	1	1.7
Nd (pg/g)	230.5	2.4	0.4	230	10	0.6
Sm (pg/g)	38.61	0.5	1.0	38	3	2.6
Eu (pg/g)	6.7	0.17	19.4	9	1	-11.1
Tb (pg/g)	3.917	0.06	2.1	4	1	0.0
Gd (pg/g)	30.35	0.72	3.2	33	2	-5.1
Dy (pg/g)	21.1	0.36	2.7	22	2	-1.5
Ho (pg/g)	4.313	0.073	-7.3	4.2	0.3	-4.8
Er (pg/g)	11.91	0.18	3.6	12	1	2.8
Tm (pg/g)	1.721	0.035	16.2	1.6	0.3	25.0
Yb (pg/g)	11.16	0.17	-1.4	10	1	10.0
Lu (pg/g)	1.756	0.024	13.9	1.7	0.3	17.6
Tl (pg/g)	7.36	0.58	8.7	17	8	-52.9
Pb (pg/g)	165	19	-1.0	200	100	-18.3
Th (pg/g)	19.8	2.7	-20.9	26.48	20.26	-40.8
U (pg/g)	70.4	1.4	4.6	70	10	5.2

[1]National Research Council Canada

*Reference Values (not certified)

[2] % Bias calculated as (Measured - Certified Value) / Certified Value *100

Appendix 3 cont.: Summary of measured AQUA-1 and SLRS-6 reference material values compared to certified and literature values.

	AQUA-1 This Study		AQUA-1 NRC-CNRC[1]			AQUA-1 Yeghicheyan et al 2021		
	Measured Concentration	**sd**	**Certified concentration**	**sd**	**% Bias[2]**	**Certified concentration**	**sd**	**% Bias[2]**
Li (pg/g)	435	11.06	526*	28*	-17.3	530	30	-17.9
Be (pg/g)	1.3	0.9						
Na (ng/g)	14207	627	13710	340	3.6	14000	400	1.5
Mg (ng/g)	2003	78	1944	40	3.0	1900	18	5.4
Al (ng/g)	52.88	1.81	54.6		-3.1	54.5	1.6	-3.0
Ga (pg/g)	9.0	1.0	7.1*	4.6*	26.8			
As (pg/g)	212.0	7.0	222	14	-4.5	220	14	-3.6
K (ng/g)	680	19	670		1.5	670	14	1.5
Ca (ng/g)	8182	256	8240		-0.7	8070	80	1.4
Sn (pg/g)	21.0	1.9						
V (pg/g)	170	4	152	8	12.1	156	4	9.2
Cr (pg/g)	259	210	87	8	198.1	86	4	201.6
Fe (ng/g)	36.7	0.8	38		-3.4	36.9	0.6	-0.5
Mn (ng/g)	2.4	0.0	2.42		-0.2	2.43	0.08	-0.6
Co (pg/g)	24.0	1.2	27.1	2.8	-11.4	26.9	0.8	-10.8
Ni (pg/g)	409.3	13.8	447	30	-8.4	443	16	-7.6
Cu (pg/g)	6712.3	277.2	7460	120	-10.0	7470	160	-10.1
Zn (pg/g)	648.0	61.3	970	80	-33.2	980	20	-33.9
Re (pg/g)	12.0	0.0	10.7*	1.6*	12.1			
Sr (ng/g)	35.3	0.2	36.02	0.48	-2.1	35.4	1	-0.4
Rb (ng/g)	1.3	0.0	1.34	0.06	-3.9	1.36	0.03	-5.3
Y (pg/g)	29.0	1.0	30.7	1.2	-5.5	31	1	-6.5
Mo (pg/g)	179	4	189	8	-5.3	193	8	-7.3
Cd (pg/g)	5.3	0.9	4.3	1.4	24.0	5.4	0.8	-1.2
Sb (pg/g)	58.0	4.9	68.2	5.6	-15.0	71	2	-18.3
Cs (pg/g)	4.0	0.0	3.2*	0.4*	25.0	3.2	0.2	25.0
Ba (pg/g)	12175	372	11890*	360*	2.4	11900	200	2.3
La (pg/g)	60.67	0.94	60*	2.6*	1.1	60.0	20.0	1.1
Ce (pg/g)	59.33	0.94	60*	3*	-1.1	61.0	2.0	-2.7
Pr (pg/g)	12.67	1.49	12.4*	0.6*	2.2	12.6	0.4	0.5
Nd (pg/g)	48.67	0.94	48.2*	2.4*	1.0	48.7	1.8	-0.1
Sm (pg/g)	7.00	1.00	7.12*	0.44*	-1.7	7.2	0.4	-2.8
Eu (pg/g)	2.00	0	1.46*	0.36*	37.0	1.5	0.2	33.3
Tb (pg/g)	0.33	0.75	0.62*	0.08*	-46.2	0.64	0.05	-47.9
Gd (pg/g)	5.67	0.75	5.9*	0.4*	-4.0	5.8	0.2	-2.3
Dy (pg/g)	4.00	0.00	3.59*	0.24*	11.4	3.71	1.24	7.8
Ho (pg/g)	0.67	1.49	0.76*	0.06*	-12.3	0.79	0.02	-15.6
Er (pg/g)	2.00	0	2.52*	0.16*	-20.6	2.51	0.1	-20.3
Tm (pg/g)			0.377*	0.04*		0.39	0.06	
Yb (pg/g)	2.00	0	2.41*	0.16*	-17.0	2.5	0.2	-20.0
Lu (pg/g)			0.439*	0.06*		0.43	0.02	
Tl (pg/g)	4.67	0.94	5.6*	3*	-16.7			
Pb (pg/g)	1322	49	1364	34	-3.1	1380	60	-4.2
Th (pg/g)	2.0	0.0						
U (pg/g)	8.0	0.0	6.95	0.52	15.1	6.9	0.4	15.9

[1]National Research Council Canada

*Reference Values (not certified)

[2] % Bias calculated as (Measured - Certified Value) / Certified Value *100

Appendix 4: Compiled major and trace element compositions for bedrock within the study sites.

Sample ID	Rock Type	Category	Reference	SiO2 wt%	TiO2 wt%	Al2O3 wt%	Fe2O3 wt%	FeO wt%	MnO wt%	MgO wt%	CaO wt%	Na2O wt%	K2O wt%	P2O5 wt%	ign %	Ni ppm	Co ppm	Cr ppm	Li ppm	Rb ppm	Cs ppm	Th ppm	U ppm
V1271	Lherzolites from Table Mtn	Ultramafic	Malpas, 1976	37.70	0.00	1.63	1.51	5.07	0.12	37.70	1.02	0.04	0.00	0.00	13.46	3300		1900		9			
V1371	Lherzolites from Table Mtn	Ultramafic	Malpas, 1976	38.34	0.21	4.50	1.70	8.13	0.10	31.20	4.00	0.21	0.60	0.05	11.30	2100		1200		15			
V1471	Lherzolites from Table Mtn	Ultramafic	Malpas, 1976	42.49	0.30	3.14	1.73	5.89	0.11	34.80	3.00	0.10	0.00	0.05	9.00	2800		1700		11			
V1571	Lherzolites from Table Mtn	Ultramafic	Malpas, 1976	38.89	0.00	2.21	1.80	5.84	0.11	36.00	2.06	0.13	0.03	0.00	11.02	2900		1800		12			
V1671	Lherzolites from Table Mtn	Ultramafic	Malpas, 1976	39.25	0.31	2.40	1.90	5.39	0.11	37.76	2.70	0.09	0.00	0.05	10.20	3000		1700		11			
JM115	Harzburgites from Bay of Islands Complex	Ultramafic	Malpas, 1976	35.76	0.40	0.38	2.15	4.30	0.10	37.50	0.80	0.01	0.00	0.10	16.91	3600		1600		10			
JM120	Harzburgites from Bay of Islands Complex	Ultramafic	Malpas, 1976	40.00	0.39	0.38	3.04	5.73	0.10	39.00	0.80	0.01	0.00	0.15	11.37	3600		1700		11			
JM122	Harzburgites from Bay of Islands Complex	Ultramafic	Malpas, 1976	56.47	0.08	0.49	1.10	4.10	0.06	27.20	1.00	0.01	0.00	0.05	9.80	3400		1900		10			
JM124	Harzburgites from Bay of Islands Complex	Ultramafic	Malpas, 1976	39.53	0.11	0.60	3.10	4.80	0.10	38.40	1.30	0.02	0.00	0.05	12.10	3500		1800		12			
JM181	Harzburgites from Bay of Islands Complex	Ultramafic	Malpas, 1976	34.20	0.02	0.20	3.13	4.22	0.11	41.50	0.00	0.00	0.02	0.00	14.54	3400		5100		7			
JM182	Harzburgites from Bay of Islands Complex	Ultramafic	Malpas, 1976	38.20	0.04	0.60	2.93	4.80	0.12	40.80	0.70	0.00	0.02	0.03	11.30	3200		2300		15			
JM183	Harzburgites from Bay of Islands Complex	Ultramafic	Malpas, 1976	35.33	0.07	0.40	2.61	5.01	0.11	41.50	0.00	0.00	0.02	0.00	13.53	3300		1800		6			
JM184	Harzburgites from Bay of Islands Complex	Ultramafic	Malpas, 1976	36.83	0.02	0.60	2.30	5.49	0.10	40.80	0.70	0.00	0.02	0.01	11.30	4200		1500		6			
JM185	Harzburgites from Bay of Islands Complex	Ultramafic	Malpas, 1976	37.54	0.07	0.60	3.01	4.56	0.11	41.03	0.60	0.00	0.02	0.00	11.84	3100		2400		5			
JM186	Harzburgites from Bay of Islands Complex	Ultramafic	Malpas, 1976	36.74	0.02	0.40	2.51	4.56	0.12	30.43	0.30	0.00	0.02	0.04	13.94	3300		2200		16			
JM187	Harzburgites from Bay of Islands Complex	Ultramafic	Malpas, 1976	37.93	0.07	0.60	3.61	3.91	0.11	42.53	0.60	0.00	0.02	0.00	10.76	3300		2500		2			
JM188	Harzburgites from Bay of Islands Complex	Ultramafic	Malpas, 1976	37.33	0.07	0.40	2.96	4.62	0.12	41.03	0.50	0.00	0.02	0.00	13.37	3300		2100		13			
JM189	Harzburgites from Bay of Islands Complex	Ultramafic	Malpas, 1976	37.69	0.09	0.40	2.41	5.17	0.11	41.50	0.60	0.00	0.02	0.05	13.09	3100		2500		13			
JM190	Harzburgites from Bay of Islands Complex	Ultramafic	Malpas, 1976	36.13	0.02	0.30	2.25	4.92	0.11	43.45	0.30	0.00	0.02	0.00	13.74	3100		1900		10			
JM191	Harzburgites from Bay of Islands Complex	Ultramafic	Malpas, 1976	33.78	0.07	0.20	2.00	5.33	0.10	41.83	0.30	0.00	0.02	0.00	16.27	3700		3900		16			
JM192	Harzburgites from Bay of Islands Complex	Ultramafic	Malpas, 1976	34.77	0.02	0.50	2.44	5.21	0.11	40.45	0.30	0.00	0.02	0.00	14.62	4200		3700		7			
JM193	Harzburgites from Bay of Islands Complex	Ultramafic	Malpas, 1976	32.77	0.04	0.20	2.04	5.57	0.12	41.73	0.00	0.00	0.02	0.01	15.65	3200		4700		7			
JMEN-V	Harzburgites from Bay of Islands Complex	Ultramafic	Malpas, 1976	45.30	0.00	2.00	1.89	4.26	0.00	20.10	19.05	0.00	0.00	0.00	7.30								
JM271	Dunites and Critical Zone Rocks	Ultramafic	Malpas, 1976	41.06	0.37	23.20	0.96	4.20	0.08	9.40	14.80	0.27	0.00	0.10	5.40	800	38	3700		5			
JM272	Dunites and Critical Zone Rocks	Ultramafic	Malpas, 1976	37.43	0.10	0.22	3.10	3.62	0.10	41.20	0.50	0.01	0.00	0.05	13.89	2400	108	5300		2			
JM274	Dunites and Critical Zone Rocks	Ultramafic	Malpas, 1976	35.76	0.81	0.18	3.84	3.48	0.10	41.50	0.60	0.01	0.00	0.05	13.63	2100	115	4200					
JM275	Dunites and Critical Zone Rocks	Ultramafic	Malpas, 1976	37.15	0.40	0.22	1.73	5.50	0.10	40.00	0.50	0.01	0.00	0.05	13.73	2200	110	4200		1			
JM276	Dunites and Critical Zone Rocks	Ultramafic	Malpas, 1976	37.81	0.12	0.21	3.69	3.81	0.12	40.09	0.60	0.00	0.01	0.01	12.91	2400	107	4500					
19472	Dunites and Critical Zone Rocks	Ultramafic	Malpas, 1976	34.88	0.02	0.20	5.18	2.64	0.12	42.63	0.30	0.00	0.02	0.00	14.68	2900		4300		8			
19572	Dunites and Critical Zone Rocks	Ultramafic	Malpas, 1976	32.28	0.12	0.20	5.88	2.14	0.11	43.43	0.30	0.00	0.02	0.00	15.41	3700		3900		6			
19672	Dunites and Critical Zone Rocks	Ultramafic	Malpas, 1976	34.39	0.02	0.20	6.27	3.64	0.15	40.23	0.30	0.00	0.02	0.00	12.53	3200		3900		13			
E2	Dunites and Critical Zone Rocks	Ultramafic	Malpas, 1976	35.24	0.00	2.46	2.53	4.70	0.11	39.30	1.40	0.40	0.00	0.00	12.42	1900	113	4100		2			
E4	Dunites and Critical Zone Rocks	Ultramafic	Malpas, 1976	46.12	0.48	15.38	0.94	5.55	0.12	10.99	14.52	1.32	0.17	0.00	2.80	90	41	390		7			
E5	Dunites and Critical Zone Rocks	Ultramafic	Malpas, 1976	46.64	0.39	15.50	1.04	3.92	0.10	10.55	17.50	1.11	0.04	0.00	4.00	210	33	830		8			
E8	Dunites and Critical Zone Rocks	Ultramafic	Malpas, 1976	44.71	0.23	11.64	0.87	6.57	0.12	14.30	14.72	0.70	0.04	0.00	4.20	300	48	750		8			
TMC1	Dunites and Critical Zone Rocks	Ultramafic	Malpas, 1976	36.79	0.40	4.98	3.13	4.69	0.11	34.10	3.21	0.10	0.01	0.01	12.50	1900	158	3100		10			
TMC2	Dunites and Critical Zone Rocks	Ultramafic	Malpas, 1976	34.61	0.32	4.76	4.00	4.10	0.12	36.07	2.13	0.10	0.00	0.01	12.78	2300	140	4600		5			
TMC3	Dunites and Critical Zone Rocks	Ultramafic	Malpas, 1976	33.90	0.10	4.80	3.80	4.00	0.11	36.01	2.60	0.10	0.00	0.02	13.63	2100	150	5800		5			
TMC4	Dunites and Critical Zone Rocks	Ultramafic	Malpas, 1976	40.81	0.07	14.10	2.30	4.70	0.10	18.01	8.76	0.60	0.01	0.00	9.89	140		320		10			
TMC5	Dunites and Critical Zone Rocks	Ultramafic	Malpas, 1976	35.30	0.08	7.10	2.98	4.43	0.11	34.10	2.46	0.15	0.01	0.01	13.30	1600	53	4700		5			
TMC6	Dunites and Critical Zone Rocks	Ultramafic	Malpas, 1976	48.90	0.10	5.10	1.01	4.38	0.10	18.16	14.30	0.19	0.00	0.00	7.58	310		3700		8			
19872	Gabbros, Bay of Islands Complex	Mafic	Malpas, 1976	45.07	0.72	19.30	1.45	4.03	0.08	13.03	10.43	1.42	n.d.	0.01	3.62	548		94		9			
19972	Gabbros, Bay of Islands Complex	Mafic	Malpas, 1976	46.73	n.d.	22.20	0.11	5.03	0.09	8.30	10.95	2.57	0.10	0.03	3.38	154		130		11			
20072	Gabbros, Bay of Islands Complex	Mafic	Malpas, 1976	47.32	0.07	24.60	0.70	2.33	0.05	5.52	12.69	2.43	0.09	n.d.	2.00	169		103		7			
20172	Gabbros, Bay of Islands Complex	Mafic	Malpas, 1976	47.77	n.d.	17.80	2.04	3.65	0.10	10.23	16.62	1.04	n.d.	n.d.	1.19	139		252		12			
20272	Gabbros, Bay of Islands Complex	Mafic	Malpas, 1976	47.77	0.78	17.60	0.12	4.48	0.09	9.01	13.62	1.57	n.d.	0.03	2.93	256		668		11			
20372	Gabbros, Bay of Islands Complex	Mafic	Malpas, 1976	50.03	n.d.	19.30	1.51	4.03	0.10	7.77	11.81	2.52	n.d.	n.d.	2.31	120		151		9			

n.d.: not detected

Appendix 4 cont.: Compiled major and trace element compositions for bedrock within the study sites.

Sample ID	Rock Type	Category	Reference	SiO2	TiO2	Al2O3	Fe2O3	FeO	MnO	MgO	CaO	Na2O	K2O	P2O5	ign	Ni	Co	Cr	Li	Rb	Cs	Th	U
				wt%	wt%	wt%	wt%	wt%	wt%	wt%	wt%	wt%	wt%	wt%	%	ppm	ppm	ppm	ppm	ppm	ppm	ppm	ppm
20572	Gabbros, Bay of Islands Complex	Mafic	Malpas, 1976	46.73	0.47	19.70	0.33	5.10	0.08	9.35	13.67	1.85	0.03	n.d.	2.90	205		524		5			
206A72	Gabbros, Bay of Islands Complex	Mafic	Malpas, 1976	45.79	n.d.	21.80	0.10	4.94	0.08	10.25	12.46	1.50	0.23	0.01	1.88	355		244		9			
206B72	Gabbros, Bay of Islands Complex	Mafic	Malpas, 1976	45.97	0.47	22.00	0.12	4.01	0.08	9.60	13.18	1.57	0.09	0.03	3.45	290		163		6			
20772	Gabbros, Bay of Islands Complex	Mafic	Malpas, 1976	42.37	0.20	22.50	0.52	2.50	0.05	11.18	12.69	1.29	n.d.	0.06	5.36	520		212		6			
28571	Gabbros, Bay of Islands Complex	Mafic	Malpas, 1976	45.22	0.31	22.20	1.05	4.10	0.09	8.50	13.60	0.75	n.d.	n.d.	4.05	112	36	391		4			
JM289	Gabbros, Bay of Islands Complex	Mafic	Malpas, 1976	47.69	0.17	15.00	1.79	5.67	0.13	5.00	15.40	1.16	0.02	0.21	7.30	63	63	189		6			
301A71	Gabbros, Bay of Islands Complex	Mafic	Malpas, 1976	48.15	0.76	16.06	0.84	5.51	0.12	8.94	13.22	2.44	0.06	0.08	1.23	57	53	111		5			
301C71	Gabbros, Bay of Islands Complex	Mafic	Malpas, 1976	48.40	0.40	16.10	0.97	4.78	0.10	8.70	13.60	2.50	0.10	n.d.	2.30	71	73	138					
31271	Gabbros, Bay of Islands Complex	Mafic	Malpas, 1976	47.40	0.90	20.30	2.07	4.07	0.10	6.80	11.90	3.20	0.50	0.10	1.90	90	40	178		5			
312A71	Gabbros, Bay of Islands Complex	Mafic	Malpas, 1976	47.70	0.79	20.91	2.31	3.98	0.10	6.73	11.49	3.22	0.48	0.10	2.30	110	41	203					
E672	Gabbros, Bay of Islands Complex	Mafic	Malpas, 1976	47.29	0.20	22.37	0.51	5.04	0.09	8.66	11.97	2.10	0.08	n.d.	1.46	134	42	243		5			
E772	Gabbros, Bay of Islands Complex	Mafic	Malpas, 1976	47.93	0.13	22.99	0.84	4.13	0.08	7.97	7.72	3.76	0.59	n.d.	4.00	143	40	205		17			
E972	Gabbros, Bay of Islands Complex	Mafic	Malpas, 1976	47.10	0.06	24.62	0.51	1.57	0.04	5.00	13.70	1.15	0.20	0.05	7.30	93	21	137		6			
E1272	Gabbros, Bay of Islands Complex	Mafic	Malpas, 1976	44.40	0.20	18.90	0.35	2.87	0.07	9.52	16.00	1.44	0.12	n.d.	4.90	212	29	833		12			
E1672	Gabbros, Bay of Islands Complex	Mafic	Malpas, 1976	43.83	0.08	23.18	0.13	0.39	0.01	7.20	15.70	0.49	0.26	0.05	8.00	126	17	85		10			
E1772	Gabbros, Bay of Islands Complex	Mafic	Malpas, 1976	47.70	0.16	18.15	0.61	2.80	0.06	10.82	15.22	1.60	0.07	n.d.	2.41	137	41	731					
E1872	Gabbros, Bay of Islands Complex	Mafic	Malpas, 1976	49.72	0.10	20.58	0.21	1.32	0.02	9.08	14.88	1.21	0.43	n.d.	1.73	160	16	549		9			
12671	Gabbros, Bay of Islands Complex	Mafic	Malpas, 1976	47.17	0.37	16.40	2.03	4.80	0.10	8.50	14.20	1.07	n.d.	0.05	1.91	93		229		13			
24471	Gabbros, Bay of Islands Complex	Mafic	Malpas, 1976	48.04	1.91	16.16	5.01	6.58	0.13	5.47	11.15	3.65	0.11	0.12	1.40	45	84	151		6			
24971	Gabbros, Bay of Islands Complex	Mafic	Malpas, 1976	48.29	0.84	15.06	0.93	6.87	0.14	8.97	12.93	2.52	0.08	n.d.	0.92	84	47	222		6			
25871	Gabbros, Bay of Islands Complex	Mafic	Malpas, 1976	48.52	0.74	19.88	0.84	5.68	0.12	6.19	12.12	2.65	0.12	0.16	2.60	60	40	152		4			
28271	Gabbros, Bay of Islands Complex	Mafic	Malpas, 1976	42.50	0.26	23.84	1.11	5.12	0.10	10.50	12.69	1.72	n.d.	0.09	2.30	208	46	163		3			
28471	Gabbros, Bay of Islands Complex	Mafic	Malpas, 1976	47.57	1.43	16.87	1.69	6.73	0.14	6.20	13.08	2.49	0.00	0.14	1.30	55	60	186		7			
WF11071	Diabases, Bay of Islands Complex	Mafic	Malpas, 1976	49.40	0.80	14.60	0.80	7.90	0.20	8.50	9.70	2.90	0.10	0.10	2.90	120	41	408		6			
WF112B71	Diabases, Bay of Islands Complex	Mafic	Malpas, 1976	46.90	0.70	19.10	1.10	5.50	0.10	7.50	9.00	2.90	1.80	0.10	4.40	79	33	243		10			
WF12371	Diabases, Bay of Islands Complex	Mafic	Malpas, 1976	49.70	1.00	14.10	2.80	7.20	0.20	7.40	8.60	3.40	0.10	0.10	3.30	42	32	164		5			
WF123A71	Diabases, Bay of Islands Complex	Mafic	Malpas, 1976	51.60	1.30	12.10	2.20	8.20	0.20	7.30	8.90	4.20	0.10	0.10	3.20	52	42	204		4			
21172	Diabases, Bay of Islands Complex	Mafic	Malpas, 1976	51.37	1.37	14.90	0.20	10.39	0.19	4.80	7.11	4.78	0.38	n.d.	1.53	28		70		14			
21772	Diabases, Bay of Islands Complex	Mafic	Malpas, 1976	46.82	0.60	15.50	2.29	7.09	0.18	8.58	10.45	2.44	1.04	0.10	2.89	112		192		17			
22172	Diabases, Bay of Islands Complex	Mafic	Malpas, 1976	50.48	0.90	16.10	1.74	6.49	0.16	8.58	10.48	2.44	0.16	0.05	2.10	208		213		13			
22472	Diabases, Bay of Islands Complex	Mafic	Malpas, 1976	47.27	0.96	16.40	0.42	8.76	0.16	9.32	9.00	2.81	1.05	n.d.	3.42	158		183		17			
22572	Diabases, Bay of Islands Complex	Mafic	Malpas, 1976	45.45	0.90	18.80	1.50	5.37	0.13	8.20	10.51	2.25	1.46	0.10	3.72	191		238		18			
294B71	Diabases, Bay of Islands Complex	Mafic	Malpas, 1976	49.57	1.31	16.08	2.04	6.70	0.16	9.00	11.50	1.35	0.63	0.10	1.70	95	43	295		8			
294C71	Diabases, Bay of Islands Complex	Mafic	Malpas, 1976	46.89	1.20	14.60	3.80	8.04	0.20	7.00	10.50	1.76	0.22	0.10	4.78	95	41	301		8			
294E71	Diabases, Bay of Islands Complex	Mafic	Malpas, 1976	49.38	1.61	15.26	1.50	6.25	0.13	8.20	11.50	0.93	0.60	0.10	4.10	121	40	212		8			
301B71	Diabases, Bay of Islands Complex	Mafic	Malpas, 1976	47.64	1.36	15.88	2.84	6.52	0.14	8.49	12.34	2.70	0.20	0.18	0.68	88	47	204		6			
Avolc	Volcanic Rocks, Bay of Islands Complex	Mafic	Malpas, 1976	45.97	0.70	15.00	4.74	4.61	0.51	6.13	12.00	3.35	0.18	0.10	5.08	49		109		12			
Bvolc	Volcanic Rocks, Bay of Islands Complex	Mafic	Malpas, 1976	47.77	1.33	13.60	5.66	4.05	0.14	5.55	11.27	2.90	0.12	n.d.	4.95	115		216		15			
Cvolc	Volcanic Rocks, Bay of Islands Complex	Mafic	Malpas, 1976	49.13	1.36	15.00	5.53	3.84	0.16	5.95	10.82	2.81	0.08	0.05	3.63	58		137		11			
Dvolc	Volcanic Rocks, Bay of Islands Complex	Mafic	Malpas, 1976	49.01	1.01	14.10	1.90	9.10	0.30	8.53	8.70	4.60	0.01	0.15	2.80	121	41	123		6			
Evolc	Volcanic Rocks, Bay of Islands Complex	Mafic	Malpas, 1976	48.65	1.50	13.93	2.96	6.30	0.20	8.78	5.60	4.90	0.10	0.20	4.76	63	40	24		4			
Gvolc	Volcanic Rocks, Bay of Islands Complex	Mafic	Malpas, 1976	47.10	1.00	12.91	2.71	4.97	0.15	8.10	10.91	3.12	0.00	0.10	7.80	110	36	151		6			
18ZM437A01	St. Lawrence Granite, E Lobe	Granite	Magyarosi, 2022	76.90	0.11	10.63	0.44	1.28	0.05	0.01	0.17	3.44	4.91	0.00	0.41	3	3	3	52.9	285	3.4	24.6	5.7
18ZM438A01	St. Lawrence Granite, E Lobe	Granite	Magyarosi, 2022	77.30	0.12	10.80	0.73	1.54	0.05	0.01	0.14	4.04	4.58	0.00	0.58	4	3	1	145.1	358	4.1	25.6	7.1
17ZM407A01	St. Lawrence Granite, E Lobe	Granite	Magyarosi, 2022	76.67	0.14	10.87	1.56	0.77	0.01	0.01	0.10	3.17	5.08	0.00	0.45	4	5	4	21.5	269	1.5	21	7.1
18ZM423A01	St. Lawrence Granite, W Lobe	Granite	Magyarosi, 2022	76.17	0.07	11.31	0.75	1.05	0.01	0.03	0.22	4.04	4.19	0.00	0.45	3	2	1	33.6	403	6.2	36.9	8.6
18ZM424A01	St. Lawrence Granite, W Lobe	Granite	Magyarosi, 2022	77.00	0.07	11.83	0.18	1.35	0.01	0.01	0.28	4.22	4.42	0.00	0.48	4	2	3	41.2	416	4.3	34.1	10.9
18ZM463A01	St. Lawrence Granite, Winterland Porphyry	Granite	Magyarosi, 2022	67.70	0.57	12.64	3.95	1.87	0.25	0.74	1.12	3.15	6.47	0.13	1.36	9	3	4	28.8	247	5.2	12.5	4.0

n.d.: not detected

Appendix 5: Full geochemical data for all streams/rivers

Element	Li	Be	Na	Mg	Al	K	Ca	Cr	Mn	Fe	Co	Ni	Cu	Zn	V	Ga	Rb	Sr
Unit	µg/L	µg/L	µg/L	µg/L	µg/L	µg/L	µg/L	µg/L	µg/L	µg/L	µg/L	µg/L	µg/L	µg/L	µg/L	µg/L	µg/L	µg/L
BEC Values	*0.00043*	*0*	*6.09*	*0.1*	*0.3*	*1.5*	*0.6*	*0.1*	*0.01*	*0.4*	*0.0004*	*0.006*	*0.02*	*0.1*	*0.001*	*0.0002*	*8.72E-05*	*0*
Major Rivers																		
MR2201 (Terra Nova)	0.5215	0.0098	1733	354.4	61.22	273.6	1125	B.D.	18.26	106.3	0.0311	0.1593	0.2659	2.645	0.0941	0.0075	0.8738	5.017
MR2202 (Gander)	0.2999	0.0088	1908	602.5	86.36	192.6	1386	B.D.	3.299	41.46	0.0162	0.4957	0.4605	1.498	0.0357	0.0093	0.5687	6.430
MR2203 (Humber)	0.1443	0.0069	2608	807.9	55.01	494.1	3901	B.D.	1.530	63.53	0.0118	0.2697	0.8931	16.53	0.1250	0.0110	0.6012	17.84
MR2204 (Exploits)	0.0940	0.0083	1603	413.6	59.81	147.3	2241	B.D.	4.968	37.49	0.0111	0.1149	1.093	7.595	0.0516	0.0080	0.3134	7.360
MR2205 (Garnish)	0.2889	0.0062	4566	582.2	142.3	191.2	1957	B.D.	7.462	140.9	0.0194	0.0927	1.171	2.142	0.1583	0.0139	0.2103	7.938
MR2206 (Piper's Hole)	0.4822	0.0051	2210	369.7	18.43	209.2	1837	B.D.	7.610	98.83	0.0159	0.0581	0.0880	1.442	0.0724	0.0049	0.6765	8.223
Western NL Samples																		
BI2201	0.3226	0.0047	19987	4532	46.96	684.8	10581	B.D.	7.483	109.9	0.0546	0.9707	1.325	1.100	0.4731	0.0160	0.3909	40.87
BI2202	0.3837	0.0023	14299	6689	35.02	687.8	12945	1.122	4.054	62.66	0.0432	2.450	1.152	0.7535	0.3967	0.0117	0.4045	42.06
BI2203	0.8974	0.0002	14003	9352	21.43	614.7	22027	1.926	0.2950	7.066	0.0195	0.2163	0.1975	0.7888	1.2679	0.0102	0.4280	48.81
BI2205	0.0530	0.0003	6637	2353	29.69	245.7	11076	B.D.	0.2287	5.372	0.0123	0.0760	0.5650	0.4133	0.8152	0.0101	0.1604	19.86
BI2206	0.0721	0.0007	2813	962.5	60.52	133.6	1532	B.D.	0.4686	14.67	0.0238	0.5708	0.3337	0.5387	0.4826	0.0052	0.1083	6.268
BI2207	0.2681	0.0003	3908	9466	5.384	192.6	1952	B.D.	0.2634	3.225	0.0200	2.398	0.1664	0.3929	0.0433	0.0009	0.1554	11.19
BI2208	0.6398	0.0022	4539	8160	21.85	251.6	5868	0.9869	0.9385	30.86	0.0237	3.208	0.4729	0.4829	0.0696	0.0061	0.2620	30.25
BI2209	0.3595	0.0016	4019	2232	13.86	272.1	31888	B.D.	0.9371	42.96	0.0198	0.2228	0.3470	0.6592	0.0475	0.0037	0.2901	90.17
GM2201	0.2620	0.0029	3830	3014	42.23	226.2	3816	0.5080	1.053	39.53	0.0160	1.632	0.5563	0.5568	0.0977	0.0075	0.1596	14.80
GM2202	0.1184	0.0010	3878	6107	25.93	152.6	2059	0.8887	0.8600	52.68	0.0426	5.636	0.7153	1.065	0.1772	0.0054	0.1305	8.888
GM2203	0.0735	0.0002	2023	7321	2.986	98.8	548.0	1.938	0.1829	16.19	0.0337	5.770	0.1503	0.4647	0.0402	B.D.	0.0702	2.890
GM2204	0.0648	0.0001	1810	6375	2.238	91.5	383.2	1.677	0.1856	11.99	0.0288	5.053	0.1234	0.4045	0.0323	B.D.	0.0855	2.084
GM2205	0.0702	0.0002	1664	6495	2.434	78.4	371.3	1.671	0.2318	41.59	0.0349	8.005	0.0831	0.7684	0.0379	0.0008	0.0683	2.088
GM2206	0.0808	B.D.	2224	6796	3.186	105.4	801.0	0.9465	0.1281	10.04	0.0169	2.412	B.D.	0.5090	0.0252	B.D.	0.0686	2.419
GM2207	0.0821	0.0044	3211	1352	255.6	116.4	1993	1.102	2.050	196.6	0.0708	3.096	1.491	2.210	0.5967	0.0212	0.1231	7.906
GM2208	0.1969	0.0023	3194	6833	18.65	188.4	2060	1.440	0.8799	52.99	0.0459	8.177	0.4795	2.054	0.1229	0.0037	0.1896	10.71
GM2209	0.2381	0.0007	3153	8602	13.95	239.8	1841	1.177	0.5445	40.62	0.0427	9.937	0.4402	7.083	0.0706	0.0030	0.3015	13.88
GM2210	0.7152	0.0053	5129	2831	29.13	645.8	8573	0.4509	1.408	32.82	0.0335	1.963	1.044	0.7799	0.1078	0.0107	0.4790	33.34
GM2211	0.2104	0.0016	3621	5439	24.73	312.3	23682	B.D.	2.027	13.97	0.0103	0.1054	0.1607	0.3700	0.0652	0.0051	0.3395	41.96
Burin Peninsula Samples																		
BP2201	1.0212	0.1544	4871	505.5	198.9	99.4	1096	B.D.	19.11	281.0	0.0411	0.1283	0.3360	4.064	0.1518	0.0525	0.4541	7.134
BP2202	1.0229	0.0225	4947	501.6	61.97	164.8	1445	B.D.	16.26	160.4	0.0126	0.0476	0.1554	1.679	0.0592	0.0102	0.3930	12.20
BP2203	0.7172	0.0672	5855	684.8	88.86	126.0	1381	B.D.	36.61	121.4	0.0419	0.0971	0.4292	4.209	0.0674	0.0276	0.6216	9.327
BP2204	1.0642	0.0593	4228	454.6	52.07	129.7	1512	B.D.	16.85	235.8	0.0159	0.0451	0.3548	1.519	0.0672	0.0126	0.3886	10.27
BP2205	0.6014	0.0221	4636	552.5	87.73	134.2	1524	B.D.	24.29	372.8	0.0285	0.0852	0.1558	1.302	0.0898	0.0137	0.3019	8.113
BP2206	2.7770	0.1959	10723	1353	149.0	578.8	19289	B.D.	96.30	162.7	0.0356	0.1737	1.379	3.914	0.1453	0.0649	1.853	34.96
BP2207	9.6436	0.1183	45255	1065	190.6	3394.9	7164	B.D.	55.83	360.5	0.1652	0.2883	1.109	2.431	0.2436	0.2022	6.388	35.82
BP2208	1.4681	0.0516	7372	1175	63.41	346.5	3181	B.D.	658.16	478.9	0.1054	0.0939	0.1972	1.329	0.0872	0.0243	1.273	15.31
BP2209	0.7975	0.0163	5979	706.6	70.49	266.5	1646	B.D.	5.411	70.75	0.0072	0.0390	0.2094	0.9199	0.0514	0.0164	0.5357	11.79
BP2210	0.5345	0.0104	6333	1129	62.67	289.9	3165	B.D.	45.97	247.8	0.0312	0.0506	0.1545	0.6132	0.1856	0.0124	0.4339	18.19
BP2212	2.2462	0.0435	7003	1389	45.09	256.5	3670	B.D.	292.7	560.9	0.0499	0.0943	0.1898	1.477	0.1085	0.0196	0.9772	20.84
Spring Waters																		
BI2204	0.0091	B.D.	13276	3026	4.687	190.6	8534	1.853	0.0667	4.008	0.0345	0.8697	0.9622	0.4848	2.419	0.0130	0.0432	29.27
GM2212	0.4412	0.0005	6947	4042	2.355	711.2	57288	B.D.	0.0297	0.6726	0.0084	0.0355	0.1215	3.935	0.0049	0.0012	0.2121	218.3
BP2211	0.7819	0.1174	12571	1777	187.1	661.8	5506	0.1292	52.86	420.4	0.0567	0.2459	0.1864	7.900	0.1432	0.0531	2.072	17.43

B.D: below detection, set at 3 times the background equivalent concentration (BEC)

Appendix 5 cont: Full geochemical data for all streams/rivers

Element	As	Y	Cd	Sn	Mo	Cs	Ba	Sb	La	Ce	Pr	Nd	Sm	Eu	Gd	Tb
Unit	µg/L	µg/L	µg/L	µg/L	µg/L	µg/L	µg/L	µg/L	ng/L	ng/L	ng/L	ng/L	ng/L	ng/L	ng/L	ng/L
BEC Values	*0.001*	*2.942E-05*	*0*	*0*	*0.007*	*2.11E-05*	*0.005*	*0.001*	*0.40108*	*2.78E-02*	*4.41E-03*	*3.70E-02*	*1.57E-02*	*0*	*8.69E-02*	*0*
Major Rivers																
MR2201 (Terra Nova)	0.3132	0.0623	0.0027	0.0632	0.1561	0.0449	0.9986	0.0157	88.21	146.5	19.58	76.99	14.50	2.876	13.29	1.850
MR2202 (Gander)	0.3380	0.0884	0.0020	0.3628	0.0531	0.0230	1.278	0.3450	95.92	139.6	24.98	103.6	23.66	4.678	21.31	3.368
MR2203 (Humber)	0.1184	0.1532	0.0050	0.1175	0.0629	0.0021	7.941	0.0275	190.4	233.3	44.86	194.8	40.51	8.554	36.34	5.114
MR2204 (Exploits)	0.1816	0.1027	0.0287	0.0353	0.0677	0.0041	33.70	0.0195	89.15	114.2	21.71	94.34	18.84	5.126	19.94	2.768
MR2205 (Garnish)	0.1242	0.1689	0.0052	0.0433	0.0247	0.0114	4.243	0.0235	137.9	232.9	38.14	165.4	35.39	9.188	36.00	5.222
MR2206 (Piper's Hole)	0.0909	0.0407	0.0017	0.0248	0.0536	0.0260	1.370	0.0155	38.67	53.31	8.988	36.91	7.604	1.628	7.364	1.162
Western NL Samples																
BI2201	0.2886	0.1502	0.0027	0.1356	0.1208	0.0026	6.482	0.0553	98.13	126.0	27.65	122.0	27.54	7.948	31.82	4.836
BI2202	0.2079	0.1419	0.0030	0.0523	0.3897	0.0025	8.462	0.0257	63.82	68.10	19.04	81.88	21.77	6.004	24.58	3.768
BI2203	0.4864	0.0092	0.0016	0.0222	0.0663	0.0015	16.66	0.0071	9.958	14.28	1.074	5.008	1.492	1.452	1.784	0.4560
BI2205	0.0888	0.0379	0.0017	0.0072	0.0794	0.0017	2.073	0.0178	7.604	7.432	2.448	13.60	3.454	1.382	5.070	0.9520
BI2206	0.0749	0.0331	0.0031	0.0091	B.D.	0.0013	1.669	0.0121	12.60	22.04	4.006	18.70	4.656	2.168	6.228	1.164
BI2207	0.0415	0.0034	0.0005	0.0087	B.D.	0.0020	3.167	0.0057	2.476	2.254	0.7740	2.702	0.5520	0.3220	0.5980	0.2320
BI2208	0.1470	0.0400	0.0026	0.0138	0.1025	0.0052	3.385	0.0163	18.63	22.00	5.706	25.99	8.134	2.384	9.434	1.334
BI2209	0.0984	0.0365	0.0024	0.0165	0.0919	0.0043	5.160	0.0171	17.37	17.05	4.434	20.16	5.860	2.182	5.930	1.024
GM2201	0.1055	0.0923	0.0022	0.0280	0.0366	0.0014	5.256	0.0188	55.53	82.47	18.19	81.75	20.05	5.806	22.41	3.236
GM2202	0.0913	0.0328	0.0019	0.0208	B.D.	0.0012	2.912	0.0110	19.54	20.41	5.324	22.80	6.170	1.684	6.358	1.106
GM2203	0.1212	0.0049	0.0009	0.0260	B.D.	0.0005	0.2253	0.0099	4.012	2.844	1.468	4.838	0.8540	0.2540	1.286	0.2500
GM2204	0.0397	0.0038	0.0005	0.0198	B.D.	0.0007	0.1591	0.0175	2.676	2.782	0.9120	3.834	0.8920	0.1640	0.9240	0.2100
GM2205	0.0438	0.0052	0.0009	0.0194	B.D.	0.0005	0.1634	0.0121	3.484	7.482	1.126	4.992	1.068	0.2300	0.9600	0.2160
GM2206	0.0250	0.0015	0.0006	0.0115	B.D.	0.0008	0.0970	0.0103	B.D.	7.770	0.2000	0.9740	0.1020	0.0740	B.D.	0.1340
GM2207	0.1896	0.1738	0.0128	0.0340	0.0263	0.0013	0.9374	0.0299	72.90	145.7	23.63	104.7	27.04	8.436	32.79	4.784
GM2208	0.1094	0.0751	0.0015	0.0297	B.D.	0.0023	5.675	0.0101	29.80	42.02	10.31	51.44	13.26	4.290	15.73	2.462
GM2209	0.1213	0.0258	0.0015	0.0238	B.D.	0.0027	3.215	0.0149	19.87	22.28	5.152	23.86	4.470	1.480	4.910	0.8000
GM2210	0.2162	0.1565	0.0020	0.0175	0.1186	0.0065	22.41	0.0159	90.61	71.63	28.01	125.5	32.12	9.668	35.90	4.856
GM2211	0.0906	0.0420	0.0013	0.0112	0.1131	0.0009	9.346	0.0093	33.41	32.85	9.440	37.16	8.930	1.970	7.664	1.192
Burin Peninsula Samples																
BP2201	0.1694	2.370	0.0189	0.0360	0.1445	0.1235	8.774	0.0298	531.1	1286	168.466	690.3	203.9	9.044	264.3	51.58
BP2202	0.1149	0.4505	0.0050	0.0172	0.0372	0.0501	6.271	0.0188	156.5	249.2	40.228	163.9	37.02	4.178	45.62	8.410
BP2203	0.1375	1.546	0.0164	0.0603	0.1131	0.1095	26.84	0.0197	394.2	666.1	101.484	395.3	103.9	4.332	135.7	24.77
BP2204	0.1228	0.3207	0.0131	0.0642	0.0904	0.0637	12.99	0.0199	207.1	318.3	51.574	205.2	42.62	5.356	48.19	7.084
BP2205	0.6107	0.2609	0.0059	0.0824	0.1034	0.0289	12.23	0.0405	205.3	401.3	50.744	223.4	43.54	6.866	45.73	6.236
BP2206	0.3084	2.091	0.0420	0.0887	0.4393	0.1745	146.6	0.0648	724.0	1255	203.928	837.0	219.9	16.78	260.9	42.03
BP2207	2.636	1.747	0.0947	0.0748	70.01	0.3724	36.62	2.603	648.5	1505	186.1	766.7	201.0	16.10	246.7	38.91
BP2208	1.429	0.2983	0.0093	0.0531	0.4904	0.1656	47.15	0.0186	239.2	554.6	70.282	323.7	71.79	15.39	69.98	9.012
BP2209	0.1175	0.1896	0.0034	0.0251	0.0680	0.0253	11.59	0.0118	208.0	387.0	58.178	237.8	44.78	8.840	46.87	5.894
BP2210	0.5264	0.1605	0.0019	0.0329	0.0416	0.0046	13.87	0.0155	87.86	154.3	30.51	144.6	38.03	10.82	40.99	5.228
BP2212	0.6633	0.4149	0.0062	0.0401	1.284	0.0933	12.11	0.0231	235.1	565.2	68.132	302.9	70.64	10.35	73.61	10.55
Spring Waters																
BI2204	0.0393	0.0070	0.0003	0.0151	0.0969	0.0012	1.634	0.0136	0.9080	0.6060	0.174	0.9040	0.3740	0.386	0.5220	0.2080
GM2212	0.0299	0.0869	0.0008	0.0108	0.1423	0.0108	38.14	B.D.	19.08	1.230	4.094	19.32	5.018	7.058	7.434	1.158
BP2211	0.4107	0.3020	0.1155	0.0673	0.0767	0.4351	59.99	0.0253	365.5	689.5	108.384	463.6	96.39	17.276	85.61	10.56

B.D: below detection, set at 3 times the background equivalent concentration (BEC)

Appendix 5 cont: Full geochemical data for all streams/rivers

Element	Dy	Ho	Er	Tm	Yb	Lu	Re	Tl	Pb	Th	U
Unit	ng/L	ng/L	ng/L	ng/L	ng/L	ng/L	ng/L	ng/L	ng/L	ng/L	ng/L
BEC Values	*0*	*0*	*0*	*0*	*1.49E-02*	*0*	*6.72E-03*	*0.2069*	*1.063*	*0*	*1.31E-02*
Major Rivers											
MR2201 (Terra Nova)	11.092	2.160	6.632	0.9520	5.748	0.8500	0.7560	2.526	26.36	26.19	140.1
MR2202 (Gander)	18.568	3.570	9.662	1.202	7.594	1.388	0.6180	1.660	21.76	16.72	77.28
MR2203 (Humber)	28.008	5.884	14.92	2.042	12.65	1.952	0.8980	2.798	86.87	18.08	54.33
MR2204 (Exploits)	17.2	3.708	10.16	1.176	7.598	1.330	0.8880	10.74	358.2	9.572	42.12
MR2205 (Garnish)	28.298	5.596	15.66	1.996	12.39	1.914	0.7020	1.566	42.50	14.61	19.33
MR2206 (Piper's Hole)	5.974	1.334	4.452	0.7540	3.842	0.6220	0.7520	1.942	13.34	11.61	80.91
Western NL Samples											
BI2201	28.13	5.354	16.51	2.336	14.08	2.420	1.054	3.760	92.29	11.43	18.55
BI2202	22.24	4.894	15.11	1.440	13.19	2.136	2.110	3.774	100.2	10.72	73.64
BI2203	2.198	0.4560	1.418	0.2400	1.594	0.4260	1.254	1.498	7.498	0.9000	22.73
BI2205	5.498	1.168	3.662	0.6020	3.368	0.6300	0.9000	2.722	6.104	0.9360	6.252
BI2206	5.914	1.236	3.190	0.5140	3.118	0.4720	0.7400	1.224	25.37	1.750	2.266
BI2207	0.5720	0.1800	0.3940	0.1380	0.2620	0.0500	0.8360	0.944	5.828	4.936	0.6600
BI2208	7.990	1.352	3.952	0.3800	3.462	0.5820	1.070	2.174	20.80	4.330	20.27
BI2209	4.994	1.180	3.300	0.3800	3.288	0.5020	1.022	1.882	9.970	4.566	75.99
GM2201	17.04	3.206	8.258	1.252	6.760	1.010	0.9720	1.308	26.79	8.692	12.26
GM2202	4.922	1.166	2.980	0.4660	2.718	0.4540	0.9780	1.072	30.79	2.562	2.642
GM2203	0.8520	0.2000	0.4720	0.0560	0.4160	0.0940	0.7780	B.D.	9.262	0.7060	0.5720
GM2204	0.6120	0.0760	0.1860	0.0160	0.5940	0.0260	1.176	2.338	8.656	0.6700	0.4600
GM2205	0.6080	0.1600	0.4000	0.0700	0.4920	0.0320	0.6960	B.D.	27.58	0.8120	0.8120
GM2206	0.2520	0.0480	0.1560	0.0140	0.0720	0.0160	0.4720	B.D.	7.738	0.4180	0.7620
GM2207	28.99	6.086	16.84	2.524	14.15	2.386	0.9380	1.916	235.1	7.998	5.778
GM2208	11.57	2.416	6.650	1.002	5.218	0.6600	0.6660	1.212	46.70	2.440	6.200
GM2209	4.288	0.8400	2.160	0.2240	2.410	0.2740	0.6820	0.8240	40.09	2.452	4.224
GM2210	26.85	5.126	13.48	1.776	14.37	2.052	0.5380	2.918	38.31	7.734	26.27
GM2211	7.352	1.426	4.124	0.6800	3.670	0.5140	0.6780	2.556	B.D.	4.560	122.7
Burin Peninsula Samples											
BP2201	337.3	71.13	199.0	25.15	159.5	22.62	0.6960	3.450	267.6	140.6	618.7
BP2202	49.21	11.42	33.22	5.008	30.83	4.558	0.6520	1.964	65.84	24.17	107.2
BP2203	172.3	40.39	124.3	16.66	121.5	18.80	0.6100	3.568	53.64	79.50	193.8
BP2204	42.60	8.932	25.53	3.660	23.99	3.420	0.4360	1.474	148.6	23.22	226.0
BP2205	35.64	7.220	19.84	2.816	18.06	2.750	0.8040	2.124	74.68	18.73	61.35
BP2206	255.5	50.44	140.7	19.20	137.5	23.60	1.102	7.176	1136	75.53	1038
BP2207	231.6	45.39	123.1	16.38	113.2	18.58	3.536	38.12	799.7	83.21	4272
BP2208	50.55	9.318	24.09	3.206	19.70	3.178	0.6820	4.580	123.2	11.30	10.30
BP2209	31.70	5.620	15.24	2.240	11.61	1.714	0.6300	1.300	23.37	12.62	47.42
BP2210	28.02	5.630	13.33	1.486	10.39	1.662	0.4300	1.326	27.13	9.664	10.45
BP2212	60.53	12.70	36.18	4.908	30.72	4.708	0.7360	2.148	40.86	12.06	32.88
Spring Waters											
BI2204	0.8200	0.1800	0.574	0.1260	0.742	0.0880	2.034	1.054	B.D.	0.6420	1.132
GM2212	6.004	1.492	4.802	0.5720	4.518	0.8540	0.342	1.118	15.63	0.4880	281.2
BP2211	55.45	10.85	27.384	2.948	21.162	3.078	0.778	9.560	94.69	10.51	8.396

B.D: below detection, set at 3 times the background equivalent concentration (BEC)